

University of Nottingham
UK | CHINA | MALAYSIA

The Effect of Gestational Diabetes on Human Umbilical Mesenchymal Stem Cells and Their Ability to Influence Endothelial Permeability

By: Samar Salem
Ph.D. Thesis

Supervisors:

Dr. Lopa Leach
Prof. David Bates

Faculty of Medicine and Health Sciences
University of Nottingham, United Kingdom

March 2023

ABSTRACT

Gestational diabetes mellitus (GDM) is associated with short-term adverse complications, such as macrosomia and postnatal fetal hypoglycaemia and long-term metabolic and cardiovascular health consequences for offspring. Placental pathophysiology in gestational diabetes which includes increased insulin resistance and glucose transporters expression, glucose transfer to the fetus, inflammation, and fetoplacental endothelial dysfunction, suggests that GDM may also have an impact on the fetal stem cells from the cord. Therefore, this study aimed to investigate the influence of GDM and its treatment either diet or metformin on Wharton's Jelly Mesenchymal Stem Cells (WJ-MSCs).

WJ-MSCs were isolated from term human umbilical cords (n=35) after elective caesarean sections, from normal pregnancies (nWJ-MSCs) (n=13) and those complicated by GDM (gWJ-MSCs) (n=22); either diet-controlled, (d-GDM) and metformin-treated (m-GDM). The effect of GDM on the migratory and secretory properties, doubling time, and cell morphology of WJ-MSCs was investigated. The number of migrated cells from each cord piece was recorded after 7 days. The concentration of VEGF-A in culture supernatant per $1x10^6$ cells was quantified by ELISA. A phenotypic profile for the expression of mesenchymal and hematopoietic markers in gWJ-MSCs using flow cytometry was performed. PKH-26-labelled nWJ-MSC or gWJ-MSCs were added to confluent monolayers of isolated human umbilical vein endothelial cells (HUVEC) and transendothelial migration of the gWJ-MSCs and their effect on endothelial VE-cadherin junctional occupancy were assessed by selective random sampling. nWJ- MSCs or gWJ-MSCs were added on a confluent HUVEC monolayer growing on transwell inserts to investigate tracer leakage across the endothelial monolayer. Statistical comparisons between two groups were performed by independent samples *t*-test, and among the three groups by One-Way ANOVA, and p-value ≤ 0.05 was considered statistically significant.

Compared with nWJ-MSCs, gWJ-MSCs showed a 65 % increase in the number of migrated cells from each cord piece ($p < 0.005$). The concentration

of VEGF-A on culture supernatant secreted from gWJ-MSCs was 3.8-fold higher than nWJ-MSCs (p <0.001). On sub-culturing gWJ-MSCs displayed a 20% less elongated spindle shape. gWJ-MSCs were positive for CD-44, CD-90, CD-105 & CD-73, and negative for CD-14, CD-19& HLA-DR. However, they displayed 17 % higher CD-105 (Endoglin) (ENG) expression (p <0.05). On co-culture with HUVEC, gWJ-MSCs could transmigrate to the sub-endothelium, open the endothelial junctions (observed in significantly reduced VE-cadherin at 2h co-culture time), and resume the junctional occupancy (observed in the VE-cadherin junctional expression at 24h co-culture time), but junctional VE-cadherin counts were 28 % less in the co-cultures HUVEC+ gWJ-MSCs compared to HUVEC+ nWJ-MSCs (p <0.05). The permeability studies revealed that nWJ-MSCs when co-cultured on top of the HUVEC monolayer enhanced the endothelial barrier integrity and decreased the tracer leakage after transmigration to the sub-endothelial niche. However, gWJ-MSCs did not do so evidenced by increased tracer leakage concentration by 19% compared to nWJ-MSCs.

Endoglin silencing in WJ-MSCs after ENG siRNAs transfection was done to investigate whether the compromised ability of gWJ-MSCs to tighten the endothelial barrier when co-cultured with HUVEC and the increased permeability is via an ENG-dependent mechanism. WJ-MSCs from normal pregnancy were transfected with ENG siRNAs, and gene knockdown was confirmed at the protein level by flow cytometry. The effect of ENG silencing on the VEGF secretion by WJ-MSCs was assessed by ELISA. Permeability assay and immunocytochemistry localization of VE-cadherin at the endothelial junctions after co-culturing with either silenced WJ-MSCs ($ENG^{-/-}$) or non-silenced WJ-MSCs ($ENG^{+/+}$) were performed.

The concentration of VEGF-A secreted in culture from WJ-MSCs was doubled after ENG silencing ($p \leq 0.0001$). ENG loss in WJ-MSCs reduced the stem cell attachment to the endothelial monolayer by 53%. Loss of ENG in WJ-MSCs can impair the ability of the stem cell to maintain the endothelial barrier integrity observed in increased tracer leakage concentration in the co-culture HUVEC + $ENG^{-/-}$WJ-MSCs ($p \leq 0.05$) and reduced number of

junctions displaying continuous VE-cadherin expression by 75.33% compared to the non-silenced cells HUVEC + $ENG^{+/+}$WJ-MSCs.

These changes in vascular permeability, even in well-controlled gestational diabetes, suggest an impaired ability of gWJ-MSC, to maintain/increase endothelial integrity after transmigration. However, the differences found in the comparison between the fetal mesenchymal stem cells from GDM complicated pregnancy and normal pregnancy elucidate the need to do more investigations on the pathogenesis of GDM. ENG mediates multiple endothelial cell responses in response to angiogenic signals from VEGF, and its loss in stem cells leads to increased VEGF-A secretion, reduced stem cell attachment, and deteriorating effect on the endothelial barrier integrity, thus its role in GDM needs to be further investigated.

PUBLICATIONS

PEER-REVIEWED ABSTRACTS

SALEM, S., BATES, D.O. & LEACH, L. 2021. Effect of Human Umbilical Mesenchymal Stem Cells Isolated from Normal and Gestational Diabetic Pregnancies on the Permeability of Human Umbilical Vein Endothelial Cells. *Placenta*, *112*, e40-e41.

SALEM, S., BATES, D.O. & LEACH, L. 2022. Effect of gestational diabetes mellitus on human umbilical mesenchymal stem cells: a flow cytometry study. *Microcirculation,* 29**,** e12739.

SALEM, S., BATES, D.O. & LEACH, L. 2022. Transfection Studies Into The Role of Endoglin in Regulation of Monolayer Permeability of Human Umbilical Vein Endothelial Cells (HUVECs) in Joint Meeting of British Microcirculation and Vascular Biology Society (BMVBS) and Gesellschaft Für Mikrozirkulation Und Vaskuläre Biologie (GFMVB).

These were presented as posters at the BMVBS, IFPA, and Joint BMVBS & GMFVB conferences.

AWARDS

NIH New Investigator Award 2021 from the International Federation of Placenta Associations in recognition of the excellence of the abstract submitted for the IFPA Meeting, 30 Aug-2 Sep Amsterdam.

BMVBS Student Assistance Scheme Award 2022 from the British Microcirculation and vascular biology Society to present the submitted abstract for the joint meeting of the British Microcirculation and Vascular Biology society (BMVBS) and the Gesellschaft für Mikrozirkulation und Vaskuläre Biologie (GFMVB) held 7 & 8 July in Berlin.

ACKNOWLEDGEMENTS

I would like to thank my supervisor, Prof Lopa Leach for her guidance and advice throughout this project and for being supportive at every step of my PhD. Her expertise and research experience have helped to keep my project on track. As an overseas student, I am truly grateful for having an amazing supervisor whom I can share everything with her. Special thanks to Prof. David O. Bates for all the helpful and valuable input to my publications and thesis. I would also like to thank my viva examiners, Dr Luisa Martinez-Pomares and Dr Dean Kavanagh for their very helpful comments and suggestions.

I wish to thank all the clinical staff and midwives at the Labour Ward, Queens Medical Centre, Nottingham University Hospital for the timely retrieval of the placenta and the mothers who agreed to be part of the study and donated their umbilical cords. I would like to acknowledge and thank Dr David Onion for teaching me the flow cytometry technique and analysis. I would like to thank The Egyptian Ministry of Higher Education and the British Council in Cairo for funding the Newton Mosharafa scholarship granted to me.

I would like to express my gratitude to my family who has always supported and believed in me. A great deal of thanks to my mother for encouraging me to pursue a PhD abroad and a special thank-you and remembrance for my late father, who inspired me to seek greater heights. To my husband, my daughters, and my son, thank you so much for being a part of this journey, for always bringing me laughs through the ups and downs of my studies and I hope I can always make you proud.

CONTENTS

Contents

ABSTRACT ..... **I**
PUBLICATIONS ..... **IV**
ACKNOWLEDGEMENTS ..... **V**
CONTENTS ..... **VI**
FIGURES ..... **X**
TABLES ..... **XII**
ABBREVIATIONS ..... **XII**
1 CHAPTER 1 General Introduction **1**

1.1 Gestational Diabetes Mellitus **2**
1.1.1 Diagnosis of Gestational Diabetes Mellitus 2
1.1.2 Glucose Regulation during Healthy Pregnancy 3
1.1.3 Pathophysiology of Gestational Diabetes 5
1.1.4 Placental dysfunction 7
1.1.5 Management of Gestational Diabetes 8
1.1.6 Fetal and Maternal Outcomes of Pregnancy Complicated with Gestational Diabetes (Clinical) 9
1.1.7 Outcomes of GDM on the Mother 11

1.2 Human Placenta **11**
1.2.1 Development of the Placenta 11
1.2.2 Haemochorial Placentation 14
1.2.3 Development of the Umbilical Cord 14
1.2.4 Gross Anatomy of the Human Placenta and Umbilical Cord 16
1.2.5 Effect of GDM on Placenta and Cord Anatomy 18
1.2.6 Angiogenesis Changes in a GDM Placenta 18

1.3 Fetoplacental Endothelial Barrier **19**
1.3.1 VE-Cadherin Molecule Structure 21
1.3.2 VE-Cadherin Disassembly and its Role in Vascular Permeability Factors 22
1.3.3 VEGF and Vascular Permeability 23
1.3.4 Endothelial Cell Junctional Dysfunction and Gestational Diabetes 25
1.3.5 Transmigration of the Cells across the Endothelium 25

1.4 Stem Cell Biology **27**
1.4.1 Stem Cells Classifications upon Their Origin 28
1.4.2 Fetal Mesenchymal Stem Cells 29
1.4.3 WJ-MSCS Embryological Origin 30
1.4.4 Mesenchymal Stem Cells Derivatives 31
1.4.5 The Correlation of Area of WJ with Antenatal and Perinatal Pathology 32

1.5 Thesis Hypothesis 33
1.6 Aims and Objectives 33

2 CHAPTER 2 General Material & Methods 34

2.1 Materials 35
2.1.1 Study Design and Subjects 38
2.2 Methods 38
2.2.1 Isolation of WJ-MSCs 38
2.2.2 Proliferation of WJ-MSCs 41
2.2.3 Cell Freezing and Thawing 41
2.2.4 Morphological Observation and Measurement 42
2.2.5 WJ-MSCs Labelling with Pkh26 Red Fluorescent Cell Linker for General Cell Membrane Labelling 42
2.2.6 Isolation of Human Umbilical Endothelial Cells (HUVECs) 42
2.2.7 HUVECs Subculture, Counting, and Freezing 45
2.2.8 Statistical analysis 45

3 CHAPTER 3 The Phenotype and Behaviour of WJ-MSCs from Normal and Gestational Diabetes and their Influence on Endothelial Barrier Integrity 46

3.1 Introduction 47
3.1.1 WJ-MSCs Phenotypic Characterization 47
3.1.2 WJ-MSCs Immunomodulatory Properties 48
3.1.3 Pericytes 49
3.1.4 Stem cell niche 49
3.1.5 Role of WJ-MSCs in vascular repair 50
3.1.6 Effect of GDM on the Fetal Cells 51
3.1.7 WJ-MSCs and HUVECS Cross-Talk 52
3.2 Aim 53
3.3 Materials and Methods 53
3.3.1 Materials 53
3.3.2 Study Design and Subjects 55
3.3.3 Characterization of MSCs Using Flow Cytometry 56
3.3.4 Doubling Time Calculation 58
3.3.5 VEGF-A Quantification in the Cell Culture Supernatant 58
3.3.6 Co- Cultures Studies, VE-Cadherin Immunocytochemistry 59
3.3.7 Quantitative Analysis of Junctional VE-Cadherin Expression 60
3.4 Results 61
3.4.1 Comparison of Maternal Characteristics 61
3.4.2 WJ-MSCs Retrieval and Migration 68
3.4.3 Morphological Analysis 70
3.4.4 Doubling Time 74
3.4.5 Characterization of MSCs Using Flow Cytometry 74
3.4.6 VEGF-A Secreted from WJ-MSCs in Culture 84

3.4.7 Co-Culture Studies of WJ-MSCs with HUVECs 85
3.5 Discussion 94

4 CHAPTER 4 Effect of Human Umbilical Mesenchymal Stem Cells Isolated from Normal and Gestational Diabetic Pregnancies on Monolayer Permeability of Human Umbilical Vein Endothelial Cells 101

4.1 Introduction 102
4.1.1 Structural Heterogeneity of the Endothelial Cells 102
4.1.2 Breaking Down VE-Cadherin Junctions and the Endothelial Barrier Permeability 102
4.1.3 Endothelial Permeability Pathways 104
4.1.4 Signalling Mechanisms Regulating Paracellular Endothelial Permeability 107
4.1.5 Regulation of Transcellular Endothelial Permeability 108
4.1.6 The Interaction between Mesenchymal Stem Cells and Endothelial Cells and Endothelial Permeability Restoration 108
4.2 Aim 109
4.3 Materials 110
4.3.1 Chemical and Reagents: 110
4.3.2 Tissue Culture Plates, Accessories, and Devices 110
4.3.3 Study Design and Subjects 111
4.4 Methods 112
4.4.1 Co-culture permeability assays 112
4.4.2 Co- Cultures Studies, VE-Cadherin Immunocytochemistry 114
4.5 Results 115
4.6 Discussion 118

5 Chapter 5 The role of Endoglin in Endothelial Permeability 121

5.1 Introduction 122
5.1.1 Endoglin Role in Mesenchymal Stem Cells 122
5.1.2 Membrane Endoglin Role in Endothelial Cells 123
5.1.3 Endoglin's Molecular Structure and Its Role as an Adhesion Molecule in Endothelial Cells 125
5.1.4 Regulation of Endoglin Expression 125
5.1.5 Endoglin Role in Vessel Branching, Maturation and Quiescence 126
5.1.6 Soluble Endoglin 127
5.1.7 Knockdown of Gene Expression 128
5.2 Aim 128
5.3 Materials and Methods 129
5.3.1 Study Design and Subjects 129
5.3.2 WJ-MSCS and HUVEC Transfection by siRNA Endoglin. 130

5.3.3 Flow Cytometry for Transfected Cells 132
5.3.4 ELISA Quantification of VEGF Secreted from ENG^{--}WJ-MSCS 133
5.3.5 Co- Cultures Studies, VE-Cadherin Immunocytochemistry and Systemic Random Sampling 133
5.3.6 Quantitative Analysis of Junctional VE-Cadherin Expression. 134
5.3.7 Effect of ENG Knockdown in WJ-MSCs on the Permeability of HUVEC (Co-Culture Permeability Study) 134

5.4 Results 136

5.4.1 Confirmation of ENG Silencing by Flow Cytometry 136
5.4.2 Cell Attachment and Morphological Changes after ENG Silencing 138
5.4.3 Cell Viability % (Trypan Blue Staining), Sub-culturing and Cell Proliferation after ENG siRNA Transfection 141
5.4.4 ELISA Quantification of VEGF-A Secreted from WJ-MSCs after Endoglin Silencing 142
5.4.5 ENG Reduction in WJ-MSCs Affects the Stem Cells Attachment to the Endothelial Monolayer 143
5.4.6 Effect of ENG Knockdown in WJ-MSCs on the Permeability of HUVEC 146

5.5 Discussion 148

6 Chapter 6 General Discussion and Future Work 153

6.1 Summative Discussion 154

6.2 WJ-MSCs and Regenerative Medicine 156

6.3 Metformin Use in Pregnancy 158

6.4 Future Work 162

APPENDIX 163

CONSENT FORM 164

CASE REPORT FORM 165

PARTICIPANT INFORMATION SHEET 166

REFERENCES 168

FIGURES

Figure 1-1 Regulation of glucose transport across the placenta. 4
Figure 1-2 Diagram showing transplacental transport of high glucose levels results in fetal hyperglycaemia and hyperinsulinemia.. 10
Figure 1-3 Human blastocyst of day-13 post-fertilization. 12
Figure 1-4 Schematic overview of placental- fetal circulation and placental villi morphology. . 14
Figure 1-5 Umbilical cord development (week 3-4). 15
Figure 1-6 Diagram displaying the umbilical cord development (week 5). 16
Figure 1-7 Diagram displaying the anatomy of the placenta and umbilical cord. 17
Figure 1-8 Diagram displaying the VE-cadherin endothelial junctional complex 22
Figure 1-9 Diagram displaying the evolution and derivatives of mesenchymal stem cells. 28
Figure 1-10 Diagram displaying the embryological origin of mesenchymal stem cells 31
Figure 2-1 Diagram showing WJ-MSCs isolation method from cord samples 40
Figure 2-2 Diagram showing the HUVEC isolation technique 44
Figure 3-1 Systematic diagram for WJ-MSCs phenotypic characterization using flow cytometry 57
Figure 3-2 Graph displaying the VEGF ELISA cell culture supernatant standard curve. 59
Figure 3-3 Representative micrograph displaying the continuous and interrupted junctions 61
Figure 3-4 Graph displaying increased body mass index of mothers in the GDM groups 63
Figure 3-5 Graph displaying increased birth weight percentile in the GDM group. 63
Figure 3-6 Graph displaying increased placental weight in the GDM group 64
Figure 3-7 Graph displaying increased placental-to-fetal weight ratio in the GDM compared to normal pregnancy group 64
Figure 3-8 Graphs displaying the correlation of the placental weight to the birth weight centile 65
Figure 3-9 Graphs displaying the correlation between the maternal body mass index and birth weight centile 66
Figure 3-10 Graph displaying the gestational age of the study population 67
Figure 3-11 Graph displaying the maternal age of the study population 67
Figure 3-12 Representative phase contrast micrographs of primary cultures of nWJ-MSCs and gWJ-MSCs (passage 0) day 7 69
Figure 3-13 Graph displaying increased WJ-MSCs migration from UC samples from d-GDM group and m-GDM group compared to normal pregnancy 70
Figure 3-14 Representative micrographs displaying the mixed morphology of PKH-26 red labelled MSCs (passage 2). 71
Figure 3-15 Representative phase contrast micrographs displaying the whirl appearance of the confluent WJ-MSCs at passage-0 72
Figure 3-16 Graph showing no significant difference in cell surface area measurements between the GDM group compared to the normal pregnancy group 73
Figure 3-17 Graph showing decreased percentage of WJ-MSCs exhibiting the elongated spindle-shaped cells after 24h culture in the GDM group). 73
Figure 3-18 Graph displaying no significance difference between the nWJ-MSCs and gWJ-MSCs in doubling time calculation. 74
Figure 3-19 Density diagrams displaying the mesenchymal markers and the haematopoietic markers expression in nWJ-MSCs. 77
Figure 3-20 Density diagrams displaying the mesenchymal markers expression and the haematopoietic markers in gWJ-MSCs 79
Figure 3-21 Density diagrams displaying the mesenchymal markers and the haematopoietic markers expression in gWJ-MSCs. 81
Figure 3-22 Graphs displaying no significant difference between Normal and GDM groups in CD90 (A), CD73 (B), CD14, CD19, and HLA-DR (C) expression (passage-2). 82
Figure 3-23 Graph displaying increased percentage of Endoglin expression in gWJ-MSCs compared to nWJ-MSCs, (passage-2). 83

Figure 3-24 Graph displaying the correlation between increased placental weight and increased Endoglin expression 83
Figure 3-25 Graph showing increased VEGF-A concentration in the supernatant per 1 X106 gWJ-MSCs compared to nWJ-MSCs. 84
Figure 3-26 Graph showing increased VEGF-A concentration in the supernatant of d-GDM group compared to m-GDM and normal pregnancy..... 85
Figure 3-27 Phase contrast microscopic image showing the confluent HUVEC monolayer control and its characteristic cobblestone..... 86
Figure 3-28 Representative micrographs showing cell shape changes in WJ-MSCs after 2h co-culture with HUVEC 87
Figure 3-29 Phase contrast representative microscopic images of HUVEC+ WJ-MSCs co-cultures on coverslips..... 88
Figure 3-30 Representative micrographs displaying reduced junctional VE-cadherin expression after 2h in the co-cultures from HUVEC+ n WJ-MSCs..... 89
Figure 3-31 Micrographs of PECAM localization in HUVEC with and without WJ-MSCs, showing junctional and intracellular expression of PECAM in the HUVEC monolayer 90
Figure 3-32 Effect of WJ-MSCs on Junctional VE-cadherin expression. 91
Figure 3-33 Representative micrographs of co-culture HUVEC + nWJ-MSCs..... 92
Figure 3-34 Representative micrographs of co-culture HUVEC + gWJ-MSCs..... 93
Figure 3-35 Reduced VE-cadherin junctional expression after 24h co-culture of the HUVEC +gWJ-MSCs compared to the HUVEC + nWJ-MSCs..... 94
Figure 4-1 Diagram showing the effect of VEGF on VE-cadherin phosphorylation 103
Figure 4-2 Schematic diagram of transport pathways in continuous endothelium 104
Figure 4-3 Phase contrast micrograph displaying the HUVEC monolayer growing on a transwell insert. 112
Figure 4-4 Schematic diagram displays the co-culture permeability assay experimental design .. 113
Figure 4-5 Graph displaying the standard curve used to interpolate the tracer concentrations. 114
Figure 4-6 Graph displaying the amount of albumin transferred to the basal chamber across the bilayer cell culture model at 0, 4 and 24-hours culture time..... 115
Figure 4-7 Graphs displaying nWJ-MSCs decreased tracer leakage while gWJ-MSCs increased it after 24h co-culture time. 116
Figure 4-8 Graph displaying the effect of GDM treatment mode on the endothelial integrity enhancing ability of WJ-MSCs. 117
Figure 5-1 Schematic diagram illustrating the Endoglin role in angiogenesis, TGF-b and BMP9 signalling pathways in endothelial cells..... 123
Figure 5-2 Diagram displaying the workflow for gene interference using siRNA transfection. Created with BioRender.com..... 132
Figure 5-3 Diagram illustrating the co-culture permeability assay done after the ENG silencing in WJ-MSCs. 134
Figure 5-4 Graph displays the standard curve used to interpolate the unknown FITC-albumin concentrations. 135
Figure 5-5 Flow cytometry analysis of Endoglin expression after ENG siRNA transfection in WJ-MSCS..... 137
Figure 5-6 Density diagrams displaying the Endoglin expression in HUVEC after ENG siRNA transfection 138
Figure 5-7 Representative phase contrast microscopic images of WJ-MSCs displaying no morphology changes after ENG siRNA transfection. 139
Figure 5-8 Representative micrographs displaying no morphological changes observed after ENG knockdown in WJ-MSCs (PKH-67 labelled)..... 139
Figure 5-9 Representative phase contrast microscopic images of transfected HUVECs 140
Figure 5-10 Graph presents the cell viability percentage in WJ-MSCs after ENG-siRNA transfection counted by Trypan blue dye 141
Figure 5-11 Phase contrast microscopic images displaying reduced number of the silenced WJ-MSCs attached to the plate 24 h after passaging compared to the non- silenced WJ-MSCs. 142

Figure 5-12 Graph showing increased VEGF secretion in culture supernatant after Endoglin silencing. 143
Figure 5-13 Representative phase contrast micrographs for co-cultures of HUVEC with silenced or non-silenced WJ-MSCs 144
Figure 5-14 Representative micrographs displaying VE-Cadherin localisation in co-cultures from HUVEC+ ENG$^{-/-}$MSCs and HUVEC+ ENG$^{+/+}$ MSCs 145
Figure 5-15 Graph displays the percentage of continuous VE-cadherin junctional expression after 24h co-culture with silenced or non-silenced WJ-MSCs 146
Figure 5-16 Graph displaying the constant increase in the tracer concentration in the basal compartment in the co-culture group (HUVEC+ ENG$^{-/-}$WJ-MSCs). 147
Figure 5-17 Graph displaying increased FITC-albumin transfer across the co-culture bilayer after ENG silencing 147
Figure 5-18 Schematic diagram displaying the effect of ENG-expressing WJ-MSCs on the endothelial barrier integrity 149
Figure 5-19 Diagram displaying no homophilic binding of the extracellular parts of VE-cadherin, wide intercellular space, and disturbed adherens junctions, when the endothelial cells were co-cultured with ENG silenced WJ-MSCs. 149

TABLES

Table 2-1 Antibodies Used in this Thesis 35
Table 2-2 List of Chemicals and Reagents 36
Table 2-3 Tissue Culture Plates and Devices 37
Table 3-1 List of Antibodies and Kits 53
Table 3-2 List of Reagents 54
Table 3-3 List of Tissue Culture Plates and Devices 54
Table 3-4 Clinical characteristics of the study population used for morphological and phenotypic characterization. 55
Table 4-1 List of Chemical and Reagents used in the Permeability Studies 110
Table 4-2 List of Tissue Culture Plates, Accessories, and Devices used in the Permeability Studies 110
Table 4-3 Clinical characteristics of the study population used for HUVEC+WJ-MSCs permeability assays. 111
Table 5-1 List of chemicals and reagents used in the transfection studies. 129
Table 5-2 Clinical characteristics of the study population used for Endoglin knockdown in WJ-MSCs and the followed permeability assays. 130

ABBREVIATIONS

AGM	Aorta-gonad-mesonephros
AVMs	Arteriovenous malformations
AJs	Adherens junctions
ALK	Activin receptor-like kinase
ANG-2	Angiopoietin-2

CI	Confidence Interval
DM	Diabetes Mellitus
DMEM-LG	Dulbecco's Modified Eagle's Medium - low glucose
DPBS	Dulbecco's Phosphate Buffered Saline
dsRNA	Double-stranded RNA
ECM	Extracellular matrix
ECs	Endothelial cells
EGM	Endothelial growth medium
ENG	Endoglin
eNOS	Endothelial nitric oxide synthase
ESCs	Embryonic stem cells
EVT	Extra villous trophoblast
FAK	Focal adhesion kinase
FGF	Fibroblast growth factor
FoxO1	Forkhead box factor
GDM	Gestational diabetes Mellitus
GLUT	Glucose transports
HAECs	Human amniotic epithelial cells
hCAT	Human cationic amino acid transporter
HCMSCs	Human chorionic mesenchymal stromal cells
HCTCs	Human chorionic trophoblast cells
HHT	Hereditary haemorrhagic telangiectasia
HLA	Human leucocyte antigen
HSCs	Haematopoietic stem cells
HUVECs	Human umbilical vein endothelial cells
ICAM-1	Intracellular adhesion molecule-1

ICM	Inner cell mass
MMPs	Matrix metalloproteinases
MSCs	Mesenchymal stem cells
NO	Nitric oxide
PAK	p21-activated kinase
PE	Preeclampsia
PECAM-1	Platelet endothelial cell adhesion molecule
PFA	Paraformaldehyde
PGCs	Primordial germ cells
PGE2	Prostaglandin E2
PiRNA	Piwi-interacting RNAs
PlGF	Placental growth factor
RNAi	RNA interference
ROS	Reactive oxygen species
SD	Significant difference
sENG	Soluble endoglin
siRNA	Short interfering RNA
SMC	Smooth muscle cell
TGF	Transforming growth factor
TJs	Tight junctions
UC	Umbilical cord
VE-cadherin	Vascular endothelial cadherin
VEGF	Vascular endothelial growth factor
VEGFR2	VEGF receptor-2
VVO	Vesiculo-vacuolar organelle
WJ-MSCs	Wharton's jelly mesenchymal stem cells

1 CHAPTER 1 General Introduction

1.1 Gestational Diabetes Mellitus

Gestational diabetes mellitus (GDM), a common medical complication of pregnancy, is defined as any degree of glucose intolerance with onset or first recognition during pregnancy (American Association of Diabetes, 2018). The impact of pregnancy complications on placental function and the compromised barrier integrity of human fetoplacental vessels from gestational diabetic pregnancies (Young et al., 2010, Leach et al., 2004, Villota et al., 2021) suggests that extraembryonic stem cells in the placenta and their effect on the fetoplacental vascular permeability (Ebrahim and Leach, 2015) may also be affected.

1.1.1 Diagnosis of Gestational Diabetes Mellitus

According to the NICE guidelines updates, women with risk factors such as; obesity, previous GDM, glycosuria detected by routine antenatal testing, previous macrosomic baby, an ethnicity with a high prevalence of diabetes, or family history are recommended to have the 75-g 2-hour oral glucose tolerance test (OGTT) at 24–28 weeks done for them to test for gestational diabetes (NICE, 2021). American Diabetes Association (ADA) for the first time recommended that all pregnant women, not known to have prior diabetes, undergo a 75-g OGTT at 24–28 weeks of gestation, whether or not indicated in the first trimester in high-risk women. This recommendation was in response to the International Association of Diabetes and Pregnancy Study Groups (IADPSG)/WHO 2013 criteria (World Health Organization, 2013).

GDM is diagnosed by an OGTT or a fasting glucose concentration. Based on the results, GDM is present if the fasting plasma glucose level is 5.6 mmol/litre or above or the 2-hour plasma glucose level is 7.8 mmol/litre or above (NICE, 2021). GDM is currently the most common medical complication of pregnancy, it was estimated to occur in approximately 14.7 % of all pregnancies by a meta-analysis study that has been done to report the frequency of GDM using the new IADPSG criteria (Saeedi et al., 2021). GDM is the most prevalent type of diabetes that may happen during pregnancy

comprising approximately 90 % of diabetic pregnancies (Lappas et al., 2011). The prevalence of undiagnosed hyperglycaemia and even overt diabetes in young women is increasing (McIntyre et al., 2019a).

Despite the same diagnostic criteria and screening methods being applied the prevalence of gestational diabetes varies from 1 to 28 % (Hunt and Schuller, 2007, Fadl et al., 2015, Behboudi-Gandevani et al., 2019, McIntyre et al., 2019b). The prevalence of gestational diabetes varies depending on population characteristics, such as age, ethnicity, overweight/obesity, lifestyle (physical activity, diet), and type 2 diabetes mellitus prevalence in the background population (Coton et al., 2016).

1.1.2 Glucose Regulation during Healthy Pregnancy

Glucose transfer across the fetoplacental barrier is regulated by several factors: glucose supply, placental glucose metabolism, uteroplacental blood flow, and placental glucose transporter density (Baumann et al., 2002, Lager and Powell, 2012, Walker et al., 2019). The human placenta has been reported to express seven isoforms of the glucose transporter, GLUT1, 3, 4, 8, 9, 10, and 12 on the microvillous membrane, plasma basal membrane of the syncytiotrophoblast in the human placenta, and endothelial cells (Figure 1-1) (Rivas et al., 2008, Mueckler and Thorens, 2013, Pujol-Giménez et al., 2013).

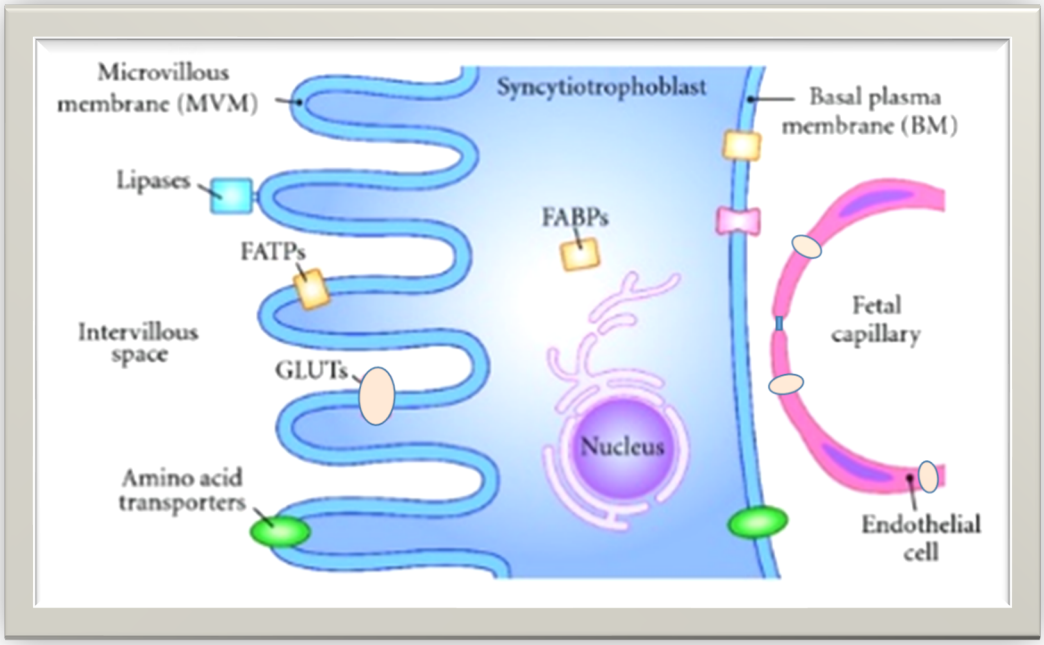


Figure 1-1 **Regulation of glucose transport across the placenta.**

The syncytiotrophoblast is the primary barrier for the transfer of nutrients from mother to fetus. Maternal blood pools in the intervillous space and bathes the microvillous membrane. The basal plasma membrane of the syncytiotrophoblast is facing fetal circulation. Transporters mediating the transfer of amino acids, glucose (GLUTs), and fatty acids (FATPs) are expressed in both plasma membranes of the syncytiotrophoblast, modified from (Lager and Powell, 2012).

A series of physiological changes must occur during pregnancy to support the demands of the growing fetus. Glucose metabolism is one of these changes as maternal insulin sensitivity typically decreases towards the end of the first trimester to maintain glucose supply to the fetus (Lain and Catalano, 2007). Insulin response to a glucose load is increased in the first trimester, but in late pregnancy, OGTTs have indicated that insulin action in late pregnancy is much lower than in non-pregnant women (Catalano et al., 1991). A progressive increase in fasting and 2h postprandial insulin concentrations is perceived with advancing pregnancy (Catalano et al., 1991) (Catalano et al., 1992, Sibiak et al., 2022).

1.1.3 Pathophysiology of Gestational Diabetes

Maternal insulin resistance

During early pregnancy, lower fasting glucose level is paralleled by increasing insulin sensitivity, to facilitate the uptake of glucose into adipose tissues for storage preparing for the increasing energy demands of later pregnancy (Plows et al., 2018). As pregnancy advances, a progressive increase in placental hormones, including progesterone, oestrogen, and placental growth hormone that are predominantly secreted by the syncytiotrophoblast. These hormones promote a decrease in maternal insulin sensitivity and a 50% increase in maternal insulin levels, which is accompanied by a progressive increase in postprandial blood glucose levels and a prolonged glucose peak (Hadden and McLaughlin, 2009, Lain and Catalano, 2007), and this glucose is going to be transported across the placenta to the fetus (Di Cianni et al., 2003). Gestational diabetes mellitus develops if pancreatic beta-cell function decreases, insulin resistance is excessive, β-cell compensation is insufficient, or any combination of these (Landon and Gabbe, 2011).

Insulin sensitivity progressively starts to decrease during the second trimester to the same levels of insulin resistance seen in diabetes mellitus type 2. Despite this insulin resistance, most pregnant women remain normoglycaemic because of adequate β-cell compensation (Hadden and McLaughlin, 2009). Insulin resistance in healthy pregnancies in animal studies leads to increased glucose-stimulated insulin secretion, β-cell hypertrophy, and hyperplasia (Plows et al., 2018). A balance between increased maternal insulin resistance and β-cell hyperplasia ensures optimum glucose supply to the fetus. Increased insulin resistance or the inability to increase insulin secretion accordingly disrupts maternal physiological modulation of glucose metabolism and may cause GDM (Stern et al., 2021).

Decreased insulin-stimulated glucose uptake in response to increased insulin resistance contributes to hyperglycaemia and overworking β-cells (Ashcroft et al., 2017). Therefore, once β-cell dysfunction begins, a vicious cycle of insulin resistance, hyperglycaemia, and more β-cell dysfunction starts.

Women with gestational diabetes are known to have increased insulin resistance compared to others with normal gestation, however, this resistance is suggested to be present preceding pregnancy and to persist across pregnancy (Catalano, 2014). These maternal changes will impact placental and fetal physiology.

Changes in the maternal plasma glucose concentration will change the maternal-fetal glucose concentration gradient, causing an altered rate of glucose transfer. Therefore, changes in blood glucose, such as those seen in maternal circulation as a result of diabetic hyperglycaemia, will increase glucose transfer to the fetus (Baumann et al., 2002). Higher maternal blood glucose levels result in fetal hyperglycaemia and fetal β-cell hypertrophy. This again means fetal hyperinsulinemia and greater fetal utilization of glucose. This phenomenon will explain several changes found in newborns as macrosomia (Pedersen, 1977, Catalano and Hauguel-De Mouzon, 2011, Walker et al., 2019).

Inflammation

During pregnancy, there is physiologic regulation of the innate immune responses to prevent the rejection of the fetal allograft. The balance of Th1 (cell-mediated immunity) and Th2 (humoral immunity) cytokines is characterized by an initial prevalence of the anti-inflammatory profile characterized by Th2 cytokines (such as IL-4, IL-6 and IL-10) to improve materno-fetal tolerance and improve pregnancy outcomes, followed by a progressive shift towards the inflammatory profile characterized by Th1 cytokines (such as interferon-gamma and tumour necrosis factor-alpha) late in gestation (Saito et al., 2010). GDM may alter this balance and initiate and exaggerate the cascade of inflammatory cytokine production involved in adverse pregnancy outcomes (Gomes et al., 2013).

Moderate inflammation during pregnancy is associated with insulin resistance and gestational diabetes. Higher levels of serum leukocyte counts and inflammatory cytokines, including interleukin -6 and tumor necrosis factor (TNF) in women with GDM suggest that GDM exposes the fetus to a pro-

inflammatory environment. Moreover, levels of anti-inflammatory cytokines, such as interleukin-10 and interleukin-4 were reduced (Atègbo et al., 2006). Placental mRNA and protein expression of inflammatory mediators also appear to be upregulated in GDM (Pantham et al., 2015). Inflammatory cytokines impact the insulin receptor signalling as TNF reduces tyrosine phosphorylation of the insulin receptor and increases phosphorylation of insulin receptor substrate-1which contributes to the insulin- resistant state (Hotamisligil, 2003).

Increased secretion of pro-inflammatory cytokines has been distinguished to occur in early pregnancy, followed by insulin resistance in the third trimester, therefore suggesting that pro-inflammatory cytokines and chemokines may be involved in the development of insulin resistance (Abell et al., 2015). Environmental exposure to a pro-inflammatory environment within the uterus may impact diabetes risk by influencing the fetal epigenome at this early stage (Kwak and Park, 2016).

1.1.4 Placental dysfunction

The fetus depends on obtaining glucose from the mother via the placenta. To accommodate this without significant fetal gluconeogenesis the maternal state becomes insulin resistant, allowing placental uptake and transfer of glucose to the fetus. GDM is associated with several metabolic disruptions as altered placental glucose metabolism (Jansson and Powell, 2006), amino acid transport (Jansson et al., 2002) and lipid concentrations (Segura et al., 2017). GLUTs have been reported to show increased expression in response to maternal hyperglycemia (Jansson et al., 2001, Bibee et al., 2011, Stanirowski et al., 2022). GDM trophoblasts display increased GLUT-1 expression and increased glucose uptake in the trophoblast basal membrane (Gaither et al., 1999). Fetal endothelial cell by its role expresses GLUT-3 which participates in glucose transfer to the fetus after trans-syncytial transport contributing to increased fetal weight (Hay Jr, 2006).

GDM placentas display increased Leptin expression along with its receptor (Perez-Perez et al., 2013). Leptin is known to have an anti-apoptotic

effect on trophoblast cells (Magariños et al., 2007). Reduced trophoblast apoptosis accounts for functional adaptations in the GDM placentas to optimize fetal growth leading to higher placental weight to increase the surface area for nutrients transfer (Magee et al., 2014).

1.1.5 Management of Gestational Diabetes

The first line of treatment for gestational diabetes is a balanced diet, together with weight management and physical activity (Yamamoto et al., 2018, American Diabetes Association, 2017, NICE, 2015). It has been suggested that modifying lifestyle alone is sufficient to control blood glucose levels in 70–85% of the women diagnosed with GDM. If blood glucose targets are not met with medical nutrition therapy and physical activity changes within 1 to 2 weeks, metformin is recommended. However, if metformin is intolerable to the woman or contraindicated, insulin is recommended (NICE, 2015). The standard medical therapy for women diagnosed with gestational diabetes requiring drug treatment is insulin. Insulin gives good blood sugar control, but pregnant women may find oral medications more acceptable than insulin injections (Tieu et al., 2017). Oral hypoglycaemic agents have been viewed as potential alternatives since Langer and his colleagues compared glibenclamide with insulin (Langer et al., 2000). Later on, other oral agents like metformin became widely used, more preferable and an attractive alternative because of their easy route intake and low-cost (Heilmaier, 2014, Camelo Castillo et al., 2014).

Metformin decreases insulin resistance by decreasing glycogenolysis, and the activity of hepatic glucose-6-phosphatase as well as increasing glycogen synthesis, insulin receptor tyrosine kinase, and GLUT4 activity (Scarpello and Howlett, 2008). It also does not lead to maternal hypoglycaemia, improves insulin sensitivity, and reduces the maternal weight gain. In GDM-complicated pregnancies controlled by metformin, serum samples from umbilical cords, placental, and fetal tissues have displayed metformin concentrations to be equal to or higher than maternal levels, suggesting active transport of metformin from the maternal circulation across the placenta and into fetal tissues (Vanky et al., 2005). Perfusion studies

confirmed that metformin transfers readily across the placenta from the maternal to the fetal side (Nanovskaya et al., 2006, Kovo et al., 2008, Tertti et al., 2010).

1.1.6 Fetal and Maternal Outcomes of Pregnancy Complicated with Gestational Diabetes (Clinical)

The International Diabetes Federation announced that 21.3 million births (16.2%) worldwide in 2017 were affected by maternal hyperglycaemia, with GDM contributing 86.4% of these cases (Cho et al., 2018). Higher blood glucose in the maternal circulation can pass across the placental barrier and stimulate fetal pancreatic β-cells to produce more insulin. Fetal hyperinsulinemia leads to more accumulation of fat and protein and therefore, macrosomia, which increases the incidence of shoulder dystocia and birth trauma (Kamana et al., 2015) (Wendland et al., 2012).

Weiss et al 1998, found that cord insulin levels were over 50μU/mL in 10% of infants born to diabetic mothers. Furthermore, a larger percentage of these infants had cord blood insulin concentrations of over 20μU/mL, compared to those of normoglycemic mothers (6.9μU/mL) (Weiss et al., 1998). The increased angiogenesis in fetoplacental vessels may be linked to fetal hyperinsulinemia rather than maternal hyperinsulinemia (Figure 1-2). Hyperinsulinemia can influence angiogenesis, as insulin showed angiogenesis stimulation in primary human fetoplacental endothelial cells thereby contributing to the placental hypervascularization that occurs in diabetes (Lassance et al., 2013). High insulin level is associated with increased vascular endothelial growth factor (VEGF), endothelial junctional disruption, and vascular leaks (Nelson et al., 2009).

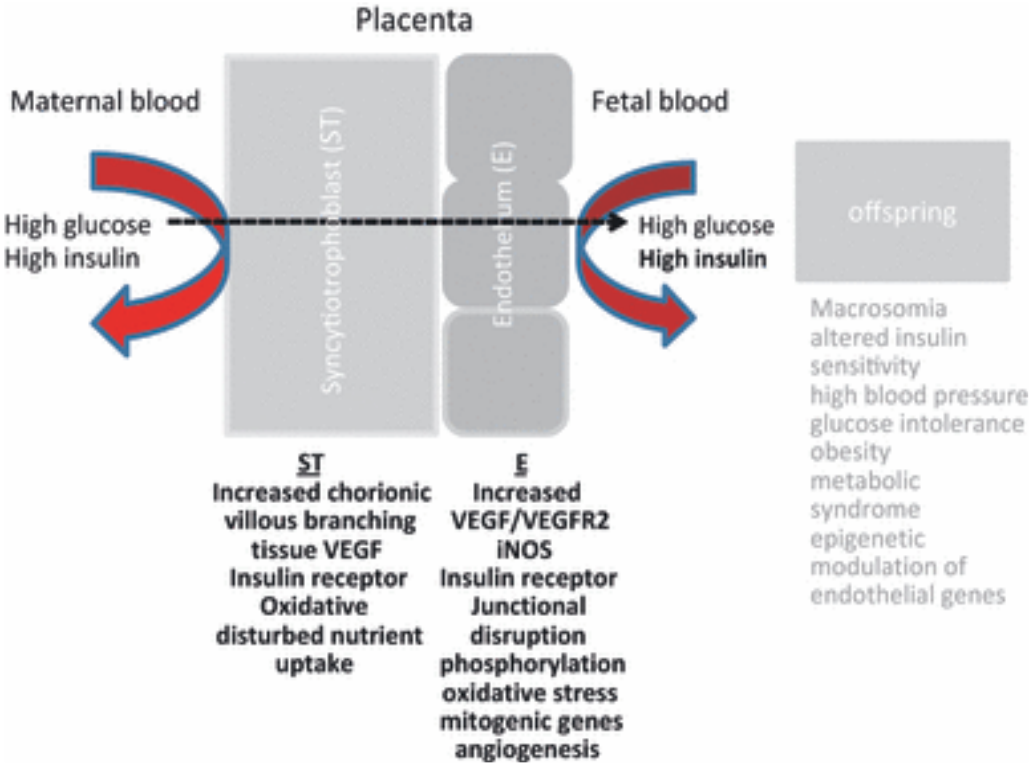


Figure 1-2 Diagram showing transplacental transport of high glucose levels (broken arrow) results in fetal hyperglycaemia and hyperinsulinemia. Both maternal and fetal circulation can cause vascular changes in the fetoplacental vessels. The risks to the offspring are written in grey taken from (Leach, 2011).

Postnatal fetal hypoglycaemia as the newborn is still hyperinsulinaemic can be one of the adverse outcomes of gestational diabetes that lead to increased risk of neonatal unit admission (Billionnet et al., 2017). Gestational diabetes is also known to be associated with an increased risk of neonatal respiratory distress (Mortier et al., 2017). One retrospective cohort study was carried out on over six hundred women with a singleton term pregnancy from 2004 to 2016 displayed the prevalence of macrosomia was higher in infants born to GDM complicated pregnancies (16.4%) compared to the controls (11.2%) and had a higher prevalence of any birth defect (1.0%) compared with the controls (0.8%) (Yang et al., 2019).

GDM was reported to be associated with an increased risk specific subtypes of congenital anomalies such as cyanotic congenital heart diseases, cleft lip with/ without cleft palate, Down syndrome, and Meningomyelocele/spina bifida in a study that included all live births from

2011 to 2018 in the U.S (Wu et al., 2020). Another cohort study including 57 629 infants born to GDM mothers in 2012, showed an increase in the perinatal mortality probabilities by 30% in full-term infants born to mothers whose pregnancies were complicated with GDM compared with the normal gestation population (Billionnet et al., 2017). Increased rates of childhood and adulthood obesity and increased cardiometabolic risk are considered to be long-term risks for offspring born to mothers with GDM (Murray and Reynolds, 2020).

1.1.7 Outcomes of GDM on the Mother

Women whose pregnancies complicated with GDM are twenty times at a higher risk of developing DM type 2, three times more likely to develop ischemic heart disease, and twice as likely to develop hypertension (Daly et al., 2018). The prevalence of gestational diabetes in a population reflects the prevalence of type 2 DM in that population; therefore, ethnic and racial populations with a high prevalence of type 2 DM are at higher risk of gestational diabetes (Hunt and Schuller, 2007).

1.2 Human Placenta

1.2.1 Development of the Placenta

Development of the placenta passes through four stages; pre-implantation stage, pre-lacunar stage, Lacunar stage and villous stage reviewed in (Huppertz, 2008). The human placenta develops from the trophectoderm, which forms at day-5 post fertilisation. At this stage, the blastocyst is segregated into two lineages: the inner cell mass (ICM) and the outer trophoectoderm. The ICM will give rise to the embryo and the umbilical cord, and the trophoblast will form most of the placenta and the fetal membranes. At days 6–7 post-fertilization, the blastocyst hatches from the zona pellucida to attach to the uterine epithelium (pre-implantation stage) (Aplin, 2000, Boyd and Hamilton, 1970).

The ICM localisation in the blastocyst defines which part of the trophoblast that makes the final attachment to the uterine epithelium referred to as polar trophoblast. As soon as the blastocyst attaches to the implantation site.

The polar trophoblast initiates the syncytial fusion of mononucleated cells to generate the oligonucleated syncytiotrophoblast that will allow the blastocyst to penetrate the uterine epithelium. The inner trophoblast layer will be the cytotrophoblast which acts as stem cells, divides frequently and fuses with the outer syncytiotrophoblast layer, resulting in a continuous expansion of the latter (pre-lacunar stage) (Pötgens et al., 2002).

Eight days post-fertilization, fluid-filled spaces occur within the syncytiotrophoblast and soon coalesce to form larger lacunae. The remaining syncytiotrophoblastic masses in between the lacunae are termed as trabeculae and are of great importance for the development of the villous trees. At this stage, the placenta can be defined to have three zones: the early chorionic plate facing the embryo, the villous tree, and the lacunar system. The lacunar system and the trabeculae develop into the intervillous space. The syncytiotrophoblast invades and penetrates the interstitium of the endometrium and finally encounters maternal capillaries and venous plexus of the endometrium (Figure 1-3). Erosion of these blood vessels leads to the presence of maternal blood within the lacunae (Carter, 1997).

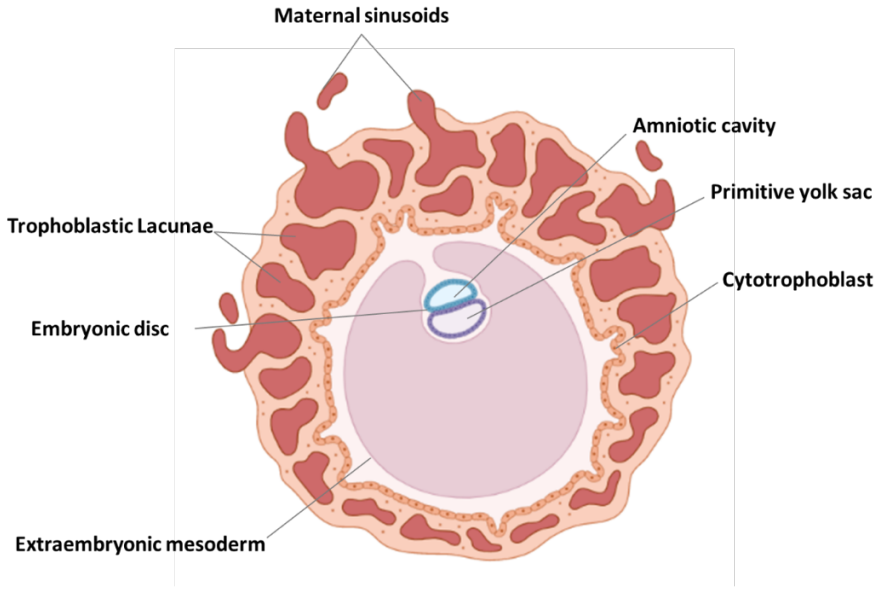


Figure 1-3 **Human blastocyst of day-13 post-fertilization**.

The trophoblastic lacunae are in open communication with the maternal sinusoids, and the uteroplacental circulation has started (Carter, 1997) (created with Bio-render).

Then the cytotrophoblast of the chorionic plate penetrates the syncytiotrophoblastic mass of the trabeculae and differentiates into extravillous cytotrophoblasts (EVT). The EVT invades the endometrial stroma and invades the walls of spiral arteries from the interstitium, lastly entering the lumen of these vessels destructing the muscular wall and replacing the endothelium with trophoblast. This ensures arteries remain open, stay dilated and are no longer under maternal control (lacunar stage)(Kaufmann et al., 2003).

Numerous columns of cytotrophoblastic cells covered by the syncytiotrophoblast grow out of chorionic plate. They branch and elongate. Majority of these branches project into the intervillous space and float free in maternal blood which are called primary villi. When the extraembryonic mesodermal cells of the chorionic plate penetrate the trabeculae of the primary villi giving them a mesenchymal core, they are called secondary villi. At about day 20 post-fertilization, placental blood cells and endothelial cells first develop from haematopoietic progenitor cells independent of the vascular system of the embryo proper forming the first placental vessels and transforming the secondary villi into tertiary villi (Demir et al., 1989, Kingdom et al., 2000, Zygmunt et al., 2003).

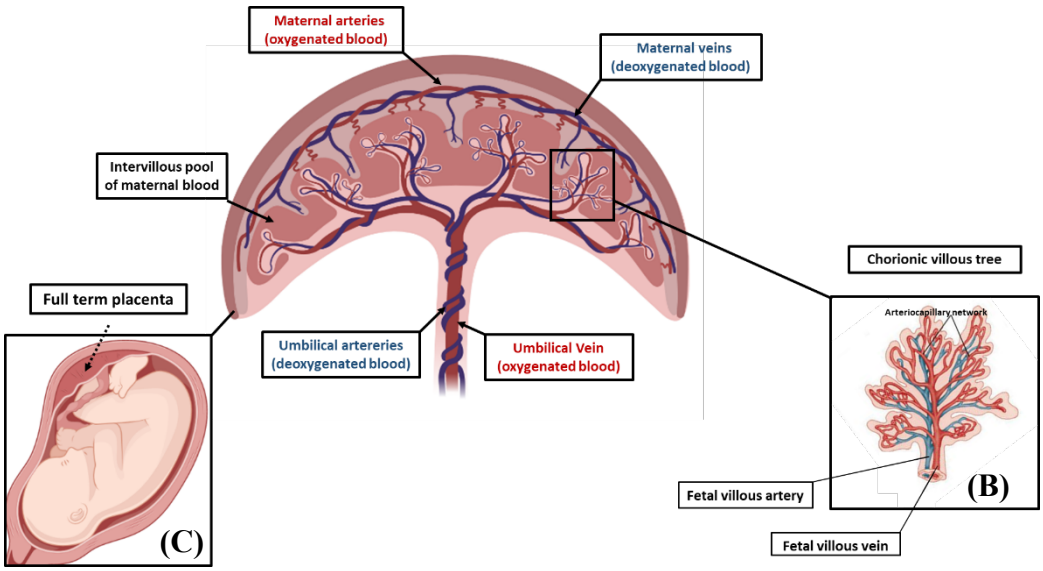


Figure 1-4 **Schematic overview of placental- fetal circulation and placental villi morphology.** (**A**) Deoxygenated blood from the fetus can come into the placental fetal vessels, via the umbilical arteries, pick up oxygen and nutrients and take them back to the fetus via the umbilical vein. (**B**) Tertiary chorionic villus is formed of extra-embryonic mesoderm core and arterocapillary network surrounded by a layer of syncytiotrophoblast (**C**) Full term placenta embedded in the upper posterior surface of the uterine endometrium with the umbilical cord attached to the center of its fetal surface (created with Bio-render) figure (**B**) was taken with permission from (Gude et al., 2004).

1.2.2 Haemochorial Placentation

Mammals display a massive diversity of placental development regarding the degree of trophoblast invasion into uterine tissues and the number of cell layers between the maternal and fetal circulations (Roberts et al., 2016). Both the laboratory mouse and primates have a haemochorial type of placenta, where the trophoblast invades through the uterine epithelium, stroma and maternal arterial walls to come into direct contact with maternal blood (Georgiades et al., 2002). In humans, the decidualisation process- when trophoblast penetrates the epithelium and its basement membrane (Denker, 1990)-is evident at day-5 after the embryo makes contact with the stroma. However, in rats and mice, the trophoblastic penetration of the stroma is less extensive, and decidualisation is evident in the earliest phase of implantation (Chang and Sauer, 2002, Aplin and Kimber, 2004), which makes a significant difference in placental morphogenesis (Myren et al., 2007).

1.2.3 Development of the Umbilical Cord

By the end of the 3rd week of development, the embryo is attached to placenta through the connecting stalk. At 25 days the yolk sac forms and by 28 days at the level of the anterior wall of the embryo, (Figure 1-5) the yolk sac is pinched down to a vitelline duct, which is surrounded by a primitive umbilical ring. The connecting stalk progresses ventrally as a result of the craniocaudal flexion of the embryo and fuses with the yolk sac stalk to form the umbilical cord.

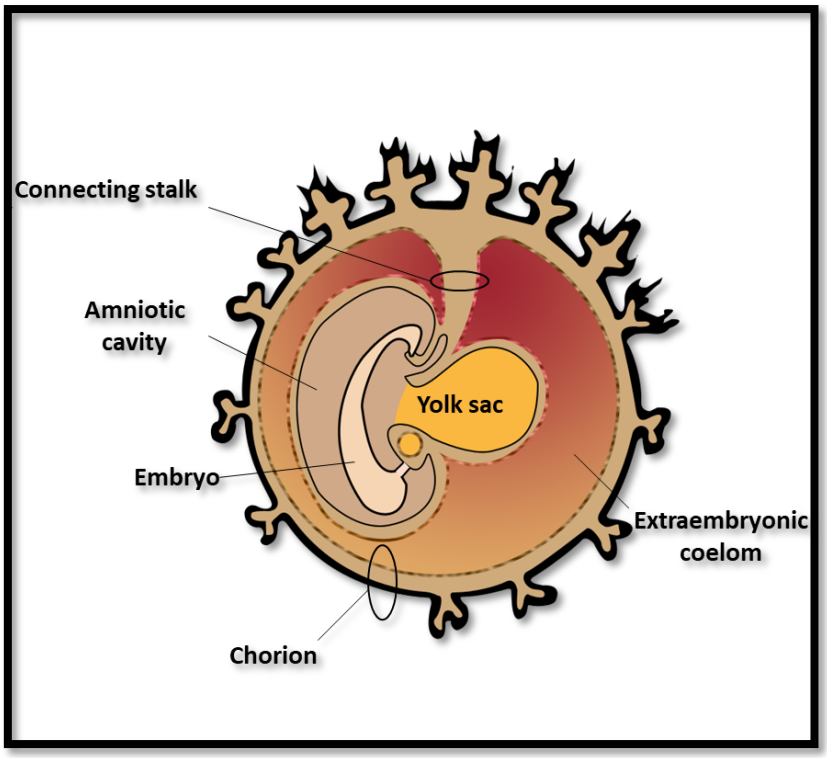


Figure 1-5 **Umbilical cord development (week 3-4).**

Diagram displaying the separation of the embryo from the developing placenta and still linked by a connecting stalk. Within this stalk are the beginnings of the early circulatory system, modified from (Pansky, 1982).

Two stalks are seen by the end of the 5th week: the yolk sac stalk, containing the vitelline duct and vessels and the connecting stalk, containing the allantois and umbilical vessels (Figure 1-6). By the 10th week the gastrointestinal tract has developed and herniates through the umbilical ring forming the physiological umbilical hernia. The intestinal loops retract to the abdominal cavity by the end of the 3rd month. The cord is covered by the amniotic membrane which is continuous with the outer epithelial layer of the embryo, and is inserted in the lower ventral region of the embryo **(**Pansky, 1982**)**.

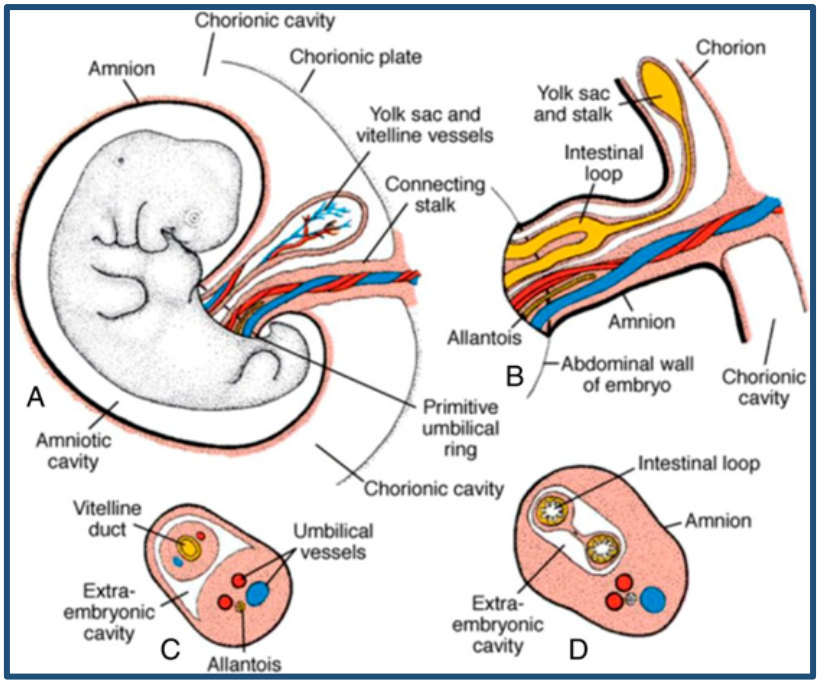


Figure 1-6 **Diagram displaying the umbilical cord development (week 5**).

The yolk sac stalk, containing the vitelline duct and vessels and the connecting stalk, containing the allantois and umbilical vessels are seen by the end of the 5th week. Later the umbilical cord brings together the connecting stalk and the vitelline duct and vessels(Sadler, 1985).

1.2.4 Gross Anatomy of the Human Placenta and Umbilical Cord

The term placenta is a discoid organ with an average diameter of 22 cm and central thickness of 2.5 cm (Bouw et al., 1976). The fetal side of the placenta contains the chorionic plate that is covered by the amnion and the umbilical cord attaches to its centre (Figure 1-7A). The umbilical cord vessels are continuous with vessels in the chorionic plate, which then go on to supply the villi. The maternal side of the placenta (basal plate) is composed of the extravillous trophoblasts and maternal cells. The basal plate is lobulated and contains the villous trees of the fetus. The villous trees are immersed in maternal blood to absorb nutrients and metabolic products (Huppertz, 2008).

The umbilical cord (UC) is a coiled structure, 40-60 cm in length and 1–2 cm in diameter at full term. It is surrounded by the amnion that encloses a mucoid connective tissue through which two arteries and a vein connect the fetal vascular system with the placental vascular system (Figure 1-7B). The umbilical vessels are different from other vessels of similar diameter as they have no tunica adventitia. The adventitial roles are known to be vascular support and contractile function that are considered to be fulfilled by the Wharton's jelly (Davies et al., 2017, Debebe et al., 2020). The umbilical vein carries oxygenated blood from the mother to the fetus and the umbilical arteries carry deoxygenated blood and waste products from the fetus to the placental villi (Gude et al., 2004).

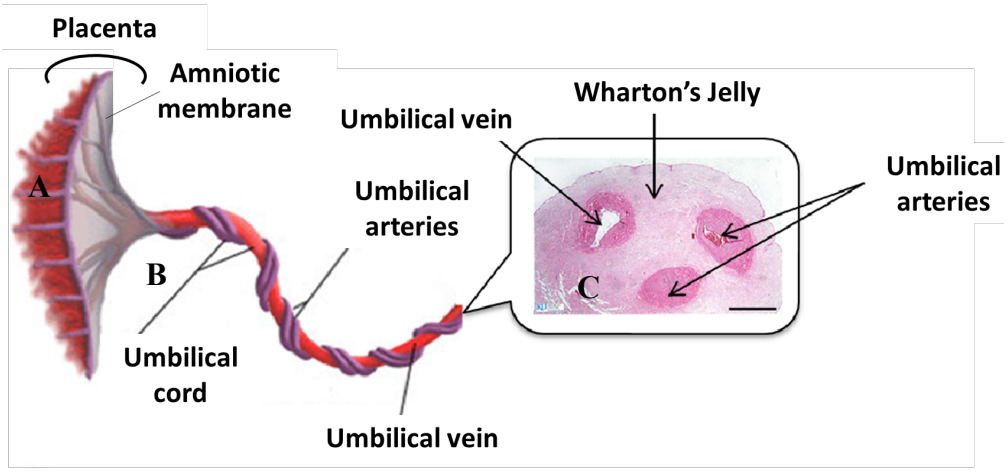


Figure 1-7 **Diagram displaying the anatomy of the placenta and umbilical cord**. The placenta is a discoid organ, its maternal side is red in colour and divided into cotyledons (**A**), its fetal surface is grey, translucent and shiny, covered by the amnion with the umbilical cord attaches to its centre (**B**). (**C**) Haematoxylin and Eosin-stained transverse section in the umbilical cord showing two umbilical arteries and one umbilical vein embedded in the Wharton's Jelly. Modified from (Courtesy of University of Birmingham Medicine, 2008 and university of Kansas medical centre, 2011).

Wharton's Jelly

Wharton's jelly is consisted of a mucoid structure consisting a ground substance of mucopolysaccharides, accumulated around the umbilical vessels, and was described for the first time by Thomas Wharton in 1656 (Wharton,

1730, Balzano et al., 2019). It contained regularly distributed elongated spindle-shaped fibroblast cells and different degrees of differentiation from mesenchymal cells to myofibroblasts (Vázquez Blanco et al., 2011). WJ is important to protect the vessels from torsion and compression in response to fetal movements and its absence has been reported in incidences of perinatal death (Thomson and Hoo, 1996, Labarrere et al., 1985, Takechi et al., 1993). WJ arises from the mesoderm of the primitive streak and surrounds embryonic blood island cells during their migration to the aorta-gonad mesonephros region from the yolk sac region prior to day E 10.5 (Sadler, 2004, Troyer and Weiss, 2008).

1.2.5 Effect of GDM on Placenta and Cord Anatomy

The placentas of poorly controlled diabetic women are enlarged and heavy, which may explain the significantly lower fetal-to-placental weight ratios in GDM pregnancies (Cetin et al., 2005, Taricco et al., 2009). On the macroscopic level, *Panthak et al., 2010*, demonstrated that GDM placentas revealed no significant anatomical difference when compared with normal placentas regarding the eccentricity index. The latter index indicates the placental shape ranging from circular to elliptical. The cord centrality and cord coiling indexes, which describe the umbilical cord insertion from the chorionic plate margin and the coiling direction and numbers of coils, respectively, also revealed no significant difference (Pathak et al., 2010). On the microscopic level, GDM placentas show fibrinoid necrosis and vascular lesions more often when compared with normal placentas (Madazlı et al., 2008, Daskalakis et al., 2008). Villous edema, fibrin deposits in the syncytiotrophoblast, and marked hyperplasia of the cytotrophoblast were associated with poorly controlled GDM placentae (Al-Okail and Al-Attas, 1994).

1.2.6 Angiogenesis Changes in a GDM Placenta

The human placenta has a vascular complex that is totally fetal in origin and continuous with the fetal vasculature. The fetoplacental vessels are found in the chorionic villi bathed in the maternal blood allowing any hemodynamic changes like maternal hyperglycaemia to affect the functioning of fetoplacental vessels (Leach et al., 2005). Placentation includes extensive angiogenesis in

maternal and fetal placental tissues, accompanied by an increase in uterine and umbilical blood flows (Magness, 1998). The villous vascularization and formation of terminal villi is under continuous control of angiogenic factors, such as fibroblast growth factor-2 (FGF), placental growth factor (PlGF), Leptin, VEGF, Erythropoietin, Adiponectin, and Angiopoietins. Increased angiogenesis of fetoplacental vessels frequently observed in placentas exposed to hyperglycaemia (Leach et al., 2009).

GDM occurs in the 2nd trimester sparing the vasculogenesis (developing of vessels from hemangioblastic precursor cells) and early angiogenesis (developing of vessels from existing vessels) that occur in early embryonic development but placentas from GDM exhibit enhanced vascularization, and there is junctional perturbations observed in the GDM placentas. Moreover, placentas from GDM mothers have more surface area of exchange in terms of peripheral villous and capillary surface area and wider intervillous space (Leach et al., 2009). These changes were recorded to be associated with permeability changes in GDM placentas (Villota et al., 2021).

1.3 Fetoplacental Endothelial Barrier

The placental barrier in the first trimester consists of five layers: syncytiotrophoblast layer, cytotrophoblast, trophoblastic basal lamina, connective tissue, and fetal endothelium. This specialized barrier changes during pregnancy: the syncytiotrophoblast is largely reduced in thickness, the cytotrophoblast becomes discontinuous, villus structure enlarges to facilitate the exchange processes between mother and fetus (Kaufmann, 1992, van der Aa et al., 1998, Sibley, 2009). The placental barrier separates the maternal intervillous space and fetal circulation, and plays an essential role in fetal development by tightly regulating the exchange of materials between the mother and the fetus. (Spencer et al., 2014, Blundell et al., 2016).

Endothelial cells (ECs) line the luminal surface of the blood vessels forming a barrier between the blood and the surrounding tissues. The endothelial barrier is maintained by inter endothelial junctions; adherens junctions (AJs), and tight junctions (TJs), so the barrier function is tightly

regulated and plays a central role in human placental microvessels (Lampugnani, 2017). The adherens junctional molecules are important for forming continuous monolayers, regulation of vascular permeability, endothelial survival, tubulogenesis, and angiogenesis. The vascular permeability is facilitated by opening and closing of the endothelial junctions. The permeability of the endothelial junctions determines the level of passive diffusion across the capillary lining (Leach and Firth, 1992, Desforges and Sibley, 2009).

Both adherens and tight junctions join adjacent cells together and can adapt rapidly to changes in the perivascular microenvironment, such as angiogenic/antiangiogenic signals (Gavard, 2013). Tight junctions are localized at the outermost part of interendothelial junctions but can also be intermingled with AJs (Dejana and Orsenigo, 2013, Guo et al., 2007). Tight junctions are composed of several adhesive proteins; occludins, claudins, and cytosolic zonula occluden (ZO)-1, ZO-2, and ZO-3 proteins (Hirase et al., 1997) that assemble as zipper-like structures along the rim of endothelial cells (Itoh et al., 1999) (Komarova et al., 2017).

AJs are composed of VE-cadherin and associated α-, *β*-, and p120-catenin complexes (Lampugnani et al., 1995). AJs initiate cell-to-cell contacts and promote their maturation, playing an important role in tissue integrity. AJs are characterized by two opposing membranes separated by 20 nm (Leach and Firth, 1992). VE-cadherin adhesion is the main adhesion event during vascular development (Breier et al., 1996). VE-cadherin–mediated adhesion promotes activation of forkhead box transcriptional factor FoxO1 that upregulates the gene encoding the tight junction adhesive protein claudin-5.

Endothelial cells express other adhesive proteins, as Platelet endothelial cell adhesion molecule (PECAM-1). PECAM - also known as CD-31 - is concentrated in the intercellular clefts but is not specifically confined to the adherens or tight junctions (Nasdala et al., 2002). PECAM is member of the Immunoglobulin Superfamily that is concentrated at intercellular contacts in the endothelium, that can modulate cell adhesion and migration by interacting with matrix adhesion receptors, reviewed in (Woodfin et al., 2007).

1.3.1 VE-Cadherin Molecule Structure

VE-cadherin, the AJ protein,– known as, cadherin 5 and CD144 was first identified in 1991 by Suzuki, Sano, and Tanihara (Suzuki et al., 1991), who cloned the cDNAs for eight novel cadherin family members, one of which (VE-cadherin) could be found in endothelial cells. In 1992, *Lampugnani et al 1992*, found an endothelial-specific cadherin that plays a role in the organization of endothelial junctions localized at the intercellular boundaries of endothelial cells in vitro (Lampugnani et al., 1992).

VE-cadherin expression is exclusive to the endothelial cells (Prandini et al., 2005), and is specifically responsible for endothelial adherens junctions assembly and barrier architecture (Gavard, 2013). VE-cadherin has extracellular domains which mediate the homophilic binding and adhesion between adjacent endothelial cells. The extracellular domain of VE-cadherin consists of five cadherin-like repeats that form a rodlike structure. These domains are stabilized by the binding of calcium ions to the intervening sequences located at the base of each domain (Leckband and Sivasankar, 2000). The intracellular domain of VE-cadherin is linked to the actin filaments by a complex of proteins, including α- and *β*-catenins, plakoglobin (γ-catenin), p120-catenin, vinculin and α-actinin, which are necessary for the dynamic opening and closing of junctions and also for junctional stability (Figure 1-8) (Azzi et al., 2013, Koch et al., 1999). Opening and closing of the endothelial junctions must occur during normal physiological processes such as acute inflammatory responses, immune surveillance, and antigen recognition (Mehta and Malik, 2006). The integrity of the endothelial cell-cell junction depends on the VE-cadherin expression and the ability to assemble with the underlying actin cytoskeleton (Vincent et al., 2004).

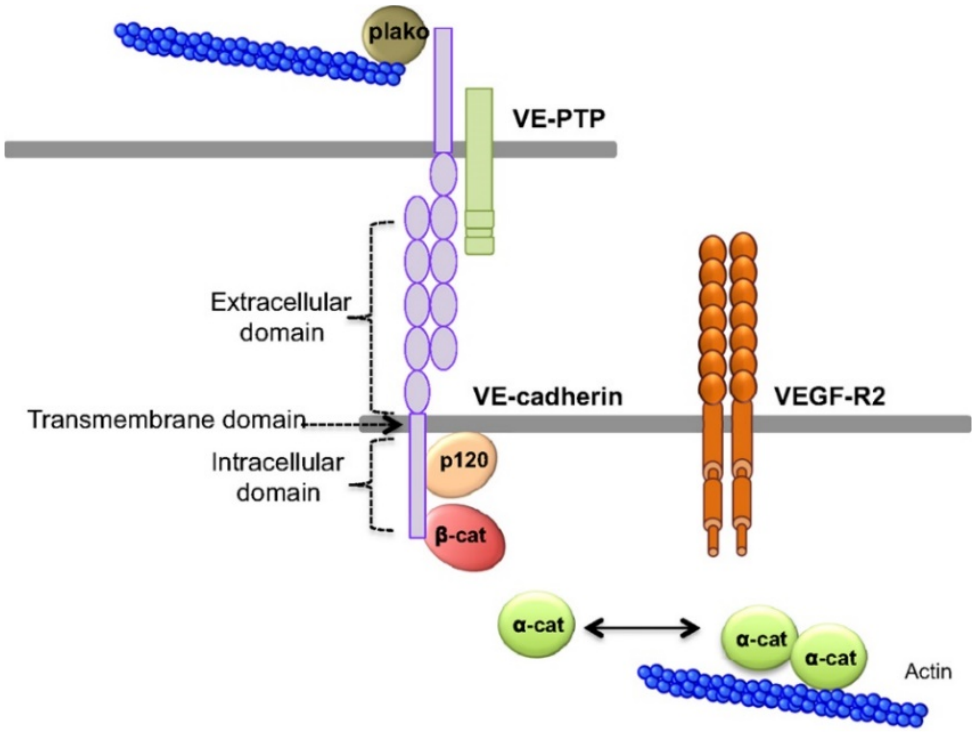


Figure 1-8 **Diagram displaying the VE-cadherin endothelial junctional complex**. VE-cadherin has extracellular and intracellular domains. The intracellular domain is linked to the actin cytoskeleton by α- and *β*-catenins to maintain the junctional stability, taken from (Azzi et al., 2013).

1.3.2 VE-Cadherin Disassembly and its Role in Vascular Permeability Factors

VE-cadherin is a key regulator of vascular permeability in response to permeability-inducing factors, such as thrombin and VEGF, which makes the adherens junctions remodel, and the endothelium becomes more permeable. Changes in vascular permeability are important for leukocytes and stem cells transmigration and tissue fluid homeostasis (Pulous et al., 2019, Ebrahim and Leach, 2016). VE-cadherin can also form complexes with different transmembrane signalling systems, such as VEGF receptor-2 (VEGFR2), vascular endothelial phosphotyrosine phosphatase, transforming growth factor (TGF) *β* receptor complex, and fibroblast growth factor receptor-1. These complexes are vital for regulating the activities of these systems at endothelial junctions (Lampugnani et al., 2006, Dejana and Giampietro, 2012, Cao et al., 2012).

Breaking the junctions starts with phosphorylation of the VE-cadherin C-tail and associated catenins. PAK (p21-activated kinase), Src, and FAK (focal adhesion kinase) catalyze the VE-cadherin phosphorylation. This phosphorylation leads to cadherin-catenin complex dissociation. Then, followed by internalization into clathrin-coated vesicles, which depends on p120-catenin (cat) and VE-cadherin phosphorylation (Gavard, 2013), this mechanism may be behind WJ-MSC migration (Ebrahim and Leach, 2016).

VE-cadherin expression is regulated either at the transcriptional level through miRNA and transcription factors or at the protein level through extracellular shedding or intracellular cleavage and lysosomal degradation (Gavard, 2013). In vitro silencing of VE-cadherin provided evidence that this adhesion molecule is essential for AJ formation and endothelial barrier maintenance. Other proteins as PECAM-1 may also contribute to the permeability control. PECAM-1 can be phosphorylated by permeability-increasing agents or inflammatory cytokines (Nasdala et al., 2002).

1.3.3 VEGF and Vascular Permeability

Vascular endothelial growth factor A is a member of a family of proteins including VEGF-B, VEGF-C, VEGF-D, VEGF-E, and PlGF reviewed in (Ferrara and Adamis, 2016). Alternative exon splicing of VEGF-A generates multiple isoforms including VEGF165, VEGF189, VEGF121, and VEGF206. VEGF165 is the most frequently expressed isoform in tissues and is known as VEGF. Heparin-binding ability is the feature that distinguishes these isoforms, reviewed in (Apte et al., 2019).

Alternative splicing of VEGF165 (exon 8) generates two isoforms, represented by proangiogenic VEGF-A_{165}a and antiangiogenic VEGF-A_{165}b. The two isoforms have opposing actions on vascular permeability and angiogenesis. VEGF-A_{165}b prevents the VEGF-A_{165}a effects on vascular permeability, angiogenesis, and vasodilatation (Woolard et al., 2004).

VEGF can stimulate cell differentiation, proliferation, migration, and survival. It plays a dual role in sprouting, on one hand activating endothelial tip cell formation and actin dynamics to induce cell migration, on the other

hand loosening AJs by the same pathway that triggers the VEGF-mediated increase in vascular permeability (Vestweber, 2014). The various cellular functions of VEGF-A result from its ability to initiate a diverse, complex and integrated network of signalling pathways through its receptor (Zachary, 2003, Ge et al., 2018).

VEGF promotes angiogenesis in health and disease via VEGF receptor-2 (VEGFR-2) (Ferrara, 2009). It disrupts the endothelial barrier function via disruption of the paracellular junctions and this initial barrier disruption must be maintained throughout the process of endothelial cell migration that takes place during angiogenesis. VE-cadherin becomes tyrosine-phosphorylated disrupting the adherens junctions in response to VEGF (Esser et al., 1998).

Pang et al., 2017, demonstrated that the anti-angiogenic VEGF-A165b does not disturb the VE-cadherin junctional occupancy or induce paracellular tracer leakage in the placental microvascular bed and HUVEC monolayers. VEGF-A165b can reverse the VEGF-A165a-mediated increases in fetoplacental endothelial permeability and loss of junctional VE-cadherin (Pang et al., 2017). Changes in this ratio may be behind MSCs transmigration which needs investigation.

Endothelial cells play a vital role in various conditions, such as angiogenesis, inflammation, surgical trauma, ischaemia–reperfusion, and immune responses (Lee Jang et al., 2017). In organ transplantation, the host immune system is brought into direct contact with the endothelial lining of graft vessels, where the graft endothelial cells play a vital role in allograft vasculopathy and overall long-term survival of the grafted tissue (Al-Lamki et al., 2008). Therefore, understanding the molecular mechanisms of vascular permeability could lead to new potential therapeutic strategies for the altered endothelial barrier function that occurs in many disorders (Rahimi, 2017, Weis, 2008, Carmeliet and Jain, 2011). The role of WJ-MSCs in vascular repair is an emerging field that requires further investigation and was part of this Ph.D. project.

1.3.4 Endothelial Cell Junctional Dysfunction and Gestational Diabetes

Endothelial dysfunction of the fetoplacental circulation is one of the main alterations detected in GDM. Endothelial dysfunction is associated with paracellular extravasation of large tracers, which are normally retained in the vascular compartment. GDM placentas display disruption in the tight and adherens junctions leading to reduced junctional restrictiveness, increased solute transfer time, and vascular leaks, all affecting the optimal nutrient transfer to the growing fetus and impairing the placental barrier function (leach, 2011). Endothelial dysfunction can be defined as a state of imbalance between vasodilatation and vasoconstriction (Nguyen-Ngo et al., 2019). GDM is characterized by increased inflammatory cytokines expression and increased oxidative stress, both can lead to endothelial dysfunction (Sobrevia et al., 2011).

Accumulation of reactive oxygen species (ROS) promotes the transcription of endothelial dysfunction markers including vascular cell adhesion molecule 1, intracellular adhesion molecule 1 (ICAM-1), and inflammatory cytokines. ROS interferes with vascular haemostasis by reducing nitric oxide (NO) production, which is a potent vasodilator by suppressing endothelial NO synthase activity (Sprague and Khalil, 2009). In normal pregnancy, vasodilation is a typical feature to reduce peripheral vascular resistance and enable an increase in uteroplacental blood flow. In gestational diabetes-complicated pregnancy, endothelial function is impaired in the uterine arteries that control blood flow to the placenta, along with the arteries involved in regulating systemic vascular resistance (Chirayath et al., 2010, Mrizak et al., 2013).

1.3.5 Transmigration of the Cells across the Endothelium

Leukocytes can transmigrate across the endothelial barrier via a paracellular junctional pathway as well as a transcellular pathway, with the paracellular one being more preferred (Carman and Springer, 2004). The process of leukocyte transendothelial migration involves an interaction

between leukocyte integrins and endothelial receptors, acting as adhesion molecules (Ley et al., 2007). Endothelial cell junctions have to be opened to let leukocytes pass through the endothelial barrier with VE-cadherin downregulation (Del Maschio et al., 1996). Stem cells have also shown similar transmigration taking a period of hours as in WJ-MSCs or minutes as in bone marrow stem cells (Teo et al., 2012). WJ-MSCs demonstrate transmigration to the sub-endothelial layer and influence VE-cadherin junctional expression, with VE-cadherin perturbation as an early event followed by paracellular migration and full junctional VE-cadherin occupancy (Ebrahim and Leach, 2015). The ability of stem cells to migrate to the injury site is a main factor in determining their therapeutic effect of cell-based therapy (Liu et al., 2016).

Fetomaternal Microchimerism

Fetal cells pass into maternal circulation during gestation, as fetal cells and amplified fetal DNA sequences were demonstrated in the maternal circulation at all gestational ages from 6 weeks (Jackson, 2003). Moreover, XY metaphases in fetal lymphocytes were detected in the peripheral blood of pregnant women carrying male fetuses (Walknowska et al., 1969). *O'donoghue et al., 2006,* identified fetal MSCs in the maternal blood of first trimester pregnancy confirming migration of the fetal MSCs to the mother across the placenta (O'Donoghue and Chan, 2006). Microchimerism seems to be more common in diseased tissues than in blood, as observed in spleen, lung, and skin of women with systemic sclerosis (Johnson et al., 2001). Moreover, fetal cells in the maternal blood were found in women with systemic lupus erythematosus (da Silva Florim et al., 2016), suggesting that fetomaternal microchimerism might have a role in the pathogenesis of autoimmune diseases, which have a preference for women after pregnancy (Khashan et al., 2011).

The presence of fetal cells in healed maternal caesarean scar suggested that fetal cells migrate to the site of damage to become involved in maternal tissue repair, or proliferate locally (Mahmood and O'Donoghue, 2014). There is also maternal microchimerism where mother cells can be found in fetal tissues (Maloney et al., 1999). Increased levels of maternal cells have been

described in many human autoimmune disorders, including juvenile dermatomyositis (Reed et al., 2000), idiopathic inflammatory myopathies (Artlett et al., 2000), and biliary atresia (Kobayashi et al., 2007). Whether these genetically foreign maternal cells are harmful and initiate alloreactivity, or otherwise provide regenerative properties remains uncertain (Bianchi et al., 2021). Fetal and maternal microchimerism both might be for the education of maternal and fetal immune systems respectively. Maternal microchimeric cells prevent the fetal immune system from rejecting noninherited maternal alloantigens, and fetal cells remained in women also support fetal tolerance during following pregnancies, since the fetus is considered an allograft (Deshmukh and Way, 2019).

1.4 Stem Cell Biology

Stem cells are undifferentiated cells with the ability to self-renew, differentiate and repopulate a host in vivo. Their potency is ranging from totipotent to unipotent cells. Totipotent cells (germ cells [oocyte and sperm]) can differentiate into all cell types including the placenta. Pluripotent cells (Embryonic stem cells [ESCs]) can differentiate into all cells of the three germ layers, endoderm, mesoderm and ectoderm. Multipotent cells (Haematopoetic stem cells [HSCs] and Mesenchymal stem cells [MSCs]) are lineage-restricted based on the organ of origin that differentiate into cells of more than one type. Unipotent cells differentiate into only one type of cell (spermatogonia give rise only to sperms), (Figure 1-9) reviewed in (Abdulrazzak et al., 2010).

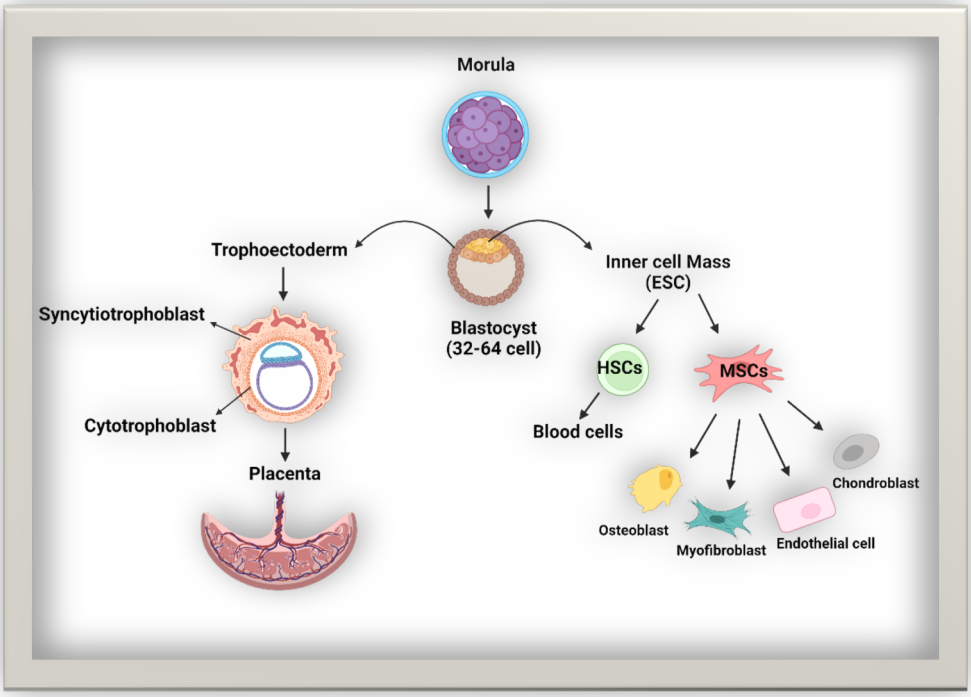


Figure 1-9 **Diagram displaying the evolution and derivatives of mesenchymal stem cells.** A fluid-filled cavity opens in the morula to form a blastocyst with inner cell mass surrounded with a single layer called trophoblast that gives rise to the placenta, ICM can give rise to all three germ layers (ectoderm, endoderm, and mesoderm) of the adult body. Embryonic stem cells give Haematopoietic and mesenchymal stem cells that differentiate into different types of cells (Evans and Kaufman, 1981), created with BioRender.com.

1.4.1 Stem Cells Classifications upon Their Origin

Adult stem cells

Adult stem cells are multipotent cells that give rise to cell types of one specific tissue to maintain the function of the organs. Adult stem cells can be found in the brain, bone marrow (Friedenstein et al., 1976), blood, teeth, heart, eye and liver (Herrera et al., 2006, Caglayan et al., 2019), and are supposed to reside in specific niches.

Embryonic stem cells

Embryonic stem cells which are derived from the inner cell mass of pre-implanted embryo first used by Yasuhiro Takashima, possess the capability of

unlimited self-renewal and expansion (Takashima et al., 2007). They are pluripotent in culture as they can differentiate into all cell types under a specific culturing condition (Madigan and Atoui, 2018, Kim and De Vellis, 2009). Major limitations regarding the use of ESCs include ethical concerns, immune rejection, and their malignant transformation following transplantation (Hao et al., 2014, Broughton et al., 2013) (Barzegar et al., 2019).

Fetal stem cells

Fetal stem cells and stem cells isolated from extraembryonic tissues or cord blood have emerged as a - halfway house - between ESCs and adult stem cells. Fetal stem cells can be divided into neural crest stem cells, hematopoietic stem cells, and mesenchymal stem cells (Ullah et al., 2015). Fetal stem cells are found at a higher frequency than adult stem cells. These include umbilical cord (Ebrahim and Leach, 2015), cord blood (Park et al., 2011), amnion membranes (Díaz-Prado et al., 2011), placental tissues (Vellasamy et al., 2012), and amniotic fluid (Phermthai et al., 2010).

1.4.2 Fetal Mesenchymal Stem Cells

- ***Placental stem cells*** can be divided into the amniotic epithelial cells (hAECs) obtained from the amnion membrane **(**Barbati et al., 2012**)**, chorionic mesenchymal stromal cells (hCMSCs), and chorionic trophoblast cells (hCTCs). The hCMSCs and hCTCs can be obtained from chorionic villus sampling as early as 11 weeks of gestation and the heterogeneous population of cells can be obtained at delivery from the placenta by enzymatic digestion and mechanical dissociation (Antoniadou and David, 2016) (Vellasamy et al., 2012).

- ***Amniotic fluid MSCs*** can be obtained as early as 15 weeks of gestation through amniocentesis or later at the caesarean section. Amniotic fluid contains fetal cells from the amnion, skin, and respiratory system that can differentiate into MSCs or HSCs (Sagar et al., 2018, Phermthai et al., 2010).

- ***Umbilical cord blood stem cells*** can be obtained from cordocentesis during pregnancy or at delivery and the cord blood contains both hematopoietic and mesenchymal stem cells (Antoniadou and David, 2016).

- ***Wharton's jelly mesenchymal stem cells*** (WJ-MSCs) are considered to be an ideal source of mesenchymal cells, as they presented a high capacity to promote tissue regeneration and repair (Kamolz et al., 2014) (Au - Beeravolu et al., 2017).

1.4.3 WJ-MSCS Embryological Origin

There are two possible theories on how stem cells existed in the WJ. One theory suggested that WJ-MSCs are actually primitive MSCs originating from the mesenchyme in the umbilical cord matrix. Their function might be to secrete the glycosaminoglycans, mucopolysaccharides, and extracellular matrix (ECM) proteins forming the Wharton' s jelly substance to prevent strangulation of the cord vessels (Jeon and Kennedy, 1973). The other one was provided by *Wang et al., 2008* that the WJ-MSCs originate from the primordial germ cells (PGCs), and during the migration waves some got trapped in the WJ and retained there. PGCs migrate from the base of the allantois through the hindgut and enter into the genital ridges. This migration occurs between weeks 5 and 8 of gestation. Some of these cells migrate through the allantois to be latter the WJ-MSCs (Figure 1-10) (Wang et al., 2008). Comparative characterization of cells for stemness markers from different regions of 40-day old embryos after termination of pregnancies suggested that the MSCs of the WJ originated from the aorta-gonadal mesonephros (AGM) of the fetus during migration (Wang et al., 2008).

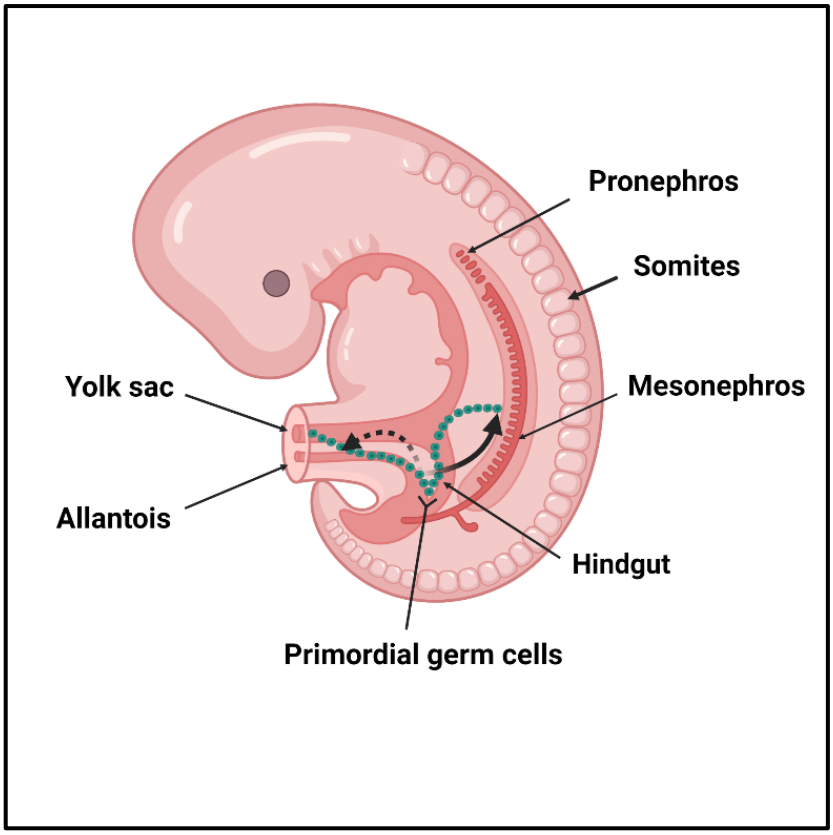


Figure 1-10 **Diagram displaying the embryological origin of mesenchymal stem cells.** Primordial germ cells migrate through the hindgut to the genital ridges (headed arrow), and some other cells migrate (dashed arrow) to the umbilical cord and reside there in the Wharton's Jelly to be the WJ-MSCs (Wang et al., 2008), created with BioRender.com.

1.4.4 Mesenchymal Stem Cells Derivatives

Mesenchymal stem cells are multipotent stromal cells -first discovered by *Friedenstein* in 1977 in mouse bone marrow (Friedenstein et al., 1976) MSCs are approved to be a multipotent progenitor cell whose progeny gives rise to skeletal tissues: cartilage, bone, tendon, ligament, marrow stroma, and connective tissue (Johnstone et al., 1998). Comparative characterization of the stromal cells from various compartments of the fetal tissues showed that they all had stemness properties with the Wharton's jelly compartment having the largest number of cells and the highest degree of stemness and consequently clinical utility (Subramanian et al., 2015).

1.4.5 The Correlation of Area of WJ with Antenatal and Perinatal Pathology

Pathological studies and case reports correlated a thin umbilical cord with adverse pregnancy outcome (Qureshi and Jacques, 1994, Sun et al., 1995). A thin umbilical cord at birth was reported to be associated with oligohydramnios and fetal distress (Silver et al., 1987). A recently published meta-analysis of the UC coiling index based on 27 studies included involved 9553 pregnant women stated that both hypo-coiled and hyper-coiled cords were associated with increased prevalence of smaller for gestational age neonates, meconium stained liquor, preterm birth, Apgar scores < 7 at 5 min, fetal anomalies, and fetal death (Pergialiotis et al., 2020).

Wharton's jelly is known to be altered in the presence of pregnancy complications, such as GDM (Weissman and Jakobi, 1997) and preeclampsia (Bańkowski, 1999). *Debebe et al, 2020*, demonstrated that fetal growth restriction and indicated postpartum severe placental pathology examination were associated with smaller Wharton's jelly area measured by ultrasound at mid and late gestation (Debebe et al., 2020).

The intrauterine environment during pregnancy could affect the biology of fetal stem cells isolated from extraembryonic tissues. Thus, studies that provide understanding of stem cells isolated from women experienced gestational diabetes are necessary to guide future clinical applications (Chen et al., 2020). The Wharton's jelly mesenchymal stem cells can be a useful indicator of the adverse effects of gestational diabetes on fetal tissues that represents the fetus, genetically, and physiologically (Kong et al., 2019) for that reason this study is going to test whether the WJ-MSCs from diabetic pregnancies (gWJ-MSCs) will be able to transmigrate across the endothelial barrier by disrupting the junctions and repair it back, and if they can do will it be in the same time period or to some extent slightly delayed.

1.5 Thesis Hypothesis

The hypothesis of this study is that WJ- MSCs from gestational diabetic pregnancies are phenotypically different from normal pregnancies in their ability to transmigrate across endothelial monolayers, influence cell-cell junctions, junctional integrity, and endothelial permeability.

1.6 Aims and Objectives

To test this hypothesis, the aims are:

I. Phenotypic characterization of WJ-MSCs from GDM complicated pregnancies.
II. Effect of GDM on the migratory properties and proliferation of the WJ-MSCs.
III. VEGF-A secretion from WJ-MSCs in culture in Normal and GDM pregnancies.
IV. Effect of the WJ-MSCs from Normal and GDM pregnancies on the endothelial monolayer permeability (HUVEC + WJ-MSCs) co-culture permeability assay on the trans-well inserts).

2 CHAPTER 2 General Material & Methods

2.1 Materials

Table 2-1 Antibodies Used in this Thesis

Antibody	Species	Source	Product No.	Concentration used
CD144 (Clone 55-7H1)	Purified Mouse anti-human	BD Biosciences, UK	555661	5 µg/ml
CD105 PE (SN6)	Monoclonal mouse anti-human	BD Biosciences, UK	12-1057-42	5µl/(1mg) Test
CD34 PE (Clone:581)	Monoclonal mouse anti-human	BD Biosciences, UK	51-9007661	5 µl/Test
CD11b PE (Clone: ICRF44)	Monoclonal mouse anti-human	BD Biosciences, UK	51-9007661	5 µl/Test
CD19 PE (Clone: HIB19)	Monoclonal mouse anti-human	BD Biosciences, UK	51-9007661	5 µl/Test
CD45 PE (Clone: HI30)	Monoclonal mouse anti-human	BD Biosciences, UK	51-9007661	5 µl/Test
HLA-DR PE (Clone: G46-6)	Monoclonal mouse anti-human	BD Biosciences, UK	51-9007661	5 µl/Test
mIgG1, κ PE (Clone: X40)	Monoclonal mouse anti-human	BD Biosciences, UK	51-9007662	5 µl/Test
mIgG2a, κ PE (Clone: G155-178)	Monoclonal mouse anti-human	BD Biosciences, UK	51-9007662	5 µl/Test
mIgG1, κ PerCP-Cy5.5 (Clone: X40)	Monoclonal mouse anti-human	BD Biosciences, UK	51-9007664	5 µl/Test
mIgG1, κ APC (Clone: X40)	Monoclonal mouse anti-human	BD Biosciences, UK	51-9007664	5 µl/Test
mIgG1, κ PerCP-Cy5.5 (Clone: X40)	Monoclonal mouse anti-human	BD Biosciences, UK	51-9007664	5 µl/Test

mIgG1, κ FITC	Monoclonal mouse anti-human	BD Biosciences, UK	51-9007664	5 µl/Test
APC- CD73 (Clone: AD2)	Monoclonal mouse anti-human	BD Biosciences, UK	51-9007663	5 µl/Test
FITC-CD90 (Clone: 5E10)	Monoclonal mouse anti-human	BD Biosciences, UK	51-9007663	5 µl/Test
CD31	Monoclonal mouse anti-human	R&D Systems, UK	BBA7	5 µg/ml
IgG (Whole molecule)-FITC	Goat anti-mouse	Sigma Aldrich, UK	F0257	1: 50
IgG (Whole molecule)-TRITC	Goat anti-mouse	Sigma Aldrich, UK	T5393	1: 50

Table 2-2 List of Chemicals and Reagents

Reagent	Company
Dulbecco's Phosphate Buffered Saline (DPBS); without calcium and magnesium	Sigma-Aldrich, UK
Dulbecco's Modified Eagle's Medium - low glucose (DMEM); with 1000 mg/L glucose, L-glutamine, and sodium bicarbonate, and Trypsin-EDTA solution	Sigma-Aldrich, UK
Paraformaldehyde (PFA)	Sigma-Aldrich, UK
Bovine Serum Albumin (BSA)	Sigma-Aldrich, UK
Endothelial cell growth supplement from bovine neural tissue (ECGS)	Sigma-Aldrich, UK
Heparin sodium salt from porcine intestinal mucosa; Grade 1-A	Sigma-Aldrich, UK
Albumin–fluorescein isothiocyanate conjugate (FITC-Albumin)	Sigma-Aldrich, UK
Trypsin-EDTA solution	Sigma-Aldrich, UK
PKH26 Red Fluorescent Cell Linker Kit for General Cell Membrane Labelling	Sigma-Aldrich, UK
PKH67 Green Fluorescent Cell Linker Kit for General Cell Membrane Labelling	Sigma-Aldrich, UK

Medium 199 (1x) with L-glutamine, 25Mm HEPES, L-amino acids, sodium pyruvate	Gibco, UK
Medium 199, no phenol red, Dulbecco's Modified Eagle's Medium - low glucose (DMEM), no phenol red	Gibco, UK
Type II collagenase powder	Gibco, UK
VECTASHIELD® Antifade Mounting Medium	Vector laboratories, UK).

Table 2-3 Tissue Culture Plates and Devices

Product	Company
Cell culture flasks (25cm2 and 75 cm2)	Corning, USA
Petri dishes (100mm)	Corning, USA
Cell culture plates (6, 12 and 24 wells)	Corning, USA
Centrifuge tubes (15 mL and 50mL)	Corning, USA
Glass Coverslips (19mm)	Corning, USA
96-well plate black bottomed	Corning, USA
Transwell inserts 0.4µm pore size 12 well format	Corning, USA
Emerald syringe (10mL)	Becton Dickinson, UK
Glass pipettes 5ML, 10ML, and 25ML	Greiner bio-one, Germany
Centrifuge tubes (15 mL and 50mL)	Greiner bio-one, Germany
Pipette tip 20, 200, 1000µL	Sarstedt, Germany
Syringe Filters Plus (2um)	Sarstedt, Germany
Micro tubes 0.5, and 1.5 µL	Sarstedt, Germany
FACS 5mL tubes	Sarstedt, Germany
Cryopreserevation tubes	Sarstedt, Germany
Tc counting slides	Bio-Rad, UK
3-way stopcocks	Vycon UK Ltd., Gloucester, UK
Vicryl suture (2/0, 75cm)	Davies and Geck, Gosport, UK
Scissors, forceps, scalpels, steel trays	Jencons-PLS, Leighton Buzzard, UK

Device	Company
TC20 Automated Cell Counter	Bio-Rad, UK
BD FACS CANTO II Cytometer	BD-biosciences
The SpectraMax M2e Multimode Microplate Readers	Molecular Devices, UK
The SpectraMax M2e Multimode Microplate Readers	Molecular Devices, UK

2.1.1 Study Design and Subjects

Term umbilical cords (UC) were obtained after elective caesarean sections (n = 35; >37 weeks' gestation) from normal pregnancies (n=13) and GDM (n=22) controlled either by diet (n = 13) or metformin (n = 9), with informed patient consent and full ethical approval (REC: OG010101) Nottingham University Hospitals, NHS Trust UK. This study was carried out following The Code of Ethics of the World Medical Association (Declaration of Helsinki). Pregnant women with singleton pregnancies were included, pregnancies complicated with hypertension, pre-eclampsia, pre-gestational diabetes, anaemia, fetal congenital anomalies, smoking were excluded. Women in both groups were not taking any other medications. Norm glycaemic and gestational diabetes state was confirmed by OGTT between 24 and 28 weeks (NICE, 2021). Birth weight (BW) was measured for the newborns after delivery (Villar et al., 2014). Birthweight percentiles corrected for gestational age were calculated using the INTERGROWTH-21st standards.

2.2 Methods

2.2.1 Isolation of WJ-MSCs

WJ-MSC were non-enzymatically isolated from human umbilical cord (UC) that was stored, for a maximum of 24h, in sterile 0.9% NaCl saline contained 100 IU/mL penicillin and 100µg/mL streptomycin at 4ºC, using the method described by (De Bruyn et al., 2011) (Figure 2-1). UC was divided into small pieces 5cm each with a sterile scalpel, each piece was cut longitudinally to expose WJ, small incisions were done in the inner surface, and then the cord

pieces were washed with sterile saline antibiotic solution to remove any residual blood. Each piece was placed in a separate 10 cm petri dish with the Wharton's jelly facing downwards, 15 mL growth medium was added (DMEM/low glucose, 100 IU/mL penicillin, 100µg/mL streptomycin, 0.25µg/mL Amphotericin B and 15% FBS). Dishes were incubated at 37 ºC and 5% CO_2 in air for seven days without disturbance with carefully replace the media with pre-warmed fresh media every 2-3 days.

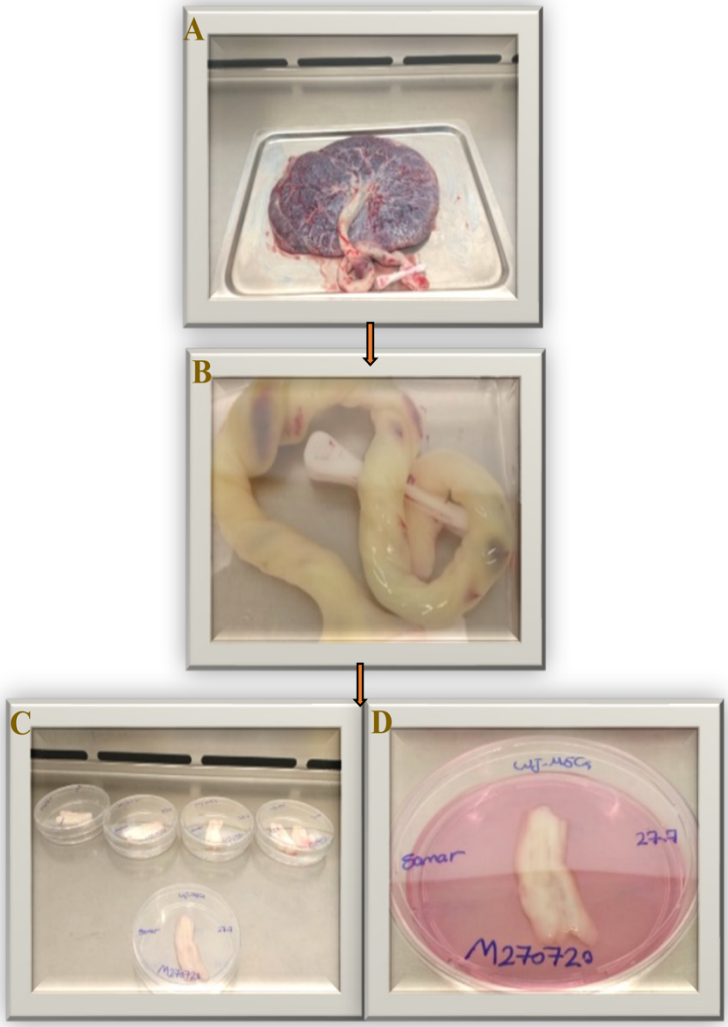


Figure 2-1 **Diagram showing WJ-MSCs isolation method from cord samples.** WJ-MSCs from N and GDM groups were isolated from freshly collected umbilical cords. Image (**A**); one placenta specimen in a sterile tray inside the hood before cutting the umbilical cord. Image (**B**); the cord is washed and kept in an antibiotic saline solution at 4 °C to be used within 24h. Images (**C**) and (**D**); UC cord pieces 5cm each are cut longitudinally to expose WJ, small incisions are done in the inner surface, are placed in a petri-dish with the inner surface facing downwards and left for 5mins to dry and attach before adding the media.

2.2.2 Proliferation of WJ-MSCs

After seven days, UC pieces were removed and pre-warmed growth medium at 37ºC was used to feed up the attached cells every 2-3 days. The migration of the cells from each cord piece was monitored using Olymus inverted microscope. All the migrated cells were imaged at day-7 to be counted later. When the cells reached 80-90% confluence, the medium was changed, and 10mL of DPBS was used to wash any remaining residues of the media from the petri dish. The cells were detached by incubation with 2mL of trypsin/EDTA (0.05 %trypsin and 0.02% EDTA) for 5 minutes at 37%. After checking that the cells were detached under the microscope, the reaction was stopped by adding a pre-warmed growth medium equivalent to four times the trypsin volume. WJ-MSCs were collected by centrifugation (1000 rpm for 5 min) and the cell pellet was re-suspended in 3ml complete media for counting. 10 µL cell suspension was mixed with 10 µL trypan blue, and 10 µL of the mixture was loaded into one counting slide chamber, and the reading was recorded by TC20 Automated Cell Counter. 1×10^6 cells/ml were seeded on a 75 cm^2 culture flask in the same culture conditions for confluence.

2.2.3 Cell Freezing and Thawing

When the cells reached 80-90% confluence, the medium was changed, and the cells were washed and detached using trypsin/EDTA as described in the previous section. WJ-MSCs were collected by centrifugation (1000 rpm for 5 min). After counting, one million cells were resuspended in one mL freezing mixture (90% full growth medium and 10% DMSO). The cell suspension was transferred quickly to the cryovial (1ml/vial) labelled with sample ID, passage number and the date. Then cryovials were put in Mr Frosty container and placed at -80º freezer overnight to ensure the cells freeze slowly (1°c/min). The cryovials were transferred into the liquid nitrogen container on the next day (British oxygen company, UK) Dewar. Stored cells were taken from the liquid nitrogen and thawed quickly in a warm water bath. The cells were gently pipetted into the centrifuge tube with growth medium, centrifuged at 1000 rpm for 5 min, and transferred into a T-75 flask. The growth medium was changed

after 24 h to remove any remaining DMSO and unattached cells. The cells were passaged when confluent.

2.2.4 Morphological Observation and Measurement

Changes in cell morphology were detected by a phase contrast microscope. To analyze the cell length, 5 images with the same magnification were taken from each sample from passages 0–2. Single cells that appeared clearly separated were used for analysis by Image J. The images were opened by Image-J software and were adjusted by changing the contrast and brightness until the cell margins were clearly defined. To measure cell lengths, a line tool was drawn based on the longest axis from the cell periphery and its length was measured to represent individual cell length. No more than 150 cell populations were counted for each umbilical cord sample to maintain sampling efficiency.

2.2.5 WJ-MSCs Labelling with Pkh26 Red Fluorescent Cell Linker for General Cell Membrane Labelling

The cell suspension was placed in a conical tube (5×10^6 cells), washed once with media without FBS and centrifuged at 400 rpm for five minutes to obtain a loose pellet. One mL of diluent C was added to the pellet and another mL was added to PKH26 stain (4µL). The dye solution was added to the cell suspension and mixed immediately. The dye/cell suspension mix was incubated for 5min at RT with periodic mixing. Two ml of FBS was added to stop the stain and the cells were incubated for 1 minute at RT to allow binding of excess dye, then centrifuged (400 rpm for 5 min). The pellet was suspended in 10mL complete media and washed twice to ensure the removal of unbound dye. Finally, the cells were centrifuged and re-suspended to the desired final concentration of viable cells.

2.2.6 Isolation of Human Umbilical Endothelial Cells (HUVECs)

Umbilical cords were collected and stored in 0.9% saline at 4ºC until isolation (within 24 hours). The isolation of human umbilical vein endothelial cells was performed as described by (Hamilton and Leach, 2011) (Figure 2-2).

A 1cm long piece of cord at both ends was resected with a scalpel. The vein at each end was cannulated by a 3-way stopcock and the cannula was fixed using vicryl suture (2.0) around the cord end. The vein was washed with a pre-warmed saline antibiotic solution to remove any residual blood and be sure that the cord was not damaged and there was no leakage at any point. One mg /mL collagenase type II was added in 10 mL M0 (M199 containing 100 IU/mL penicillin, 100µg/mL streptomycin and 0.25µg/mL amphotericin B) and injected into the cannulated vein until it become firm. The cord was put in a water bath with a pre-warmed saline antibiotic solution at 37ºC for 10 min, then a 10 mL syringe was attached to the stopcocks at each cord end, and the solution was passed back and forth through the vein to ensure that endothelial cells were detached from the vessel wall.

HUVECs were collected in M 20 (M 0 and 20% heat-inactivated FBS), centrifuged at 1000rpm for 5 min at RT, then re-suspended in endothelial growth medium (EGM) (M 20 with 75µg/mL ECGS and 50µg/mL heparin) and allowed to attach to gelatin-coated tissue culture flasks. Isolated HUVECs were seeded on a 1% gelatin-coated T-25 flask. After 24 hours, unattached cells were removed and attached cells were fed up with pre-warmed growth media every 48-72 h. In all experiments, HUVECs were grown and used only up to the third passage. 1 % gelatin in sterile water was autoclaved for flask coating. 2mL gelatin solution was added in T-25 flask, 5mL in T-75 flask, and one mL for each coverslip in 6 well plate or 400µL in 12 well plate. The coated flasks and plates were incubated at 37 ºC with 5% co_2 for 90 min, gelatin was removed and air-dried in a laminar flow hood under UV light for sterilization.

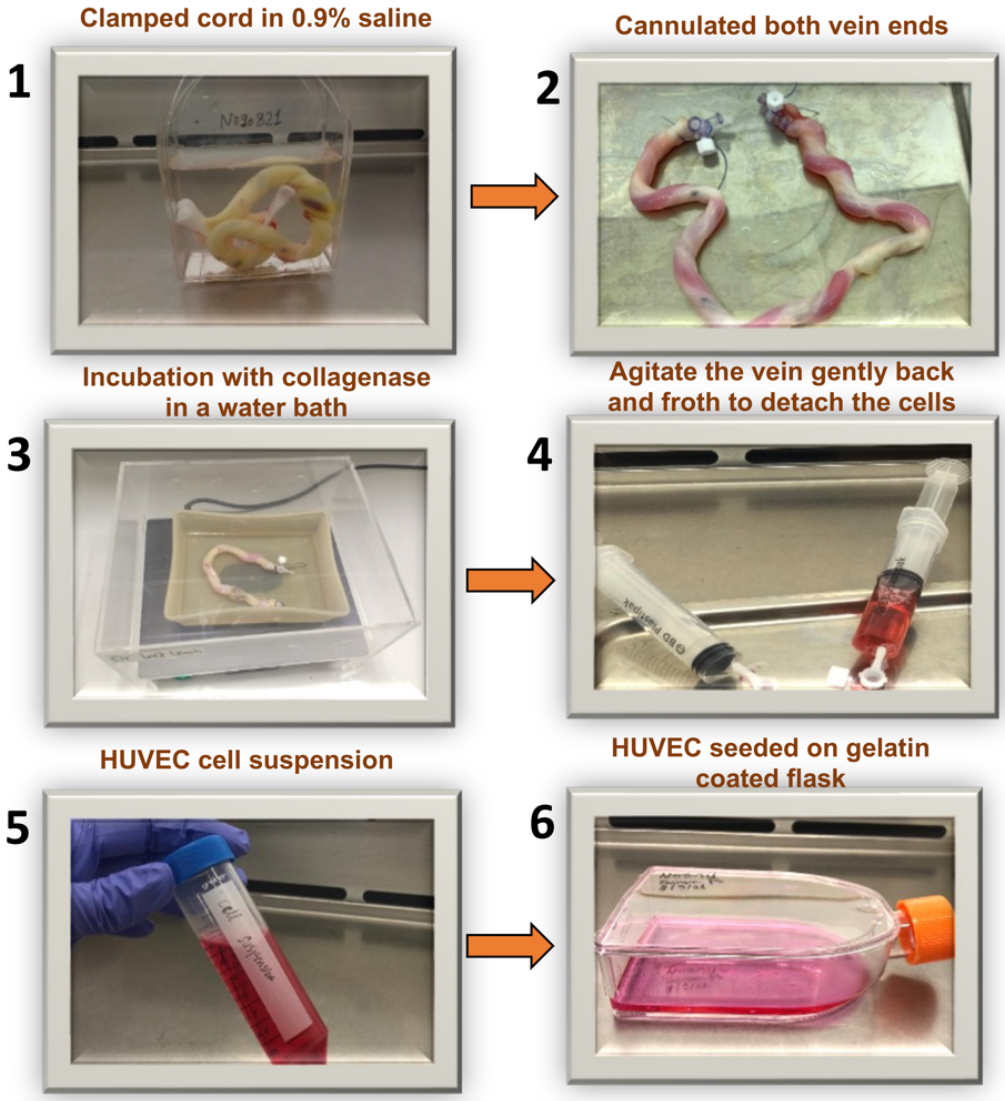


Figure 2-2 **Diagram showing the HUVEC isolation technique.** (**1**) The cord's both ends were clamped and washed in 0.9% saline. (**2**) The vein ends were cannulated with 2-way stopcock and flushed with 0.9 % saline twice to get rid of any blood or blood clots. (**3**) The vein was filled with 0.1% collagenase type II and incubated for 10min in a water bath at 37ºC. (**4**) M20 solution was passed back and forth through the vein to ensure that endothelial cells were detached from the vessel wall. (**5**) The cell suspension was collected in M20 media and centrifuged. (**6**) The isolated HUVECs were growing on gelatine coated flasks in EGM, and media was changed after 24 hours.

2.2.7 HUVECs Subculture, Counting, and Freezing

When HUVECs reached 80-90% confluence (T-25 flask), the media was removed, and any remaining residues were washed with 5 mL pre-warmed DPBS. The cells were detached by incubation by 1mL trypsin/EDTA (0.05% / 0.03%), rock gently from side to side and incubate at 37°C for 1 minute. The reaction was stopped by 4 mL pre-warmed M20. HUVECs were collected by centrifugation (1000rpm for 5min), the supernatant was removed and 3mL pre-warmed growth medium was used to re-suspend the pellet. The suspension was seeded on 1% gelatin coated T-75, then growth media was refreshed every 48-72 h. When the cells reached confluence, they were harvested, and the pellet was re-suspended in 3mL freezing mixture (90% FBS and 10% DMSO). The cells were counted and frozen as described before.

2.2.8 Statistical analysis

The data obtained were tested for the normality of distribution by D'Agostino–Pearson test with a confidence interval (CI) of 95%. Study population, phenotypic characterization, Endoglin expression and tracer leakage were normally distributed. Statistical comparisons between two groups were performed by unpaired *t* test, and among the three groups by One-way ANOVA and Tukey post-hoc tests or two-way ANOVA where appropriate. Results of birth weight in all groups, cell migration, and VEGF-A secretion in gWJ-MSCs were not normally distributed and performed by Mann–Whitney U test and Kruskal–Wallis test. Pearson's or Spearman's rank correlation coefficients were used according to the data distribution. All statistics were calculated, and graphs plotted using the GraphPad Prism software 9.0, USA. P-value < 0.05 was considered statistically significant.

3 CHAPTER 3 The Phenotype and Behaviour of WJ-MSCs from Normal and Gestational Diabetes and their Influence on Endothelial Barrier Integrity

3.1 Introduction

3.1.1 WJ-MSCs Phenotypic Characterization

WJ-MSCs showed necessary MSC characteristics, such as plastic adherence, the ability to self-renew, multipotency with osteogenic, chondrogenic, and adipogenic differentiation potentials, and expression of mesenchymal makers, such as CD105, CD44, CD90, CD29, and CD73 while lacking expression of haematopoietic markers; CD14, CD34, CD45, and human leukocyte antigen-DR (HLA-DR). WJ-MSCs have the ability to be expandable over several passages in vitro (Ebrahim and Leach, 2015) based on the minimal criteria of MSCs published by the International Society for Cellular Therapy (ISCT) in 2006 (Dominici et al., 2006).

CD-90, also known as Thy-1, is a glycosylphosphatidylinositol-anchored glycoprotein expressed on mesenchymal stem cell surfaces. It plays a role in many signalling pathways, including regulating the activity of Rho GTPases on fibroblast cells. It has been known to regulate cell adhesion, apoptosis, fibrosis, and migration (Ode et al., 2013, Rosati et al., 2022). CD-105, also known as Endoglin, is expressed on mesenchymal stem cells and is a part of TGF-β that plays a vital role in angiogenesis, vascular physiology, and vascular remodelling (Schoonderwoerd et al., 2020). Endoglin is also expressed in endothelial cells and its expression is increased during active angiogenesis when sprouting takes place (Barnett et al., 2014, Jin et al., 2017).

CD-73 is a purine catabolic enzyme and an adhesion molecule that is important for lymphocyte endothelial binding (Linden, 2001, Deaglio et al., 2007). CD-73 is a marker for gastric cancer stem cells that regulates tumour initiation, self-renewal, metastasis, and chemoresistance (Lee et al., 2019, Xu et al., 2020, He et al., 2021).

CD-14, known as human monocyte differentiation antigen, is a pattern recognition receptor that enhances innate immune responses and induces the synthesis of tumor necrosis factor (Wright et al., 1990, Deaglio et al., 2007). CD34 is an L-selectin ligand and one of the haematopoietic stem cell markers

(Baum et al., 1992). Human Leukocyte antigen HLA-DR isotope is a major histocompatibility antigen class II cell surface receptor which constitutes a ligand for the T-cell receptor (Basham and Merigan, 1983) that presents extracellular antigens to T-lymphocytes, these antigens stimulate T-cells multiplication, by their role stimulate antibody-producing B cells. Mismatches at the HLA-DR locus reveal the greatest responsibility for graft rejection (first six months) (Kaczmarek et al., 2006, Kwon et al., 2021).

3.1.2 WJ-MSCs Immunomodulatory Properties

WJ-MSCs display very low expression of HLA class I and do not express class II. WJ-MSCs also don't express CD86 or CD80, the co-stimulatory antigens that activate B cells and T cells (Jyothi Prasanna and Sowmya Jahnavi, 2011, Marino et al., 2019). Moreover, WJ-MSCs synthesize extensive amounts of the anti-inflammatory cytokine; interleukin-10, and up-regulate the TGF-β. TGF- β reduces the expression of MHC class II molecules. Decreased MHC class II expression reduces the potential of inducing a T helper cell response (Prasanna et al., 2010, Vasandan et al., 2016). MSCs affect immune response through their interactions with the cellular components of the innate and adaptive immune systems. Mesenchymal stem cell immunomodulation can occur via cellular contact and/or secretory properties (Meisel et al., 2004, Ryan et al., 2007, Castro-Manrreza and Montesinos, 2015).

MSCs can cause in vitro inhibition of immune cell proliferation. They can stop a variety of immune functions, such as cytotoxicity of T and natural killer cell, B cell stimulation, antibody production, antigen presentation, and dendritic cell activation generating a tolerogenic environment during wound healing. MSCs can stop an immune response during tissue repair contributing to the maintenance of immune homeostasis (Castro-Manrreza and Montesinos, 2015, Chen et al., 2016, Shpichka et al., 2019).

3.1.3 Pericytes

Pericytes were first recognized as sub-endothelial cells resident in small and large vessels in 1871 (Eberth, 1871). Pericytes have been considered as MSCs progenitors with the ability to be expanded in vitro for many passages and have the tri-lineage differentiation potential. Moreover, Pericytes express the MSCs surface marker combination of CD44, CD73, CD90, and CD105 in situ (Crisan et al., 2008, Pittenger et al., 2019). They can be isolated as $CD146^{+}$ (melanoma cell adhesion molecule)and $CD34^{-}$ cells from different tissues (Crisan et al., 2008).

Pericytes cannot be distinguished from mesenchymal stem cells in vitro and in vivo. However, an in-vivo animal study demonstrated that pericytes in different tissues (heart, brain, adipose tissues, and skeletal muscles) do not behave as multipotent tissue-resident progenitors as they behave in vitro. These in-vitro and in-vivo differences might be a consequence of the cell culture environment (Guimarães-Camboa et al., 2017). *Blocki et al 2013,* stated that not all pericytes are mesenchymal stromal cells, but all MSCs can act as pericytes (Blocki et al., 2013), as they are also located in a perivascular niche (Wu et al., 2010, Wong et al., 2015, de Souza et al., 2016). Pericytes are believed to be the in vivo perivascular source of MSCs, support the endothelial cells and monitor and react to signals that play a vital role in angiogenesis and vascular maintenance. However, heterogeneous populations of mesenchymal stem cells, both fibroblastic or pericytic in origin may explain the reported vascular repair potential of mesenchymal stem cells (Traktuev et al., 2009).

3.1.4 Stem cell niche

Stem cell niche is composed of microenvironmental cells that cultivate stem cells enabling them to maintain tissue homeostasis. A proper spatiotemporal crosstalk between stem and niche cells is needed to accomplish lifelong demands for differentiated cells (Moore and Lemischka, 2006). Niche cells provide an environment that seizes stem cells from differentiation and apoptosis in response to stimuli that would challenge stem cell reserves. The niche also prevents excessive stem cell production that could lead to tumour.

Stem cells must activate to produce progenitors that are committed to produce differentiated cell lineages. A balance of stem cell quiescence and activity is necessary for a functional niche (Moore and Lemischka, 2006).

3.1.5 Role of WJ-MSCs in vascular repair

Mesenchymal stem cells participate in neo-vasculogenesis of both the placental and umbilical circulation. They also modify the microenvironment and trigger angiogenesis (Edwards et al., 2014, Todeschi et al., 2015) promoting tissue repair processes by cell-to-cell interactions and/or secreted cytokines, including antioxidant, anti-apoptotic and growth factors, such as epithelial growth factors, vascular endothelial growth factor, transforming growth factor α and *β*, fibroblast growth factor, and insulin-like growth factor type 1 (Murphy et al., 2013, Richardson et al., 2016, Ebrahim and Leach, 2016). Advances have been made in the development of allogeneic MSCs as a therapy for cardiovascular diseases (Huang and Li, 2008, Sorrell et al., 2009, Pankajakshan and Agrawal, 2014, Butler et al., 2017, Hare et al., 2017).

The essential role of MSCs in the vasculogenesis of many pathological processes has been confirmed in myocardial infarction, wound healing, and bone repair by promoting local revascularization via secreting angiogenic growth factors (Pu et al., 2017). MSCs can respond to injury, infection, or disease by locally secreting the cytokines. This ability might be because of the distribution of perivascular MSCs precursors in almost all the vascularized tissues of the body (Bai et al., 2012, Blocki et al., 2013, Murphy et al., 2013). Human MSCs delivery into the injured heart has demonstrated stimulation of neovascularization and endogenous tissue regeneration, immunomodulation, and reduction of fibrosis (Butler et al., 2017, Hare et al., 2017, Hare et al., 2012). *Ge et al., 2018*, suggested that the presence of MSCs may enhance the *in vitro* endothelial differentiation of endothelial progenitor cells, through a paracrine mechanism by secretion of cytokines, including VEGF, instead of direct cell-cell contacts **(**Ge et al., 2018**)**.

3.1.6 Effect of GDM on the Fetal Cells

Wharton's Jelly Mesenchymal Stem Cells

One previous study showed that WJ-MSCs from GDM-complicated pregnancies have more adipogenic differentiation potential that may play a role in the development of metabolic dysfunction and its progression into an irreversible diabetic state. Increased adipogenesis may also be associated with neonatal adiposity and obesity (Tsai et al., 2013). Moreover, WJ-MSCs from GDM-complicated pregnancies were proved to have lower osteogenic and chondrogenic differentiation potentials which may explain the reduced bone strength and the frequency of craniofacial anomalies among infants of diabetic mothers (Kim et al., 2015).

Chorionic Mesenchymal Stem Cells

Chorionic mesenchymal stem cells (CMSCs) in the GDM group significantly displayed increased adipogenic ability than those in the Normal gestation group accompanied by increased transcriptional responsiveness of two adipogenic factors; PPARγ and ADIPOQ induction (Chen et al., 2019). Another study from the same research group revealed that CMSCs in the GDM group displayed upregulation of 162 genes that are associated with increased migration ability, epithelial development, and growth factor-associated signal transduction while downregulation of another 269 genes that are linked to angiogenesis and cellular metabolic processes (Chen et al., 2020).

Amniotic Mesenchymal stem Cells

Amniotic Mesenchymal stem cells in the GDM group displayed an impaired proliferation and osteogenic potential, overexpression of genes involved in the inflammatory response including; TNFα, MCP-1, CD40, and CTSS, and downregulation of the anti-inflammatory interleukin-33 compared to the Normal gestation group (Algaba-Chueca et al., 2019).

Human umbilical cord Perivascular stem cells

Perivascular stem cells isolated from umbilical cord blood vessels displayed no significant difference in phenotypic expression and adipogenic differentiation potential between Normal and GDM groups. However, stem cells from the GDM group displayed decreased initial rates of cell yield and proliferation early passage and a reduced ability to promote wound healing (An et al., 2017).

Fetoplacental Arterial and Venous Endothelial Cells

A transcriptome and methylation analysis study identified variation between Normal and GDM pregnancy in gene expression linked to DNA methylation. These differentially methylated genes were proved to be associated with cell morphology and cellular movement, and advanced functional analysis revealed that GDM-exposed cells had altered actin organisation and barrier function (Cvitic et al., 2018).

3.1.7 WJ-MSCs and HUVECS Cross-Talk

WJ-MSCs from normal pregnancies displayed trans-endothelial migration across HUVEC monolayers and tighten the endothelial barrier by 24h after reaching sub-endothelial niches associated with initial increase and followed by decrease in VEGF levels (Ebrahim and Leach, 2015). Moreover, the proximity between WJ-MSCs and HUVECs in situ and their developmental origins makes the use of umbilical vein endothelial cells appropriate for this study.

Therefore, this chapter aimed to test whether the WJ-MSCs from diabetic pregnancies express the same markers similarly as the ones from normal pregnancy and will be able to transmigrate across the endothelial barrier by disrupting the junctions and repairing it back and if they can do will it in the same time or to some extent slightly delayed.

3.2 Aim

The aim of this chapter is to compare the WJ-MSCs from Normal and diabetic pregnancies in the following functions:

- Migration and morphology.
- Mesenchymal stemness markers expression.
- Cell doubling time and viability.
- VEGF-A secretion.
- Transmigration through the HUVEC monolayer.

3.3 Materials and Methods

3.3.1 Materials

Table 3-1 List of Antibodies and Kits

Antibody	Company
FITC Mouse Anti-Human CD90	BD Biosciences, UK
PE Mouse Anti-Human CD44	BD Biosciences, UK
PerCP-Cy™5.5 Mouse Anti-Human CD105	BD Biosciences, UK
APC Mouse Anti-Human CD73	BD Biosciences, UK
PE Mouse Anti-Human CD34	BD Biosciences, UK
PE Mouse Anti-Human CD45	BD Biosciences, UK
PE Mouse Anti-Human CD19	BD Biosciences, UK
PE Mouse Anti-Human CD11b	BD Biosciences, UK
PE Mouse Anti-Human HLA-DR	BD Biosciences, UK
mIgG1, κ FITC	BD Biosciences, UK
mIgG1, κ PerCP-Cy5.5	BD Biosciences, UK
mIgG1, κ APC	BD Biosciences, UK
mIgG1, κ PE	BD Biosciences, UK
Mouse anti VE-cadherin (CD144)	BD Biosciences, UK
Human VEGF Quantikine ELISA Kit	R & D systems, USA
Mouse anti CD31 antibody	R & D systems, USA
Anti-goat IgG-FITC antibody	Sigma Aldrich, UK

Table 3-2 List of Reagents

Reagent	Company
Dulbecco's Phosphate Buffered Saline (DPBS); without calcium and magnesium	Sigma-Aldrich, UK
Dulbecco's Modified Eagle's Medium - low glucose (DMEM); with 1000 mg/L glucose, L-glutamine, and sodium bicarbonate	Sigma-Aldrich, UK
Trypsin-EDTA solution	Sigma-Aldrich, UK
Paraformaldehyde (PFA)	Sigma-Aldrich, UK

Table 3-3 List of Tissue Culture Plates and Devices

Product	Company
Cell culture flasks (25cm2 and 75 cm2)	Corning, USA
Petri dishes (100mm)	Corning, USA
Cell culture plates (6, 12 and 24 wells)	Corning, USA
Centrifuge tubes (15 mL and 50mL)	Corning, USA
Glass Coverslips (19mm)	Corning, USA
96-well plate black bottomed	Corning, USA
Emerald syringe (10mL)	Becton Dickinson, UK
Glass pipettes 5ML, 10ML, and 25ML	Greiner bio-one, Germany
Centrifuge tubes (15 mL and 50mL)	Greiner bio-one, Germany
Pipette tip 20, 200, 1000µL	Sarstedt, Germany
Syringe Filters Plus (2um)	Sarstedt, Germany
Micro tubes 0.5, and 1.5 µL	Sarstedt, Germany
FACS 5mL tubes	Sarstedt, Germany
Tc counting slides	Bio-Rad, UK

Device	Company
TC20 Automated Cell Counter	Bio-Rad, UK
BD FACS CANTO II Cytometer	BD-biosciences
The SpectraMax M2e Multimode Microplate Readers	Molecular Devices, UK

3.3.2 Study Design and Subjects

For phenotypic characterization with flow cytometry, cells were taken from normal pregnancies (n=9) and Gestational Diabetes GDM (n=17) (diet-controlled (n = 9), Metformin-treated (n = 8). The Clinical characteristics of the study population that had samples used for morphological and phenotypic characterization are shown in (Table 3-4). HUVECs were isolated from 6 normal pregnancies.

Table 3-4 Clinical characteristics of the study population used for morphological and phenotypic characterization.

Characteristic	Normal (n = 9)	d-GDM (n = 9)	m-GDM (n = 8)
Maternal age, years	33.5 ± 6.5	34.9 ± 7.6	34.6 ± 2.8
Maternal BMI, Kg/m²	23.4 ± 3	29.3± 6.6	34.7 ± 5.6
Gestational age at delivery, weeks	39.5± 0.6	38.9 ± 1.1	38.8 ± 0.7
Placental weight, g	572.7 ± 59.5	614.4 ± 93	689.9 ± 47
Baby weight, kg	3.7 ± 0.6	3.5 ± 0.6	3.9 ± 0.7
Individual birthweight centile [gender]	61.75th[F]	74.24th[M]	92.64th[F]
	46.68th[M]	63.47th[F]	97.15th[M]
	70.73rd[M]	89.23rd[M]	76.98th[M]
	96.49th[F]	95.15th[F]	64.85th[F]
	52.25th[F]	99.87th[M]	89.65th[F]
	93.55th[F]	86.68th[F]	96.31st[F]
	98.05th[M]	78.17th[M]	100.00th[M]
	76.75th[F]	98.52nd[F]	91.36th[F]
	76.44th[F]	87.41st[F]	

Data are presented as mean (SD, [F], neonatal sex female; [M], neonatal sex male.

3.3.3 Characterization of MSCs Using Flow Cytometry

In order to prepare the cell suspension for flow cytometry, WJ-MSCs from both groups (nWJ-MSCs and gWJ-MSCs) were grown in T-75 flask, detached when become 90% confluent using Trypsin/ EDTA solution for 5min. The cell suspension was centrifuged at 1000 rpm room temperature, washed with washing Solution (1 x PBS, 1% FBS, and 0.09% sodium azide) and re-suspended at a concentration of 5x10^6 cells/ml. Then 5µl of each of the following antibodies: FITC Mouse Anti-Human CD90, PE Mouse Anti-Human CD44**,** PerCP-Cy™5.5 Mouse Anti-Human CD105, APC Mouse Anti-Human CD73, PE Mouse Anti-Human CD34, PE Mouse Anti-Human CD45, PE Mouse Anti-Human CD11b, PE Mouse Anti-Human CD19, PE Mouse Anti-Human HLA-DR were added to a 100 µl cell suspension. For the isotope control (5µl) each of the following antibodies mIgG1, κ FITC, mIgG1, κ PerCP-Cy5.5, mIgG1, κ APC as isotope controls, and mIgG1, κ PE as negative isotope control was added to 100 µl cell suspension in a separate tube.

Cell suspension (100 µL) with no added antibodies was used as a negative control. The stained cells were incubated in the dark for 30 minutes at room temperature. Then cells were washed twice and re-suspended at 300 µl in the previous buffer according to the manufacturer's instructions. Cells were analysed for positivity and negativity on the flow cytometer BD FACS CANTO II. Results were analyzed using Kaluza software and presented as histograms (Figure 3-1).

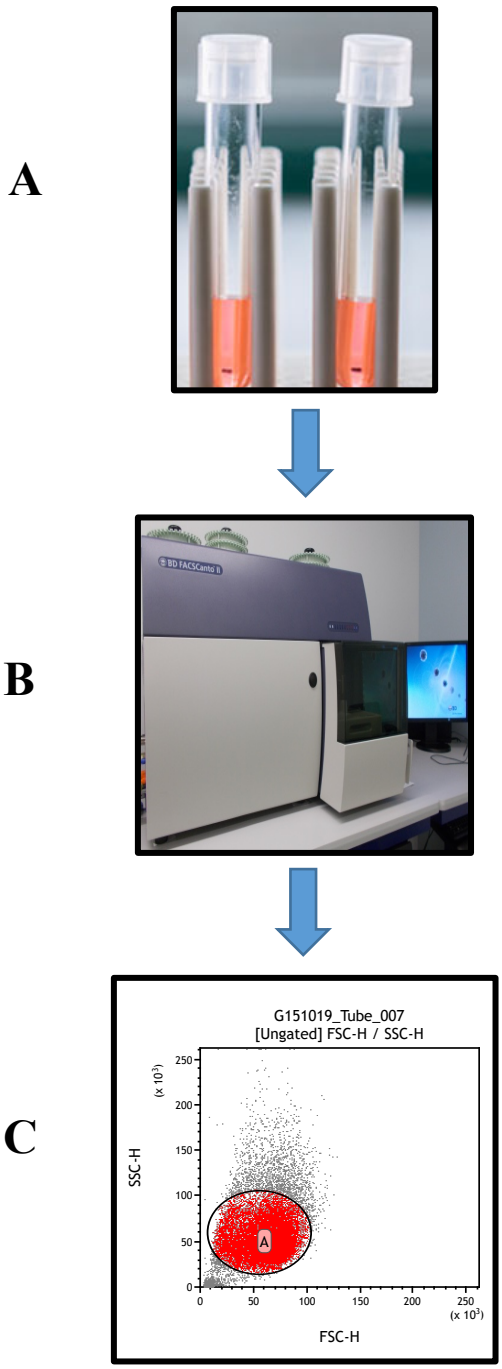


Figure 3-1 **Systematic diagram for WJ-MSCs phenotypic characterization using flow cytometry.** WJ-MSCs from both groups were split and stained with the conjugated antibodies, a final cell suspension (A) in FACS tubes were used to be processed by the suitable cytometer; BD FACS CANTO II cytometer (B), and the results were analysed by the Kaluza flow cytometry software (C).

3.3.4 Doubling Time Calculation

WJ-MSCs were harvested from one T-75 after 5min incubation with Trypsin. The cells were centrifuged at 1000 rpm and resuspended in 3 mL prewarmed growth media. 10 µL cell suspension was mixed with 10 µL trypan blue, and 10 µL of the mixture was loaded to one counting slide chamber, and the reading was recorded by TC20 Automated Cell Counter. Cell passaging was done twice per week. Doubling time was calculated using the following equation (Roth V., 2006);

$$\text{Doubling Time} = \frac{\textit{Duration} * \log(2)}{\log(\text{Final Concentration}) - \log(\text{Initial Concentration})}$$

3.3.5 VEGF-A Quantification in the Cell Culture Supernatant

The supernatant was collected from a confluent T-75 flask after 72 hours since the last time the media was changed. The cells were counted after splitting. The supernatant was centrifuged to remove any particles, aliquoted and kept at -20 till processed. ELISA assay was done as prescribed by the manufacturer's instructions. Fifty µL of Assay Diluent RD1W were added to each well and mixed with 200 µL of standard, control, or sample per well. Then an adhesive strip was used to cover the plate to be incubated for 2 hours at room temperature.

Three proper washes were done using 400 µL wash buffer per well. Afterwards, 200 µL of Human VEGF Conjugate was added to each well, covered with a new adhesive strip and the plate was incubated for 2 hours at room temperature. Three washes were done again, then 200 µL of Substrate Solution was added, and incubated for 20 minutes at room temperature. Finally, 50 µL of stop solution was added to each well. The optical density of each well was determined within 30 minutes, using a microplate reader set to 450 nm. The samples were run in duplicates and a standard curve was created by reducing the data using Prism software generating a four-parameter logistic

(4-PL) curve fit (Figure 3-2). The concentration read from the standard curve was multiplied by the dilution factor.

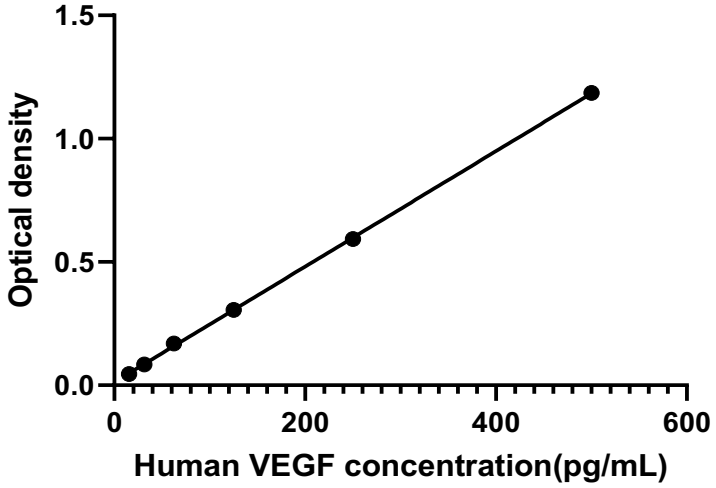


Figure 3-2 Graph displaying the VEGF ELISA cell culture supernatant standard curve.

3.3.6 Co- Cultures Studies, VE-Cadherin Immunocytochemistry

To obtain co-cultures of HUVEC 100,000 cells were seeded on 1% gelatin-coated coverslip (19mm diameter) and incubated in endothelial media till reached 70% confluence, the media was changed to mixed media (50% EGM and 50% stem cell media). When the cells reached full confluence (18-24h), 20,000 PKH-26 red dye labelled WJ-MSCs were seeded on top of the HUVEC monolayer (1:5) per coverslip in 1mL mixed media.

To localise VE-cadherin in HUVEC and monitor the effect of labelled WJ-MSC from Normal and GDM groups on VE-cadherin, co-culture slides of the (HUVEC and WJ-MSC) were fixed with 4% PFA in 1X PBS at different intervals (2 and 24 hours). Permeabilization was done using 0.15% triton X-100 in 0.1% BSA/PBS for 10min followed by blocking with 5% goat serum in PBS for 30min at room temperature, then overnight incubation at 4° C with mouse anti-human CD144 (VE-cadherin) 10µg/mL. Cells were washed with 0.1% PBS/BSA and incubated with FITC goat anti-mouse IgG (1:100) for two hours in the dark at room temperature.

The coverslips were washed three times for 5min then three times for 10min with 0.1% PBS/BSA, and a final wash with PBS for 10 min. The coverslips were mounted using Vectorsheild and analyzed by a Nikon fluorescence microscope with the appropriate filter to allow visualization of both PKH26 (The optimum excitation wavelength Ex is 551 nm, and the emission wavelength Em 567 nm) and FITC ((Ex max 494 nm/Em max 520 nm). The slides from the two groups; normal and gestational diabetic were labelled and blinded. Three co-culture coverslips per sample were immunostained and ten images per coverslip were taken by NIS systems software (duration of co-culture and the donor number were blinded), and the counting was done using Image J software.

HUVEC staining with PECAM

To confirm the absence of VE-cadherin from adherens junctions in the 2h co-culture coverslips, HUVECs were stained for PECAM (CD-31). The cells in the coverslips were permeabilized using 0.15% triton X-100 in 0.1% BSA/PBS for 10min, then blocked with 5% goat serum in PBS for 30min at room temperature. Incubation with mouse anti-human CD31 (PECAM) 5µg/mL was done overnight at 4° C. Cells were washed with 0.1% PBS/BSA and incubated with FITC goat anti-mouse IgG diluted (1:50) in 0.1% BSA/PBS for two hours in the dark at room temperature. The following steps were the same as VE-cadherin immunostaining.

3.3.7 Quantitative Analysis of Junctional VE-Cadherin Expression

Systematic random sampling was used to acquire 10 images per coverslip three repeats for each group. After blinding, stored images were used to count the % of paracellular junctions and were characterised according to VE-cadherin staining pattern: continuous or interrupted. A grid was used to ensure that all junctional regions had the same chance of being counted, and junctions were counted using the unbiased ‘forbidden line ’counting principle (junctions that cross the left or lower side of each square are excluded) to ensure that no junctions were counted twice and no more than 150 junctions per population to ensure the efficient random sampling method (Gundersen

and Jensen, 1987) used before by (Leach et al., 2004) and (Ebrahim and Leach, 2015) (Figure 3-3).

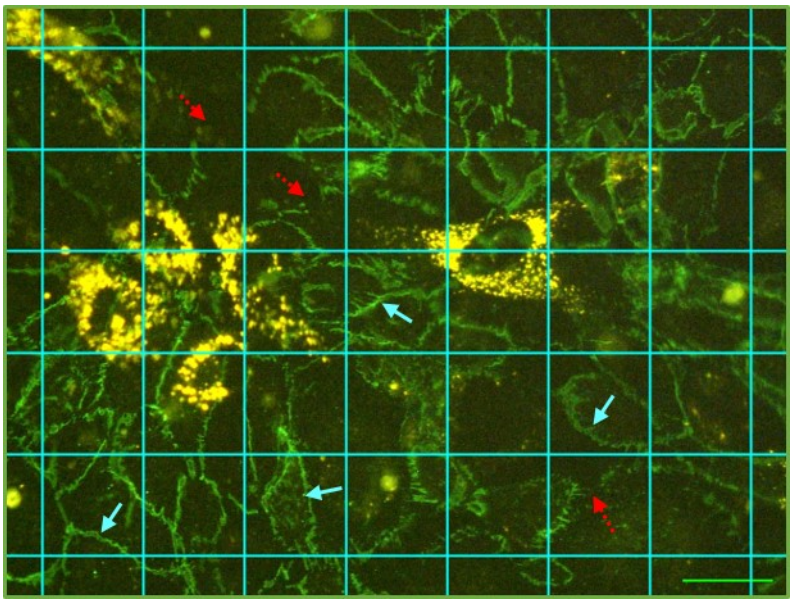


Figure 3-3 Representative micrograph displaying the continuous (blue arrows) and interrupted (red dashed arrows) junctions, and the junctional counting method using a grid placed on the centre of the image (Gundersen and Jensen, 1987), scale bar=40µm.

3.4 Results

3.4.1 Comparison of Maternal Characteristics

Maternal BMI in the study population showed a significant increase in d-GDM group (29.3 Kg/m^2± 6.6) (P-value < 0.005), and m-GDM group (34.9 Kg/m^2± 5.6) (P-value<0.0001) compared to BMI in the normal pregnancy group (23.4 Kg/m^2 ±3) (Figure 3-4). BMI of mothers in the study population regardless of the glycaemic state was positively correlated to the birth weight centile (Pearson r= 0.4) (P-value < 0.05). However, it was not correlated to the BW centile in both Normal (Pearson r=0.3) and m-GDM groups (Spearman r= -0.4) and displayed a positive correlation to birth weight centile in the d-GDM group (Pearson r= 0.6) (P-value < 0.05). Birth weight displayed no statistical difference between the groups, but birth weight centile corrected for the gestational age was higher in the GDM group (87.67± 11.5) compared to the

Normal pregnancy group (72.9± 16.3) (*P*-value < 0.05) (Figure 3-5). Placental weight was higher in the GDM group (642.7g± 85.9) compared to the Normal pregnancy group (572g± 59.5) (*P*-value < 0.05) (Figure 3-6) Placental to fetal weight ratio was higher in the gestational pregnancy group (181.3± 20) than the normal pregnancy group (169.8± 15) (*P*-value < 0.05) (Figure 3-7). Placental weight was positively correlated to the birth weight centile in both Normal pregnancy (Pearson r=0.8) (*P*-value< 0.001), and GDM group (P-value < 0.05) (Spearman r=0.6) (*P*-value<0.001) (Figure 3-8) and did not correlate with any of the maternal variables considered (maternal and gestational ages).

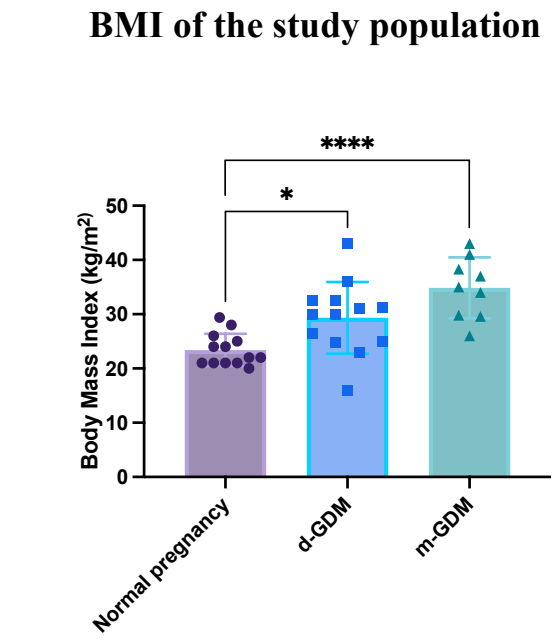


Figure 3-4 Graph displaying increased body mass index of mothers in the GDM groups ; m-GDM (n=9) and d-GDM (n=13) compared to Normal pregnancy (n=13) (One-Way ANOVA, *P*<0.0001).

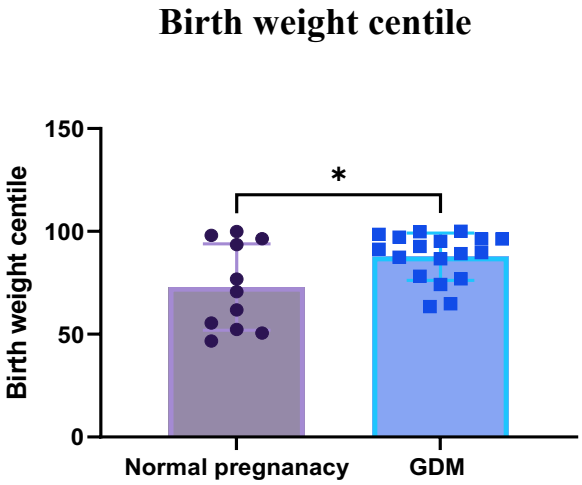


Figure 3-5 Graph displaying increased birth weight percentile in the GDM group (n=18) compared to the normal pregnancy group (n=11), (Unpaired *t*-test, *P*-value<0.05).

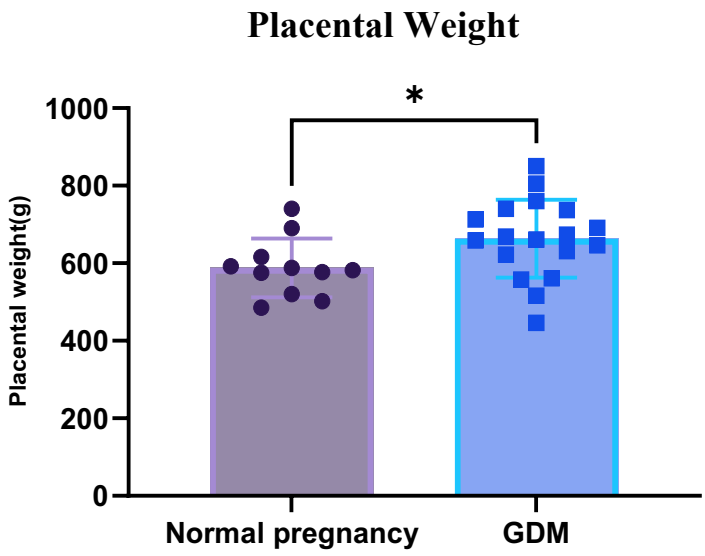


Figure 3-6 Graph displaying increased placental weight in the GDM group (n=18) compared to the normal pregnancy group (n=11) (Unpaired *t*-test *P*-value<0.05).

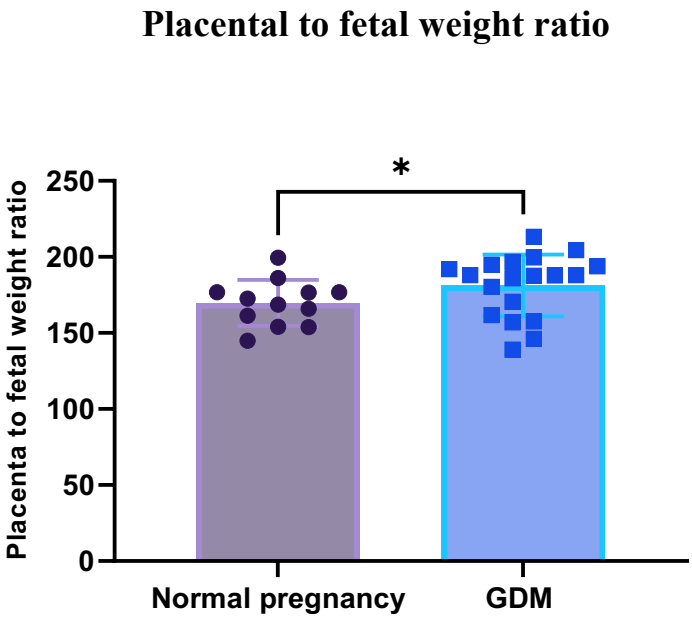
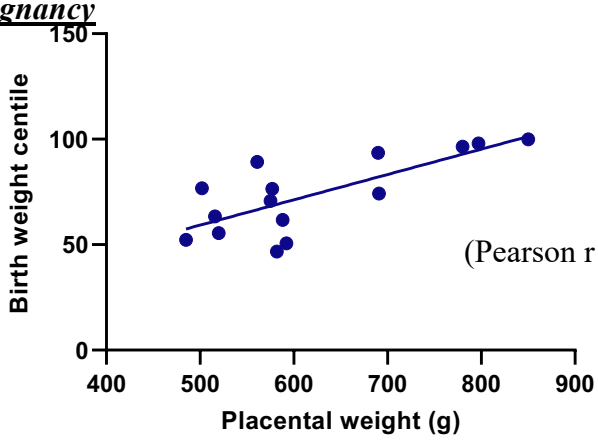


Figure 3-7 Graph displaying increased placental-to-fetal weight ratio in the GDM (n=19) compared to normal pregnancy group(n=12), (Unpaired *t*-test *P*-value<0.05).

Correlation of Placental weight to Birth weight centile in the study population

Normal pregnancy



GDM pregnancy group

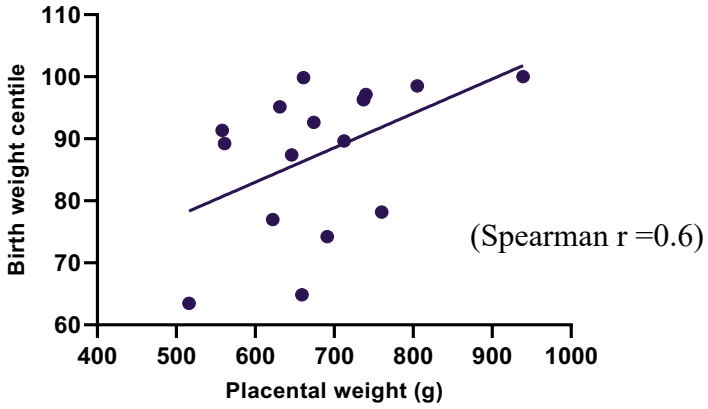
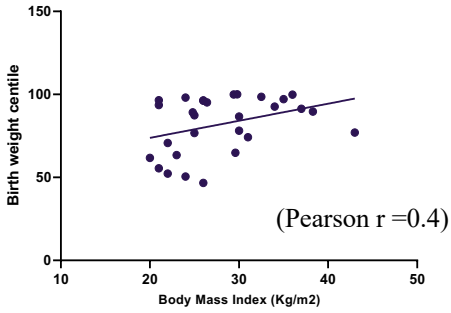
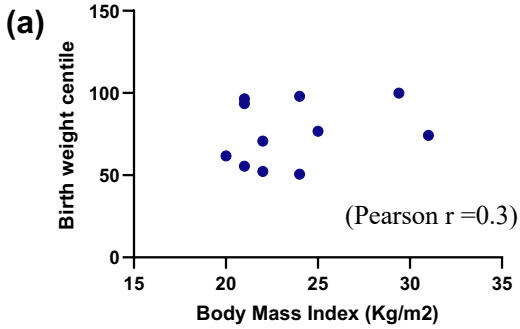


Figure 3-8 Graphs displaying the positive correlation of the placental weight to the birth weight centile in normal pregnancy (P-value < 0.001), and GDM group (P-value < 0.05).

Correlation between BMI of mothers to the birth weight centiles in the study population



Normal pregnancy



GDM pregnancy group

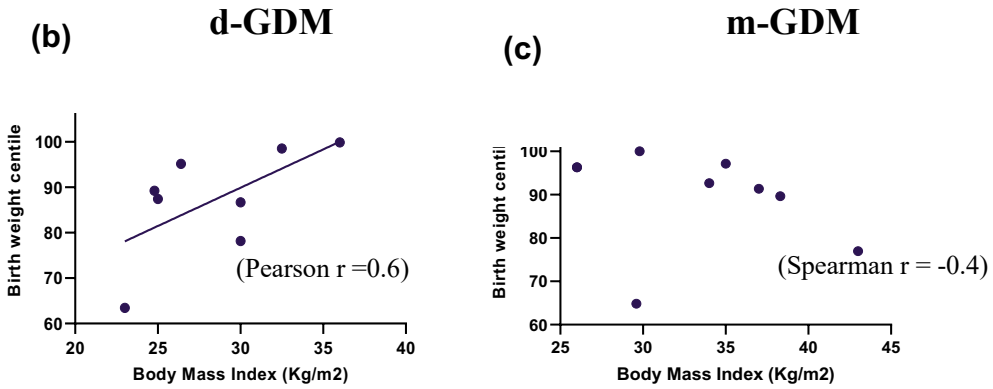


Figure 3-9 Graphs (**a** & **c**) displaying no correlation between the maternal body mass index and birth weight centile in Normal pregnancy (**a**) (Pearson r= 0.3) and m-GDM groups (Spearman r=-0.4). Graph (**b**) displaying positive correlation between in d-GDM group, (Pearson r=0.6) (*P*-value <0.05).

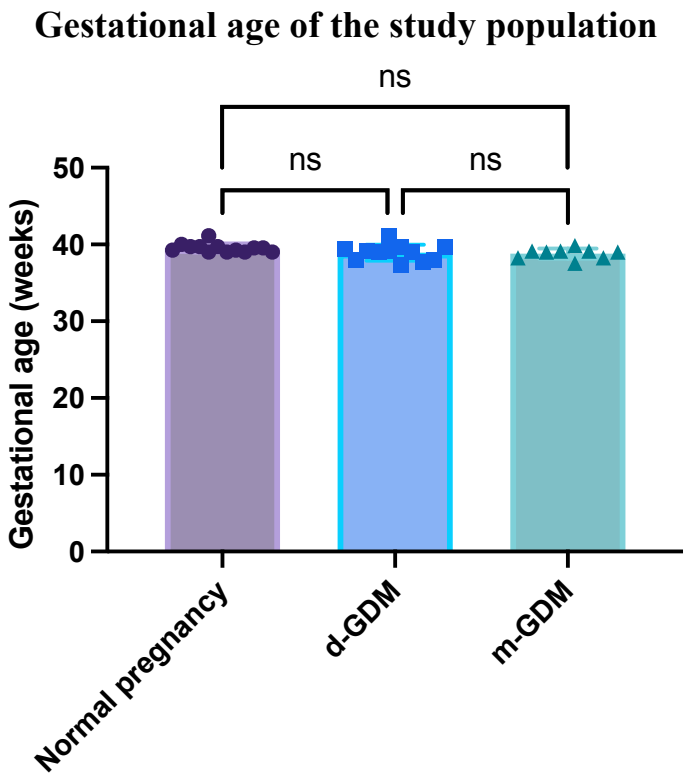


Figure 3-10 Graph displaying the gestational age of the study population in the normal (n=13), d-GDM (n=12), and m-GDM groups (n=9). *P*-value=0.09.

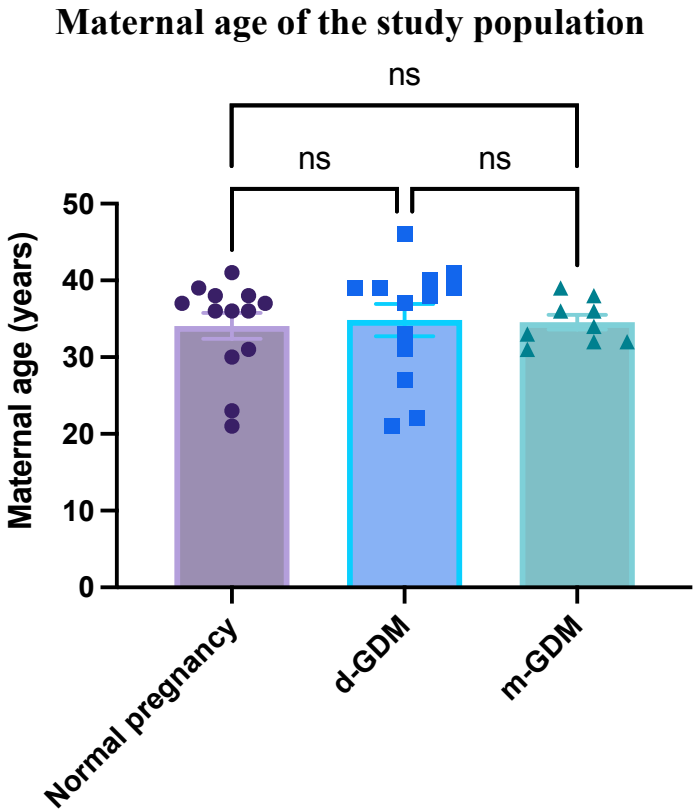


Figure 3-11 Graph displaying the maternal age of the study population in the normal (n=13), d-GDM (13), and m-GDM groups (n=9). *P*-value=0.9.

3.4.2 WJ-MSCs Retrieval and Migration

The migratory properties recorded at passage (0) by the number of MSCs migrated from each UC piece, showed the differences between nWJ-MSCs (282.2 ± 49.48) and gWJ-MSCs from d-GDM group (769.7 ±207) and m-GDM group (864.9 ±187.6). The diet-controlled GDM and metformin treated GDM were 2.5-fold and 4-fold higher compared to the control (normal pregnancy), however there is no significant statistical difference between the two treatment modes (*P*-value=0.1456) (Figure 3-13).

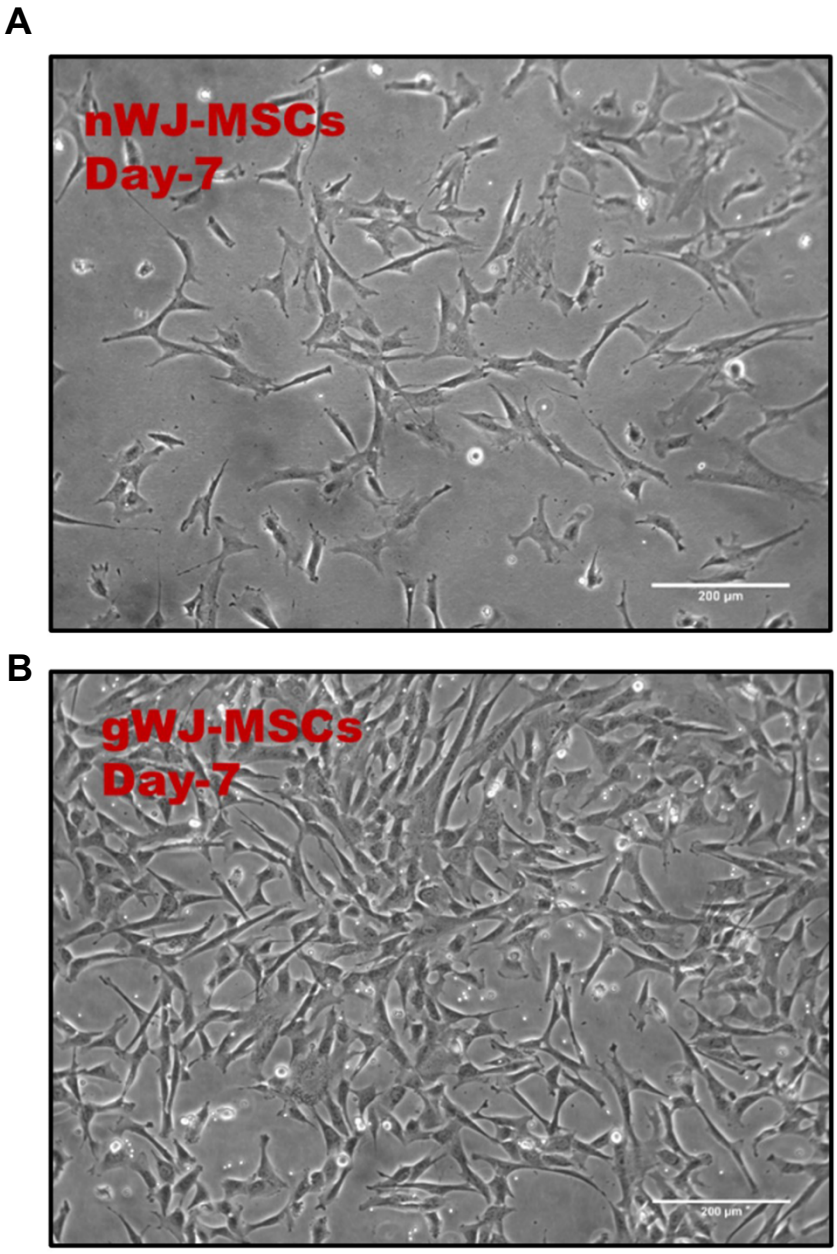


Figure 3-12 Representative phase contrast micrographs of primary cultures of nWJ-MSCs and gWJ-MSCs (passage 0) day 7 showing increased number of migrated WJ-MSCs from each UC piece. Image (**B**) primary cultures of gWJ-MSCs show more MSCs migrated from an UC piece in one of the GDM samples compared to the control normal pregnancy; image (**A**) scale bar 200µm.

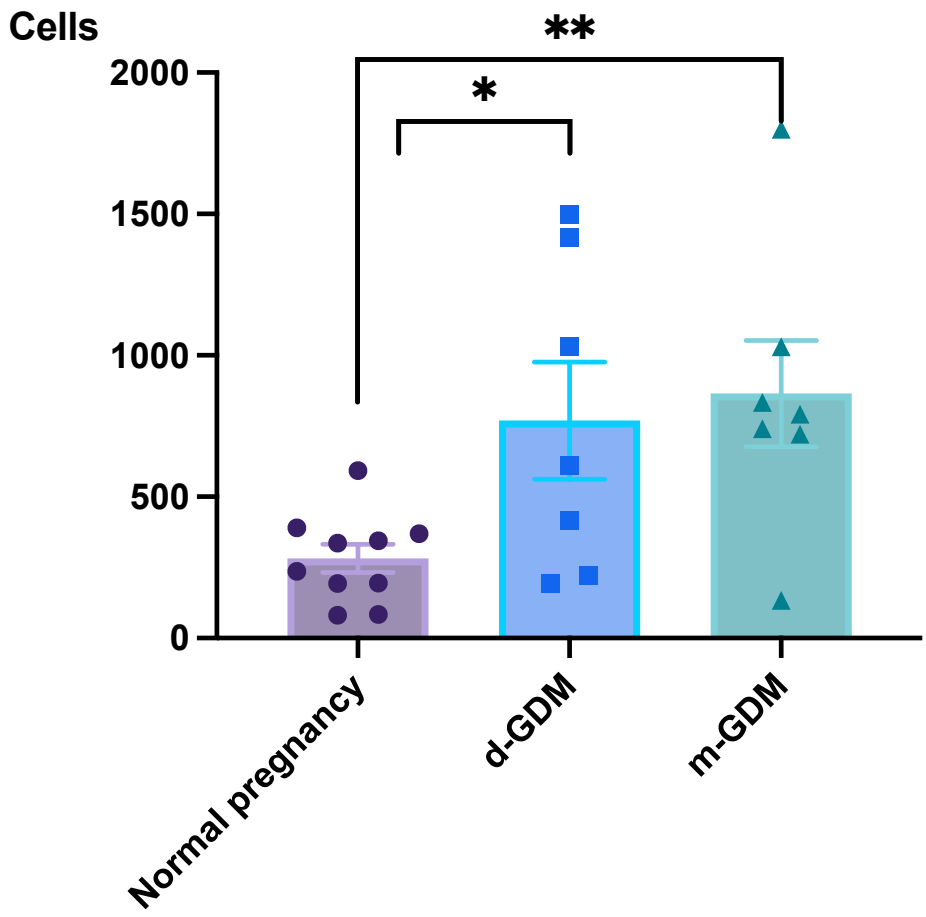


Figure 3-13 Graph displaying increased WJ-MSCs migration from UC samples from d-GDM group and m-GDM group compared to normal pregnancy (One-Way ANOVA, *P*-value < 0.05). Three different isolates were tested per sample (Normal pregnancy n=10, d-GDM n= 7, and m-GDM n=7).

3.4.3 Morphological Analysis

gWJ-MSCs exhibited similar elongated fibroblast, rounded and triangular morphologies (Figure 3-14). They form whirls when become confluent in culture (Figure 3-15), it took 22 days ± 4 in the normal pregnancy group, 20 days ± 4 in the d-GDM group, and 22days ± 3 in the m-GDM group. They maintained stable morphological features during subsequent culture.

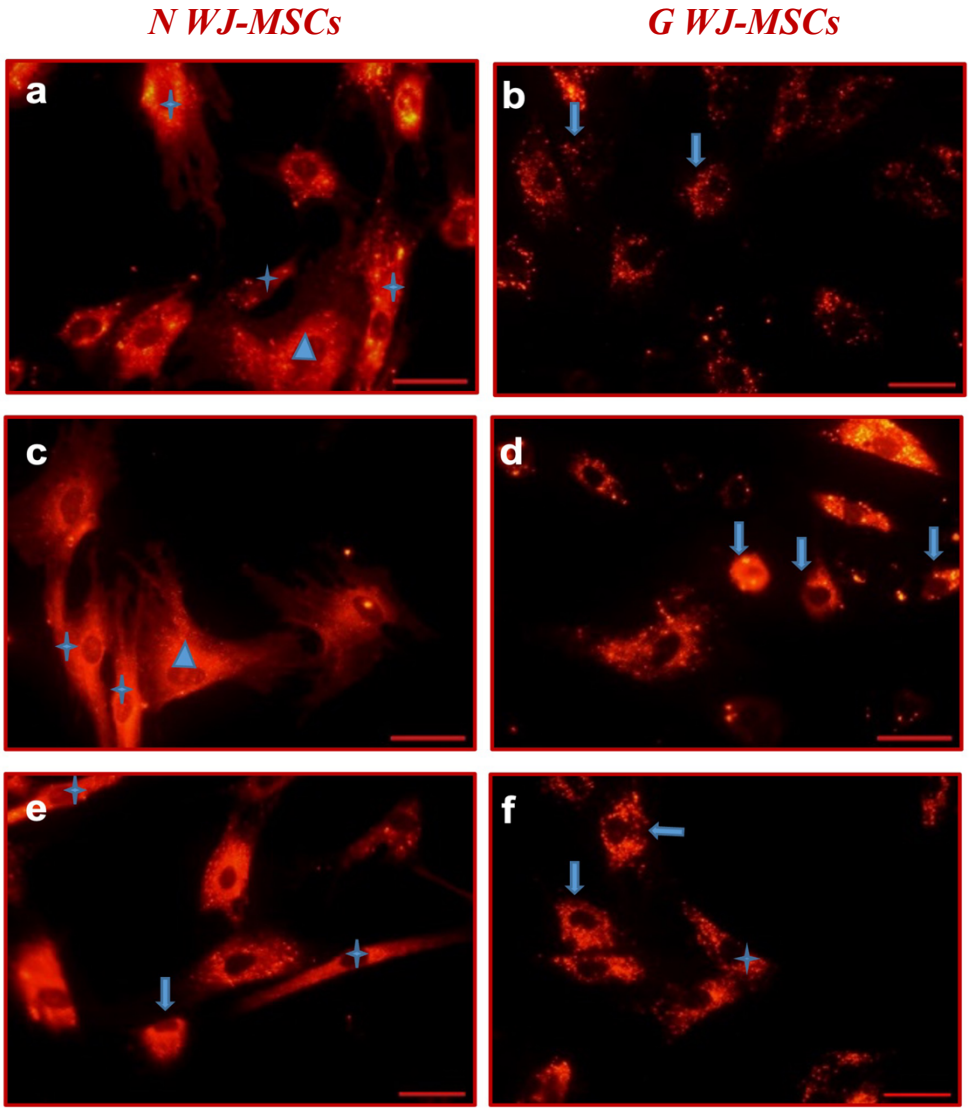


Figure 3-14 Representative micrographs displaying the mixed morphology of PKH-26 red labelled MSCs (passage 2) with their elongated (star), rounded (arrow), and triangular (triangle) morphology from Normal pregnancy group; images (**a**, **c** & **e**) and GDM group; images (**b**, **d** & **f**) Displayed images are from three different population in each group (scale bar=40µm).

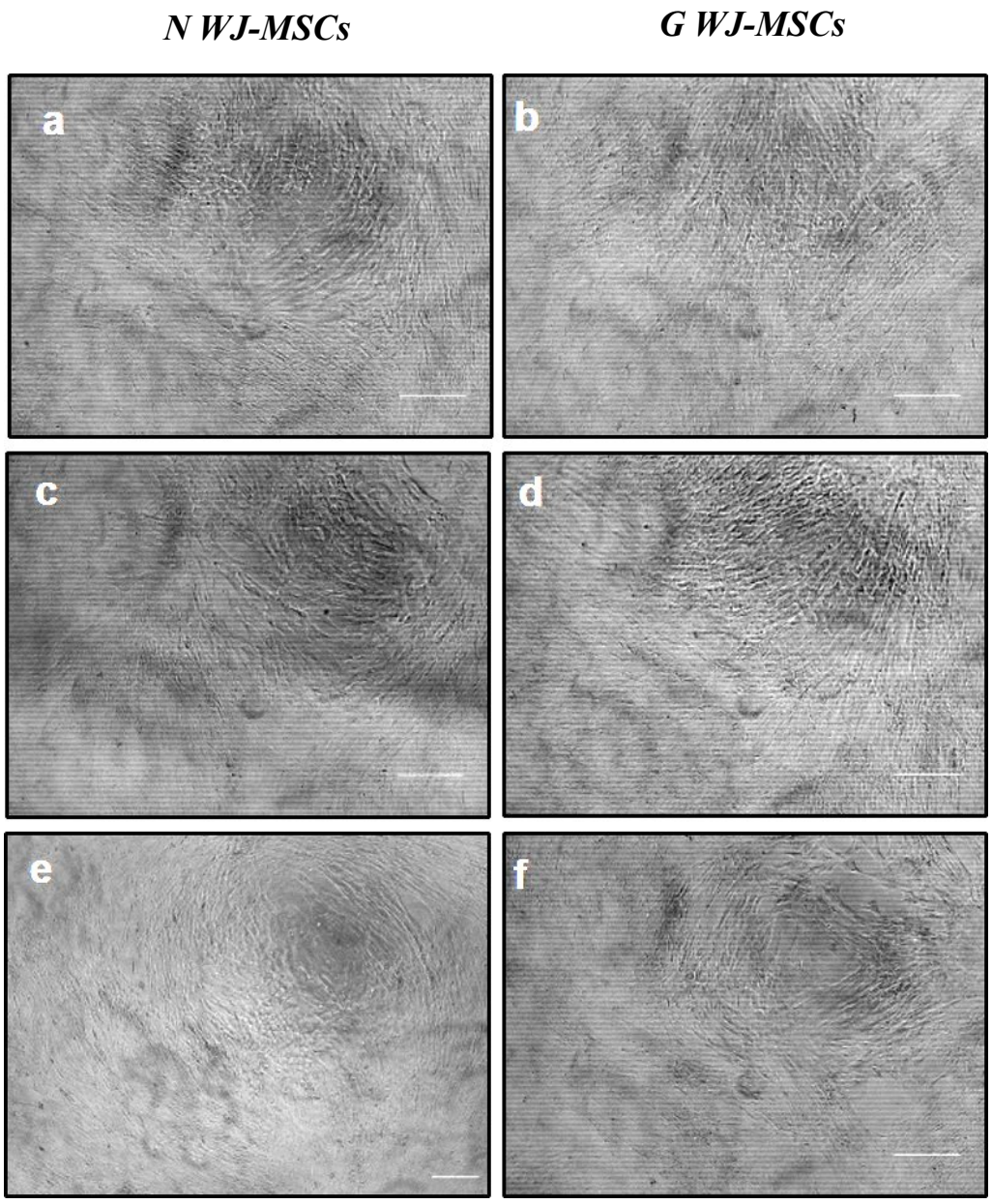


Figure 3-15 Representative phase contrast micrographs displaying the whirl appearance of the confluent WJ-MSCs at passage-0 from Normal pregnancy group; images (**a, c & e**) and GDM group; images (**b, d & f)**) similarly. Displayed images are from three different population in each group (scale bar=200µm).

Cell surface area measurements displayed no significant difference between nWJ-MSCs and gWJ-MSCs (P =0.4 (Figure 3-16). However, gWJ-MSCs showed a significantly lower percentage of elongated spindle-shaped cells, after 24h (43.8%) compared to nWJ-MSCs (64.1%) P<0.005) (n=5) (Figure 3-17).

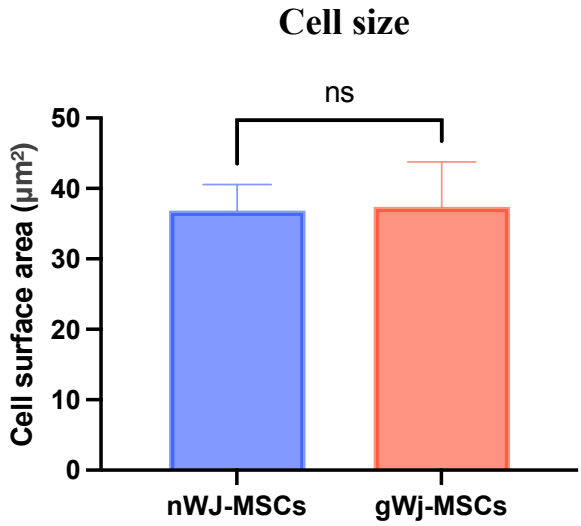


Figure 3-16 Graph showing no significant difference in cell surface area measurements between the GDM group (n=14) compared to the normal pregnancy group (n=10) (Unpaired *t*-test *P*=0.4).

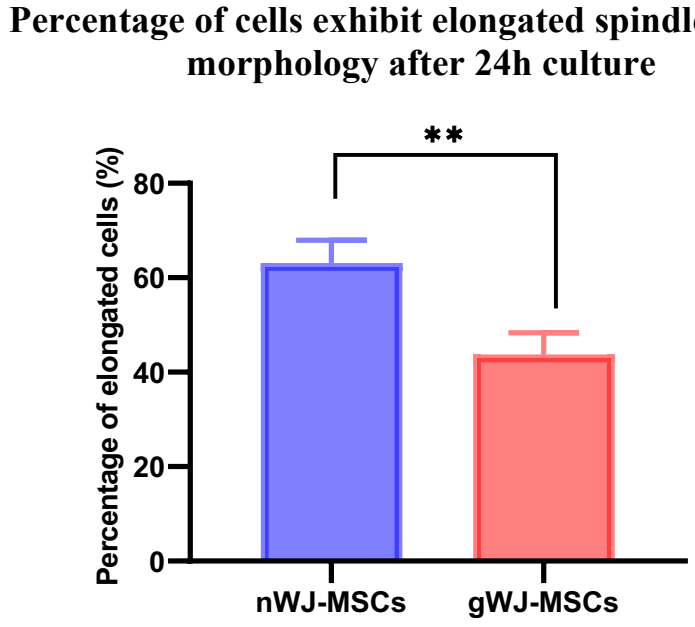


Figure 3-17 Graph showing decreased percentage of WJ-MSCs exhibiting the elongated spindle-shaped cells after 24h culture in the GDM group (n=14) compared to the normal pregnancy group (n=10) (Unpaired *t*-test *P*<0.005).

3.4.4 Doubling Time

gWJ-MSCs showed no significant difference in the doubling time (3.3 ± 0.4) compared to n WJ-MSCs (3.2 ± 0.4) (Figure 3-18).

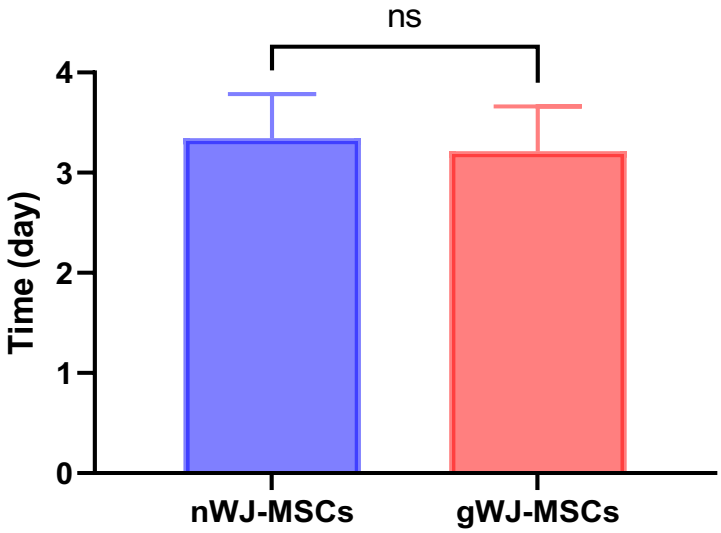


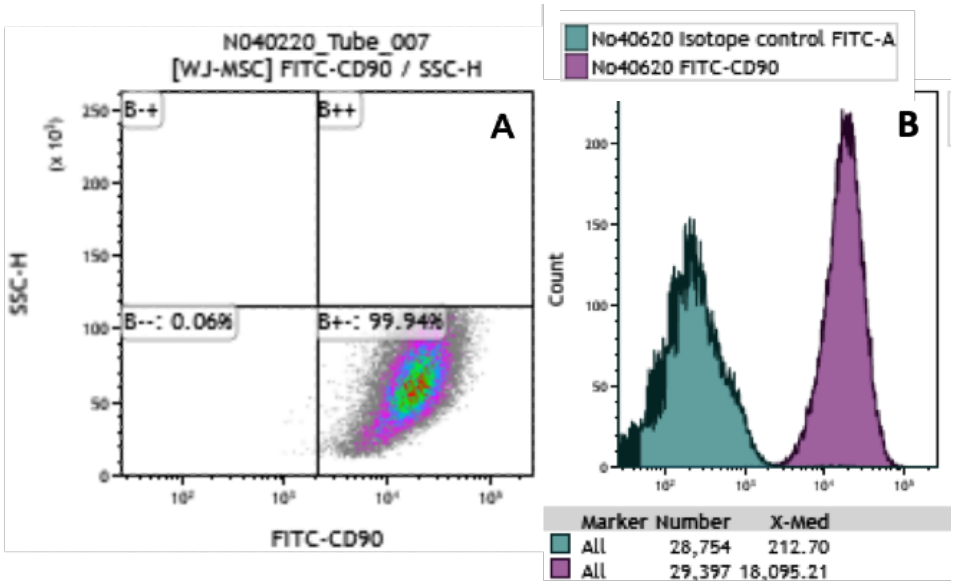
Figure 3-18 Graph displaying no significance difference between the nWJ-MSCs and gWJ-MSCs in doubling time calculation. The cells were stained with trypan blue dye for counting and the doubling time was calculated using the equation; Doubling Time = duration ∗ log (2) log/ (Final Concentration) – log (Initial Concentration). *P*-value= 0.4.

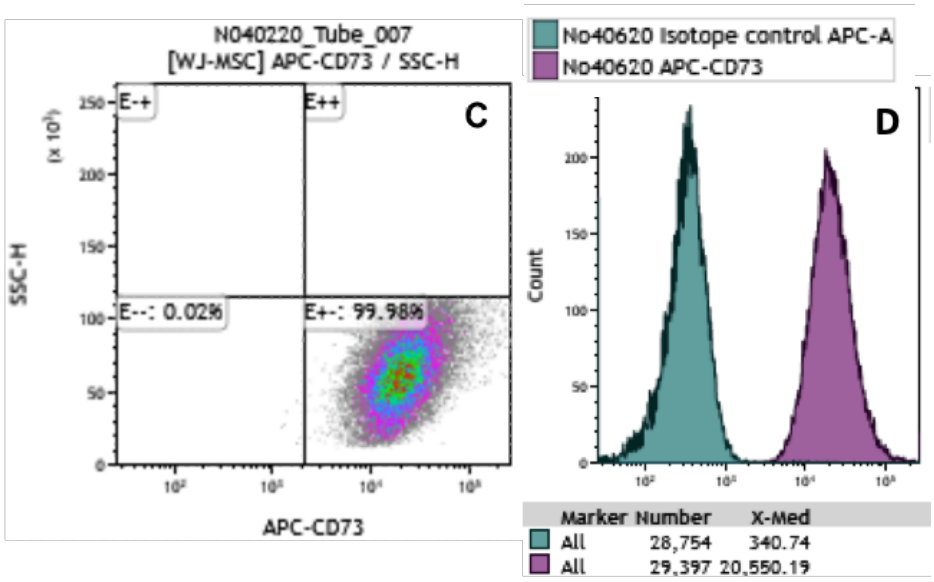
3.4.5 Characterization of MSCs Using Flow Cytometry

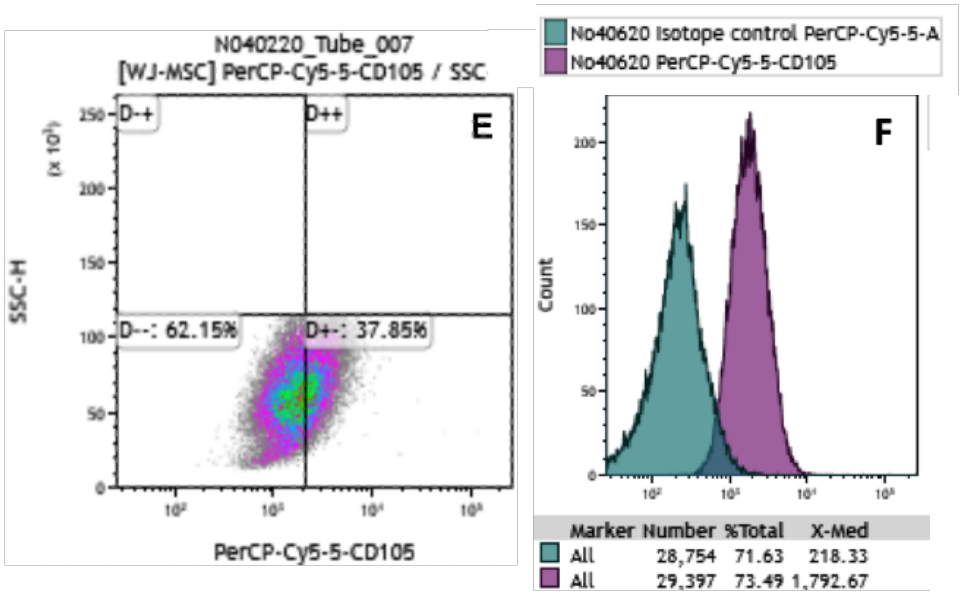
The immunophenotype of nWJ-MSCs and gWJ-MSCs were comparable and displayed high levels of expression of typical MSC markers; CD73, CD90, CD105, and low levels of hematopoietic markers; CD14, CD19, and HLA-DR. One representative experiment from each group (Normal pregnancy, d-GDM, and m-GDM) are shown in (Figures; 3-19 & 3-20 & 3-21) respectively. gWJ-MSCs expressed CD-90 (99.01%± 1.07) compared to controls (99.4%±0.11), CD73 (98.66%±1.73) compared to controls (99.71%± 0.27), and CD44 (98.44%±2.059) compared to controls (99.36%±0.4622) with no statistical difference between both groups and both passages (Figure 3-22). However, the expression of CD105 (Endoglin) was higher in P0 (99.08%±0.28) than P2 (96.08%±1.350) (*P*- value < 0.05). On the other hand, Endoglin expression was higher in gWJ-MSCs (74.12%±5.05) compared to nWJ-MSCs (56.56%±8.579) at P-2 (*P*- value < 0.05) (Figure 3-

23), with no significant difference between d-GDM and m-GDM groups (P-value =0.4449). Increased CD-105 was correlated to the increased placental weight in both groups (*P*- value < 0.05) (r= 0.4) (Figure 3-24).

Flow cytometry analysis of WJ-MSCs (P2) from Normal pregnancy group







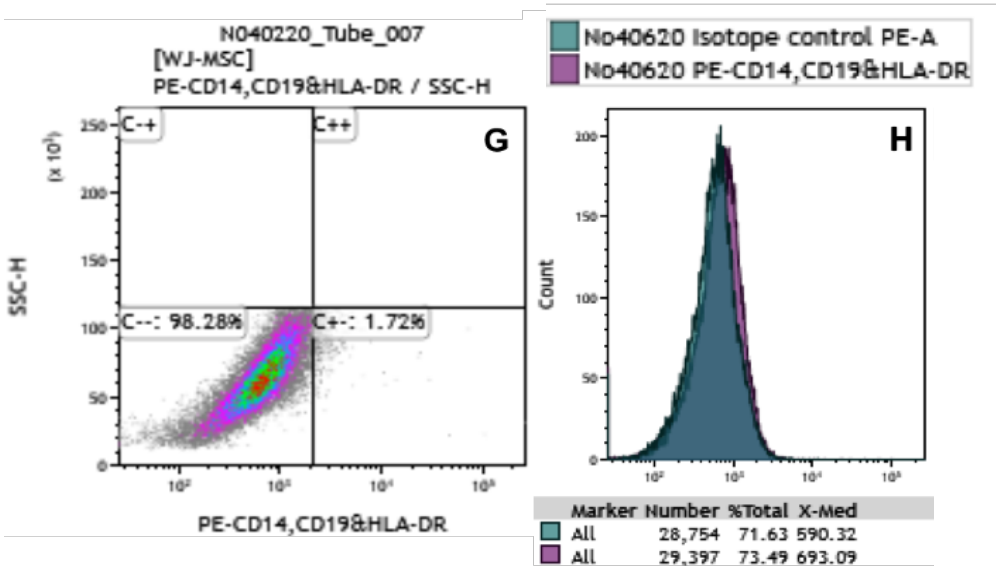
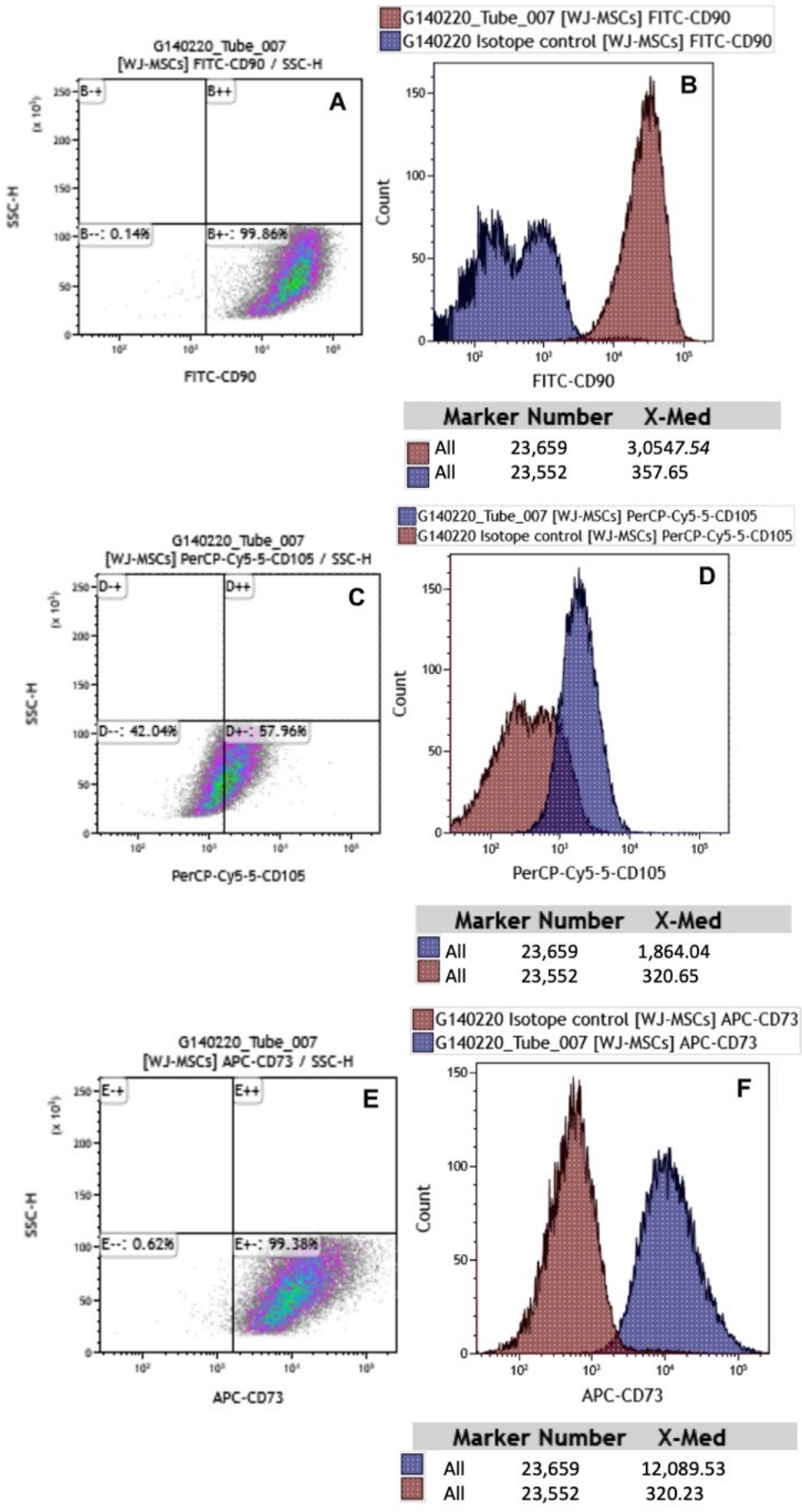


Figure 3-19 **Density diagrams displaying the mesenchymal markers expression in nWJ-MSCs** ; CD-90, CD-73 and CD-105 (**A**, **C** & **E**) and the haematopoietic markers (CD14, CD34, and HLA-DR) (**G**). Histograms displaying the number of nWJ-MSCs expressing the mesenchymal markers (**B**, **D** & **F**) and haematopoietic markers (**H**) (Data represented of one population analysis from the normal pregnancy group).

Flow cytometry analysis of WJ-MSCs (P2) from d-GDM group



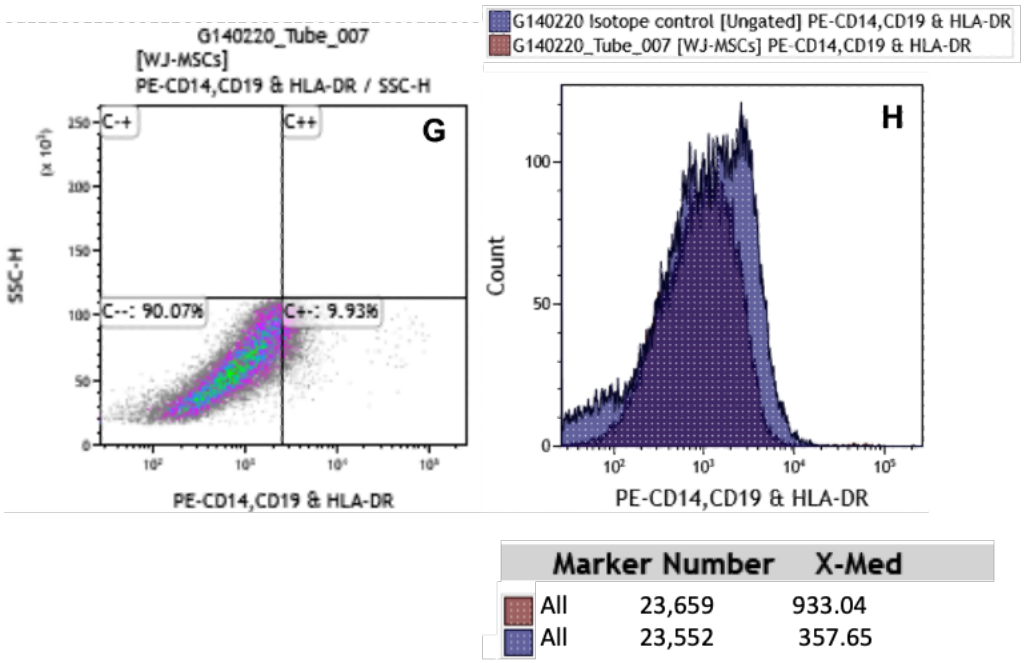
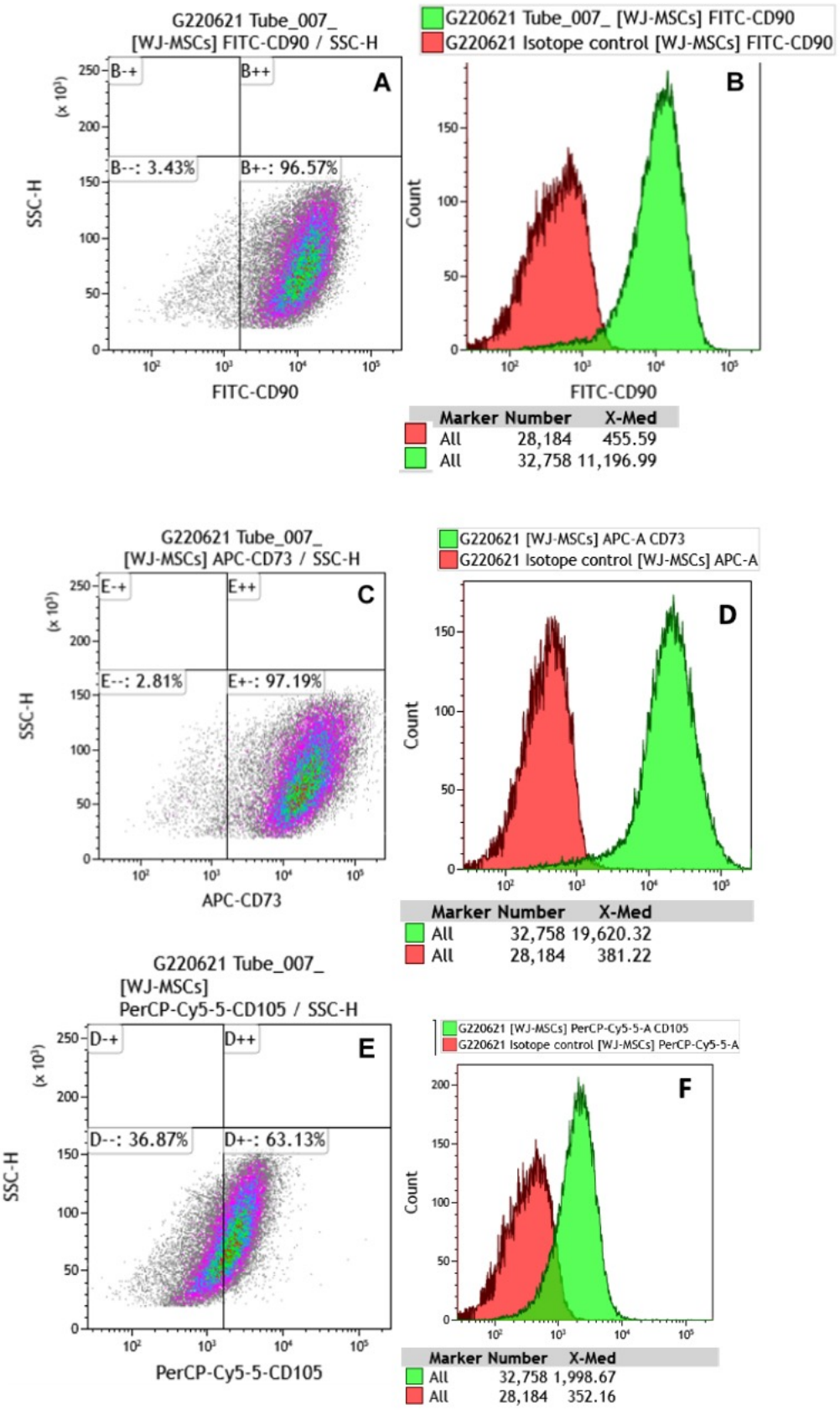


Figure 3-20 **Density diagrams displaying the mesenchymal markers expression in gWJ-MSCs** ; CD-90, CD-73 and CD-105 (A, C & E) and the haematopoietic markers (CD14, CD34, and HLA-DR) (G). Histograms displaying the number of gWJ-MSCs expressing the mesenchymal markers. (Data represented one population analysis from the diet-controlled group).

Flow cytometry analysis of WJ-MSCs (P2) from m-GDM group



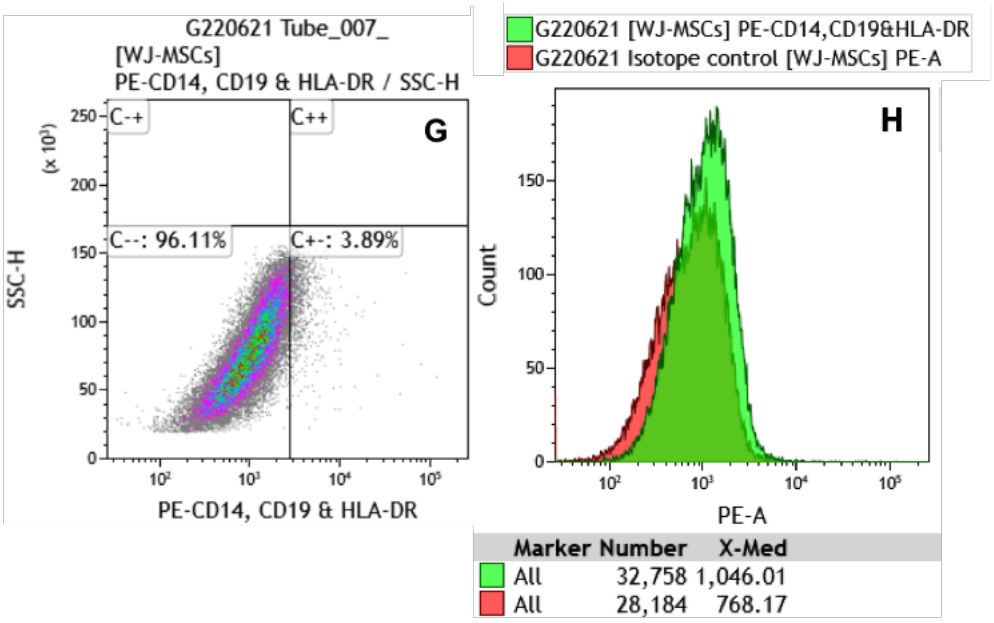


Figure 3-21 **Density diagrams displaying the mesenchymal markers expression in gWJ-MSCs** ; CD-90, CD-73 and CD-105 (A, C & E) and the haematopoietic markers (CD14, CD34, and HLA-DR) (G). Histograms displaying the number of gWJ-MSCs expressing the mesenchymal markers. (Data represented one population analysis from the metformin-treated group).

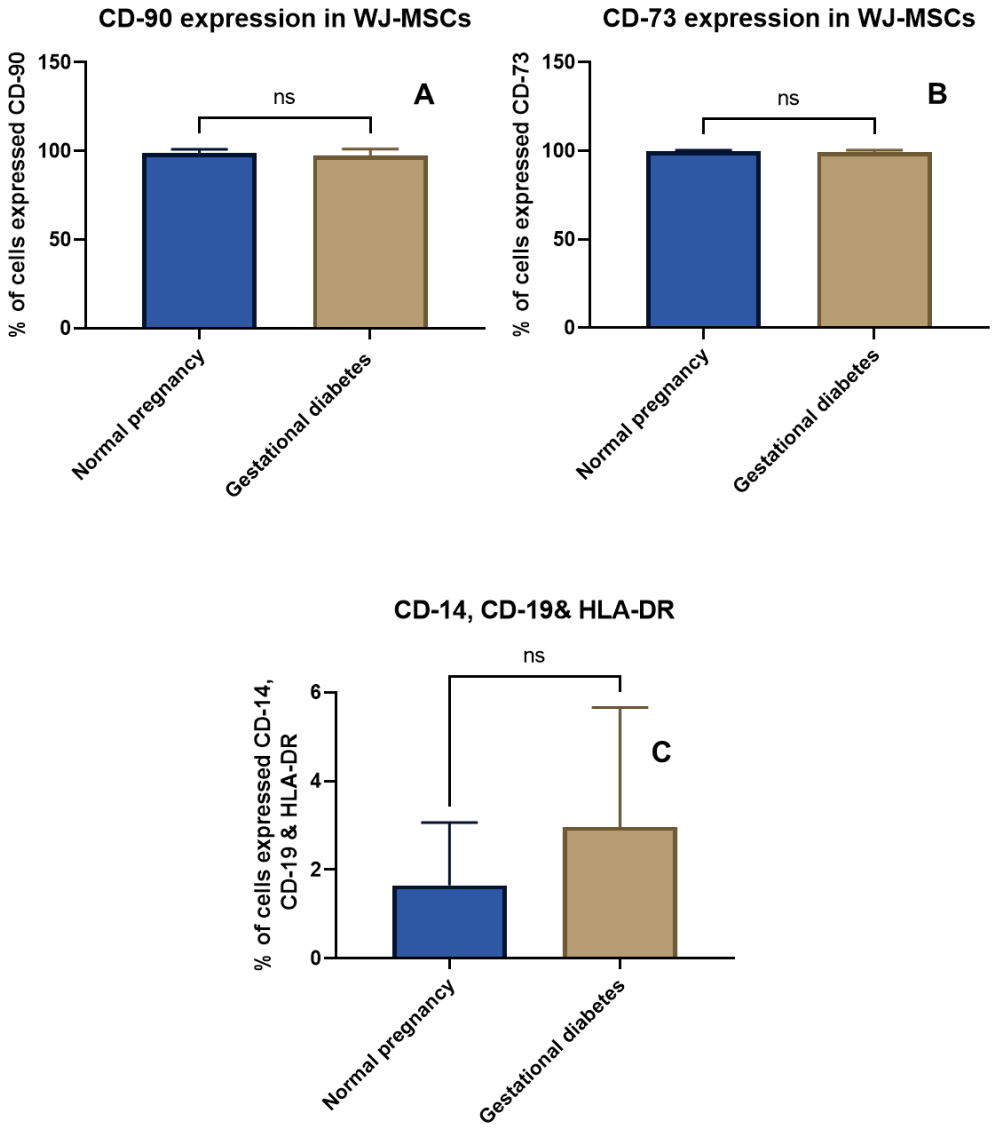


Figure 3-22 Graphs displaying no significant difference between Normal and GDM groups in CD90 (A), CD73 (B), CD14, CD19, and HLA-DR (C) expression (passage-2).

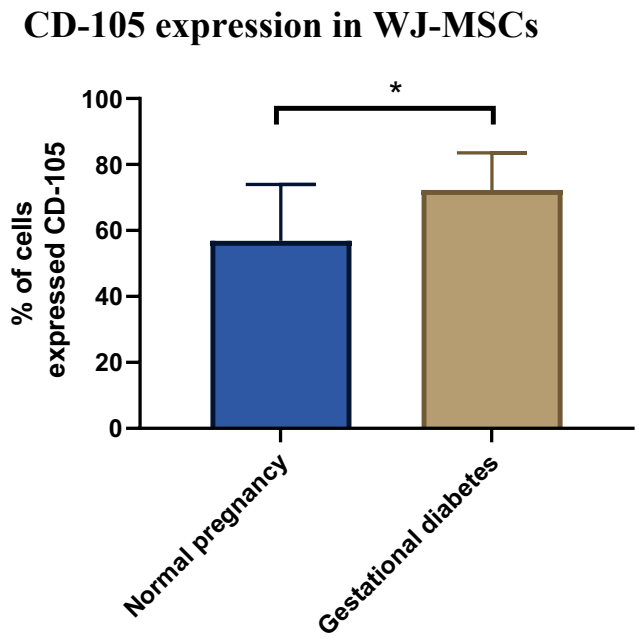


Figure 3-23 Graph displaying increased percentage of Endoglin expression in gWJ-MSCs compared to nWJ-MSCs, (passage-2) (*P*- value < 0.05).

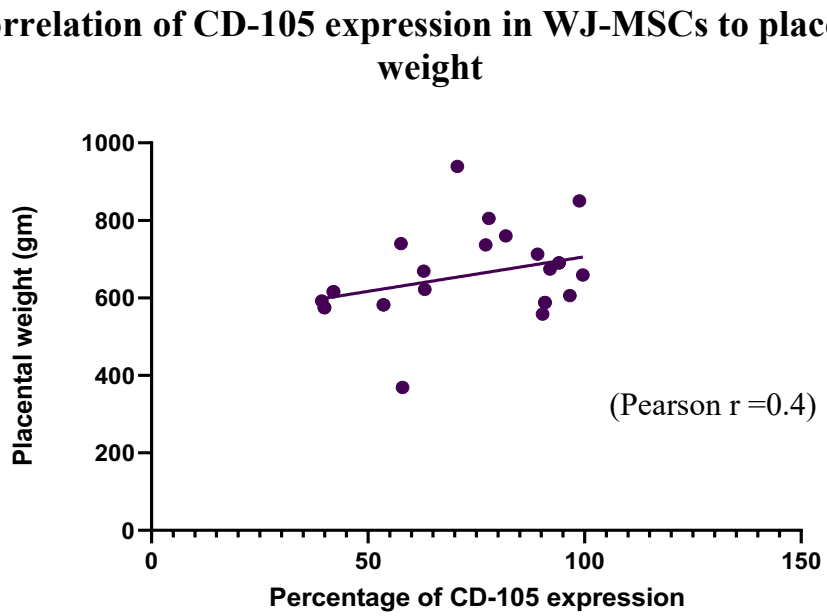


Figure 3-24 Graph displaying the correlation between increased placental weight and increased Endoglin expression (P- value < 0.05).

3.4.6 VEGF-A Secreted from WJ-MSCs in Culture

VEGF-A secretion in culture was altered in gWJ-MSCs samples as VEGF-A concentration was 3.8-fold higher in supernatant from gWJ-MSCs than in supernatant samples from n-WJ-MSCs ($P \leq 0.0001$) (Figure 3-25).

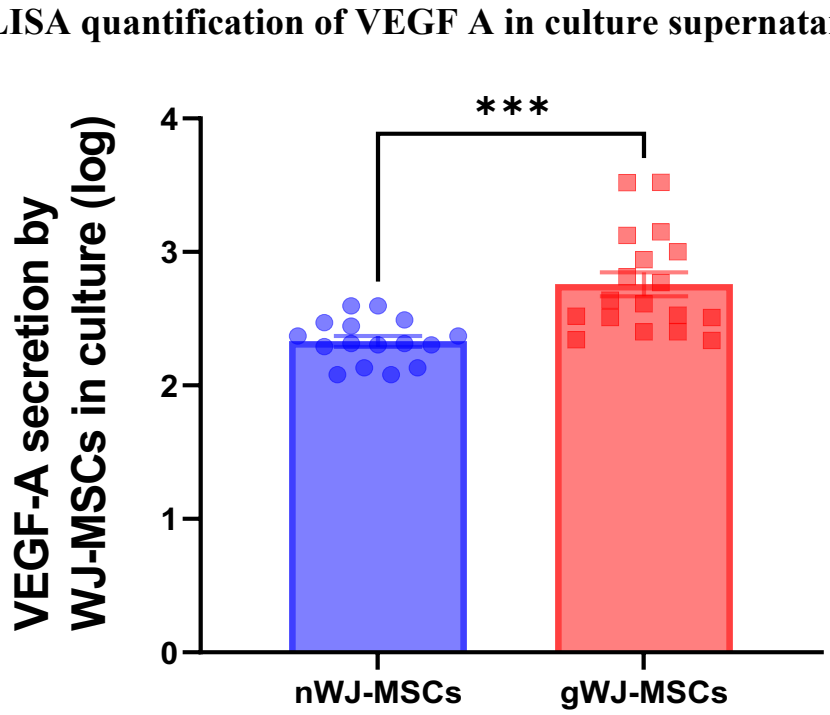


Figure 3-25 Graph showing increased VEGF-A concentration in the supernatant per 1 x 10^6 gWJ-MSCs compared to nWJ-MSCs. Three different isolates were tested per sample (Normal pregnancy group n=16 and GDM group n= 18) (Unpaired *t*-test, $P \leq 0.001$).

Increased VEGF-A secreted in culture supernatant collected from d-GDM group (1042 pg/ml ±353.1) compared to normal pregnancy group (248.0 pg/ml ± 248.0) *P*-value=0.01. There is no SD between m-GDM (1659 pg/ml ± 1148) and d-GDM and normal pregnancy (P-value = 0.365) (Figure 3.26).

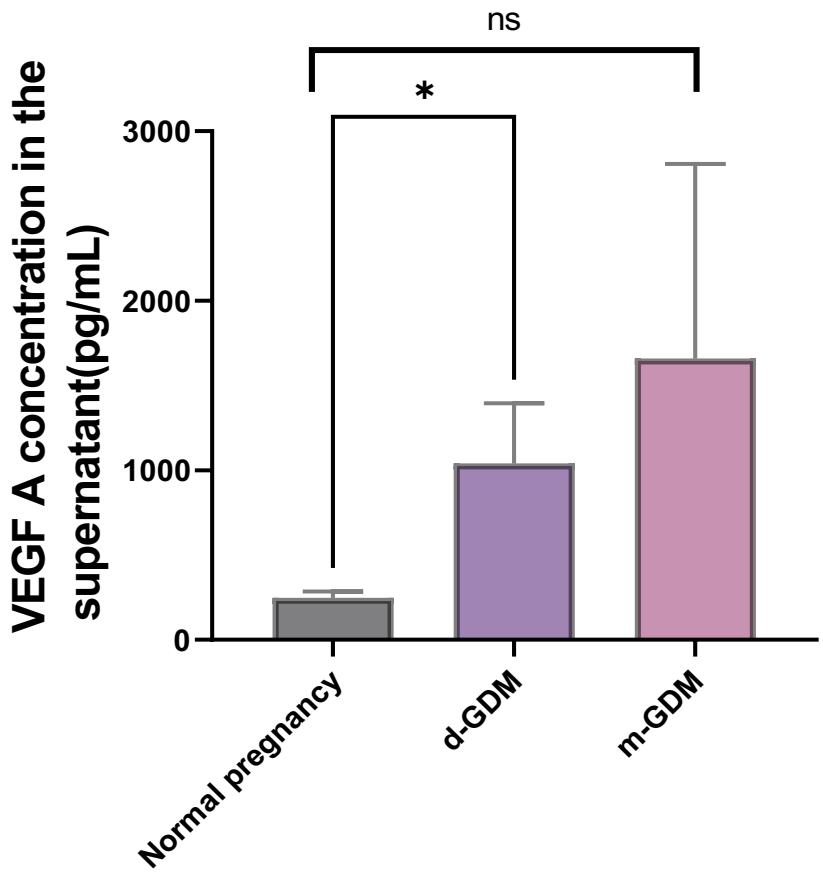


Figure 3-26 Graph showing increased VEGF-A concentration in the supernatant of d-GDM group compared to m-GDM and normal pregnancy (*P*-value<0.05).

3.4.7 Co-Culture Studies of WJ-MSCs with HUVECs

HUVECs usually take 24 h to be confluent and give the characteristic cobblestone appearance (Figure 3-27) when the seeding density was beyond 1x 10^5 per well (12 well-plate templates).

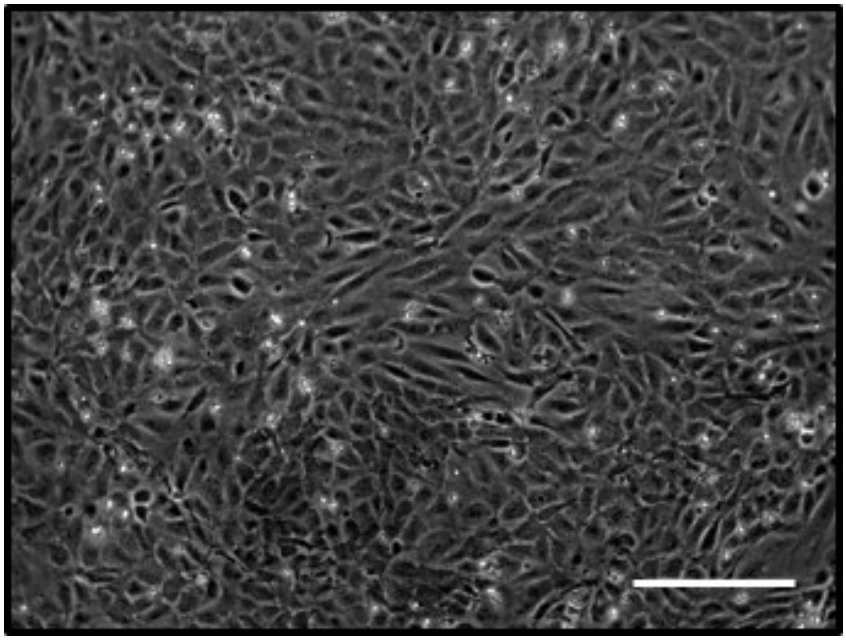


Figure 3-27 Phase contrast microscopic image showing the confluent HUVEC monolayer control and its characteristic cobblestone, scale bar=200 μm.

Behaviour of cells at 2h. Co-culture

GWJ-MSCs attached to the HUVEC monolayer and began to transform from the rounded to the spindle shape similarly as nWJ-MSCs observed at 2 hours co-culture time (Figures 3-28 & 3-29).

Stem cells shape changing 2h after co-culture with HUVECs

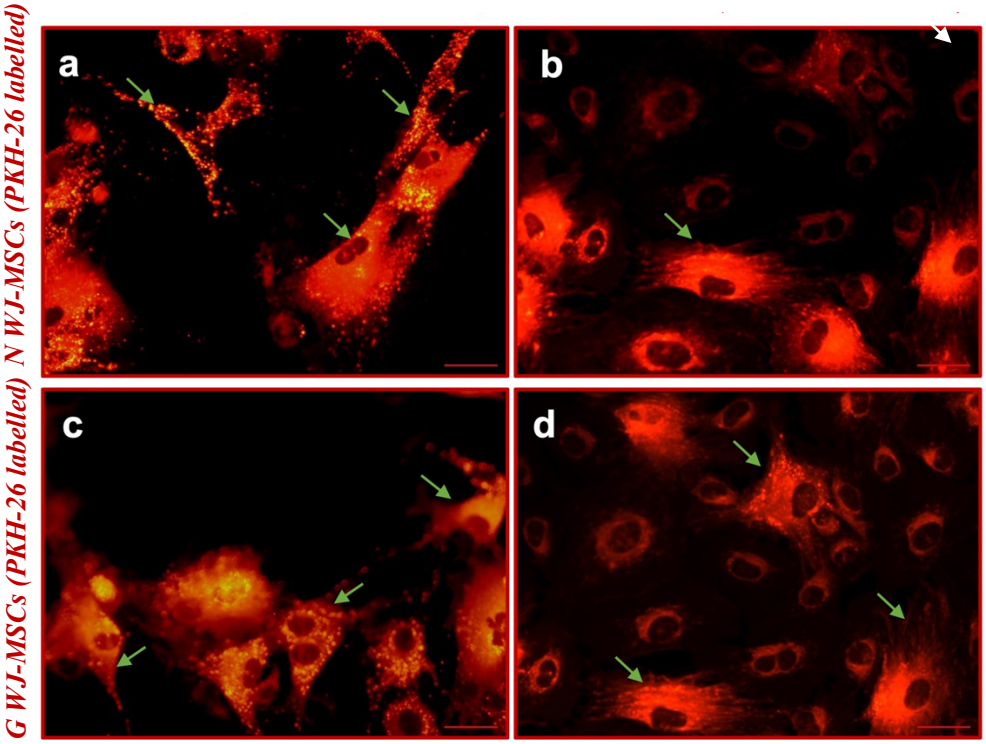


Figure 3-28 Representative micrographs showing cell shape changes in WJ-MSCs after 2h co-culture with HUVEC. PKH-26 labelled WJ-MSCs from Normal (images a & b) and GDM (images c & d) groups began to transform into elongated shape (arrows) after 2h seeding on top of the HUVEC monolayer, scale bar= 40 µm.

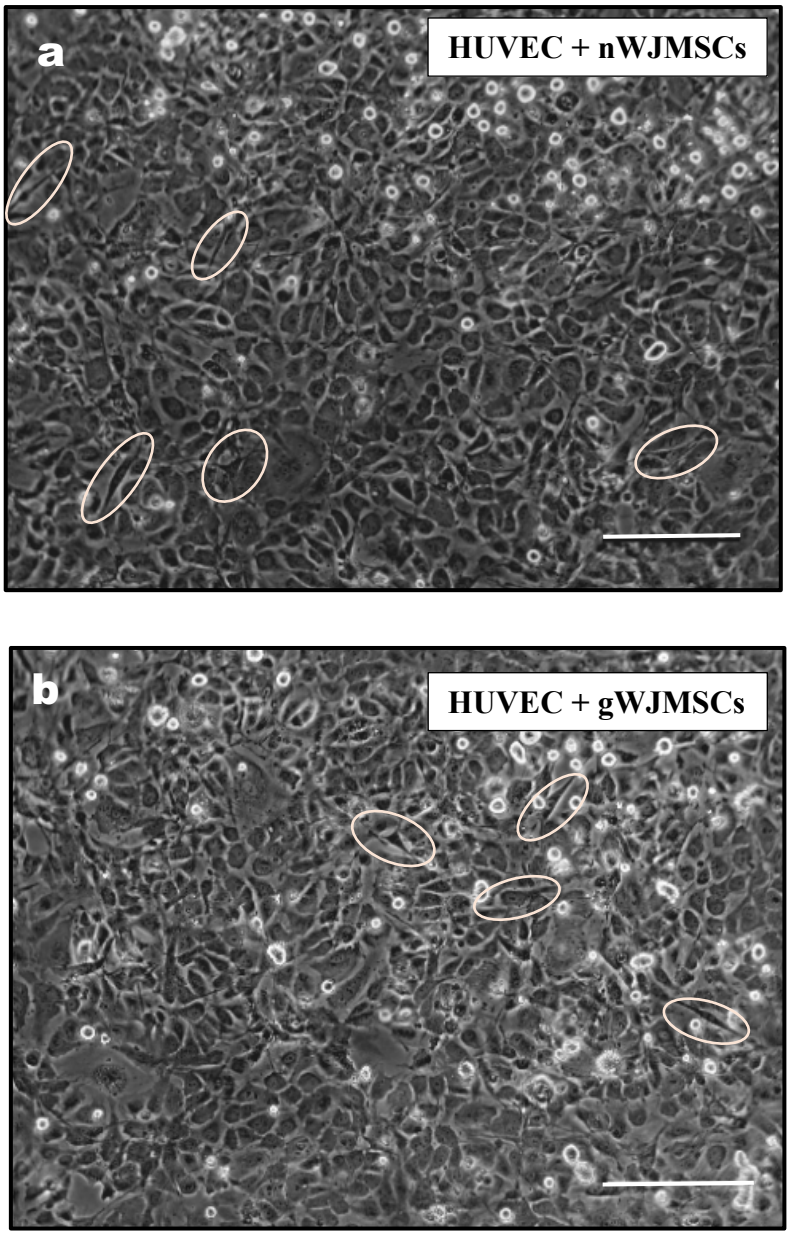


Figure 3-29 Phase contrast representative microscopic images of HUVEC+ WJ-MSCs co-cultures on coverslips. Images (a & b) are showing the spindle shaped nWJ-MSCs (a) and gWJ-MSCs (b) (white circles) attached to the HUVEC monolayer after 2h co-culture time, scale bar=200 µm.

VE-cadherin junctional localization in the co-culture images HUVEC+ gWJ-MSCs showed significant reduction in its junctional counts at 2h (Figure 3-30), and almost lost junctional expression at the sites of cell contact with the stem cells clarifying that gWJ-MSCs used the para cellular pathway to migrate via the endothelial monolayer.

Reduced VE-cadherin junctional expression after 2h co-culture with PK-H2 labelled WJ-MSCs

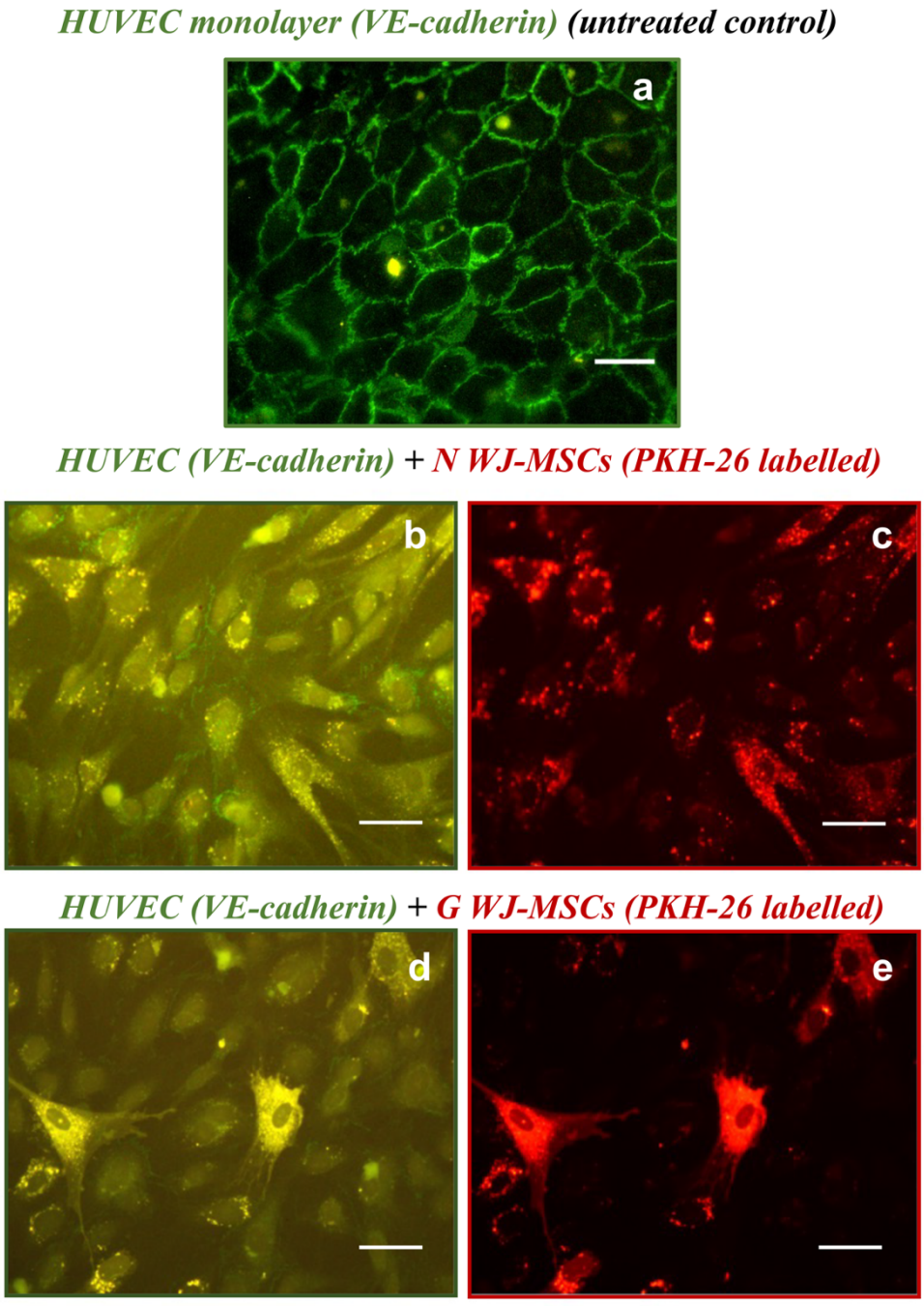


Figure 3-30 Representative micrographs displaying reduced junctional VE-cadherin expression after 2h in the co-cultures from HUVEC+ n WJ-MSCs (images b & c), and HUVEC + gWJ-MSCs (images d & d), compared to the untreated HUVEC monolayer control (image a) displaying junctional VE-cadherin expression, scale bar = 40µm.

To confirm the absence of the junctional VE-cadherin in the co-culture coverslips, HUVECs were stained for PECAM, and the co-culture images confirmed the opened junctions at 2h co-cultures, as PECAM was lost at the intercellular junctions that are in direct contact with stem cells compared to the HUVEC monolayer (Figure-3-31). The counts of continuous junctional counts were significantly reduced in the co-culture compared to the endothelial monolayer ($P < 0.05$) (Figure 3-32).

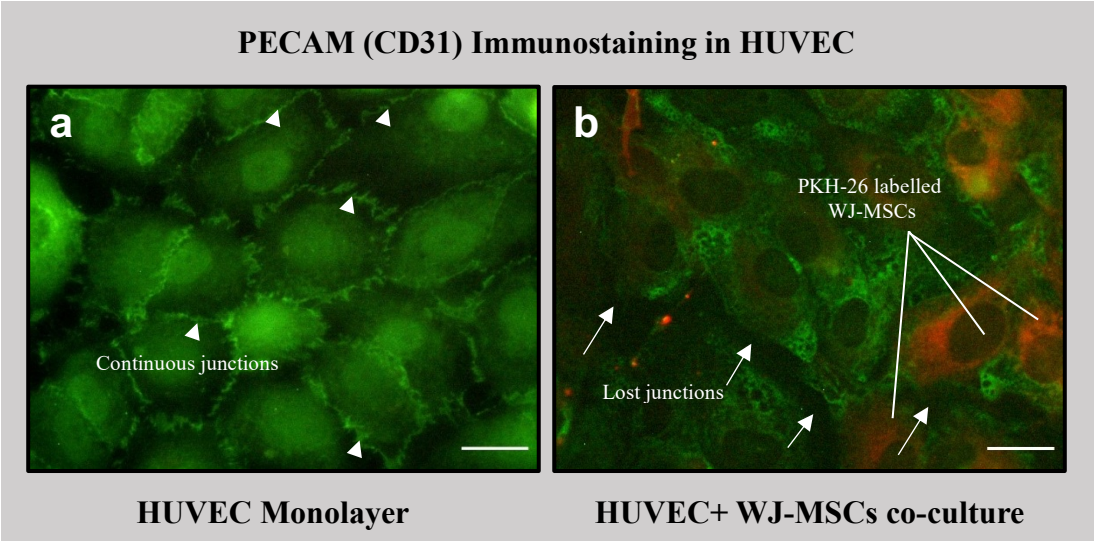


Figure 3-31 Micrographs of PECAM localization in HUVEC with and without WJ-MSCs, showing junctional and intracellular expression of PECAM in the HUVEC monolayer (**a**) (FITC) , and lost junctional expression but persistent intracellular expression in the co-culture HUVEC (green)+WJ-MSCs (red) (**b**) (mixed TRITC & FITC), scale bar = 20µm.

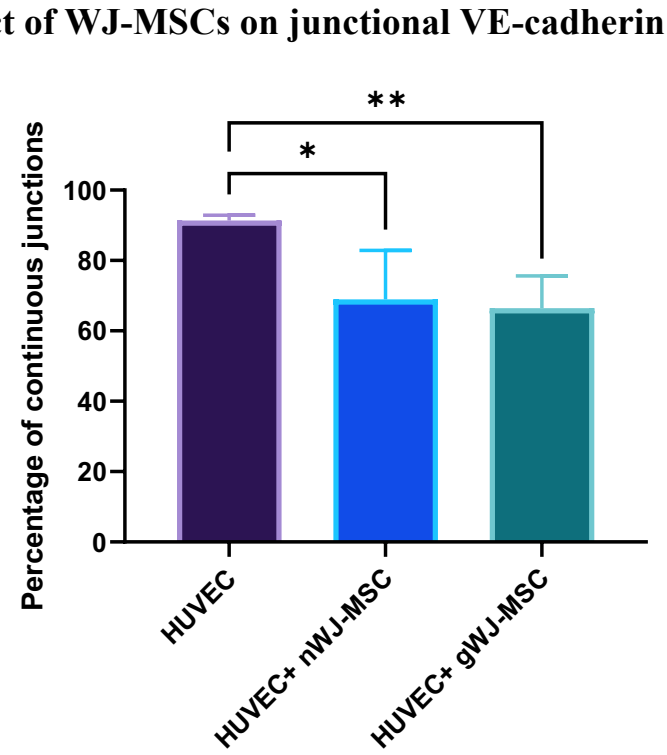


Figure 3-32 Effect of WJ-MSCs on Junctional VE-cadherin expression. VE-cadherin expression was reduced after 2hours co-culture time compared to the HUVEC monolayer due to opening of the junctions ($P < 0.05$).

Behaviour of cells after 24h. Co-culture

Full occupancy of the VE-cadherin at cell –cell junctions was found at the 24-hour interval when most of the gWJ-MSCs were found resident in the sub-endothelium suggesting the subsequent repair of endothelial junctions and return of VE-cadherin to adherens junctions. Five independent experimental repeats were done. Three different co-cultures from each group were presented; (normal pregnancy) (Figure 3-33), and (GDM) (Figure 3-34).

Transmigration of nWJ-MSCs across the HUVEC monolayer and VE-cadherin localisation

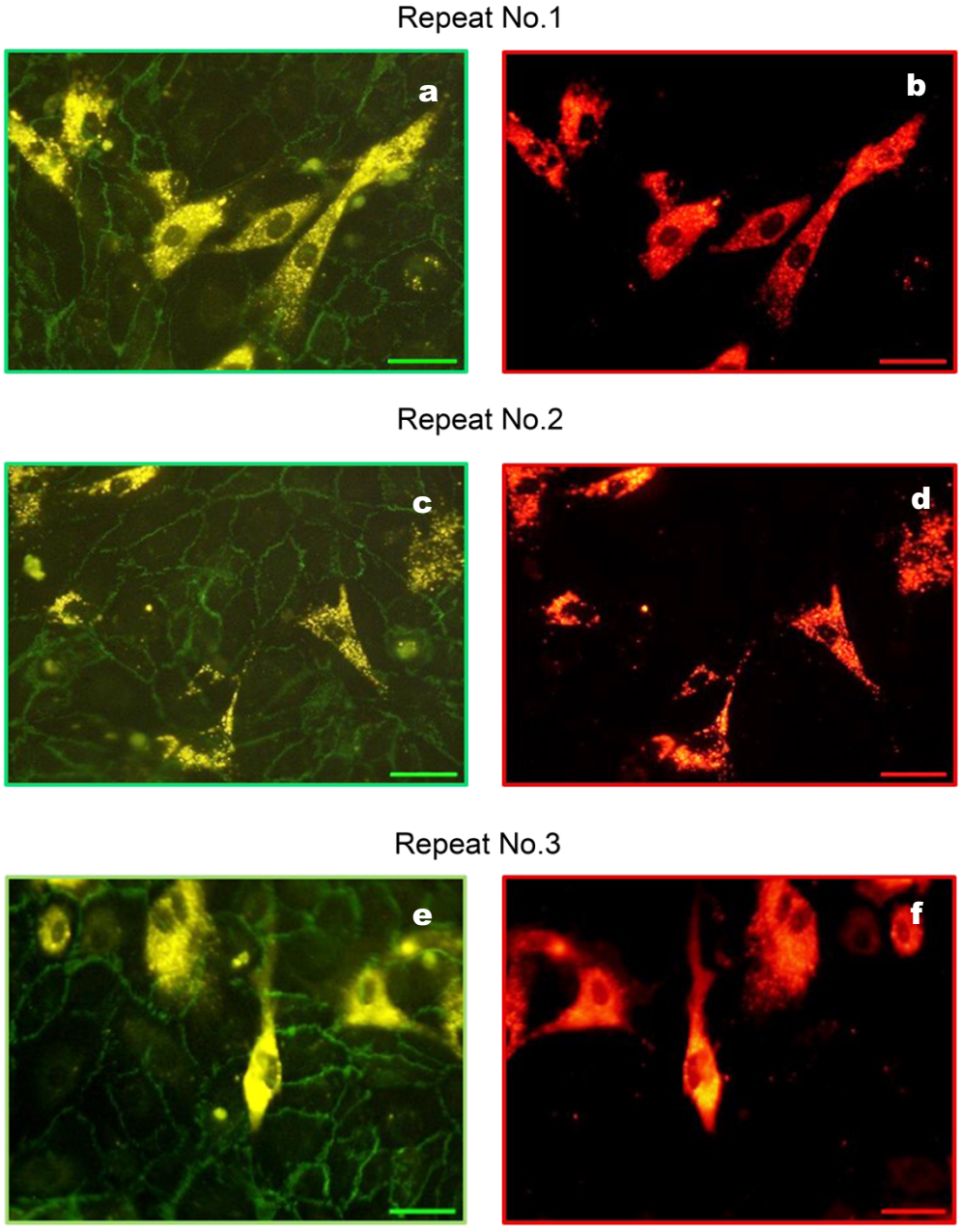


Figure 3-33 Representative micrographs of co-cultured HUVEC + nWJ-MSCs (from three different populations) showing full VE-cadherin occupancy after 24 hours. Images (**b**, **d**, and **f**) showing VE-cadherin labelled HUVEC (Green) and PKH-26 labelled WJ-MSCs (Yellow) (FITC filter). Images (**a**, **c**, and **e**) showing PKH-26 labelled WJ-MSCs (red) (TRITC filter), scale bar=40µm.

Transmigration of gWJ-MSCs across the HUVEC monolayer and VE-cadherin localisation

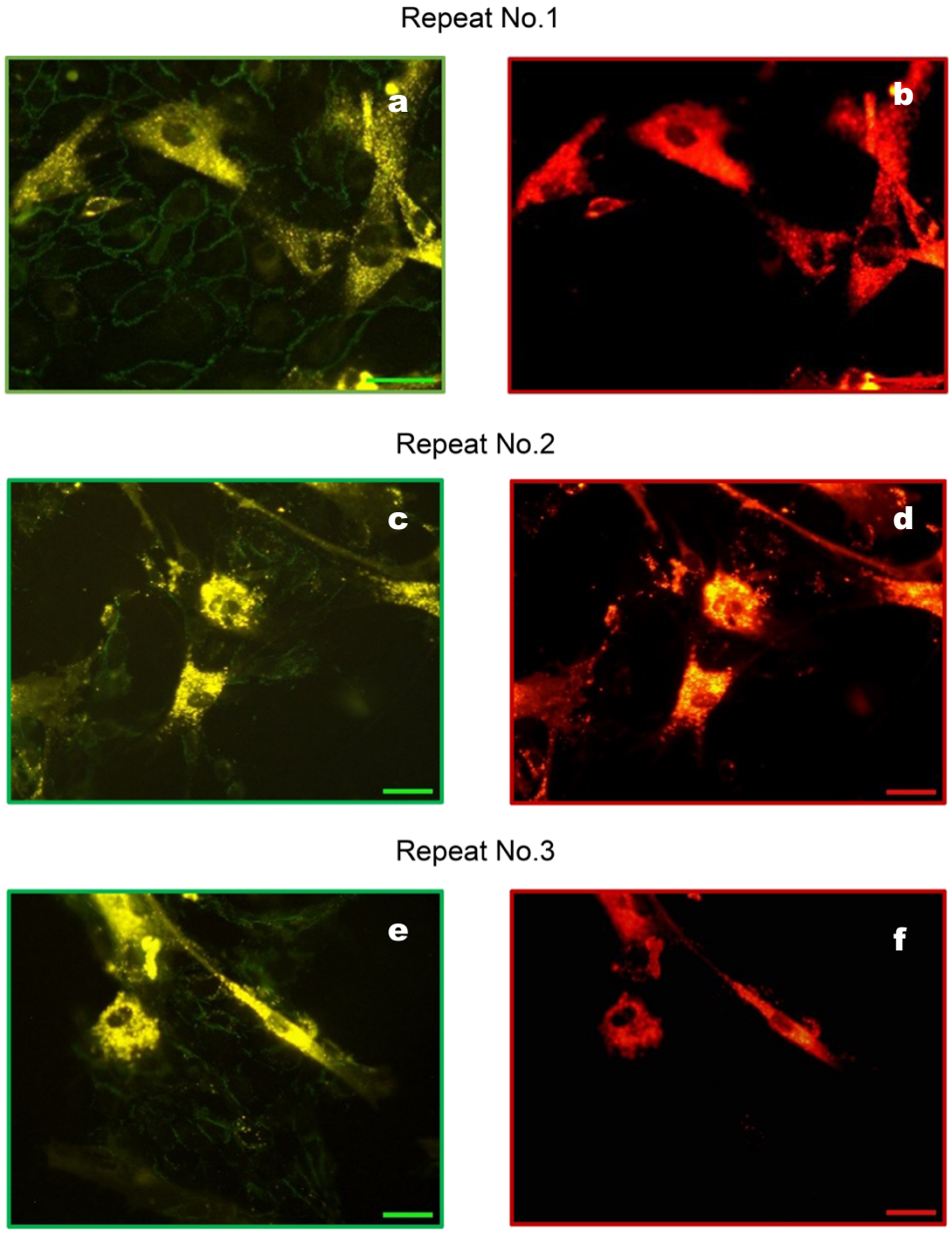


Figure 3-34 Representative micrographs of co-cultured HUVEC + gWJ-MSCs (from three different populations) showing reduced junctional VE-cadherin expression after 24 hours. Images (**a**, **c**, and **e**) showing VE-cadherin labelled HUVEC (Green) and PKH-26 labelled WJ-MSCs (Yellow) (FITC filter). Images (**b**, **d**, and **f**) showing PKH-26 labelled WJ-MSCs (red) (TRITC filter), scale bar=40µm.

The systematic random sampling for counting of the VE-cad junctional expression revealed 28% reduction in the number of continuous junctions in HUVEC +gWJ-MSCs compared to the HUVEC + nWJ-MSCs (Figures 3-35). This was shown in five experimental repeats.

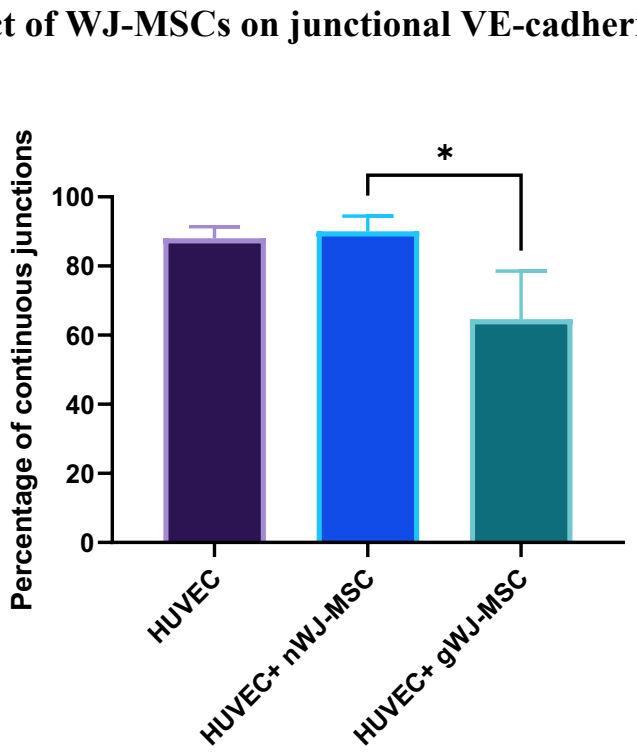


Figure 3-35 Reduced VE-cadherin junctional expression by 28 % after 24h co-culture of the HUVEC +gWJ-MSCs compared to the HUVEC + nWJ-MSCs (One-Way ANOVA test, P <0.05).

3.5 Discussion

The data shown in this chapter suggests that GDM affects migration, VEGF secretion, morphology, and phenotype expression of WJ-MSCs. Furthermore, gWJ-MSCs have a differential effect on endothelial barrier integrity in co-cultures compared to nWJ-MSCs.

Women with higher BMI have an increased risk of GDM (Dennedy and Dunne, 2010) (Martin et al., 2015). Our clinical data revealed that the BMI of the women in the GDM groups was 25% higher than those from the normal pregnancy group (P <0.001). The BMI of mothers in the metformin-treated

group was significantly higher compared to Normal pregnancy group. Women with BMI above 30 kg/m2 are recommended to be offered OGTT at the booking appointment (NICE, 2015). This is to be expected given that metformin is preferred for women with higher BMI to reduce maternal weight gain and insulin dosage and improved glycaemic control (Feig et al., 2020).

Our results demonstrated that increasing maternal BMI positively correlates to increased fetal weight in the study population independent of the glycaemic status (Pearson r =0.4), this is consistent with previous reports that stated the association between the maternal BMI and birth weight (Black et al., 2013, Martin et al., 2015) (Martino et al., 2016). Given that all the women had well-controlled glycaemic state, BMI was positively correlated to the birth weight centile in the d-GDM group (Pearson r= 0.6) (P <0.05), but not in the m-GDM group (Spearman r= -0.4) (P >0.05). Infants for obese mothers are exposed to the level of maternal lipids due to placental expression of lipoprotein receptors, fatty acid–binding proteins, and different lipase activities allowing the transfer of maternal fatty acids to the fetus, therefore the higher cord blood fatty acid levels are associated with higher maternal lipids (Schaefer-Graf et al., 2008). Metformin use during pregnancy by women with GDM and type 2 diabetes has been linked to lower infant birth weights(Tarry-Adkins et al., 2019) (Feig et al., 2020).

Placental weight was higher in the GDM group compared to the Normal pregnancy group (P-value < 0.05). Placental weight was positively correlated to the birth weight centile in both the Normal pregnancy (Pearson r=0.8) (P-value< 0.001), and GDM group (Spearman r=0.6) (P-value < 0.05) has been described before (Taricco et al., 2003) (Pathak et al., 2010). Pathologists have shown changes in the GDM placentas as; fibrinoid necrosis, cholangiosis, and the presence of nucleated red blood cells (Daskalakis et al., 2008). *Evers et al., 2003,* suggested that increased placental weight might be due to chronic fetal hypoxia as a result of the increased diffusion distance between the intervillous space and fetal capillaries that is compensated with increasing the placental weight to increase the surface area (Evers et al., 2003).

Our data revealed no statistical difference in fetal weight between the groups, but the placental-to-fetal weight ratio was higher than in normal pregnancy. *Daskalakis et al 2008* suggested that increased placental-to-fetal weight ratio in the GDM group was because of the more placental growth that occurs in the first half of gestation, well before GDM diagnosis and treatment (Daskalakis et al., 2008). Furthermore, GDM treatment can modulate the fetal weight proportionally more than the placental weight (Taricco et al., 2003).

The number of MSCs migrated from umbilical cord pieces from GDM placenta exceeds those migrated from normal ones by 65% (P <0.005), which agreed with *Chen et al., 2020,* who found that chorionic membrane stem cells from GDM donors displayed enhanced motility and upregulated expression of AQP1, FLNB, CELSR1, and CD24. These upregulated genes have important roles in cell movement (CD 24 & AQP1) and cytoskeletal remodelling (CELSR1 &FLNB)(Chen et al., 2020). The altered migratory properties seen in gWJ-MSCs suggest that they have similar expression as recorded in chorionic stem cells from GDM pregnancy given that they have the same embryological origin. Furthermore, HUVECs isolated from GDM-complicated pregnancies have also shown an increased migration ability (Troncoso et al., 2017). It might be explained as an increased number of stem cells in samples from the GDM group rather than increased cell migration. This finding makes GDM not an obstacle for stem cell therapy from the point of migration.

The number of cells migrated from each cord sample was 4-fold higher in the metformin-treated GDM group and 2.5-fold higher in the diet-controlled GDM group compared to the control. However, no significant difference was found between the diet and metformin treatment. *Bao et al., 2012* investigated the effect of metformin on cancer stem cells and found it significantly decreased cell viability, clonogenicity, wound-healing capacity, sphere-forming capability, and the expression of cancer stem cell markers (Bao et al., 2012). Moreover, Metformin was known to decrease the HUVEC and endothelial progenitor cell migration by downregulated matrix metalloproteinase-2 (MMP-2) and MMP-9 expression (Esfahanian et al., 2012). This data suggests that metformin may have an impact on fetal stem

cells that draws attention to its use during pregnancy as a drug crosses the placenta. A recent study on 1451 metformin-exposed offspring associated the preconception paternal metformin use with major birth defects (Wensink et al., 2022).

Primary cultures of gWJ-MSCs displayed same mixed morphology, the same whirl appearance when confluent. However, on sub culturing, they displayed 20% less elongated spindle shape than nWJ-MSCs and more rounded shape. The predominant rounded morphology of gWJ-MSCs may be associated with enhanced differentiation potential towards certain lineages. Cell shape has a role in many important biological processes as morphogenesis, differentiation, division, and apoptosis. *McBeath et al., 2004*, demonstrated that cell shape modulates commitment of MSCs to adipocyte or osteoblast fate by modulating endogenous RhoA activity. Expressing dominant-negative RhoA committed mesenchymal stem cells to differentiate into adipocytes, while constitutively active RhoA committed mesenchymal stem cells to differentiate into osteoblasts (McBeath et al., 2004). Adipocytes are known to be rounded with fat accumulation (Gregoire et al., 1998), while osteoblasts can be elongated or cuboidal, depending on matrix deposition activity (Sikavitsas et al., 2001). This variation in cell morphology may arise from changes in the expression of integrins, cadherins, and cytoskeleton proteins during stem cell commitment (Gumbiner, 1996). Therefore, g WJ-MSCs display a more rounded than elongated cell shape suggesting that gWJ-MSCs have more adipogenic differentiation potential. Previous studies reported that GDM can alter the adipogenic and osteogenic MSCs differentiation potentials. Kim et al., 2015 stated that WJ-MSCs from GDM complicated pregnancies have lower chondrogenic and osteogenic differentiation potential (Kim et al., 2015). Moreover, WJ-MSCs from GDM donors are well known to display more adipogenesis than the ones from Normal gestation (Pierdomenico et al., 2011, Tsai et al., 2013) that might explain the association between GDM and the higher risk for long-term childhood overweight and increased abdominal circumference by approximately 60–80% (Nehring et al., 2013).

It has been suggested that WJ-MSCs from GDM complicated-pregnancies displayed lower proliferation rates with earlier cellular senescence accompanied by expression of p16 and p53 compared to normal gestation (Kim et al., 2015). Alternatively, *Pierdomenico et al, 2011*, demonstrated that WJ-MSCs obtained from GDM complicated-pregnancies displayed higher proliferative ability and increased expression of the following markers; CD166, CD44, CD73, and CD29(Pierdomenico et al., 2011). However, in this study, the doubling time calculation showed no significant difference in the proliferation between nWJ-MSCs and gWJ-MSCs.

ELISA assays revealed increased secretion of VEGF protein in gWJ-MSCs 3.8 fold higher than nWJ-MSCs (P <0.001), in agreement with *Wajid et al., 2015,* who also reported increased VEGF protein expression in WJ-MSCs from GDM donors (Wajid et al., 2015). Increased VEGF in endothelial cells has been shown in the retinal tissues of diabetic rats (Yan and Su, 2014). WJ-MSCs release many growth factors including VEGF (Li et al., 2016, Ebrahim and Leach, 2016) which promotes angiogenesis and vascular permeability (Pang et al., 2017). VEGF disrupts the endothelial barrier function by disrupting the VE-cadherin-mediated intercellular junctions. This barrier function disruption must be maintained during endothelial cell migration that is necessary to initiate angiogenesis (Eliceiri et al., 1999, Weis et al., 2004). The dynamic architecture of endothelial cell junctions is vital to maintain the feto placental barrier integrity that separates the maternal intervillous space and fetal circulation allowing the exchange of endogenous and exogenous materials between the mother and the fetus (Leach and Firth, 1992). MSCs of the mesoderm differentiate into and participate in neo-vasculogenesis of the umbilical and placental circulation. They also modify the microenvironment and trigger angiogenesis (Edwards et al., 2014, Todeschi et al., 2015). GDM placentas displayed increased angiogenesis evidenced by increased villous vascularity frequently associated with thickened immature villi capillaries and placental hypo perfusion (Alqudah et al., 2021) (Daskalakis et al., 2008). This may be the mechanism behind the increased number of migrated cells in the GDM groups. However, VEGF-A secreted from MSC may have a major

impact on the endothelial permeability and needed to be further investigated to elucidate the diabetic state effect on fetal stem cells (see chapter 4).

This study showed that WJ-MSCs isolated from pregnancy complicated with gestational diabetes regardless the treatment was diet or metformin, were positive to CD44, CD90, CD105&CD73 and negative to CD14,CD19& HLA-DR, this is in agreement with findings from two previous studies; (Kong et al., 2019) that characterized WJ-MSCs from GDM donors and (Chen et al., 2019) that characterized Chorionic membrane MSCs from GDM donors. However, the flow cytometry analysis revealed that GDM displayed higher Endoglin expression compared to nWJ-MSCs by 17% (P <0.05). Endoglin mediates multiple endothelial cell responses, including proliferation, migration against flow and cellular footprint in response to angiogenic signals from VEGF. It is upregulated in proliferating endothelium as in tumour vessels of brain, breast, colon, lung, and stomach cancer (Minhajat et al., 2006). ENG is involved in haematopoiesis angiogenesis, NO-dependent vasodilatation, and also plays a key role in cellular transmigration as a TGF-β co-receptor (Fonsatti and Maio, 2004).

This study is the first to report that higher Endoglin expression is positively correlated with placental weight (Pearson r = 0.4) (P <0.05), but it wasn't correlated to the birth weight, maternal weight, or the maternal age. Endoglin is a major marker antigen of mesenchymal and endothelial cells. However, it is soluble form has been proven to be increased in PE and diabetes (Leaños-Miranda et al., 2019) causing increased vascular permeability and inhibition of capillary formation, its role in gestational diabetes is still unclear. Endoglin's expression in the endothelium increases during active angiogenesis when sprouting takes place (Barnett et al., 2014, Jin et al., 2017). It might reflect the pro-angiogenic state in the GDM placenta observed in the increased placental blood vessels per chorionic villi, VEGFR2 levels, and endothelial cell markers expression compared to the control ones (Troncoso et al., 2017). The role of Endoglin on endothelial permeability was explored and will be discussed in chapter 5.

The immunofluorescence co-culture studies revealed that gWJ- MSCs could transmigrate across the endothelial monolayer and reside in the sub-endothelial niche similar to the ones from normal pregnancy. GWJ-MSCs by 2h co-culture time attached to the endothelial monolayer, transformed to the elongated shape, and opened the adherens junctions observed in lost VE cadherin and PECAM junctional staining at the sites of stem cells contact. However, gWJ-MSCs showed a deficient ability to repair the endothelial barrier after transmigration, as observed in the reduced percentage of VE-cadherin junctional expression by 28% by 24h co-culture time compared to the control nWJ-MSCs when co-cultured with HUVEC from normal donors ($P < 0.05$).

In conclusion, the data obtained in this chapter shows that the uterine environment during pregnancy has an impact on the biology of stem cells derived from extra-embryonic tissues like Wharton's jelly. Even with a well-controlled glycaemic condition, gestational diabetes can affect the WJ-MSCs' properties, Endoglin expression, and endothelial barrier enhancement. This may be one of the confounding factors that leads to a higher risk of later vascular dysfunction in the offspring.

4 CHAPTER 4 Effect of Human Umbilical Mesenchymal Stem Cells Isolated from Normal and Gestational Diabetic Pregnancies on Monolayer Permeability of Human Umbilical Vein Endothelial Cells

4.1 Introduction

4.1.1 Structural Heterogeneity of the Endothelial Cells

Endothelium in different tissues can be described as continuous or discontinuous. Continuous endothelium, can be categorized into fenestrated or non-fenestrated, see review (Aird, 2007). Non-fenestrated continuous endothelium can be found in arteries, veins, and capillaries of the brain, placenta, skin, heart, and lung, whereas fenestrated continuous endothelium can be found in exocrine and endocrine glands, gastric and intestinal mucosa, and renal glomeruli to promote filtration and trans-endothelial transport. Fenestrae are transcellular pores (70 nm in diameter) that are distributed across the whole cell (Wisse, 1970). The majority of fenestrae have a thin 5- to 6-nm non-membranous diaphragm across their opening to provide more size selectivity (Feng et al., 2002). Discontinuous endothelium is common in the liver sinusoidal vascular beds. In contrast to fenestrated continuous endothelium, liver sinusoidal ECs have larger fenestrations (100 to 200 nm in diameter) that lack a diaphragm and have gaps (or large circular pores) within individual cells(Wisse, 1970). Fetal-placental endothelial barrier is considered as a continuous non fenestrated endothelium that is maintained by adherens and tight junctions. Vascular permeability is mediated by the opening and closing of these junctions. The endothelial permeability and its signalling pathways are necessary to determine the level of passive diffusion across the capillary lining **(**Leach and Firth, 1992**,** Desforges and Sibley, 2009**)**.

4.1.2 Breaking Down VE-Cadherin Junctions and the Endothelial Barrier Permeability

Continuous endothelium forms a selective semi-permeable barrier to control bidirectional transfer between the blood and the tissues. This pivotal function depends on the dynamic architecture of the endothelial cell junctions (Dejana et al., 2008, Gavard, 2013, Rahimi, 2017). Tight junctions and adherens junctions are linked structurally and functionally. Endothelial intercellular permeability is regulated by cadherin at the AJs and

claudin/occluding at the TJs (Joffre et al., 2020, Leach and Firth, 1992). VE-cadherin expression at AJs is required for claudin-5 upregulation (Taddei et al., 2008, Vestweber et al., 2009). The exposure to acute inflammation, diabetes, cancer, or immune reactions causing release of the permeability increasing agents, such as histamine, tumour necrosis factor-alpha, VEGF and platelet activating factor. This leads to phosphorylation of the VE-cadherin intracellular domain. Phosphorylation of this VE-cadherin-catenin complex leads to dissociation of homophilic binding followed by internalization in clathrin-coated vesicles (Dejana et al., 2009, Woodcock and Woodcock, 2012), by its role will trigger the cleavage of its extracellular domain. VE-cadherin organizes the opening and closing of the endothelial barrier junctions, and is essential in paracellular permeability changes (Blaise et al., 2015).

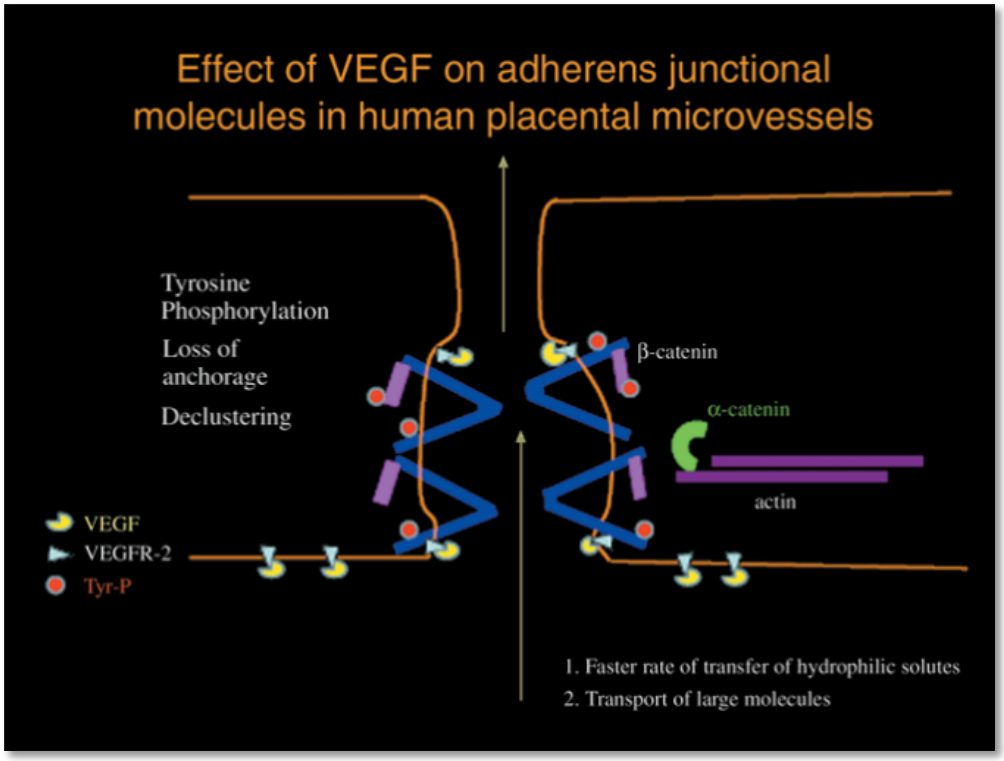


Figure 4-1 **Diagram showing the effect of VEGF on VE-cadherin phosphorylation.** VE-cadherin phosphorylation is followed by loss of anchorage to actin, cadherin-catenin dissociation, and translocation changing the cleft dimension and allowing transport of larger hydrophilic proteins, taken from (Leach et al., 2009).

4.1.3 Endothelial Permeability Pathways

Two pathways are known to regulate the permeability across the endothelial barrier: para-cellular and trans-cellular (Komarova and Malik, 2010). Trans-cellular pathway is defined as vesicle mediated transport of macromolecules, such as albumin, across the endothelial barrier in a caveolae-dependent manner. Para-cellular permeability is determined mainly by adherens junctions and tight junctions (Leach et al., 1995) (Tuma and Hubbard, 2003) that offers a passive pathway for the diffusion of protein and other small solutes. In normal physiological conditions, these junctions are impermeable to albumin and other plasma proteins. Electron micrographic studies have shown that this pathway is restricted and excludes macromolecule tracers (Predescu et al., 2004).

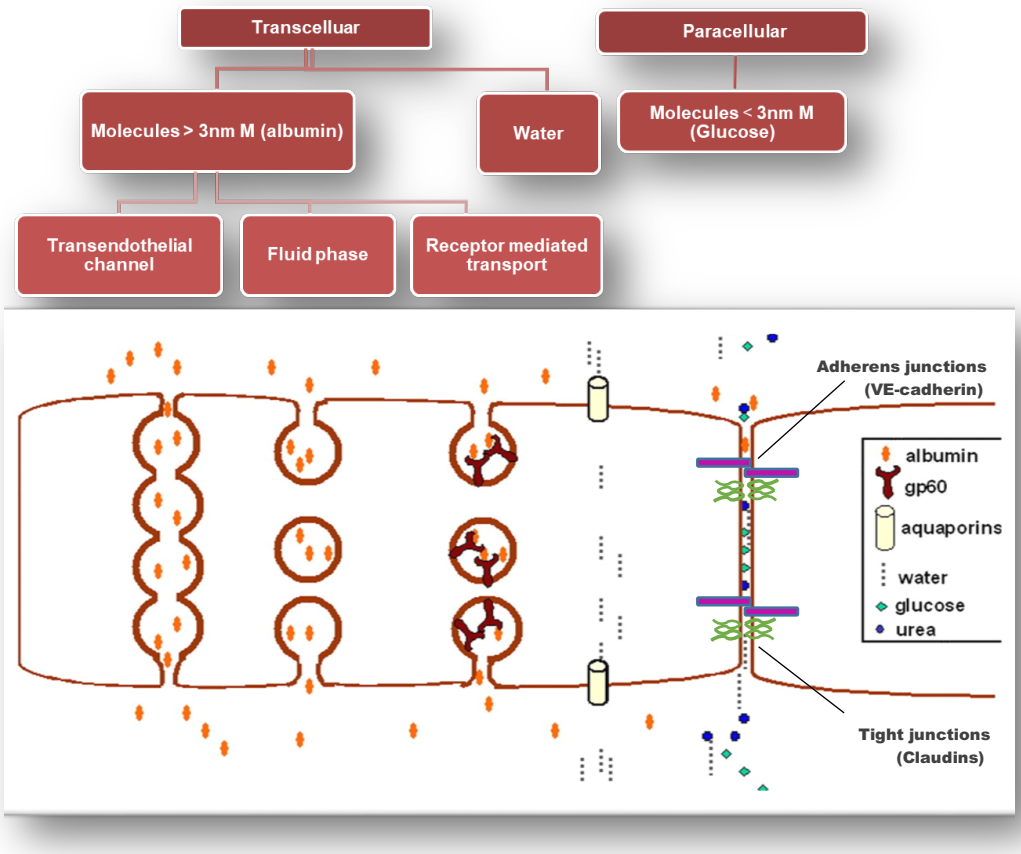


Figure 4-2 **Schematic diagram of transport pathways in continuous endothelium**. Transcellular pathway can mediate the transport of big sized plasma proteins as albumin by transcellular channels by fusion of multiple caveolae, receptor-mediated or fluid-phase pathway. Aquaporins form channels across the lipid bilayer creating a Trans endothelial pathway for water. Smaller molecules as urea and glucose are transported around individual

endothelial cells via the paracellular junctional pathway, modified from (Mehta and Malik, 2006).

Vacsular permeability in vivo

Nagy et al., 2008, classified vascular permeability, based on the different types of microvessels involved, and the molecular size of solutes into;
1- ***Basal vascular permeability*** is the rapid paracellular flow of small molecules and the extremely limited transcellular passage of plasma proteins across normal capillaries.

2- ***Acute vascular hyperpermeability*** is the time-limited passage of plasma proteins across post-capillary venules by either para cellular or transcellular routes in acute inflammation.

3- ***Chronic vascular hyperpermeability*** is the extravasation of plasma and plasma proteins from the angiogenic vessels in healing wounds, tumours, and chronic inflammation, reviewed in (Nagy et al., 2008).

Miles assay has been used in animal studies to measure vascular permeability by quantifying the amount of a dye-labelled solute that has crossed a vascular bed and accumulated in the interstitium at some time (often 30 min) after injection in response to a vascular permeabilizing agent as VEGF (Nagy et al., 2006).

Vascular permeability in vitro

Confluent-cultured endothelial cell monolayers are more permeable than the blood vessel wall in vivo as they are lacking the pericytes and vascular smooth muscle cells that normally modulate the endothelial cell behaviour. Vascular permeability develops much more slowly in cultured endothelium and reaches the peak over a period of hours not minutes as in vivo, suggesting that the experimented permeability reflects loosening of the intercellular junctions when endothelial cell are exposed to a stimulus as VEGF-A. In vitro assays mimic the chronic vascular hyper permeability model specific for pathological angiogenesis as found in tumours, healing wounds, and chronic inflammation, not the acute hyperpermeability or the basal permeability models (Nagy et al., 2008). The addition of pericytes or mesenchymal stem

cells influences the tightness of the endothelial layer in vitro (Ebrahim and Leach, 2016).

Regulation of Paracellular Permeability and Fluid Balance

The transmigration of stem cells and leukocytes into tissue for maintenance and repair of the vasculature is associated with VEGF-mediated increased para-cellular permeability of the endothelial barrier that is necessary for the transport of solutes and cellular transmigration across the endothelial monolayer (Vestweber et al., 2009, Ebrahim and Leach, 2015). Pathological conditions, such as inflammation and cancer are associated with the secretion of cytokines that induce prolonged and chronic hyperpermeability and vessel wall leakiness (Dejana et al., 2009).

There are permeability-increasing factors whereas their effect is rapid, temporary, and reversible in response to pro-inflammatory agents, such as histamine (Qin et al., 2013) and thrombin (Tsopanoglou and Maragoudakis, 2004), or their effect is sustained, as in response to proangiogenic and inflammatory cytokines, such as VEGF (Hicklin and Ellis, 2005) and kinin cleavage products (Schmaier and McCrae, 2007). There are also endothelial barrier enhancers such as Angiopoietin-1, FGF, and Sphingosine-1-phosphate that decrease the response to permeability-increasing mediators. They are present in blood plasma, for regulation of basal permeability, and continuous support for the vascular integrity (Komarova and Malik, 2010).

Angiopoietin-1, Angiopoietin-2, and their tyrosine kinase receptors, Tie1 and Tie2, also play important roles in vascular homeostasis. Angiopoietin-1 is produced by perivascular cells to inhibit the VE-cadherin internalization preventing vascular permeability during endotoxemia (Gavard, 2009, Hatanaka et al., 2012). Sphingosine-1-phosphate is released from activated platelets. It mediates the endothelial barrier enhancement through activation of the Gi protein–coupled Sphingosine-1-phosphate receptor (Maceyka et al., 2012).

4.1.4 Signalling Mechanisms Regulating Paracellular Endothelial Permeability

Src mediated signalling

Src-induced tyrosine kinase phosphorylation of Y658 or Y731 of VE-cadherin prevents the binding of p120-catenin and *β*-catenin, respectively (Potter et al., 2005). Phosphorylation of specific VE-cadherin tyrosines is induced by leukocyte or stem cell adhesion to the endothelium via ICAM-1, assisting transmigration (Turowski et al., 2008) (Ebrahim and Leach, 2015).

Ca2+ mediated signalling

The basal cytosolic Ca2+ concentration in endothelial cells is very low (∼100 nM) and significantly increases in response to extracellular stimuli (Tiruppathi et al., 2002). Some inflammatory mediators bind to heptahelical G protein-coupled receptors increasing the intracellular Ca^{2+}concentration. The rise in Ca^{2+}concentration activates the signalling pathways, which mediate cytoskeletal reorganization through myosin light chain dependent contraction, disassembly of VE-cadherin at the AJs, and enhance the endothelial permeability(Tiruppathi et al., 2002).

RhoGTPase signalling mechanisms

The RhoGTPases subfamily modulates the organization and dynamics of the actin cytoskeleton (Timpson et al., 2001). RhoA, Rac1, and Cdc42 play a pivotal role in organization of the actin cytoskeleton affecting the integrity of AJs. The balance between RhoA, Rac1, and Cdc42 at AJs is regulated by VE-cadherin. RhoA promotes the formation of actin stress fibers and actomyosin contraction generating intracellular tension at junctions that disassembles AJs. Rac1 induces the polymerization of actin filaments at the VE-cadherin adhesion site contributing AJs stabilization. Thus, a balance between RhoA and Rac1 actions is a critical control point of VE-cadherin turnover at adherens junctions reviewed in (Komarova et al., 2017).

4.1.5 Regulation of Transcellular Endothelial Permeability

The Transcellular transport pathway is mediated by specialized structures, called caveolae and vesiculo–vacuolar organelles (VVOs). Caveolae are small invaginations at the cell surface (50–100 nm in diameter) and often surround fenestrae (Levick and Smaje, 1987). The number of caveolae is highest in continuous non-fenestrated endothelium, particularly in heart, lung, and skeletal muscle except the brain where caveolae are rarely present, reviewed in (Bendayan, 2002). Determining whether solutes cross venular endothelium by inter-endothelial cell or transcellular for plasma extravasation in response to permeability factors pathways is difficult because of the tortuosity of inter-endothelial cell borders and the proximity of VVOs to these borders (Nagy et al., 2008).

Transport of the albumin from the luminal to abluminal side of the endothelium is a specialized process necessary to maintain the barrier homeostasis. Albumin transcytosis process is initiated by binding of the albumin to albumin-binding protein gp60, undergo internalization and scission, and releasing of the vesicle from the cell membrane (endocytosis). The released vesicle moves through the cytoplasm to the opposite cell surface, where they fuse with the cell membrane and release the albumin (exocytosis). Albumin can be transported in caveolae in either the fluid phase or bound to gp60, reviewed in (Minshall et al., 2002).

4.1.6 The Interaction between Mesenchymal Stem Cells and Endothelial Cells and Endothelial Permeability Restoration

Co-culture of endothelial cells with stromal cells has been shown to enhance the endothelial barrier function, for example co-culturing the brain microvascular endothelial cells differentiated from IPSCs with rat primary astrocytes (Canfield et al., 2017). Mesenchymal stem cells have been shown to restore the endothelial function, via paracrine and cell-cell contact-mechanisms (Sassoli et al., 2012, Ebrahim and Leach, 2016). Mesenchymal stem cells displayed reduction in endothelial permeability, increase in VE-cadherin levels

and enhance VE-cadherin Ajs assembly when co-cultured with HUVECs (Pati et al., 2011). Moreover, *Pati S et al., 2011*, showed that conditioned medium from mesenchymal- endothelial co-cultures, but not from HUVECs alone or MSCs alone, can decrease endothelial permeability suggesting that mesenchymal stem cells perform better and secrete more growth factors upon endothelial contact (Pati et al., 2011). Furthermore, the extracellular vesicles released by stem cells have been shown to home to the injured site similar to the parent stem cells participating as mediators of cell-to-cell communication (Turturici et al., 2014, Zappulli et al., 2016). Moreover, administration of MSC micro vesicles to human lung microvascular endothelial cells injured by a mixture of; IL-1β, TNF-α, and IFN-γ restored the endothelial permeability and was associated with an increase in Angiopoietin-1 mRNA in the injured endothelium (Hu et al., 2018).

4.2 Aim

Endothelial permeability regulation is vital for many vascular functions including the transport of molecules and cells through the endothelium without disturbing the structural integrity of blood vessels. Given that the media from MSCs-endothelial co-culture do significant reduction of the endothelial permeability. The cell-cell contact of the WJ-MSCs, and human umbilical cord endothelial cells might lead to endothelial barrier enhancement. WJ- MSCs from GDM complicated pregnancies have been shown to transmigrate across endothelial cells reaching the sub-endothelial niches similar to those from normal pregnancies. Thus, whether the GDM affects the endothelial integrity enhancing the ability of WJ-MSCs is unknown and was the aim of this chapter.

The main objectives of the chapter:

- To investigate the effect of WJ-MSC on the barrier integrity of human umbilical vein endothelial cell monolayer (HUVEC)
- To compare between gWJ-MSCs and nWJ-MSCs in their effect on the endothelial permeability

- To investigate whether the mode of GDM treatment influences the WJ-MSCs potential effects on the endothelial permeability.

4.3 Materials

Table 4-1 List of Chemical and Reagents used in the Permeability Studies

Reagent	Company
Medium 199 (1x) with L-glutamine, 25Mm HEPES, L-amino acids, sodium pyruvate	Gibco, UK
Medium 199, no phenol red, Dulbecco's Modified Eagle's	Gibco, UK
Medium - low glucose (DMEM), no phenol red	Gibco, UK
Endothelial cell growth supplement from bovine neural tissue (ECGS)	Sigma-Aldrich, UK
Heparin sodium salt from porcine intestinal mucosa; Grade 1-A	Sigma-Aldrich, UK
Trypsin-EDTA solution	Sigma-Aldrich, UK
Bovine Serum Albumin (BSA)	Sigma-Aldrich, UK
Albumin–fluorescein isothiocyanate conjugate (FITC-Albumin)	Sigma-Aldrich, UK
Dulbecco's Phosphate Buffered Saline (DPBS); without calcium and magnesium	Sigma-Aldrich, UK

Table 4-2 List of Tissue Culture Plates, Accessories, and Devices used in the Permeability Studies

Product	Company
Polycarbonate Cell Culture Inserts with 0.4-micron pore size in 12-well plate	Corning, USA
Cell culture flasks (25cm2 and 75 cm2)	Corning, USA
Cell culture plates (6, 12 and 24 wells)	Corning, USA
Centrifuge tubes (15 mL and 50mL)	Corning, USA
96-well plate black bottomed	Corning, USA
Glass pipettes 5ML, 10ML, and 25ML	Greiner bio-one, Germany

Centrifuge tubes (15 mL and 50mL)	Greiner bio-one, Germany
Pipette tip 20, 200, 1000µL	Sarstedt, Germany
Micro tubes 0.5, and 1.5 µL	Sarstedt, Germany
Tc counting slides	Bio-Rad, UK
TC20 Automated Cell Counter	Bio-Rad, UK
The SpectraMax M2e Multimode Microplate Readers	Molecular Devices, UK

4.3.1 Study Design and Subjects

The cells were taken from normal pregnancies (n = 7) and GDM pregnancies (n = 10); diet- controlled (n = 5), and Metformin-treated (n = 5). The clinical characteristics of the study population that had samples used for HUVEC+WJ-MSCs permeability assays are shown in (Table 2). HUVECs were isolated from 6 normal pregnancies.

Table 4-3 Clinical characteristics of the study population used for HUVEC+WJ-MSCs permeability assays.

Characteristic	Normal (n = 7)	d-GDM (n = 5)	m-GDM (n = 5)
Maternal age, years	34.6 ± 5.9	39 ± 5.3	33.8 ± 2
Maternal BMI, Kg/m^2	24.06 ± 3.5	25.5± 6.6	35.1 ± 5.7
Gestational age at delivery, weeks	39.5 ±0.4	38.9± 1.5	38.5 ± 0.7
Placental weight, g	672.6 ± 110.8	612.0 ± 64.75	734.5 ± 123.2
Baby weight, kg	3.8 ± 0.8	3.3 ± 0.2	3.95 ± 0.9
Individual birthweight centile [gender]	61.75th[F] 70.73rd[M] 93.55th[F] 61.73rd[F] 99.99th[M] 98.05th[M]	74.24th[M] 63.47th[F] 48.33rd[F] 51.31st[M] 87.41st[F]	97.15th[M] 76.98th[M] 64.85th[F] 89.65th[F] 100th[M]

	50.56th[M]

Data are presented as mean (SD), [F], neonatal sex female; [M], neonatal sex male.

4.4 Methods

4.4.1 Co-culture permeability assays

To investigate the effect of nWJ-MSC and gWJ-MSC on the endothelial permeability of human umbilical vein endothelial cell monolayer, the leakage of albumin-FITC was measured at specific time points after co-culture with WJ-MSCs. 5 x10^4 HUVECs from a normal umbilical cord were seeded on 1% gelatin-coated 1.12 cm^2 culture surface area 0.4µm pore transwell inserts (Figure 4-3).

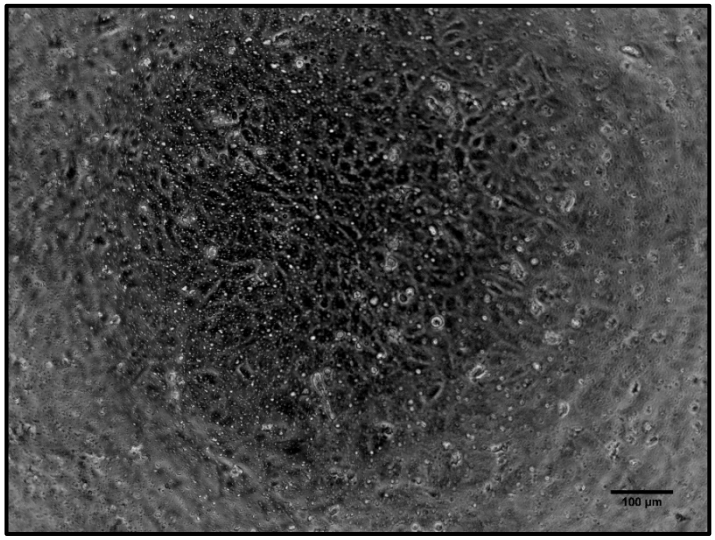


Figure 4-3 Phase contrast micrograph displaying the HUVEC monolayer growing on a transwell insert, scale bar 100µm.

Upon confluence within 24-48h, 10,000 WJ-MSC (Normal and GDM groups) were placed on top of the HUVEC monolayer using the mixed media (50% MSCs media & 50% HUVEC media) as previously described but without phenol red. FITC-Albumin (1mg/ml) of defined molecular mass (66

kDa) and fluorescence (λmax: 495 nm) was added to the apical chamber (1mg/ml) and unlabelled albumin was added to the basal chamber to maintain equal osmotic pressure. The volume in the apical and basal compartments was 500 µL and 1500 µL, respectively to maintain equal hydrostatic pressure, modified from (Pang et al., 2017) (Figure 4-4).

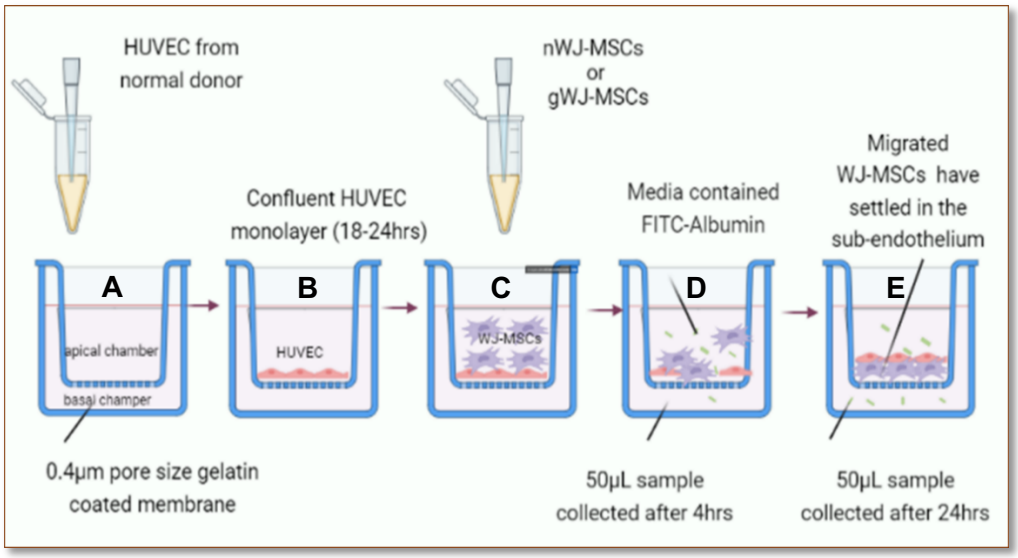


Figure 4-4 **Schematic diagram displays the co-culture permeability assay experimental design.** (**A**) The trans-well inserts were coated with gelatine. (**B**) HUVECs were seeded upon confluence. (**C**) WJ-MSCs from both groups Normal and GDM were seeded on top of the confluent HUVEC monolayer. (**D**) FITC-albumin and albumin were added to the apical and basal chambers respectively (1mg/mL) to maintain the osmotic pressure. (**E**) Tracer leakage concentration was quantified at the basal chamber at 0, 4 and 24h. Created with BioRender.com.

Fifty microliters of samples were collected at 0, 4 and 24 hours intervals from the lower compartment, and the volume was replenished with equivalent volume of fresh medium after each sample collection. The optical density was measured using by a fluorescence plate reader (SpectraMax M2e) using SpectraMax Pro7 application at an emission/excitation wavelength of 495/520 nm. Concentrations of FITC–albumin in each sample were calculated via linear regression of a serial dilution series of the tracer (Figure 4-5).

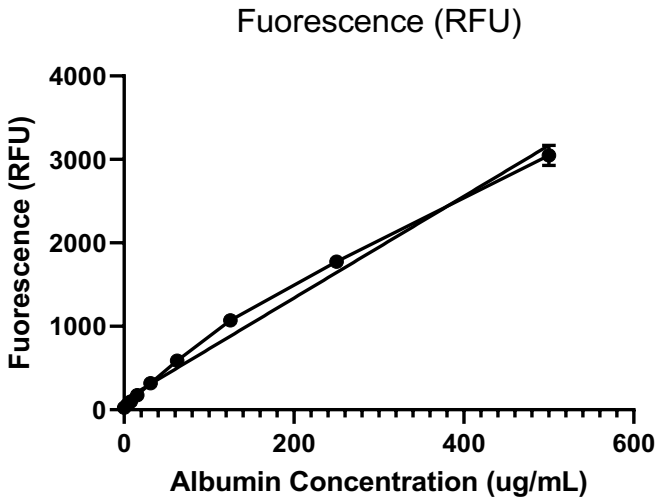


Figure 4-5 Graph displaying the standard curve used to interpolate the tracer concentrations.

The data are expressed as the amount of leaked protein to the basal compartment in the experimental groups (HUVEC+ nWJ-MSCs) and (HUVEC +gWJ-MSCs) and compared with the control conditions of untreated cells (HUVEC alone without WJ-MSC). Three replicates were performed per insert and three inserts per each sample in four independent experiments; each had its controls. To combine the data from the different repeats, the tracer concentration in the basal compartment was calculated as the percentage of endothelial barrier integrity enhancement reflecting how tightened the bilayers were, compared to the HUVEC monolayer control (HUVEC used in the repeats were isolated from different donors).

4.4.2 Co- Cultures Studies, VE-Cadherin Immunocytochemistry

The co-cultures were performed on coverslips for immunostaining parallel to growing the cells on inserts with the same culture conditions and seeding density ratio. The WJ-MSCs were labelled with red PKH-26 and the HUVEC were stained with VE-cadherin as discussed before (3.3.8).

4.5 Results

The tracer leakage values were undetectable at 0h in the three groups (HUVEC, HUVEC+ nWJ-MSC and HUVEC+ gWJ-MSC), no significant difference was recorded at 4h; the results from one repeat was as the following; (HUVEC alone 18.5 µg/mL ± 3.3), HUVEC+ nWJ-MSC (16.7 ± 4.8 µg/mL), and HUVEC+ gWJ-MSC (18 ± 4.7 µg/mL) (Figure 4-6), but the tracer leakage detected in the basal compartment after 24h co-culture time was higher in gWJ-MSC+HUVEC (151.0 µg/mL ±8.09) compared to nWJ-MSC+HUVEC (113.2 µg/mL ±4.5) (**P value 0.0027), no significant difference compared to HUVEC alone (142.5 µg/mL ±4.9) (Figure 4-7).

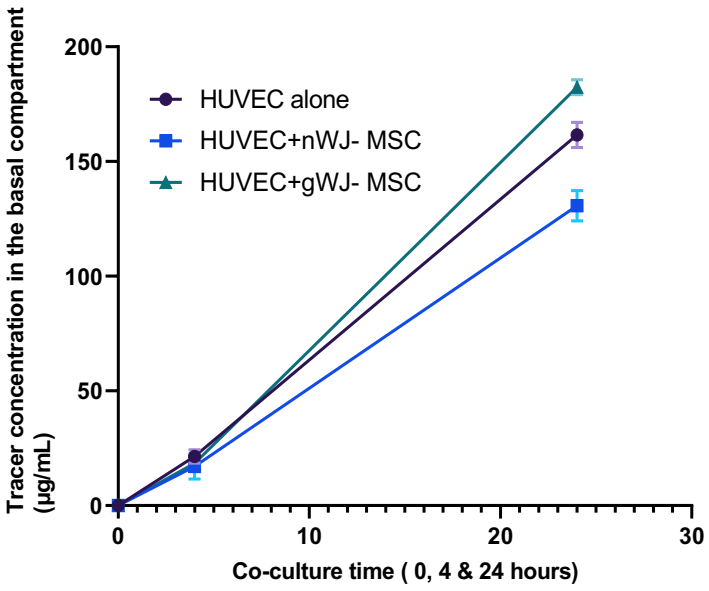


Figure 4-6 Graph displaying the amount of albumin transferred to the basal chamber across the bilayer cell culture model at 0, 4 and 24-hours culture time. No significant difference between the groups (HUVEC, HUVEC + nWJ-MSCs, and HUVEC + gWJ-MSCs) was found at 0, and 4hours time intervals between the groups, but the difference was observed after 24h co-culture time.

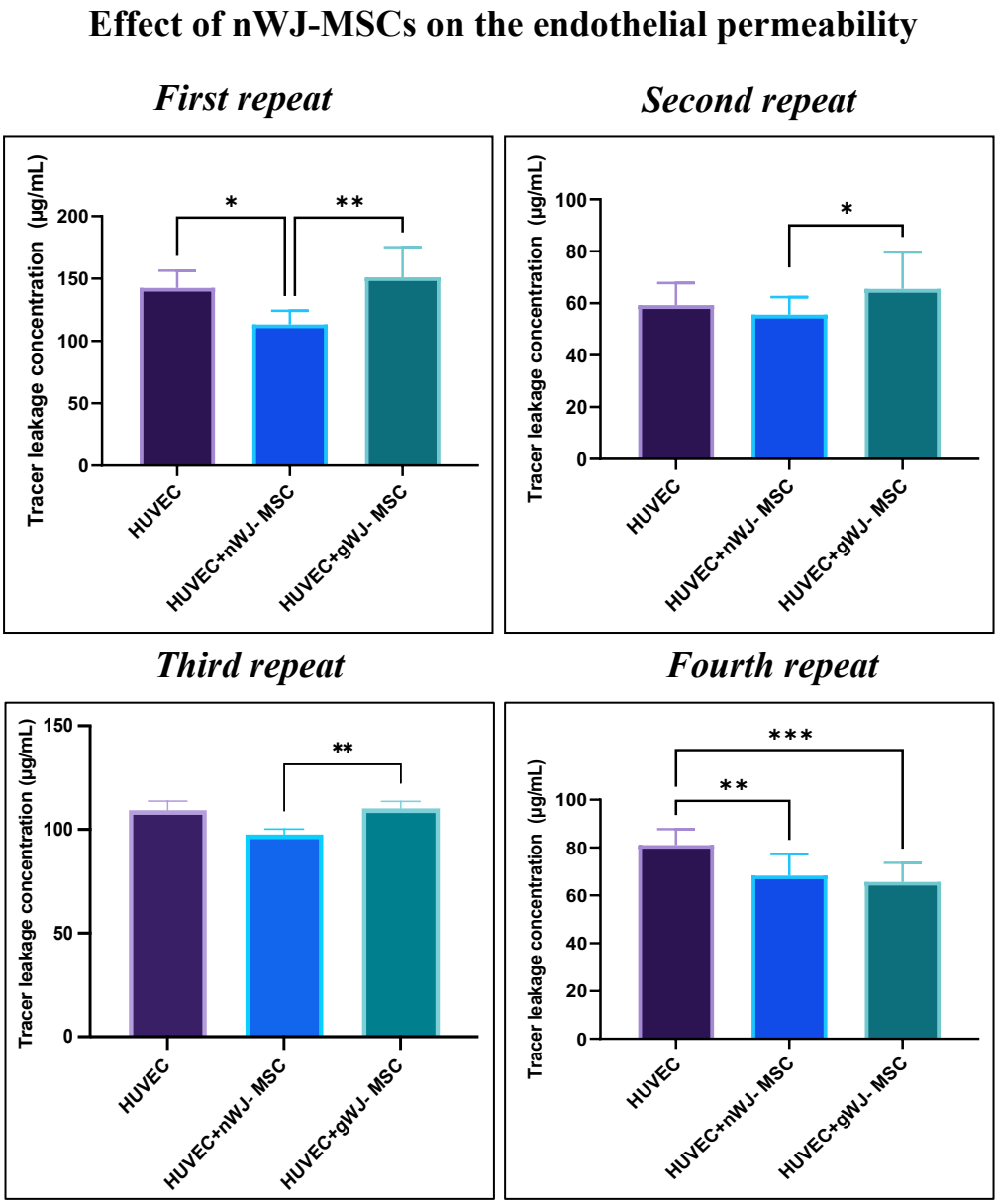


Figure 4-7 Graphs displaying nWJ-MSCs decreased tracer leakage while gWJ-MSCs increased it after 24h co-culture time. Three different isolates were tested per insert and three inserts per each sample: (Normal pregnancy n=7, d-GDM n= 5, and m-GDM n=5).

To combine the data obtained from four independent permeability studies, data is presented as the percentage of endothelial barrier integrity enhancement compared to the HUVEC monolayer control from the three experimental groups. The metformin treated-GDM achieved the lowest percentage (90.18 % ±3.987) compared to diet controlled-GDM (102.1% ±5.164) and Normal pregnancy (113.3% ±3.733) groups (Figure 4-8).

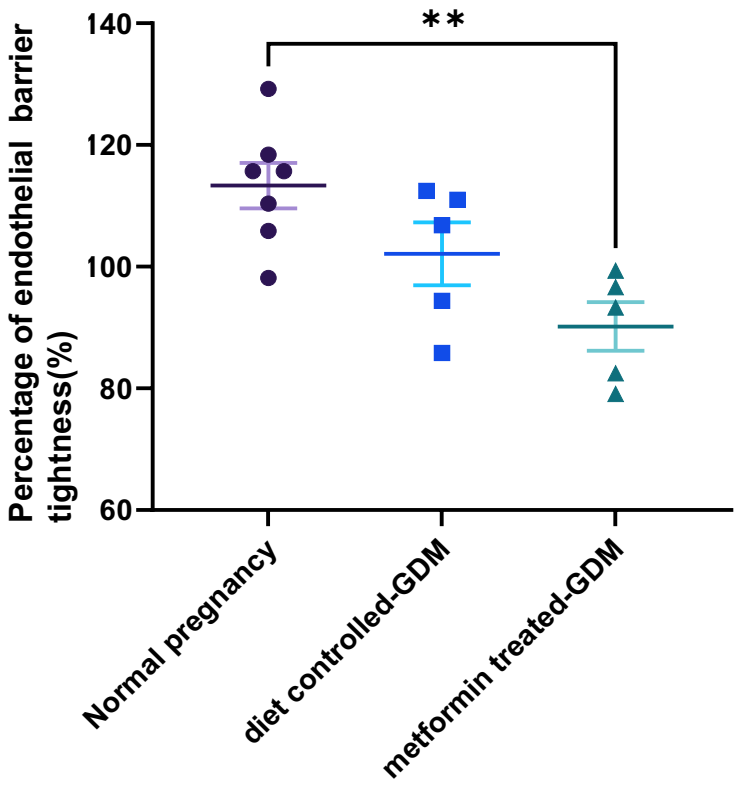


Figure 4-8 Graph displaying the effect of GDM treatment mode on the endothelial integrity enhancing ability of WJ-MSCs. Decreased % of endothelial barrier enhancement in the m-GDM group compared to the control group, (One-Way ANOVA test, P <0.005). Four independent experimental repeats were performed.

4.6 Discussion

Wharton's jelly mesenchymal stem cells have a potent stabilising effect on vascular endothelium, decreasing endothelial permeability. They have regenerative properties to restore and repair injured tissues. The data obtained provide an understanding of the effect of mesenchymal-endothelial cell contact on vascular permeability. WJ-MSCs from normal pregnancy could be able to enhance the endothelial function by improving the vascular integrity observed in the decreased tracer leakage in the co-culture (HUVEC + nWJ-MSCs) compared to the HUVEC monolayer. This effect might be dependent on increased VE-cadherin junctional expression observed in the co-culture immunofluorescence studies (3.34) Vascular permeability starts with breaking the junctions by VE-cadherin phosphorylation in response to permeability factors, such as VEGF. Decreased VE-cadherin Tyr731 phosphorylation and increased VE-cadherin in the plasma membrane were observed when HUVECs are co-cultured with MSCs (Pati et al., 2011).

The proximity between the WJ-MSCs and the HUVECs *in situ* and their developmental origins may make these stem cells more responsive to peri-vascular lineage commitment and may explain the reported vascular repair potential of WJ-MSCs. WJ-MSCs migrated to their perivascular niches across the endothelial monolayer, induced endothelial repair, and reduced permeability once the abluminal surface is reached suggesting that these cells can play a pericytic role in the vascular system (Ebrahim and Leach,2015).

Fetal cells cross the placental barrier throughout gestation and can be detected in the mother's peripheral blood from the first trimester of pregnancy and persist for decades after birth (Parant et al., 2009). Fetal cells have been demonstrated at sites of maternal injury and may have a role in the pathogenesis of maternal diseases and the repair of maternal tissues (Bianchi et al., 2021). Fetal cells in the mother's body may have important consequences for the immune status of women, influencing autoimmunity and tolerance to transplants (Dawe et al., 2007).

Our data showed that gWJ-MSCs can transmigrate across HUVEC monolayers reaching the sub-endothelial niche (3.4.7) but could not tighten the endothelial barrier as evidenced by increased albumin-FITC leakage. It can be related to the observed reduced VE-cadherin junctional localisation. Moreover, the increased VEGF secretion from gWJ-MSCs (shown in our previous chapter) might play a role in the deficient ability of those cells to maintain the endothelial barrier integrity. Endothelial cells loosen their junctions, increasing the permeability in response to VEGF (Carmeliet and Jain, 2011).

In this study, the finding revealed that gWJ-MSCs from metformin treated-GDM group made the endothelial barrier more permeable (23.2%) than the ones from normal pregnancy and (12 %) than the ones from d-GDM groups. It was observed before that mothers in the m-GDM group had the highest BMI compared to the normal and the diet group. Moreover, the cells from the m-GDM group displayed the most migration from the cord pieces, suggesting that metformin might play a role in stimulating the cell migration from the cord. Whether these findings from the metformin-treated group related to the drug itself or not, cannot be elucidated, due to the small number of samples done in the permeability study from the m-GDM group. *Villota et al 2021*, reported that placentas from metformin-treated GDM group presented stable expression of occludin gene suggesting the regulatory effect of metformin on occludin in GDM pregnancies (Villota et al., 2021). Metformin is known to cross the placenta and has been found in fetal circulation (Charles et al., 2006) and its fetal levels are similar to the maternal levels (Eyal et al., 2010) nevertheless, its use in pregnancy and effect on the offspring is still under debate (see 6.3, pages 158-160) . In future experiments, HUVEC can be incubated with metformin aiming to investigate its role in vascular permeability.

Moreover, the deficient ability of gWJ-MSCs in enhancing the endothelial barrier integrity might be related to the higher Endoglin expression in gWJ-MSCs compared to the nWJ-MSCs. *Ibanez et L 2020,* suggested that persistent ENG overexpression keeps endothelial cells in an active phase resulting in an impairment of endothelium stabilization and mural cell

recruitment (Ollauri-Ibáñez et al., 2020). Thus, investigating the role of Endoglin expressed in the WJ-MSCs on endothelial permeability was aimed in the next chapter.

5 CHAPTER 5 The Role of Endoglin in Endothelial Permeability

5.1 Introduction

Endoglin is a major marker antigen of mesenchymal stem cells. Its expression in WJ-MSCs isolated from GDM-complicated pregnancies was reported higher than those from normal pregnancies. However, it is soluble form has been proven to be increased in PE and diabetes (Leaños-Miranda et al., 2019), ENG's role in gestational diabetes is still unclear. This may be one of the confounding factors that lead to a higher risk of later vascular dysfunction in the offspring. Endoglin (Eng; 180-kDa), is a transmembrane glycoprotein acting as a co-receptor for TGF-β, binding bone morphogenetic protein 9 (BMP9) and BMP10 (Saito et al., 2017), and playing a pivotal role in vascular haemostasis, vascular remodelling, and angiogenesis (Schoonderwoerd et al., 2020). Alternative splicing of ENG mRNA generates two isoforms: the long L-Endoglin and the short S-Endoglin. The two forms differ in the structure of the cytoplasmic domain and can decrease or enhance TGF-β signalling, respectively under different conditions by interacting with ALK1 or ALK5 (Bellón et al., 1993).

5.1.1 Endoglin Role in Mesenchymal Stem Cells

Endoglin is expressed on the mesenchymal stem cell surface and also in hemangioblasts at the early hematopoietic development stage (Borges et al., 2012). ENG expression level on MSCs surface is closely connected with their differentiation state (Maleki et al., 2014) and immunomodulatory potential (Anderson et al., 2013). ENG is absent in all immune cells and is only induced by the activation of monocytes into macrophages. Its role in stem cells may be to conserve the stem cell potential, preventing the precursor cells from differentiation by modulating the TGF-β and BMP effects on lineage determination, reviewed in (Gregory et al., 2014). Studies have revealed that the absence of endoglin expression on mouse and human MSCs leads to a more differentiated MSC phenotype, with increased osteogenic gene expression (Levi et al., 2011, Rosu-Myles et al., 2010).

5.1.2 Membrane Endoglin Role in Endothelial Cells

Endoglin is predominately expressed in activated endothelial cells (Gougos and Letarte, 1988), and was first identified as a major TGF-*β* binding glycoprotein in HUVECs by (Cheifetz et al., 1992). TGF-*β* plays a vital role in angiogenesis and can have both anti-angiogenic and proangiogenic roles. TGF-β via ALK5 promotes Smad2/3 phosphorylation that inhibits proliferation and migration of the ECs whereas, via ALK1 it promotes Smad1/5 phosphorylation that promotes them (Figure 5-1). Endoglin has a pivotal role in the balance of ALK1 and ALK5 signalling to regulate endothelial cell proliferation. ENG is required for efficient TGF-β/ALK1 signalling, which indirectly inhibits TGF-β/ALK5 signalling. ENG-deficient endothelial cells stop proliferation due to reduced TGF-β/ALK1 signalling and promoted TGF-β/ALK5 signalling, suggesting that Endoglin blocking can arrest angiogenesis (Lebrin et al., 2004, Gore et al., 2014).

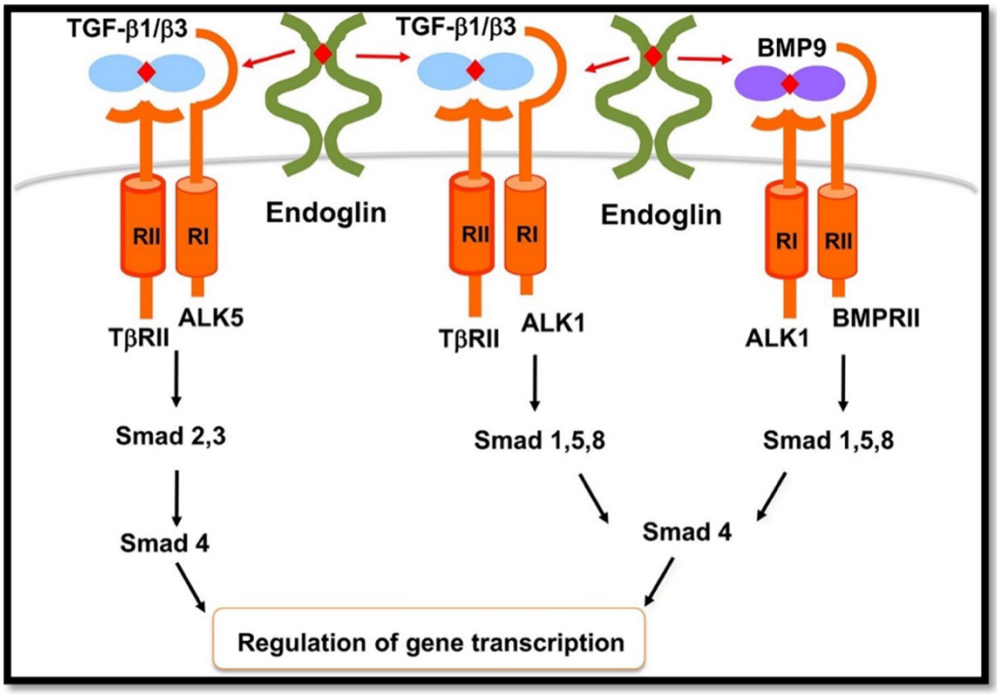


Figure 5-1 Schematic diagram illustrating the Endoglin role in angiogenesis, TGF-β and BMP9 signalling pathways in endothelial cells, taken from (Gregory et al., 2014).

Endoglin Role in Vascular Haemostatsis

Normal human pregnancy is accompanied by increased blood volume which is accommodated by systemic vasodilatation. This vasodilatation involves increased NO formation to maintain lower peripheral vascular resistance in healthy pregnant women (Toporsian et al., 2005, Williams et al., 1997). ENG can regulate NO-dependent vasodilatation. ENG upregulates eNOS expression and function via Smad2 upregulation and phosphorylation, which results in increased eNOS expression both in the absence and/or in the presence of exogenous TGF-β1 in endothelial cells (Santibanez et al., 2007). ENG was found to localize to caveolae, where it can associate with eNOS and regulate its activity and local vascular tone (Toporsian et al., 2005). Moreover, ENG-deficient endothelial cells cannot generate NO in response to Ca2+-dependent eNOS activation (Toporsian et al., 2005), suggesting that ENG is not only essential for cardiovascular development but also vascular haemostasis.

Endoglin and VEGF cooperation

ENG and VEGF are both essential markers for angiogenesis and vasculogenesis. Mice that lack either ENG or VEGF-A die at E 10.5 (Li et al., 1999) or E8.5 (Carmelie et al., 1996) respectively as a result of vascular malformation. Endoglin mutation or blocking severely affects the VEGF-induced ECs sprouting, growth, migration, and tube formation (Liu et al., 2014b). Tumour-associated angiogenesis is initiated by VEGF induced-hypoxia. ENG can also be upregulated under hypoxic conditions suggesting the cooperation between ENG and VEGF to promote tumour-associated angiogenesis. Tip cell formation and sprouting are mediated by the agonistic effect of VEGF on VEGFR2 (Gerhardt et al., 2003). ENG and VEGFR2 form a complex at the cell surface. ENG promotes its stability which contributes to maintaining tip cell phenotype and VEGF-induced sprouting (Tian et al., 2018). Loss of ENG promotes VEGFR2 internalization, it also promotes VEGFR2 trafficking to the lysosome and degradation (Gore et al., 2014).

5.1.3 Endoglin's Molecular Structure and Its Role as an Adhesion Molecule in Endothelial Cells

Endoglin is a type I integral membrane protein with an extracellular domain of 561 amino acids, a hydrophobic transmembrane domain, and a 47-intracellular domain (Gougos and Letarte, 1990). ENG has a Zona pellucida (ZP) domain of the extracellular region close to the transmembrane region that has an RGD tripeptide (Jovine et al., 2005). The RGD sequence (Arg-Gly-Asp) is the cell attachment site of adhesive ECM, and cell surface proteins (Gougos and Letarte, 1990). The RGD tripeptide is involved in integrin-based interactions with ECM proteins, including fibronectin, fibrinogen, prothrombin, and thrombospondin (Ruoslahti, 1996). Endothelial ENG interacts with leukocyte integrin α5β1 via the RGD tripeptide motif, and this adhesion process suggests a regulatory role for ENG in trans-endothelial leukocyte migration (Rossi et al., 2013).

5.1.4 Regulation of Endoglin Expression

ENG is also expressed on vascular smooth muscle cells (Bot et al., 2009), fibroblasts (St-Jacques et al., 1994), hepatic stellate cells (Meurer et al., 2019) and activated monocytes, and macrophages(Lastres et al., 1992). Changes in Eng expression are predominantly associated with several pathological conditions, including Hereditary hemorrhagic telangiectasia (HHT) (McAllister et al., 1994), cancer, angiogenesis (Minhajat et al., 2006), heart development (McAllister et al., 1994), fibrosis (Alsamman et al., 2018), and endothelial dysfunction (Vicen et al., 2019). ENG is specifically upregulated on proliferating endothelium and was found to be expressed on tumour vessels of brain, breast, colon, lung, and stomach cancer (Trentin Brum et al., 2019, Kauer et al., 2019). *Chadchan et al., 2016*, explored the role of endoglin in the uterine receptivity for embryo implantation in a murine model and identified increased endoglin expression in the endometrium during the implantation and reduced implantation index following ENG knockdown (Chadchan et al., 2016).

Induced endoglin expression by hypoxia involves synergic stimulation and formation of the Smad3/Smad4 transcriptional complex, stimulating hypoxia-inducible factor-1, leading to a cooperative effect of these factors on endoglin transcription (Sánchez-Elsner et al., 2002). TGF-β signalling, via Smad transcription factors, also potently stimulates ENG expression (Lastres et al., 1992). Tumour necrosis factor-α decreases Endoglin protein levels in endothelial cells (Li et al., 2003). Mutations in the Eng gene lead to a lower expression of the protein on the endothelial cell surface. ENG mutations are responsible for HHT type I disease, which is a vascular pathology leading to bleeding from arteriovascular malformations (AVMs), which are direct connections between arteries and veins (Ruiz-Llorente et al., 2017).

5.1.5 Endoglin Role in Vessel Branching, Maturation and Quiescence

In a healthy adult, quiescent endothelial cells have long half-lives, are ensheathed by pericytes and are protected by the autocrine action of maintenance signals, such as VEGF, Angiopoietin-1, and FGFs (Carmeliet and Jain, 2011). Quiescent endothelial cells form a monolayer of phalanx cells with a streamlined surface, interconnected by junctional molecules such as VE-cadherin, occludins, and claudins (Carmeliet, 2003, Leach et al., 2002).

When a quiescent vessel senses an angiogenic signal, such as VEGF, VEGF-C, ANG-2, FGFs, or chemokines, released by a hypoxic, inflammatory, or tumour cell, pericytes first detach from the vessel wall (in response to ANG-2) and liberate themselves from the basement membrane by proteolytic degradation which is mediated by matrix metalloproteinases (MMPs). Endothelial cells loosen their junctions, and the nascent vessel dilates. VEGF increases the permeability of the endothelial cell layer, causing plasma proteins to extravasate and lay down a provisional extracellular matrix scaffold. In response to integrin signalling, endothelial cells migrate onto this ECM surface. Activated ECs start to proliferate in response to VEGF or basic fibroblast growth factor (bFGF or FGF-2) and form a new sprout. Loosening of cell-cell contacts can also result in the fusion of capillaries to form arteries and veins (Carmeliet and Jain, 2011).

VEGF-induced receptor trafficking plays an essential role in VEGF signalling and angiogenesis, *Tian et al* stated that endoglin promotes cell surface retention of VEGFR2 by inhibiting VEGF-A mediated internalization and lysosomal degradation of VEGFR2 (Tian et al., 2018).

Considerable crosstalk between the ENG and VEGF pathways has been reported (Liu et al., 2014b, Paauwe et al., 2016, Liu et al., 2021). In an orthotopic pancreatic cancer xenograft model, Endoglin was one of three genes that significantly upregulated in response to VEGF blockage (Bockhorn et al., 2003). In colorectal cancer patient samples, it was observed that endothelial Smad1 phosphorylation was increased in response to treatment with anti-VEGF therapy (Romero et al., 2011). *Paawe et al* reported upregulated ENG pathways in response to VEGF inhibition while investigating combined targeting of the ENG and VEGF pathway that may result in enhanced inhibition of angiogenesis. (Paauwe et al., 2016).

5.1.6 Soluble Endoglin

Endoglin is cleaved by type-1 matrix metalloproteinases 14 to form soluble endoglin (sEng), which is released into the circulation (Hawinkels et al., 2010). It is known to have an anti-angiogenic effect. Increased levels of sEng were recorded in patients with early stages of preeclampsia (Leaños-Miranda et al., 2019), (Blann et al., 1996), diabetes mellitus (Blázquez-Medela et al., 2010), and familial hypercholesterolemia (Blaha et al., 2008). The observed higher levels of sEng plasma concentration in patients with advanced DM positively correlated with the severity of diabetic vascular complications, such as retinopathy that is characterized by upregulated VEGF (Blázquez-Medela et al., 2010). Increased sEng was recorded in the adipose tissue samples from women with GDM (Lappas, 2014). High levels of circulating sEng released from the placenta in pregnancies complicated with preeclampsia correlated well with disease severity, and falls after delivery (Levine et al., 2006).

sEng impairs the binding of TGF-β1 to its receptors (TβRII) and downstream signalling attenuating eNOS activation responsible for

hypertension noted in preeclampsia. sEng is known to inhibit the formation of capillary tubes in vitro and induce vascular permeability and hypertension in vivo. Excess sEng is expected to co-work with excess placenta-derived soluble VEGF receptor 1 to amplify endothelial dysfunction and induces clinical signs of severe preeclampsia, the possibility to develop HELLP syndrome (haemolysis, elevated liver enzymes, and low platelet count), and fetal growth restriction (Lappas, 2014).

5.1.7 Knockdown of Gene Expression

Gene-specific degradation of mRNA can silence individual gene expression post-transcriptionally. RNA interference (RNAi) is one of the most widely used technology to induce gene-specific RNA degradation. RNAi is a multi-step process initiated by the addition of double-stranded RNA (dsRNA). (Abudayyeh et al., 2017, Krohn-Grimberghe et al., 2020). RNA interference molecules are a group of non-coding RNAs which are composed of several categories, such as short interfering RNA (siRNA), microRNA (miRNA), and piwi-interacting RNAs (PiRNA) (He and Hannon, 2004, Aravin et al., 2007, Tam et al., 2017). The small interfering RNAs (siRNAs) are 21- to 23-nt that work as mediators of sequence-specific mRNA degradation generated by ribonuclease III cleavage from longer dsRNAs. siRNA duplexes trigger specific gene silencing in mammalian somatic cells with no unspecific interferon activation (Martinez et al., 2002).

5.2 Aim

Endoglin expression was higher in gWJ-MSCs compared to nWJ-MSCs at P-2, with no difference between d-GDM and m-GDM. Furthermore, gWJ-MSCs after transmigration did not enhance the endothelial barrier integrity and were associated with increased endothelial permeability in the co-culture studies. Therefore, the study aimed to investigate whether the compromised ability of gWJ-MSCs to tighten the HUVEC barrier is via an ENG/VEGF-dependent mechanism.

The main objectives of this chapter:

- To investigate the effect of endoglin silencing on the VEGF secretion by WJ-MSCs.
- To investigate the adhesion and transmigration of silenced WJ-MSCs through the HUVEC monolayer.
- To compare the effect of ENG $^{-/-}$ WJ-MSCs and ENG $^{+/+}$WJ-MSCs on the barrier integrity of human umbilical vein endothelial cell monolayer and the junctional VE-cadherin.

5.3 Materials and Methods

Table 5-1 List of chemicals and reagents used in the transfection studies.

Reagent	Company
Lipofectamine™ RNAiMAX Transfection Reagent	Invitrogen, USA
Opti-MEM™ I Reduced Serum Medium	Gibco,UK
SiRNA-1 (assay ID s4677) sequence 5′-UGACCUGUCUGGUUGCACAtt-3′	Ambion, Life Technology
SiRNA-2 (assay ID s4679) sequence 5′-CAAGUAUGAUCAGCAAUGAtt -3′)	Ambion, Life Technology
scrambled siRNA-1 (AM4611)	Ambion, Life Technology
scrambled siRNA-2 (AM4613)	Ambion, Life Technology
Endoglin Monoclonal Antibody (SN6), PE	eBioscience, UK
Purified mouse antihuman vascular endothelial (VE)-cadherin (CD144)	Pharminogen, BD Biosciences, UK
PK67 Green Fluorescent Cell Linker Kit for General Cell Membrane Labelling	Sigma-Aldrich, UK
Anti-goat IgG (whole molecule)–TRITC antibody produced in goat	Sigma-Aldrich, UK

5.3.1 Study Design and Subjects

Transfection studies and gene knockout experiments were done with WJ-MSCs isolated from three normal donors. The clinical characteristics of the study population that had samples used for Endoglin knockdown in WJ-MSCs and the followed permeability assays are shown in (Table 5-2).

Table 5-2 Clinical characteristics of the study population used for Endoglin knockdown in WJ-MSCs and the followed permeability assays.

Characteristic	N240621 (N-1)	N240521 (N-2)	N090321(N-3)
Maternal age, years	36	36	23
Maternal BMI, Kg/m²	21	22	20
Gestational age at delivery, weeks	40	39	39+4
Placental weight, g	690	458	588
Baby weight, kg	3.91	3.15	3.25
birthweight centile [gender]	93.55 (F)	52.25 (F)	61.75 (F)

Data are presented as individual values.

5.3.2 WJ-MSCS and HUVEC Transfection by siRNA Endoglin.

Culturing WJ-MSCs and HUVECs

One vial of each HUVECs P0 and WJ-MSCs P0 (one million cells per vial) were thawed by removing from liquid nitrogen and placing in a water bath set to 37°C for 2 minutes. All the contents of the vial were transferred into the pre-warmed T75 flask with complete media and incubated at 37°C and 5% CO_2 overnight. The next day the media was changed after

checking the attachment of cells under a microscope to remove any remaining DMSO and unattached cells.

Splitting

The media was changed every 2-3 days till the cells reached 80-90% confluence. The media was removed from cells, washed twice with sterile PBS, and split using 5mL of trypsin/EDTA per T75 flask. HUVEC and WJ-MSCs were incubated at 37°C for 2 minutes and 5 minutes respectively. Then 20 mL complete media was added to each flask to neutralise trypsin, and the cell suspension was transferred to a falcon and centrifuged at 1000 rpm for 5 minutes to pellet the cells. The cell pellet was suspended in the desired amount of cell media. Cell count was performed to ensure a viability more than 95%.

Knockdown by siRNA

To start the silencing experiment 250,000 HUVEC or WJ-MSCs (Passage-1) were plated per well (6-well plate) and incubated with 3mL complete media per well overnight. After 24h cell attachment was checked, and confluence was ensured to be around 80%. For each condition (knockdown and non-silencing control) two transfection solutions were prepared; solution-1: 30uLof Endoglin silencer 1 and silencer 2(siRNA-1and siRNA-2) or the silencer select negative control 1 and silencer select negative control 2 (at a concentration of 20uM) and 270uL Opti-MEM, and Solution-2: 22.5 uL Lipofectamine RNAiMAX and 277.5 uL Opti-MEM. Solutions 1 & 2 were mixed gently and incubated at room temperature for 5 minutes. Then both were mixed and incubated for 20 minutes at room temperature creating a 600uL (3 wells). The media was aspirated from the cells and gently the cells were washed twice with 1mL DPBS. Then 800uL of Opti-MEM was added to each well followed by 200uL dropwise of oligo/lipofectamine duplex to each well for the appropriate condition. Afterwards, the cells were incubated at 37°C for 4 hours before replacing the transfection media with complete media without antibiotics. In the second experiment, the transfection time was prolonged to 24h and 48h. For the best condition, the transfection time was set at 24h in all the following experiments then the transfection media was changed with complete media without antibiotics. Specific silencing of

targeted genes was confirmed by at least three independent experiments (Figure 5-2).

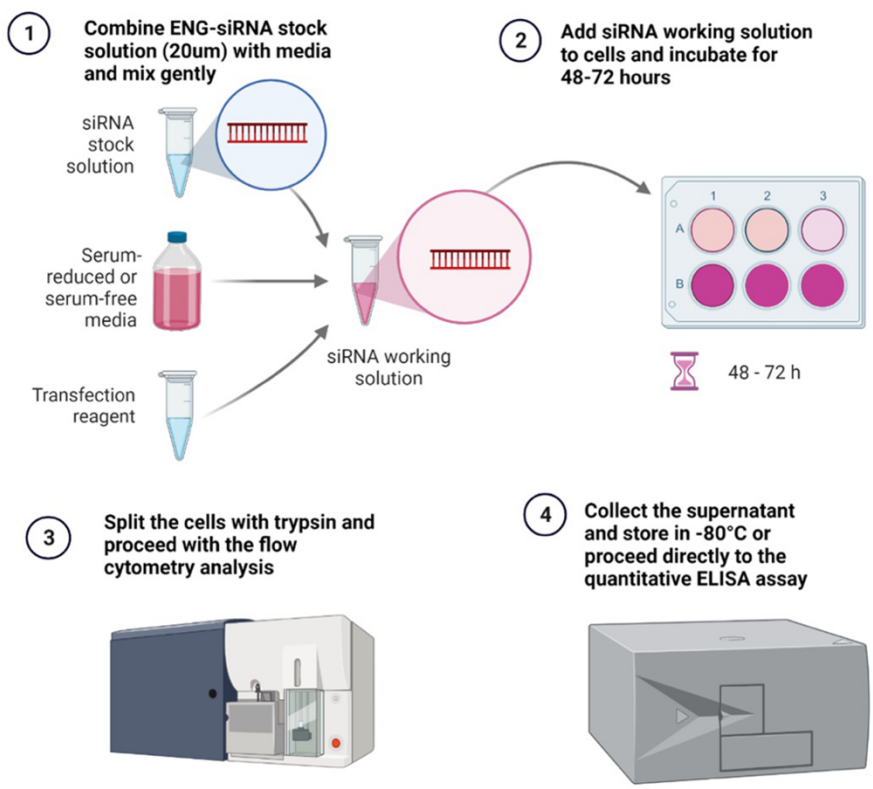


Figure 5-2 Diagram displaying the workflow for gene interference using siRNA transfection. Created with BioRender.com.

5.3.3 Flow Cytometry for Transfected Cells

The cells were harvested 72-hours post-transfection using Trypsin/EDTA after washing the cells with DPBS carefully not to detach the cells. The cells were observed every 2 minutes. WJ-MSCs and HUVEC were harvested after 5 and 2 minutes respectively with complete media four times the volume equal to the trypsin volume amount. Then the cell suspension was centrifuged at 1000 rpm for 5 min. The cells were counted and re-suspended at a concentration of $5x10^6$/mL to 1x 10^7/mL in the washing buffer (1% FBS in PBS). Then they were incubated with 5 µL Anti-Human CD105 (Endoglin) PE for 30 min at RT in the dark. Finally, the cells were washed twice before re-suspending in 300µL staining buffer to be ready for analysing by CANTO II cytometer.

5.3.4 ELISA Quantification of VEGF Secreted from ENG^{--}WJ-MSCS

The supernatant was collected from the culture well after 48 hours (2ml) centrifuged at 1900 rpm at 4°C for 10min to remove any debris or dead cells. Samples were kept in -20°C till processed. ELISA technique was done as described before (3.3.5) (pages 58 & 59).

5.3.5 Co- Cultures Studies, VE-Cadherin Immunocytochemistry and Systemic Random Sampling

To obtain co-cultures of HUVEC 100,000 cells were seeded on 1% gelatin- coated coverslip (19mm diameter) and incubated in endothelial media till reached 70% confluence, the media was changed to mixed media. When the cells reached full confluence (18-24h), 20,000 PKH-67 green dye labelled WJ-MSCs either ENG$^{-/-}$ or ENG$^{+/+}$ were seeded on top of the confluent monolayer of HUVEC (1:5) per coverslip in 1mL mixed media (50% stem cell media+ 50% EGM) (Transfected HUVECs weren't included in the co-culture or permeability studies as they didn't survive and started to detach on day-3).

Co-cultures of the HUVEC and WJ-MSC were fixed with 4% PFA in 1X PBS at different intervals (2 and 24 hours). Permeabilization was done using 0.15% triton X-100 in 0.1% BSA/PBS for 10min, blocking with 5% goat serum in PBS for 30min and incubation overnight at 4° C with mouse anti-human CD144 (VE-cadherin) 10µg/mL. Cells were washed with 0.1% PBS/BSA and incubated with TRITC goat anti-mouse IgG diluted (1:50) in 0.1% BSA/PBS for two hours in the dark at room temperature.

The coverslips were mounted using Vectorsheild and analyzed by a Nikon fluorescence microscope with the appropriate filter to allow visualization of both PKH 67 (The optimum excitation wavelength Ex is 490 nm, and the emission wavelength Em 502 nm) and TRITC ((Ex max 547 nm/Em max 572 nm). The slides from the two groups; (HUVEC+ ENG$^{-/-}$WJ-MSCs) and (HUVEC+ ENG$^{+/+}$WJ-MSCs) were labelled, ten images per

coverslip were taken by NIS systems software (the group label was blinded) and the counting was done using Image J software.

5.3.6 Quantitative Analysis of Junctional VE-Cadherin Expression

See the method as described before (3.3.7) at pages 60 & 61 (Leach et al., 2004).

5.3.7 Effect of ENG Knockdown in WJ-MSCs on the Permeability of HUVEC (Co-Culture Permeability Study)

To investigate the effect of ENG silencing in WJ-MSCs on the permeability of the endothelial cells, the tracer leakage FITC-albumin was measured in the basal compartment at three different times 24 hours after co-culturing the $ENG^{-/-}$WJ-MSCs or $ENG^{+/+}$WJ-MSCs with HUVEC. WJ-MSC (ENG^{++} and ENG^{--}) (10,000 cells) were placed on top of the HUVEC monolayer that had been seeded before on the transwell inserts using the mixed media without phenol red. After 24 hours, the wells were washed with DPBS, FITC-albumin (1mg/ml) (500µL) was added to the apical chamber, and unlabelled albumin (1500 µL) was added to the basal chamber (Figure 5-3).

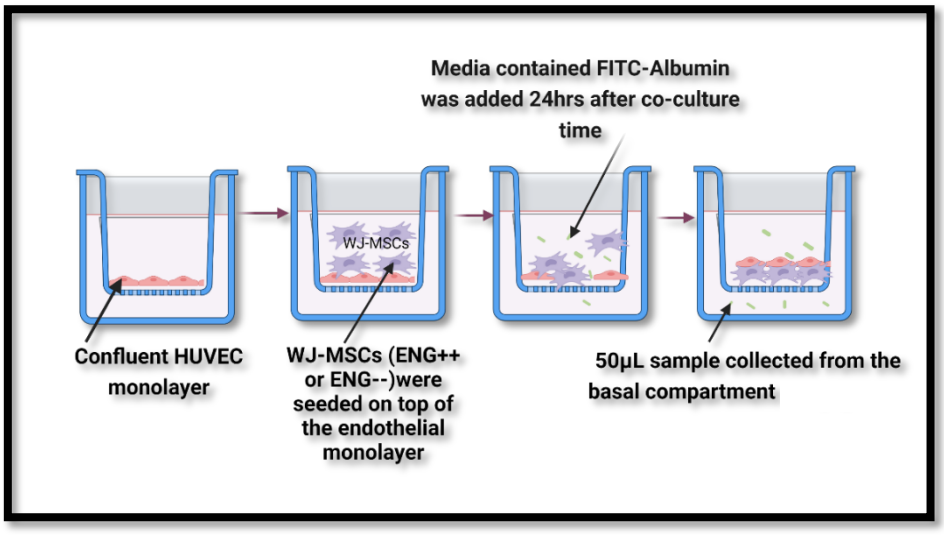


Figure 5-3 Diagram illustrating the co-culture permeability assay done after the ENG silencing in WJ-MSCs.

Samples (50 µL) were collected from the lower compartment at 2, 4, and 24 hours intervals, and replaced with the same volume of medium. The optical density was measured using by a fluorescence plate reader (SpectraMax M2e) using SpectraMax Pro7 application at an emission/excitation wavelength of 495/520 nm. Concentration of FITC–albumin in each sample was calculated via linear regression of a serial dilution series of the tracer (Figure 5-4). The data are expressed as the amount of leaked protein to the basal compartment in the two co-culture groups (HUVEC+ WJ-MSCs^{-}and HUVEC+ WJ-MSCs $^{++}$). Unpaired *t* test was used to test the statistical difference; Internal repeats (x3) from three different isolates were compared. Three experimental repeats were done to get the results.

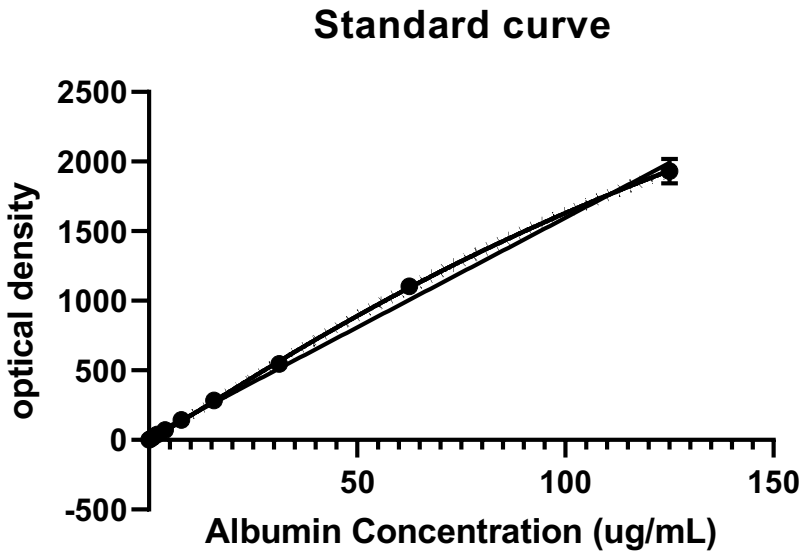


Figure 5-4 Graph displays the standard curve used to interpolate the unknown FITC-albumin concentrations.

5.4 Results

5.4.1 Confirmation of ENG Silencing by Flow Cytometry

Transfection time (4h)

Flow cytometry analyses showed that the number of HUVECs expressing CD-105 was reduced by 98.32% when the cells were incubated with the transfection duplex (siRNAs in transfection reagent) for only four hours then the duplex was replaced with complete media (Figure 5-6), unlike the WJ-MSCs, the ENG expression was only reduced by 87.79% (Figures 5-5a & d).

Transfection time (24h)

Flow cytometry analyses showed that the number of WJ-MSCs expressing CD-105 was reduced by 95.6% ± 1.87 when the cells were incubated with the transfection duplex for 24h (Figures 5-5 b & e), or 48h (Figures 5-5 c & f).

CD-105 expression in WJ-MSCs after ENG-siRNAs transfection

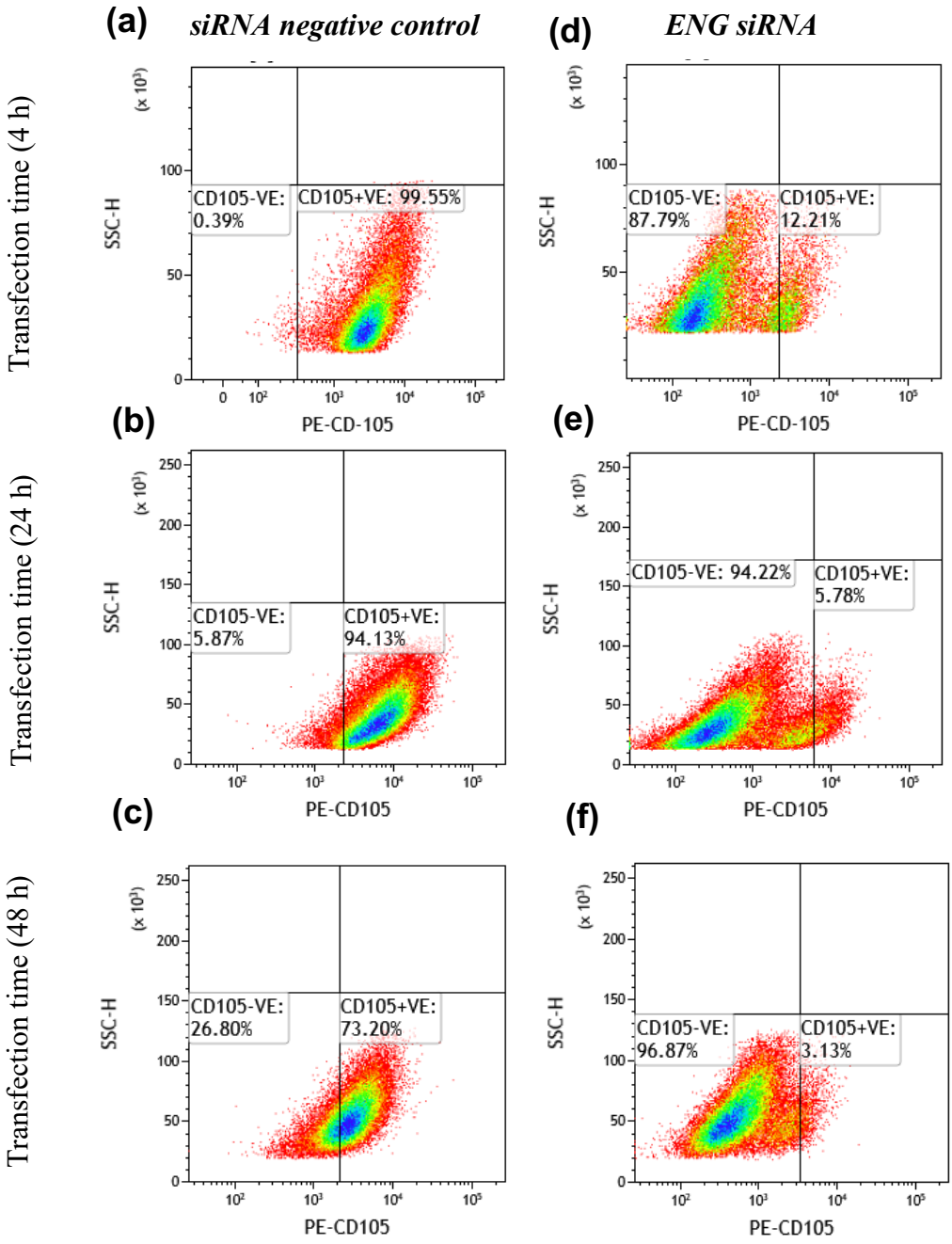


Figure 5-5 Flow cytometry analysis of Endoglin expression after ENG siRNA transfection in WJ-MSCS. Endoglin silencing was 95.6 %± 1.9 efficient confirmed by flow cytometry at the protein level. Density diagrams (**d, e & f**) displaying the percentage of Endoglin expression in WJ-MSC (P-1) after ENG siRNAs transfection and density diagrams (**a, b & c**) displaying the percentage of Endoglin expression in WJ-MSC after non-silencing siRNAs transfection as a control for 4, 24 and 24h respectively. Representative sample out of 3 experimental repeats.

CD-105 expression in HUVECs after ENGsiRNAs transfection

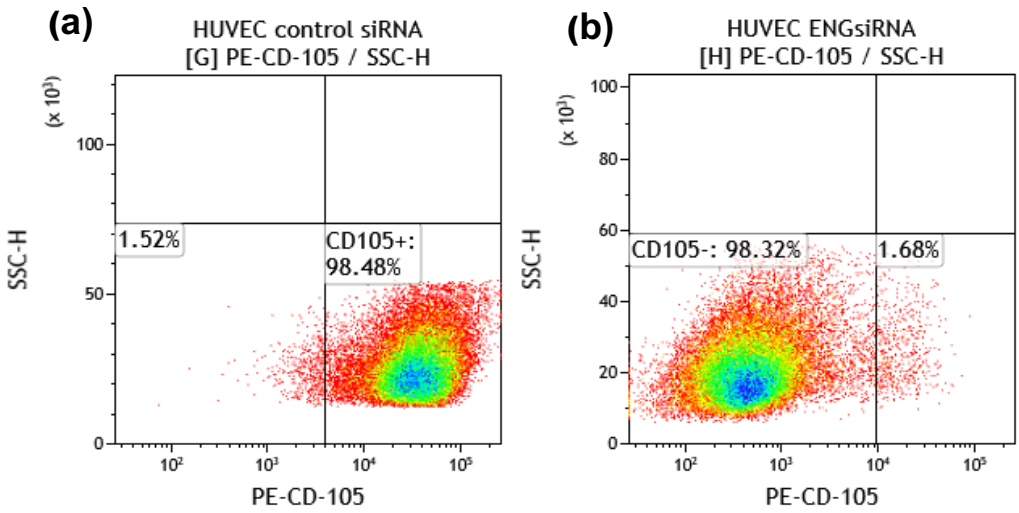


Figure 5-6 Density diagrams displaying the Endoglin expression in HUVEC after ENG siRNA transfection (**b**) and non-silencing transfection control (**a**). Representative sample out of 3 experimental repeats.

5.4.2 Cell Attachment and Morphological Changes after ENG Silencing

Incubation of the WJ-MSCs with the siRNA transfection duplex did not affect their attachment, and they displayed the same morphology compared to the siRNA-transfected control cells and the non-transfected control cells (Figures 5-7). On sub-culturing the silenced WJ-MSCs displayed the mixed morphology same as the control ones (Figure 5-8). However, the HUVECs displayed the same morphology after siRNA transfection compared to the non-silenced transfected control, the silenced HUVECs started to detach 72h after ENG silencing compared to the non-silenced HUVECs and WJ-MSCs (Figure 5-9).

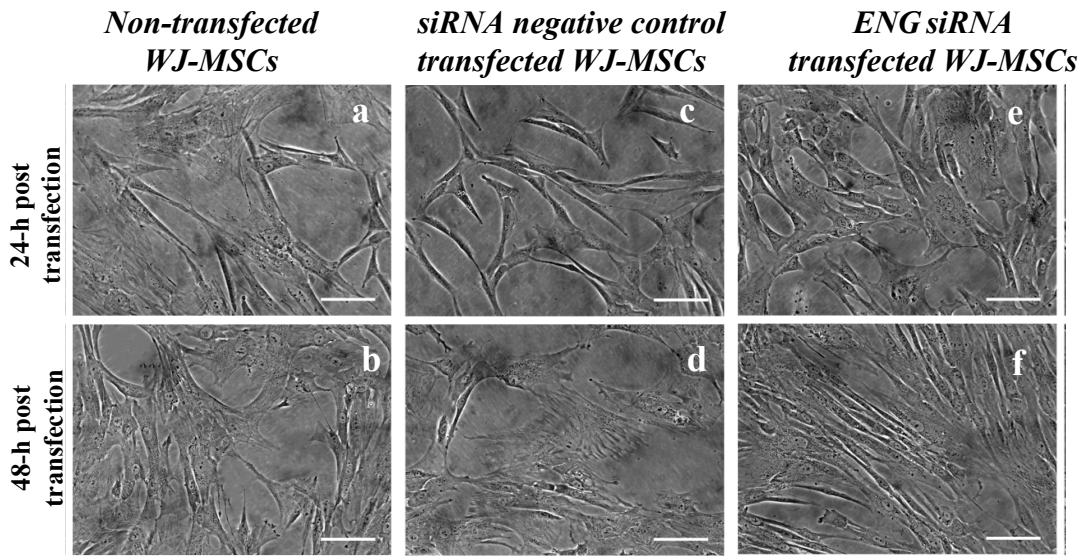


Figure 5-7 Representative phase contrast microscopic images of WJ-MSCs displaying no morphology changes after ENG siRNA transfection. Images (**e** & **f**) are showing ENG silenced WJ-MSCs, images (**c** & **d**) are showing non-silenced transfected control WJ-MSCs, and images (**a** & **b**) are showing non-transfected control WJ-MSCs, scale bar= 100µm. Representative sample out of 3 experimental repeats.

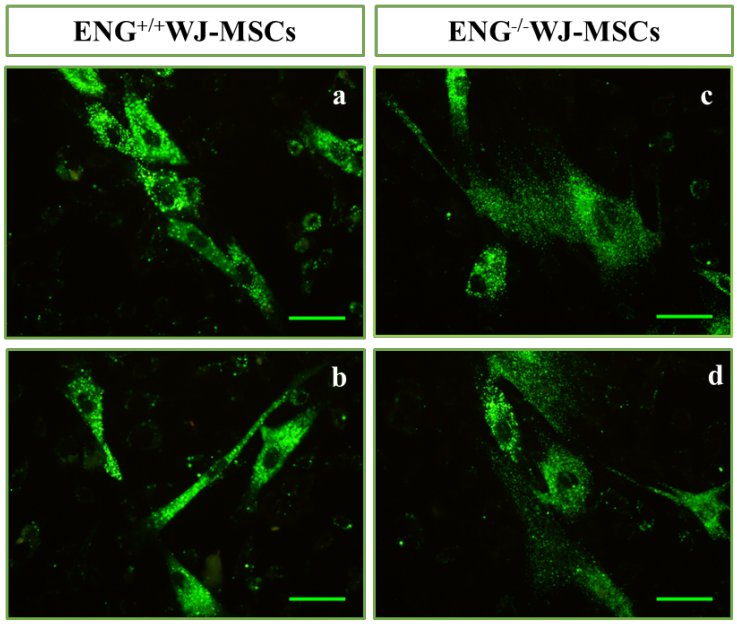


Figure 5-8 Representative micrographs displaying no morphological changes observed after ENG knockdown in WJ-MSCs (PKH-67 labelled) (**c** & **d**) compared to the control (**a** & **b**), scale bar = 40µm.

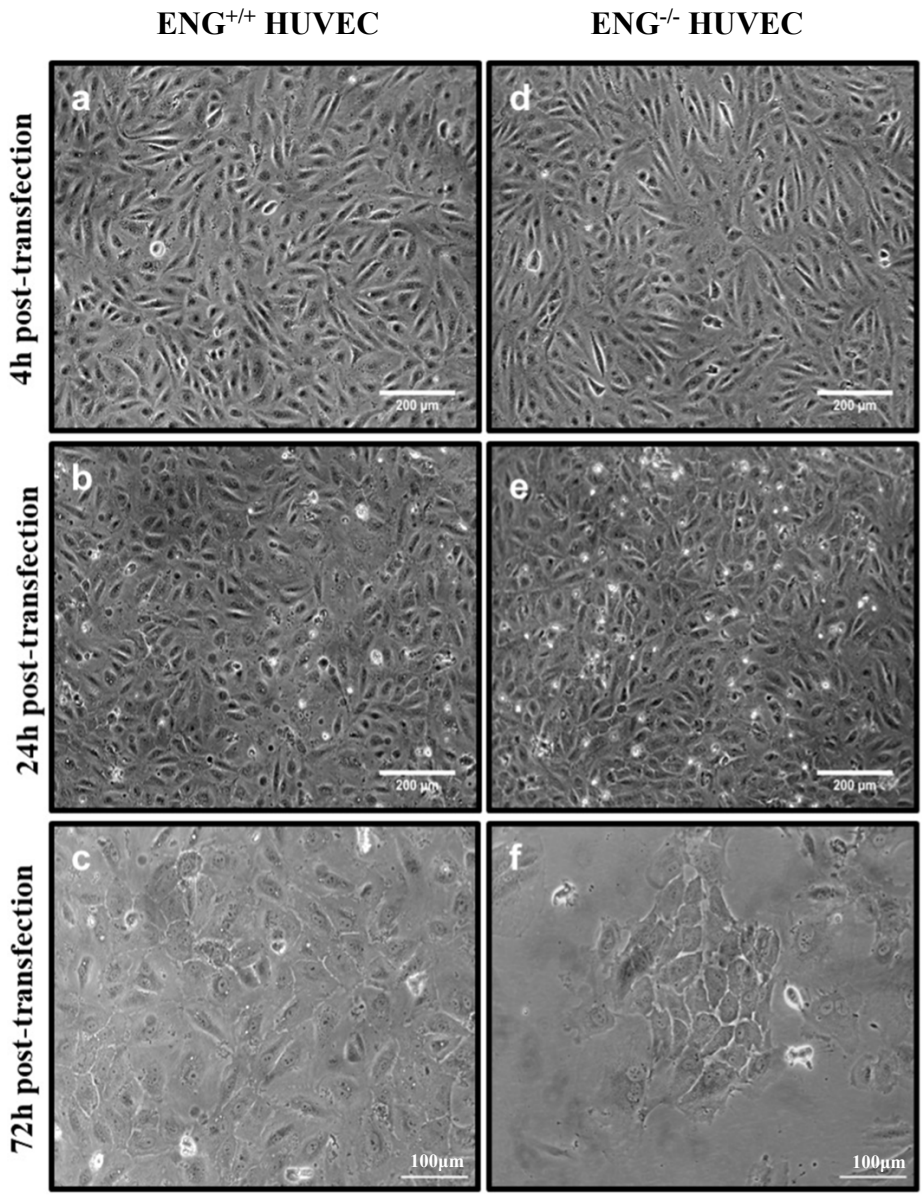


Figure 5-9 Representative phase contrast microscopic images of transfected HUVECs. Images (**d** & **e**) displaying the silenced HUVEC at 4h and 24h post silencing displaying no morphology changes compared to the non- silenced control (**a** &**b**), scale bar=200 µm. Image (**f**) displaying the silenced cells began to detach 72 h after ENG siRNA transfection compared to the non-silenced cells image (**c**), scale bar= 100µm.

5.4.3 Cell Viability % (Trypan Blue Staining), Sub-culturing and Cell Proliferation after ENG siRNA Transfection

Transfection of the WJ-MSCs has no significant effect on the cell viability (87%±2.1) compared to the (90.6%±9.5) in the siRNA non-silencing control P-value= 0.22 (Figure 5-10).

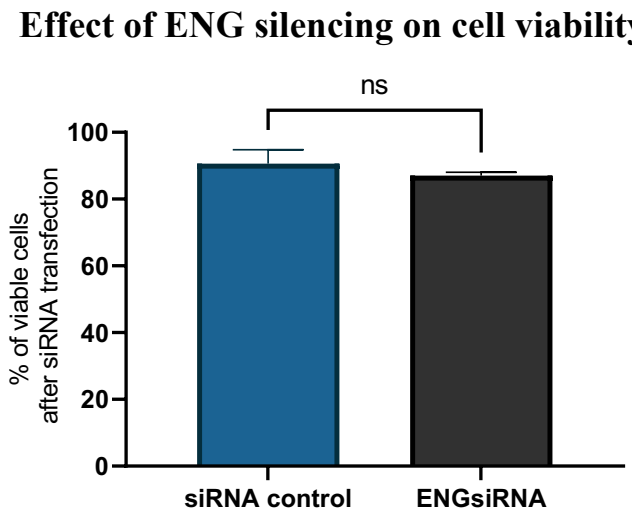


Figure 5-10 Graph presents the cell viability percentage in WJ-MSCs after ENG-siRNA transfection counted by Trypan blue dye (Unpaired *t* test P-value=0.22), Three independent experiments were performed.

After splitting the silenced and non-silenced WJ-MSCs. ENG$^{-/-}$WJ-MSCs displayed a smaller number of cells attached to the plate after 24h culture time and a smaller number of cells after 72h despite the same seeding density, compared to the control (ENG expressing cells) (Figure 5-11).

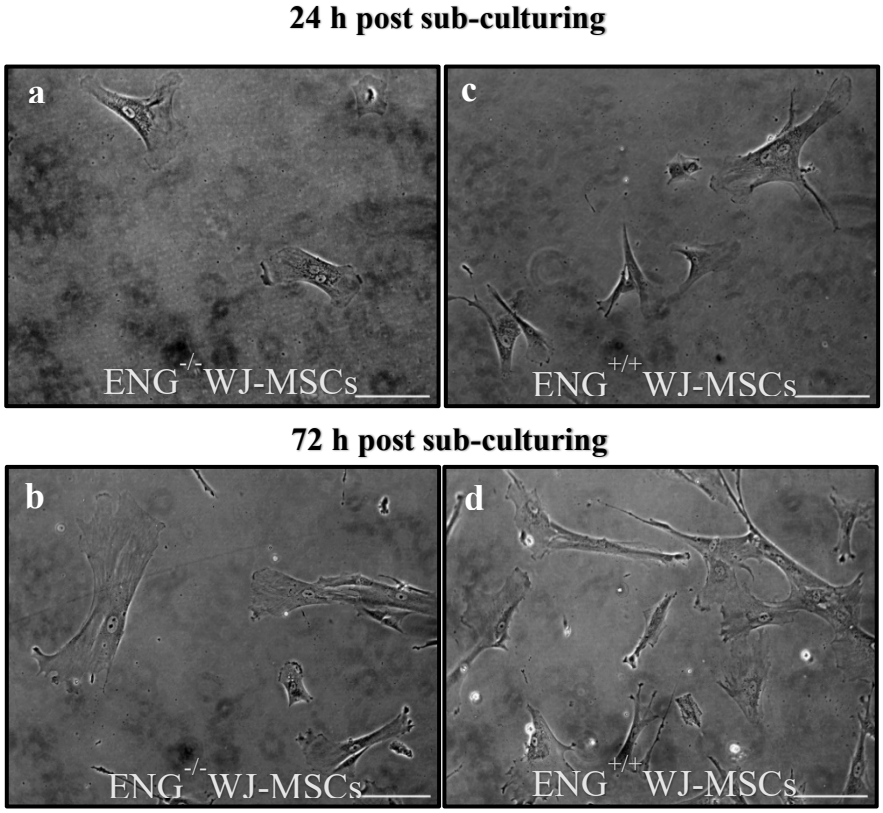


Figure 5-11 Phase contrast microscopic images (**a** & **c**) displaying reduced number of the silenced WJ-MSCs (**a**) attached to the plate 24 h after passaging compared to the non- silenced WJ-MSCs (**c**). Images (**b** &**d**) displaying a smaller number of $ENG^{-/-}$ cells 72 h after sub-culturing (**b**) compared to ENG^{++}cells (**d**), scale bar = 100µm. Representative sample out of 3 experimental repeats.

5.4.4 ELISA Quantification of VEGF-A Secreted from WJ-MSCs after Endoglin Silencing

The Endoglin deficient cells $ENG^{-/-}$WJ-MSCs secreted more VEGF-A (184.6 pg/mL ± 4.048) compared to the control group $ENG^{+/+}$WJ-MSCs (87.93 pg/mL ± 8.508) *P* value ≤0.0001, three independent experiments were done to obtain the results (Figure 5-12).

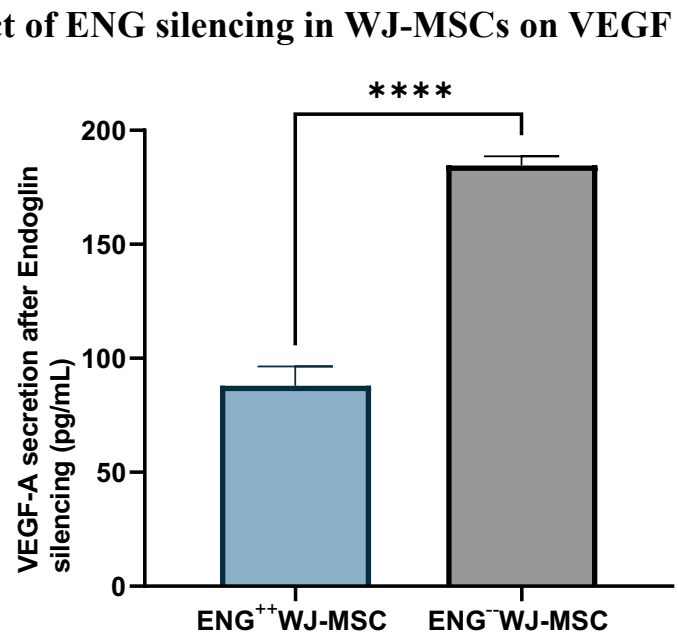


Figure 5-12 Graph showing increased VEGF secretion in culture supernatant after Endoglin silencing in ENG$^{-/-}$WJ-MSCs group compared to the negative siRNA control group, (Unpaired *t*-test *P* value ≤0.0001). Three independent experiments were performed.

5.4.5 ENG Reduction in WJ-MSCs Affects the Stem Cells Attachment to the Endothelial Monolayer

Co-culture studies of HUVEC and silenced or non-silenced WJ-MSCs revealed that ENG$^{-/-}$WJ-MSCs attached to the endothelial monolayer within two hours after seeding the same as ENG$^{+/+}$ WJ-MSCs (Figures 5-13a, b, c, &d), but the counted number of attached silenced cells to the endothelial monolayer was reduced by 53% compared to the control (P <0.0001) (Figure 5-13e). VE-cadherin showed full junctional occupancy in HUVECs co-cultured with ENG$^{+/+}$ WJ-MSCs. VE-cadherin junctional staining was less continuous and more interrupted in HUVEC + ENG$^{-/-}$WJ-MSCs co-cultures (Figure 5-14).

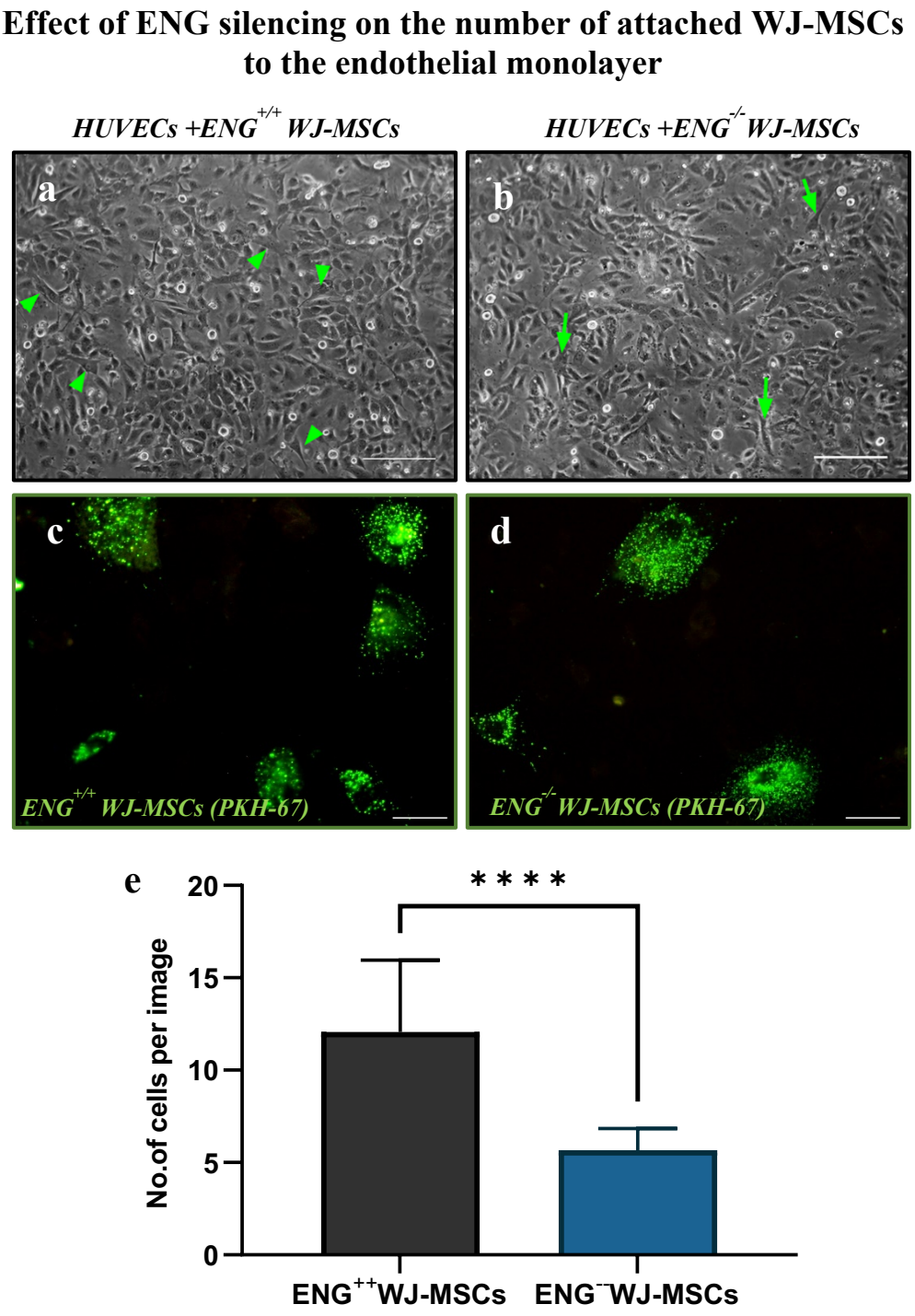


Figure 5-13 Representative phase contrast micrographs for co-cultures of HUVEC with silenced or non-silenced WJ-MSCs displaying ENG$^{+/+}$WJ-MSCs (arrows heads) (**a**) and ENG$^{-/-}$WJ-MSCs (arrows) (**b**) attached to the endothelial cell surface after 2 h co-culture time, scale bar 200µm. Images (**c, d**) representative fluorescence images displaying more attached PKH-67 labelled WJ-MSCs after 2h co-culture in the (HUVEC+ ENG$^{+/+}$WJ-MSCs) (**c**) than (HUVEC+ ENG$^{-/-}$WJ-MSCs) (**d**), scale bar 40µm. (**e**) Graph displaying reduced number of silenced cells attached to the endothelium after 2h co-culture compared to the non-silenced cells, (Unpaired *t*-test, P <0.0001). Three independent experimental repeats were performed.

Localization of VE-Cadherin in the HUVEC co-cultured with silenced and non-silenced WJ-MSCs

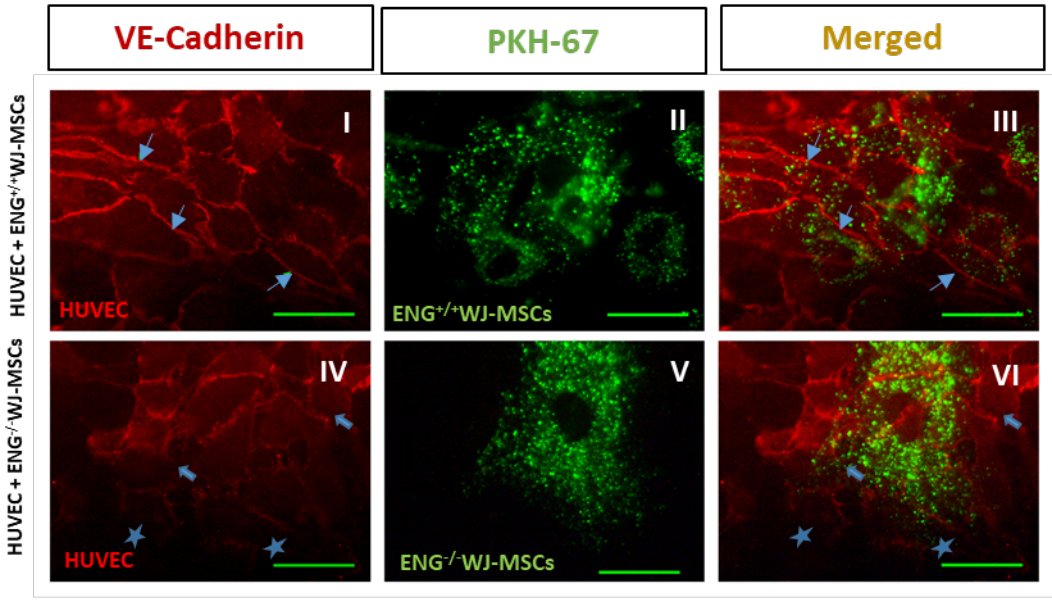


Figure 5-14 Representative micrographs displaying VE-Cadherin localisation in co-cultures from HUVEC+ ENG$^{-/-}$MSCs and HUVEC+ ENG$^{+/+}$ MSCs. Images (**I**& **IV**); showing full junctional occupancy (arrows) of VE-cadherin in the HUVECs layer in HUVEC+ ENG$^{+/+}$ WJ-MSCs (**I**) and interrupted (block arrows) and lost junctions (stars) in HUVEC+ ENG$^{-/-}$MSCs (**IV**) (TRITC filter). Images (**II & V**); showing PKH-67 labelled ENG$^{+/+}$ WJ-MSCs (**II**) and ENG$^{-/-}$ WJ-MSCs (**V**) (FITC filter). Images (**III**& **VI**) are merged images from co-culture HUVEC+ ENG$^{+/+}$ WJ-MSCs (**III**) ENG$^{-/-}$MSCs (**VI**) with the MSCs resting underneath the endothelial cells with restoring the VE-cadherin expression. Scale bar = 40µm. Representative sample out of 3 experimental repeats.

Counts revealed that the number of junctions displaying continuous VE-cadherin expression was reduced by 75.33% when the HUVECs were co-cultured with the silenced cells ENG$^{-/-}$WJ-MSCs compared to the non-silenced cells HUVEC+ENG$^{+/+}$WJ-MSCs. HUVEC + ENG$^{-/-}$WJ-MSCs displayed significantly lower VE-cadherin endothelial junctional expression (20.2 % ± 8.4) compared to HUVEC+ENG$^{+/+}$WJ-MSCs (81.9 % ± 6.7) ($P<0.0001$) (Figure 5-15).

Effect of ENG silencing in WJ-MSC on its enhancing effect on the endothelial VE-cadherin junctional expression

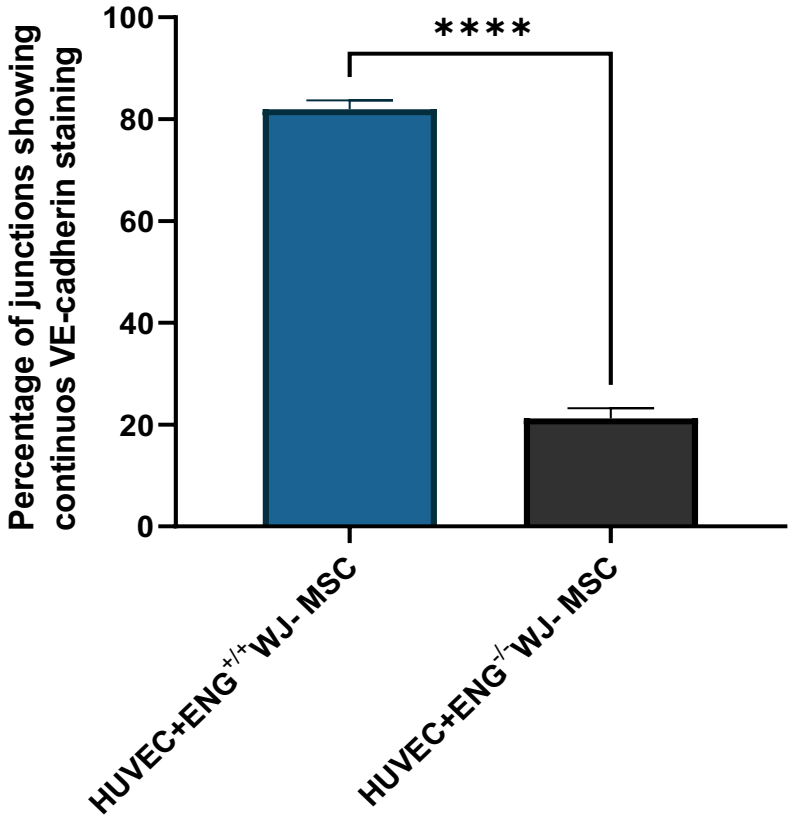


Figure 5-15 Graph displays the percentage of continuous VE-cadherin junctional expression after 24h co-culture with silenced or non-silenced WJ-MSCs, (Unpaired *t*-test, $P < 0.0001$). Three independent experiments were performed.

5.4.6 Effect of ENG Knockdown in WJ-MSCs on the Permeability of HUVEC

Permeability assays showed a significant increase in the amount of FITC-albumin that crossed the bilayer over 2h when HUVEC was co-cultured with ENG^{--} WJ-MSCs (13.11 µg/mL ±1.5) compared to the co-culture HUVEC+ ENG^{++}WJ-MSCs (10.01 µg/mL ±1.3), *p-value* ≤ 0.0001. After 4h the tracer concentration was significantly increased when HUVEC was co-cultured with ENG^{--} WJ-MSCs (24.42 µg/mL ± 1.2) compared to the co-culture HUVEC+ ENG^{++}WJ-MSCs (21.90 µg/mL ± 1.8), *p-value* ≤ 0.05 (Figure 5-16). After 24h co-culture, the tracer concentration in the basal compartment was significantly increased when HUVEC was co-cultured with

ENG^{--} WJ-MSCs (91.90 µg/mL ± 4.8) compared to the co-culture HUVEC+ ENG^{++}WJ-MSCs (81.89 µg/mL ± 6.6), *p-value* ≤ 0.05. The silencing of ENG resulted in decreasing the ability of WJ-MSCs to maintain the endothelial barrier integrity in the co-cultures (Figure 5-17).

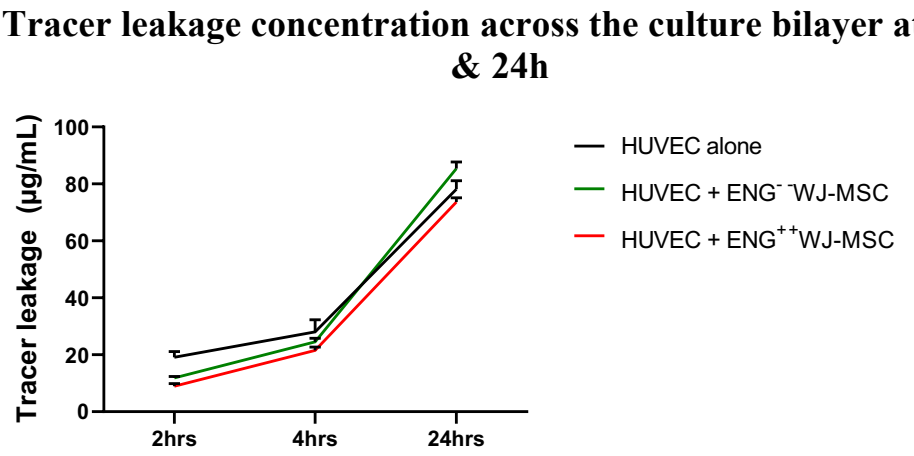


Figure 5-16 Graph displaying the constant increase in the tracer concentration in the basal compartment in the co-culture group (HUVEC+ ENG$^{-/-}$WJ-MSCs).

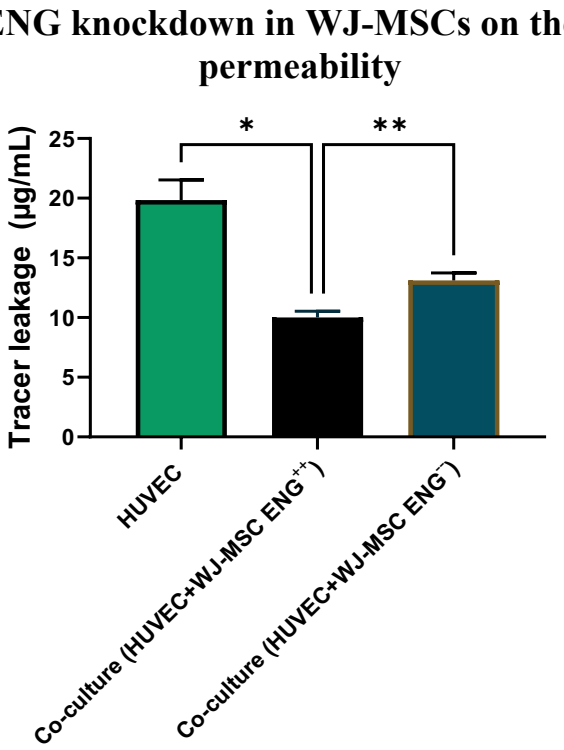


Figure 5-17 Graph displaying increased FITC-albumin transfer across the co-culture bilayer after ENG silencing (One-Way ANOVA P<0.005). Three independent experimental repeats were performed.

5.5 Discussion

The data findings in this chapter suggest that Endoglin's presence in perivascular WJ-MSCs is necessary for the enhancing effect of stem cells on the endothelial barrier after transmigration, and its loss was associated with reduced VE-cadherin junctional occupancy in the endothelial cells and increased tracer leakage. The increased VEGF secretion from the silenced WJ-MSCs may also play a part in the observed VE-cadherin binding disruption.

Endoglin was silenced in both WJ-MSCs and HUVECs. Its expression was reduced by 98% in HUVECs after 4h transfection time, but in WJ-MSCs ENG siRNA transfection needed more time (24h to be reduced by 96%). Loss of ENG in both cell types did not affect the cell morphology or cell viability, however, the HUVECs began to detach at day-3 post silencing. *Lebrin et al 2004*, demonstrated cell growth arrest after ENG silencing in the endothelial cells, and related it to reduced TGF-β/ALK1 signalling and increased TGF-β/ALK5 signalling after ENG knockdown and the survived cells adapted to this imbalance by downregulating ALK5 expression to proliferate (Lebrin et al., 2004). ENG loss was not harmful to WJ-MSCs observed by day-to-day imaging, however, on sub-culturing the silenced cells showed slower proliferation (cell counts).

Endoglin inhibition in WJ-MSCs significantly reduced their adhesion to the HUVEC monolayer by 53% compared to the ENG-expressing WJ-MSCs. In agreement with *Rossi et al., 2017*, who investigated the endoglin role in endothelial colony forming cells and MSCs interaction noting that its knockdown was associated with reduced endothelial adhesion to MSCs (Rossi et al., 2017). Moreover, lack of ENG was associated with increased permeability of the HUVEC monolayer when co-cultured with $ENG^{-/-}$WJ-MSCs observed by the increased tracer leakage in the (co-culture HUVEC+ $ENG^{-/-}$WJ-MSCs) group. These findings suggest that MSC-mediated improvement in endothelial barrier integrity was driven by WJ-MSCs adhesion

to the endothelial monolayer via endoglin expression.

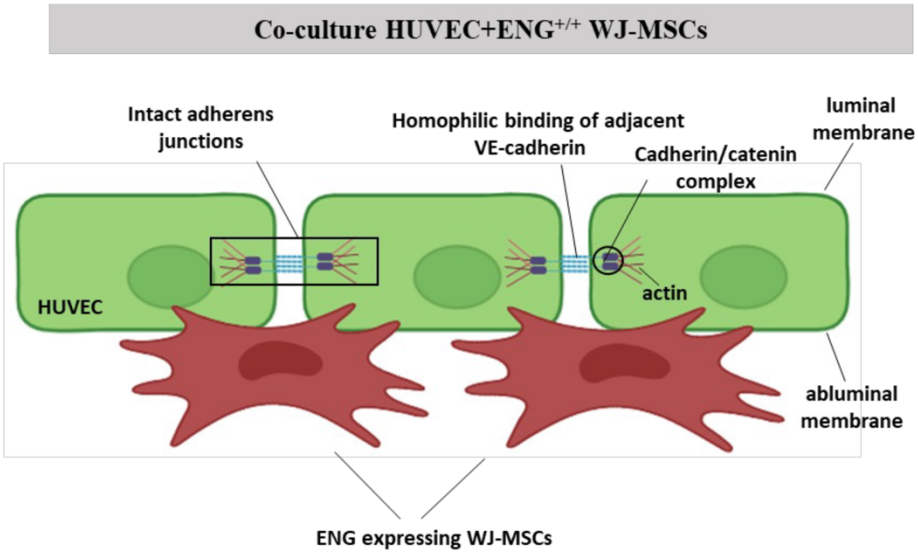


Figure 5-18 Schematic diagram displaying the effect of ENG-expressing WJ-MSCs on the endothelial barrier integrity. The adjacent adherens junctions are intact decreasing the paracellular endothelial permeability when co-cultured with WJ-MSCs.

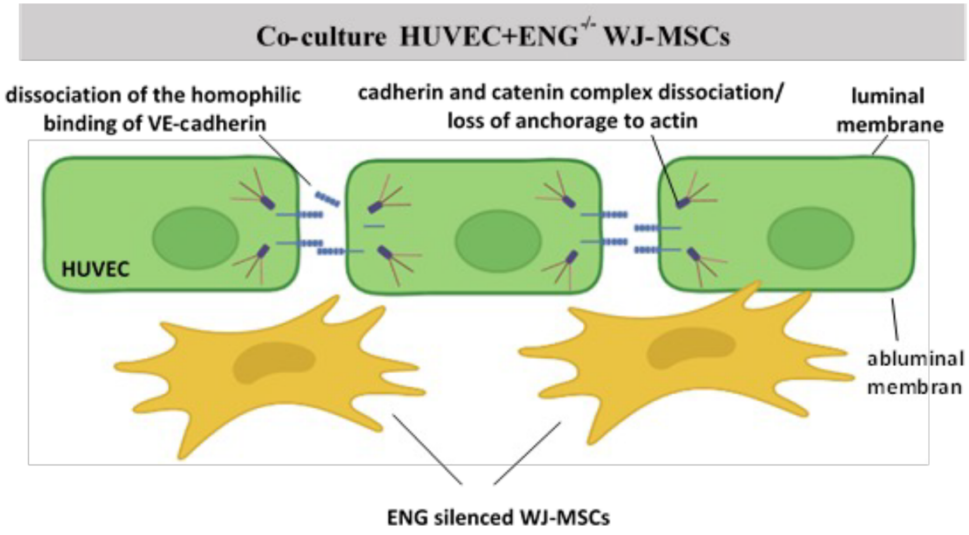


Figure 5-19 Diagram displaying no homophilic binding of the extracellular parts of VE-cadherin, wide intercellular space, and disturbed adherens junctions, when the endothelial cells were co-cultured with ENG silenced WJ-MSCs.

MSCs can differentiate into endothelial cells under certain conditions, therefore the communication between the endothelium and mesenchyme is important for angiogenesis. Mesenchymal cells signal endothelial cells via the

angiopoietin/Tie-2 signalling pathway, reviewed in (Akwii et al., 2019). Thus, cooperation between the two cell types allows perivascular cell formation and stable vessel formation. The interactions between endothelial cells and MSCs are crucial for vascular development. Endothelial cells and WJ-MSCs both express Endoglin, on their membrane. ENG in the endothelial cells interacts with leukocyte integrin α5β1 via its RGD tripeptide motif, and this Endoglin-mediated adhesion process suggests a regulatory role for ENG in trans-endothelial leukocyte trafficking (Rossi et al., 2013). Therefore, ENG silencing in WJ-MSCs was followed by reduced attachment of stem cells to the HUVECs and reduced ability to maintain endothelial barrier function.

Loss of Endoglin was also associated with less continuous and more interrupted VE-cadherin junctional staining that was visualised in HUVEC after 24h co-culture with silenced WJ-MSCs. Furthermore, the percentage of continuous VE-cadherin junctional expression in HUVEC + $ENG^{-/-}$WJ-MSCs was significantly reduced by 75.33%. Moreover, ELISA quantification of VEGF in the supernatant of WJ-MSCs displayed 2-fold increase in its concentration after ENG silencing. It substantially expands the previously described arteriovascular malformations (AVMs) development as a result of high VEGF expression occurring in ENG-deficient endothelial cells (Tual-Chalot et al., 2020). Thus, increased VEGF expression leads to reduced VE-cadherin junctional expression. VEGF disrupts the endothelial barrier function via disruption of VE-cadherin-mediated cell-cell junctions (Eliceiri et al., 1999, Weis et al., 2004).

In-vitro increased secretion of VEGF from ENG deficient cells provides added evidence that ENG inhibits VEGF signalling via activation of SMAD 1/5/8 which is proved by AVM that happens in hereditary haemorrhagic telangiectasia due to Endoglin gene mutation. *Snodgrass et al* recent published results indicate that the HHT-like phenotype in zebrafish eng mutants can be mitigated by inhibiting VEGF signalling and implicating synergistic targeting of ERK and mTOR pathways (Snodgrass et al., 2021). This is consistent with a recent report that patients with HHT have increased serum or plasma VEGF compared to healthy donors (Galaris et al., 2021). Our finding agrees with *Jin*

et al., who stated that ENG knockdown promotes the clearance of VEGFR2 from the plasma membrane elucidates the requirement of ENG in the modulation of VEGFR2 signalling (Jin et al., 2017) that might be the reason behind increased VEGF-A in the culture supernatant. MSCs are well known to release excess cytokines and chemokines key to angiogenic signalling and facilitate the possibility of delivering the mesenchymal stem cells-derived exosomes as a targeted therapy to promote angiogenesis (Mathew et al., 2020).

Endoglin- plays a crucial role in developmental angiogenesis- is upregulated in the WJ-MSCs isolated from pregnancies complicated by GDM (Salem et al., 2022). A recent study concluded that ENG promotes the normal balance of VEGF signalling in quiescent endothelial cells to maintain vessel calibre—an essential function in conditions of increased VEGF expression and ENG absence indorses abnormal endothelial proliferation in local regions of high VEGF expression, leading to arteriovenous malformations (Tual-Chalot et al., 2020). Elevated levels of VEGF-A, loss of junctional VE-cadherin, and increased vascular leakage have been reported in pregnancies complicated by maternal diabetes (Leach et al., 2009). Accumulating evidence suggests crosstalk between VEGF and Endoglin, for instance, *Tian et al*, reported that Endoglin sustained VEGFR2 on the cell surface and prevented its degradation in lysosomes that regulate VEGF signalling and biology (Tian et al., 2018). Endoglin overexpression can lead to steady activation of the endothelial cells, on the contrary, decreased Endoglin expression can lead to downregulated VE-Cadherin, both resulting in an impairment of the correct stabilization of the endothelium.

On the contrary, not only ENG deficiency is harmful, but also ENG was reported to be overexpressed in tumor tissues and was correlated to poor prognosis and metastasis (Paauwe et al., 2018). Endoglin upregulation gives rise to altered vessels with an insufficient mural coverage that allows the extravasation of blood (Ollauri-Ibáñez et al., 2020). The $ENG^{+/+}$ cells have a higher ability to maintain the endothelial barrier tight and intact, and Endoglin is essential for normal vascular development, suggesting that ENG mediates

endothelial-mesenchymal communication that is essential for angiogenesis and important to the pathogenesis of vascular disease.

6 CHAPTER 6 General Discussion and Future Work

6.1 Summative Discussion

An adverse intrauterine environment can induce long-term changes in the physiology and metabolism of the offspring. One such exposure, gestational diabetes mellitus, has been linked to the development of cardiovascular disease in offspring. Fetal stem cells can be used as an indicator for the adverse outcomes of pregnancy complications on the offspring. However, gestational diabetes mellitus is a temporary health condition that usually disappears after pregnancy, its long-term impacts on maternal health and fetal development can be observed (Kamana et al., 2015). Embryonic and mesenchymal stem cells evolving during pregnancy are likely to be adversely affected by pregnancy complications. The main purpose of this study was to examine the extent of GDM's impact on fetal stem cell biology and their vascular repair potency as the role of stem cells in vascular diseases and remodelling, suggests that vascular diseases are stem cell diseases. Furthermore, as a secondary goal, our study aimed to investigate the role of Endoglin expressed in endothelial and mesenchymal stem cells in vascular permeability.

In this study, the stem cells were isolated from human umbilical cords' Wharton's jelly. To confirm their MSCs phenotype, the cells were observed microscopically, and they displayed fibroblast-like morphology. Flow cytometry was used to examine the cell surface markers' expression to meet the minimal criteria for MSCs. Phenotypic characterization of WJ-MSCs demonstrated that both nWJ-MSCs and gWJ-MSCs, were positive to CD44, CD90, CD105 &CD73 and negative to CD14, CD19& HLA-DR. However, our findings revealed that gWJ-MSCS displayed higher CD105 expression compared to nWJ-MSCs. Wharton's Jelly MSCs isolated from gestation diabetes pregnancies (gWJ-MSCs) demonstrated greater migratory properties as observed by the number of MSCs migrated from umbilical cord pieces from GDM placenta exceeding those migrate from normal ones. However, gWJ-MSCs did not display a significant difference in cell viability or doubling time. Our results indicate a significantly increased expression of VEGF protein as assessed by ELISA in gWJ-MSCs supernatant. However, gWJ- MSCs could transmigrate across the endothelial monolayer, open the junctions, and reside

in the sub-endothelial niche similar to nWJ-MSCs, gWJ-MSCs showed a deficient ability to repair the endothelial barrier observed in the reduced percentage of VE-cadherin junctional expression by 28% compared to the control nWJ-MSCs when co-cultured with HUVEC from normal donors. Phenotypic changes in the fetal microvascular bed of the placenta and the umbilical vascular cells suggest that this dysregulation may also exist in the other developing vascular beds of the fetus. The extent of changes may not be pathological, as evidenced by successful gestation and healthy neonates. Any physiological impairment, however slight, may be enough to produce an overt pathological impact in later life if challenged with additional cardiovascular stress (Leach, 2011).

WJ-MSCs from normal pregnancy could be able to enhance the endothelial function by decreasing the permeability observed in the decreased tracer leakage in the co-culture (nWJ-MSCs + HUVEC) compared to the HUVEC monolayer. Nevertheless, our data show that gWJ-MSCs can transmigrate across HUVEC monolayers reaching the sub-endothelial niche but could not tighten the endothelial barrier as evidenced by increased albumin-FITC leakage. In this study, the findings revealed that gWJ-MSCs from the m-GDM group made the endothelial barrier more permeable and did not repair it compared to the ones from the Normal and d-GDM groups. The Developmental Origin of Health and Adult Disease paradigm suggests that long-term consequences for the offspring born to a GDM pregnancy resulting in endothelial/vascular dysfunction associated with DM type 2, obesity, metabolic syndrome, and hypertension (Xiang et al., 1999, Heindel and Vandenberg, 2015). Thus, whether gestational diabetes is an obstacle against using the cells from pregnancies complicated with such a common medical condition needs to be elucidated.

Loss of ENG in mesenchymal stem cells leads to increased VEGF secretion in culture supernatant. Lack of ENG was associated with increased permeability of the HUVEC monolayer when co-cultured with $ENG^{-/-}$WJ-MSCs observed by the increased tracer leakage in the (co-culture HUVEC+WJ-MSCs $ENG^{-/-)}$ group. The absence of Endoglin was also

associated with less continuous and more interrupted VE-cadherin junctional staining that was visualised in HUVEC after 24h co-culture with silenced WJ-MSCs. Moreover, the percentage of continuous VE-cadherin junctional expression in HUVEC + $ENG^{-/-}$WJ-MSCs was significantly reduced. Endoglin role in mesenchymal-endothelial interaction and VEGF biology may help to understand the function of endoglin in angiogenesis and many pathological diseases. We conclude that gestational diabetes disturbs both the phenotype and biological features of WJ-MSCs which are ultimately related to the fetal vascular status, WJ-MSCs might be a powerful tool for the indirect study of fetal cells in the context of gestational diabetes and vascular changes opening the possibility of new predictor or diagnostic approaches.

6.2 WJ-MSCs and Regenerative Medicine

The umbilical cord, usually discarded after delivery, is considered to be a valuable source of abundant Wharton's Jelly MSCs for regenerative medicine without ethical concerns (Forraz and McGuckin, 2011, Kim et al., 2013, Watson et al., 2015). Wharton's jelly can provide an infinite and non-controversial source of stem cells for preclinical and clinical applications. Fetal mesenchymal stem cells are not limited to a fixed number of in-vitro cellular divisions. WJ-MSCs bear a high proliferation rate and self-renewal capacity making them more preferable than adult tissue-derived MSCs (Troyer and Weiss, 2008). Mesenchymal stem cells have been suggested to be a patient-specific drugstore for injured tissues (Caplan and Correa, 2011).

Cell therapy represents an emerging area in regenerative medicine at the moment. Several health problems that have limited treatment plans or poor prognosis trigger the need for innovative therapeutic modalities implementing the stem cell field of application based on mesenchymal stem cells. WJ-MSCs among all the different tissue sources of stem cells represent a promising cell population due to their high pluripotency and regenerative properties. WJ-MSCs have attracted interest for their banking and transplantation capacities (Balzano et al., 2019).

Mesenchymal stem cells are widely used in pre-clinical & clinical applications for their primitive properties, their migratory and immunomodulatory functions expansion potential, and their lack of tumorigenicity (Lenti et al., 2007, Wang et al., 2019). The use of MSCs in clinical trials has been expanded as indicated by increased number of Investigational New Drug submissions to the FDA for MSC-based products (Mendicino et al., 2014, Rodríguez-Fuentes et al., 2021). Moreover, there were 374 registered clinical trials in the NIH clinical trial database using MSCs (Trounson and McDonald, 2015, Sagar et al., 2018). Worldwide, for the years 2011−2018, there were 1043 registered MSC clinical trials planned with a targeted enrolment of 47,548 patients (www.clinicaltrials.gov and https://celltrials.org/public-cells-data/msc-trials-2011-2018/65) (Pittenger et al., 2019). Prochymal was the first approved and licensed MSCs product to be used in severe cases of steroid-resistant graft versus host disease (Sagar et al., 2018).

WJ-MSCs can differentiate into insulin-producing cells that reduce hyperglycaemia and improve glucose intolerance when transplanted into diabetic rats (Tsai et al., 2012). *Liu et al., 2014,* conducted a phase I/II trial involving 22 diabetic patients (type 2). The patients received one intravenous injection followed by one intrapancreatic endovascular injection after five days. Treatment with WJ-MSCs decreased the HbA1c levels, fasting and, postprandial glucose levels, daily insulin, and hypoglycaemic drug dosage, and T-lymphocyte counts. However, the c-peptide level and beta cell function decreased temporarily which might happen due to the intrapancreatic injection (Liu et al., 2014a).

Guan et al., 2015, conducted a trial using allogenic WJ-MSCs to treat six diabetic patients (type 2). All six patients showed a positive response to WJ-MSCs therapy; three became insulin-free, whereas the other three required a lower insulin dosage temporarily (6–18 months) after treatment (Guan et al., 2015). *Hu et al., 2016*, reported a trial examining the long-term effects of WJ-MSC therapy involving 61 diabetic patients (type 2): 31 patients received their usual treatment and WJ-MSCs, and 30 patients received their usual treatment

and normal saline. The patients received post-treatment follow-up for three years. WJ-MSC-treated patients showed improvement in diabetes indicators and β-cell function, required lower daily insulin and oral hypoglycaemic dosage, and have a lower risk of diabetes complications (Hu et al., 2016).

The paracrine effect of MSCs contributes to their therapeutic effects. MSCs naturally secrete multiple cytokines and growth factors, promoting the survival of the surrounding cells (Rahavi et al., 2015, Lei et al., 2016) (Ebrahim and Leach, 2016). WJ-MSCs were investigated for treating the ischemic-compression model of spinal cord injury in rats (Krupa et al., 2018). Injection of bone marrow MSCs can accelerate wound healing by promoting angiogenesis and secreting numbers of growth factors, such as VEGF, FGF, TGF-β, and platelet-derived growth factor (Iqbal et al., 2013, An et al., 2018). Despite the deficient ability of gWJ-MSCs to maintain the endothelial barrier integrity, they displayed the same proliferative ability and transendothelial migration compared to nWJ-MSCs which may contribute to the future development of autologous cell therapy and regenerative medicine approaches for women who experienced GDM or their children.

6.3 Metformin Use in Pregnancy

Our study revealed that Metformin has an adverse effect on the permeability when gWJ-MSCs from the m-GDM were co-cultured with HUVEC. Metformin is known to cross the placenta, exposing the fetus to metformin levels similar to the maternal levels (Charles et al., 2006). Several studies have focused on the outcome of offspring from pregnancies treated with metformin. *Butalia et al., 2017* found no apparent reason for concerns about the short-term effects (Butalia et al., 2017), and *Ijas et al., 2015* and *Battin et al., 2015* have found no concern about the long-term effects of fetal exposure to metformin (Ijäs et al., 2015) (Battin et al., 2015).

Metformin is a biguanide compound that works as an oral hypoglycaemic drug. Its main effect is to reduce hepatic glucose production and increase insulin-stimulated glucose uptake and lower plasma triglycerides

and free fatty acids by activating 5′-adenosine monophosphate-activated protein kinase (AMPK-α2) see review (LaMoia and Shulman, 2021). Metformin is recommended for pregnant women diagnosed with GDM if the fasting glucose level is 7.0 mmol/litre or above at diagnosis, or If blood glucose targets are not met within 1 to 2 weeks after diet and exercise changes (NICE., 2015). As an anti-hyperglycaemic oral agent, metformin has the advantages of oral administration and lacks the hypoglycaemic risk compared to insulin (Nguyen et al., 2018).

Short-term outcomes of metformin use in pregnancy

One study investigated the outcome of Metformin use in pregnancy with 256 women who received metformin treatment for GDM revealed a 0.5 cm decrease in the infant abdominal circumference in the metformin-exposed group that might have a potentially significant impact on the long-term health of infants exposed to metformin (Dodd et al., 2019).

Long-term outcomes of metformin use in pregnancy

Two years follow-ups for infants exposed to metformin revealed that they have larger arm circumference and skinfold thickness measurements comparing to those exposed to insulin, despite having smaller; crown-rump and skinfold measurements at birth compared to the general population. These data suggest that metformin may alter fat distribution (Rowan et al., 2011). Another randomized controlled study on 45 metformin-exposed children revealed that they were significantly heavier at age 12 months and taller and heavier at age 18 months (Ijäs et al., 2015).

A recent study announced that preconception paternal metformin treatment is associated with major birth defects, particularly genital birth defects in boys, based on a cohort study included 1 116 779 offspring total with 1451 metformin-exposed offspring (Wensink et al., 2022). Metformin is known to reduce testosterone production in vitro. Its administration in pregnant mice was associated with reduced fetal and neonatal testicular size (Tartarin et al., 2012).

Metformin exposure in the first trimester

During early gestation, the embryo has few and relatively immature mitochondria and expresses very low levels of organic cation transporters. Metformin is transported by organic cation transporters into mitochondrial membranes, suggesting that early human embryos may be unresponsive to metformin (Lee et al., 2018).

Metformin exposure in the second and third trimester

In the second and third trimesters, the placenta and fetus express metformin transporters, show high rates of aerobic metabolism and depend more on mature mitochondrial activity. Therefore, fetal metformin levels are similar to maternal levels (Lee et al., 2018). Metformin can suppress mitochondrial respiratory complex I of the electron transport chain, reducing ATP production and increasing AMP: ATP ratios. Metformin can activate AMPK and inhibit the mechanistic target of rapamycin (mTOR) pathway, which leads to the suppression of protein synthesis and an increase in apoptosis and cell-cycle arrest. mTOR is a nutrient sensor in the placenta, and its inhibition might affect nutrient flux and fetal growth (Jansson et al., 2012).

Although metformin increases insulin gene expression, it also suppresses β-cell proliferation and enhances apoptosis through an AMPK-dependent and autophagy-mediated mechanism suggesting that metformin has a dual role in pancreatic beta cell function (Jiang et al., 2014). *Gregg et al., 2014*, showed that maternal use of metformin during pregnancy leads to more cells expressing the pancreatic progenitor marker Pdx1, but fewer cells expressing the later pancreatic endocrine progenitor marker Ngn3 in mouse embryos. The endocrine progenitors are the precursors of mature pancreatic beta cells, suggesting the effect of metformin on the future function of β-cells (Gregg et al., 2014).

Metformin has been shown to have anticancer effects, growth inhibitory properties and also to suppress mitochondrial respiration (Barbour et al., 2018, Priya and Kalra, 2018, van Weelden et al., 2018). Fetal exposure to metformin might have an antigrowth effect on pancreatic beta cells as a protective

mechanism against the metabolic changes that occur in GDM, resulting in a smaller β cell mass formed during fetal development. That may reduce the ability of metformin-exposed offspring to tolerate life-long metabolic challenges, giving rise to an increased risk of earlier beta cell dysfunction and type 2 DM (Nguyen et al., 2018). Metformin‘s adverse effects on pancreatic β-cell mass, impairing glycolysis, inhibiting thiamine uptake, and altering histone acetylation may result in epigenetic modifications, which consequently have an impact on fetal growth, differentiation, and childhood development (Barbour and Feig, 2019).

6.4 Future Work

Future work could consider placental or umbilical cord perfusion with PKH26 labelled nWJ-MSC and gWJ-MSCs to compare the cellular and molecular mechanisms employed by the stem cells to extravasate across the endothelial barriers *in vivo* and whether the cells from the GDM group will behave the same as the ones from normal pregnancy.

Our study showed that a normal level of Endoglin enhanced the endothelial barrier, and a decreased level causes increased endothelial permeability. To investigate whether the Endoglin exhibits linear or non-linear behaviour, future work should conduct a similar permeability assay but with upregulation of ENG expression instead of silencing. If endothelial permeability increases with ENG upregulation, it will suggest that it displays non-linear behaviour in which an optimal range exists. We could downregulate the ENG expression in the gWJ-MSCs, if no change occurs in endothelial permeability, it will suggest that CD105 displays linear behaviour and is not the cause of the increased permeability in co-cultures from GDM groups.

Future work should include the ENG expression in the placental samples to be correlated to the stem cell expression, determine the co-localization of the ENG and VE-cadherin in the endothelial cells and the placental tissues, and investigate the levels of miRNAs that target the VEGF and ENG in the GDM placentas.

Our study revealed that Metformin has an adverse effect on the permeability when the stem cells from the m-GDM were co-cultured with HUVEC, but due to the small sample size, we couldn't correlate this finding to any clinical characteristics. Future work should determine the possible role of metformin on the permeability of umbilical vein endothelial cells, as we can conduct a similar permeability assay by exposing the HUVECs to metformin treatment in a similar dose as the fetal exposure level for 48 hours, before adding the FITC-conjugated protein.

.

APPENDIX

University of Nottingham
UK | CHINA | MALAYSIA

Nottingham University Hospitals NHS
NHS Trust

CONSENT FORM

Final Version (4.0: 01 Oct. 15)

Title of Study: Laboratory studies of structure and function of the placenta after birth
REC ref: OGO1O1O1
Name of Researcher: Dr Lopa Leach

Name of Participant: **Please initial box**

1. I confirm that I have read and understand the information sheet version number 5.0 dated 01 Oct. 15 for the above study and have had the opportunity to ask questions. ☐

2. I understand that my participation is voluntary and that I am free to withdraw at any time, without giving any reason, and without my medical care or legal rights being affected. I understand that should I withdraw then the information collected so far cannot be erased and that this information may still be used in the project analysis. ☐

3. I understand that relevant sections of my medical notes and data collected in the study may be looked at by authorised individuals from the University of Nottingham, the research group and regulatory authorities where it is relevant to my taking part in this study. I give permission for these individuals to have access to these records and to collect, store, analyse and publish information obtained from my participation in this study. I understand that my personal details will be kept confidential. ☐

4. I understand and agree that the placenta and umbilical cord will be taken for laboratory analyses of the blood vessels and growth of cells lining the vessels. ☐

5. I agree to take part in the above study. ☐

Name of Participant	Date	Signature
Name of Person taking consent	Date	Signature

3 copies: 1 for participant, 1 for the project notes and 1 for the medical notes

CASE REPORT FORM

Study ID: …….

Date: ……

Gestational age: …… Weeks + …….. Days

Parity: ……

Gravida: …….

BMI…….

Smoking: Yes ☐ No ☐

Medication: Yes ☐ No ☐

If yes, Aspirin ☐ Clexane ☐ Metformin ☐ Insulin ☐

Others ……..

Complications:

PET ☐

DM ☐

Retinopathy ☐

Nephropathy ☐

Essential hypertension ☐

Birth weight: …….

Gender of the baby: …….

Head Circumference: …….

PARTICIPANT INFORMATION SHEET

University of Nottingham
UK | CHINA | MALAYSIA

Nottingham University Hospitals NHS
NHS Trust

Participant Information Sheet
Final version 5.0: 01. Oct.15`

Title of Study: Laboratory studies of structure and function of the placenta after birth

Name of Researcher(s): Dr Lopa Leach

We would like to invite you to take part in our research study. Before you decide we would like you to understand why the research is being done and what it would involve for you. One of our team will go through the information sheet with you and answer any questions you have. Talk to others about the study if you wish. Ask us if there is anything that is not clear.

Purpose of study

We are asking for your permission to carry out studies of your placenta (afterbirth) with attached membranes and cord after your delivery.

Normally, once the baby has been delivered and the umbilical cord clamped and cut, the placenta and attached membranes and cord are thrown away. Instead we want to carry out detailed studies in the laboratory into whether the blood vessels present in normal placenta is similar to that seen in placenta from diabetic or pre-eclamptic pregnancies.

Both diabetes and pre-eclampsia are diseases that can affect the baby throughout pregnancy.

If the placenta, which separates the mothers blood from the babies is different in structure and permeability from normal placenta then we can start planning strategies which can help alleviate the problem.

Over the next five years we wish to look at placenta from normal, diabetic and pre-eclamptic pregnancies after the baby has been delivered.

In the laboratory we will study the endothelial cells lining the blood vessels in the placenta by using a perfusion model which allows us to perfuse blood vessels in the placenta and by taking out the cells and growing them in culture. Specifically we will look at molecules which help endothelial cells stick together, regulate how leaky the vessels are and which help new blood vessels grow. Any differences in the behaviour of these molecules in the three study groups will help us understand how/why things can go wrong.
The study has the approval of the Nottingham 2 Ethics Committee (OGO1O1O1).

Why have I been chosen?

Since all the work is done in the laboratory, and we need time to make all the solutions, we are taking placentae and umbilical cord from Elective Caesarean Sections only. We can then plan to do experiments immediately after the section. Your consultant, and your notes, has advised/informed us that your afterbirth is suitable for our study.

Do I have to agree?
No. It is up to you to decide whether you agree that we may study your discarded placenta and umbilical cord. If you do decide to agree you will be given this information sheet to keep and be asked to sign a consent form. If you decide to agree you are still free to withdraw at any time and without giving a reason. This will not affect the standard of care you receive.

As stated before we want to take away your afterbirth, which is normally thrown away, to the laboratory to perform these studies. After the laboratory analyses, the tissue and endothelial cells will be destroyed.

What will happen to me if I take part?
We do not want you to do anything different from what you are doing now. This is a laboratory study, using your afterbirth. There are no side effects for you or your baby. There are no risks involved for you or your baby.

What are the possible benefits of agreeing?
There are no intended clinical benefits to you from taking part in this trial.
Will my participation be kept confidential?
All information which is collected about you during the course of the research will be kept strictly confidential. Any information about you which leaves the hospital/surgery will have your name and address removed so that you cannot be recognised from it.

What will happen to the results of this research study?
Results from this study will be published in scientific journals and presented in scientific conferences and may form part of a students PhD. However, as stated before you will not be identified in any report/publication.

Who is organising and funding the research?
This is research led by Dr L Leach. Dr Leach is an Associate Professor of Vascular Biology, School of Life Sciences, Faculty of Medicine, University of Nottingham. We have full permission of the clinical director Professor Jim Thornton, Division of Obstetrics and Gynaecology, to retrieve the placenta and cord from the labour ward and theatre at QMC and City Hospital. The project is being funded by the
University of Nottingham and the British Heart Foundation.

Who has reviewed the study?
All research in the NHS is looked at by independent group of people, called a Research Ethics Committee, to protect your interests. This study has been reviewed and given favourable opinion by Nottingham 2 Research Ethics Committee Ref. OGO1O1O1.

Contact for further information:
Dr L. Leach, School of Life Sciences, E Floor Medical School, Queens Medical Centre, Nottingham NG7 2UH. Email lopa.leach@nottingham.ac.uk.
Professor Jim Thornton, Professor of Obstetrics and Gynaecology.
Division of Obstetrics and Gynaecology, Maternity Department, City Hospital, Hucknall Road, Nottingham. Email: jim.thorntonnottingham.ac.uk
Thank you very much in anticipation for your permission.

Patient must be given a copy of the information sheet and a signed consent form to keep. A copy of signed consent should be placed in the clinical notes.

REFERENCES

ABDULRAZZAK, H., MOSCHIDOU, D., JONES, G. & GUILLOT, P. V. 2010. Biological characteristics of stem cells from foetal, cord blood and extraembryonic tissues. *Journal of the Royal Society, Interface,* 7 Suppl 6**,** S689-S706.

ABELL, S. K., DE COURTEN, B., BOYLE, J. A. & TEEDE, H. J. 2015. Inflammatory and other biomarkers: role in pathophysiology and prediction of gestational diabetes mellitus. *International journal of molecular sciences,* 16**,** 13442-13473.

ABUDAYYEH, O. O., GOOTENBERG, J. S., ESSLETZBICHLER, P., HAN, S., JOUNG, J., BELANTO, J. J., VERDINE, V., COX, D. B. T., KELLNER, M. J., REGEV, A., LANDER, E. S., VOYTAS, D. F., TING, A. Y. & ZHANG, F. 2017. RNA targeting with CRISPR-Cas13. *Nature,* 550**,** 280-284.

AIRD, W. C. 2007. Phenotypic heterogeneity of the endothelium: I. Structure, function, and mechanisms. *Circulation research,* 100**,** 158-173.

AKWII, R. G., SAJIB, M. S., ZAHRA, F. T. & MIKELIS, C. M. 2019. Role of angiopoietin-2 in vascular physiology and pathophysiology. *Cells,* 8**,** 471.

AL-LAMKI, R. S., BRADLEY, J. R. & POBER, J. S. 2008. Endothelial cells in allograft rejection. *Transplantation,* 86**,** 1340-1348.

AL-OKAIL, M. S. & AL-ATTAS, O. S. 1994. Histological changes in placental syncytiotrophoblasts of poorly controlled gestational diabetic patients. *Endocrine journal,* 41**,** 355-360.

ALGABA-CHUECA, F., MAYMÓ-MASIP, E., EJARQUE, M., BALLESTEROS, M., LLAURADÓ, G., LÓPEZ, C., GUARQUE, A., SERENA, C., MARTÍNEZ-GUASCH, L., GUTIÉRREZ, C., BOSCH, R., VENDRELL, J., MEGÍA, A. & FERNÁNDEZ-VELEDO, S. 2019. Gestational diabetes impacts fetal precursor cell responses with potential consequences for offspring. *Stem Cells Translational Medicine,* 9**,** 351-363.

ALQUDAH, A., EASTWOOD, K.-A., JEROTIC, D., TODD, N., HOCH, D., MCNALLY, R., OBRADOVIC, D., DUGALIC, S., HUNTER, A. J. & HOLMES, V. A. 2021. FKBPL and SIRT-1 are downregulated by diabetes in pregnancy impacting on angiogenesis and endothelial function. *Frontiers in endocrinology***,** 459.

ALSAMMAN, M., STERZER, V., MEURER, S. K., SAHIN, H., SCHAEPER, U., KUSCUOGLU, D., STRNAD, P., WEISKIRCHEN, R., TRAUTWEIN, C. & SCHOLTEN, D. 2018. Endoglin in human liver disease and murine models of liver fibrosis—A protective factor against liver fibrosis. *Liver International,* 38**,** 858-867.

AN, B., KIM, E., SONG, H., HA, K.-S., HAN, E.-T., PARK, W. S., AHN, T. G., YANG, S.-R., NA, S. & HONG, S.-H. 2017. Gestational Diabetes Affects the Growth and Functions of Perivascular Stem Cells. *Molecules and cells,* 40**,** 434-439.

AN, Y., LIU, W., XUE, P., MA, Y., ZHANG, L., ZHU, B., QI, M., LI, L., ZHANG, Y. & WANG, Q. 2018. Autophagy promotes MSC-mediated vascularization in cutaneous wound healing via regulation of VEGF secretion. *Cell death & disease,* 9**,** 1-14.

ANDERSON, P., CARRILLO-GÁLVEZ, A. B., GARCÍA-PÉREZ, A., COBO, M. & MARTÍN, F. 2013. CD105 (endoglin)-negative murine mesenchymal stromal cells define a new multipotent subpopulation with distinct differentiation and immunomodulatory capacities. *PloS one,* 8**,** e76979.

ANTONIADOU, E. & DAVID, A. L. 2016. Placental stem cells. *Best Practice & Research Clinical Obstetrics & Gynaecology,* 31**,** 13-29.

APLIN, J. D. 2000. The cell biological basis of human implantation. *Best Practice & Research Clinical Obstetrics & Gynaecology,* 14**,** 757-764.

APLIN, J. D. & KIMBER, S. J. 2004. Trophoblast-uterine interactions at implantation. *Reproductive Biology and Endocrinology,* 2**,** 1-12.

APTE, R. S., CHEN, D. S. & FERRARA, N. 2019. VEGF in signaling and disease: beyond discovery and development. *Cell,* 176**,** 1248-1264.

ARAVIN, A. A., SACHIDANANDAM, R., GIRARD, A., FEJES-TOTH, K. & HANNON, G. J. 2007. Developmentally regulated piRNA clusters implicate MILI in transposon control. *Science,* 316**,** 744-7.

ARTLETT, C. M., RAMOS, R., JIMINEZ, S. A., PATTERSON, K., MILLER, F. W. & RIDER, L. G. 2000. Chimeric cells of maternal origin in juvenile idiopathic inflammatory myopathies. *The Lancet,* 356**,** 2155-2156.

ASHCROFT, F. M., ROHM, M., CLARK, A. & BRERETON, M. F. 2017. Is type 2 diabetes a glycogen storage disease of pancreatic β cells? *Cell metabolism,* 26**,** 17-23.

AMERICAN DIABETES ASSOCIATION, 2017. 13. Management of diabetes in pregnancy. *Diabetes Care,* 40**,** S114-S119.

AMERICAN DIABETES ASSOCIATION, 2018. 2. Classification and Diagnosis of Diabetes: Standards of Medical Care in Diabetes—2018</em&gt. *Diabetes Care,* 41**,** S13.

ATÈGBO, J.-M., GRISSA, O., YESSOUFOU, A., HICHAMI, A., DRAMANE, K. L., MOUTAIROU, K., MILED, A., GRISSA, A., JERBI, M., TABKA, Z. & KHAN, N. A. 2006. Modulation of Adipokines and Cytokines in Gestational Diabetes and Macrosomia. *The Journal of Clinical Endocrinology & Metabolism,* 91**,** 4137-4143.

AU - BEERAVOLU, N., AU - MCKEE, C., AU - ALAMRI, A., AU - MIKHAEL, S., AU - BROWN, C., AU - PEREZ-CRUET, M. & AU - CHAUDHRY, G. R. 2017. Isolation and Characterization of Mesenchymal Stromal Cells from Human Umbilical Cord and Fetal Placenta. *JoVE***,** e55224.

AZZI, S., HEBDA, J. & GAVARD, J. 2013. Vascular Permeability and Drug Delivery in Cancers. *Frontiers in Oncology,* 3.

BAI, L., LENNON, D. P., CAPLAN, A. I., DECHANT, A., HECKER, J., KRANSO, J., ZAREMBA, A. & MILLER, R. H. 2012. Hepatocyte growth factor mediates mesenchymal stem cell–induced recovery in multiple sclerosis models. *Nature neuroscience,* 15**,** 862-870.

BALZANO, F., BELLU, E., BASOLI, V., DEI GIUDICI, S., SANTANIELLO, S., CRUCIANI, S., FACCHIN, F., OGGIANO, A., CAPOBIANCO, G. & DESSOLE, F. 2019. Lessons from human umbilical cord: Gender differences in stem cells from Wharton's jelly. *European Journal of Obstetrics & Gynecology and Reproductive Biology,* 234**,** 143-148.

BAŃKOWSKI, E. Collagen of the umbilical cord and its alteration in EPH-gestosis (preeclampsia). Proceedings of the Indian Academy of Sciences-Chemical Sciences, 1999. Springer, 207-213.

BARBATI, A., GRAZIA MAMELI, M., SIDONI, A. & DI RENZO, G. C. 2012. Amniotic Membrane: Separation of Amniotic Mesoderm from Amniotic Epithelium and Isolation of Their Respective Mesenchymal Stromal and Epithelial Cells. *Current Protocols in Stem Cell Biology,* 20**,** 1E.8.1-1E.8.15.

BARBOUR, L. A. & FEIG, D. S. 2019. Metformin for gestational diabetes mellitus: progeny, perspective, and a personalized approach. *Diabetes Care,* 42**,** 396-399.

BARBOUR, L. A., SCIFRES, C., VALENT, A. M., FRIEDMAN, J. E., BUCHANAN, T. A., COUSTAN, D., AAGAARD, K., THORNBURG, K. L., CATALANO, P. M. & GALAN, H. L. 2018. A cautionary response to SMFM statement: pharmacological treatment of gestational diabetes. *American journal of obstetrics and gynecology,* 219**,** 367. e1-367. e7.

BARNETT, J. M., SUAREZ, S., MCCOLLUM, G. W. & PENN, J. S. 2014. Endoglin promotes angiogenesis in cell-and animal-based models of retinal neovascularization. *Investigative Ophthalmology & Visual Science,* 55**,** 6490-6498.

BARZEGAR, M., KAUR, G., GAVINS, F. N. E., WANG, Y., BOYER, C. J. & ALEXANDER, J. S. 2019. Potential therapeutic roles of stem cells in ischemia-reperfusion injury. *Stem Cell Research,* 37**,** 101421.

BASHAM, T. Y. & MERIGAN, T. C. 1983. Recombinant interferon-gamma increases HLA-DR synthesis and expression. *The Journal of Immunology,* 130**,** 1492.

BATTIN, M. R., OBOLONKIN, V., RUSH, E., HAGUE, W., COAT, S. & ROWAN, J. 2015. Blood pressure measurement at two years in offspring of women randomized to a trial of metformin for GDM: follow up data from the MiG trial. *BMC pediatrics,* 15**,** 1-5.

BAUM, C. M., WEISSMAN, I. L., TSUKAMOTO, A. S., BUCKLE, A. M. & PEAULT, B. 1992. Isolation of a candidate human hematopoietic stem-cell population. *Proceedings of the National Academy of Sciences,* 89**,** 2804.

BAUMANN, M. U., DEBORDE, S. & ILLSLEY, N. P. 2002. Placental glucose transfer and fetal growth. *Endocrine,* 19**,** 13-22.

BEHBOUDI-GANDEVANI, S., AMIRI, M., BIDHENDI YARANDI, R. & RAMEZANI TEHRANI, F. 2019. The impact of diagnostic criteria for gestational diabetes on its prevalence: A systematic review and meta-analysis. *Diabetology and Metabolic Syndrome,* 11.

BELLÓN, T., CORBI, A., LASTRES, P., CALÉS, C., CEBRIÁN, M., VERA, S., CHEIFETZ, S., MASSAGUE, J., LETARTE, M. & BERNABÉU, C. 1993. Identification and expression of two forms of the human transforming growth factor-β-binding protein endoglin with distinct cytoplasmic regions. *European journal of immunology,* 23**,** 2340-2345.

BENDAYAN, M. 2002. Morphological and cytochemical aspects of capillary permeability. *Microscopy research and technique,* 57**,** 327-349.

BIANCHI, D. W., KHOSROTEHRANI, K., WAY, S. S., MACKENZIE, T. C., BAJEMA, I. & O'DONOGHUE, K. 2021. Forever connected: the lifelong biological consequences of fetomaternal and maternofetal microchimerism. *Clinical Chemistry,* 67**,** 351-362.

BIBEE, K. P., ILLSLEY, N. P. & MOLEY, K. H. 2011. Asymmetric syncytial expression of GLUT9 splice variants in human term placenta and alterations in diabetic pregnancies. *Reproductive sciences,* 18**,** 20-27.

BILLIONNET, C., MITANCHEZ, D., WEILL, A., NIZARD, J., ALLA, F., HARTEMANN, A. & JACQUEMINET, S. 2017. Gestational diabetes and adverse perinatal outcomes from 716,152 births in France in 2012. *Diabetologia,* 60**,** 636-644.

BLACK, M. H., SACKS, D. A., XIANG, A. H. & LAWRENCE, J. M. 2013. The relative contribution of prepregnancy overweight and obesity, gestational weight gain, and IADPSG-defined gestational diabetes mellitus to fetal overgrowth. *Diabetes care,* 36**,** 56-62.

BLAHA, M., CERMANOVA, M., BLAHA, V., JAROLIM, P., ANDRYS, C., BLAZEK, M., MALY, J., SMOLEJ, L., ZAJIC, J. & MASIN, V. 2008. Elevated serum soluble endoglin (sCD105) decreased during extracorporeal elimination therapy for familial hypercholesterolemia. *Atherosclerosis,* 197**,** 264-270.

BLAISE, S., POLENA, H. & VILGRAIN, I. 2015. Soluble vascular endothelial-cadherin and auto-antibodies to human vascular endothelial-cadherin in human diseases: two new biomarkers of endothelial dysfunction. *Vascular Medicine,* 20**,** 557-565.

BLANN, A. D., WANG, J. M., WILSON, P. B. & KUMAR, S. 1996. Serum levels of the TGF-beta receptor are increased in atherosclerosis. *Atherosclerosis,* 120**,** 221-226.

BLÁZQUEZ-MEDELA, A. M., GARCÍA-ORTIZ, L., GÓMEZ-MARCOS, M. A., RECIO-RODRÍGUEZ, J. I., SÁNCHEZ-RODRÍGUEZ, A., LÓPEZ-NOVOA, J. M. & MARTÍNEZ-SALGADO, C. 2010. Increased plasma soluble endoglin levels as an indicator of

cardiovascular alterations in hypertensive and diabetic patients. *BMC medicine,* 8**,** 1-12.

BLOCKI, A., WANG, Y., KOCH, M., PEH, P., BEYER, S., LAW, P., HUI, J. & RAGHUNATH, M. 2013. Not All MSCs Can Act as Pericytes: Functional In Vitro Assays to Distinguish Pericytes from Other Mesenchymal Stem Cells in Angiogenesis. *Stem Cells and Development,* 22**,** 2347-2355.

BLUNDELL, C., TESS, E. R., SCHANZER, A. S., COUTIFARIS, C., SU, E. J., PARRY, S. & HUH, D. 2016. A microphysiological model of the human placental barrier. *Lab on a Chip,* 16**,** 3065-3073.

BOCKHORN, M., TSUZUKI, Y., XU, L., FRILLING, A., BROELSCH, C. E. & FUKUMURA, D. 2003. Differential vascular and transcriptional responses to anti-vascular endothelial growth factor antibody in orthotopic human pancreatic cancer xenografts. *Clinical Cancer Research,* 9**,** 4221-4226.

BORGES, L., IACOVINO, M., MAYERHOFER, T., KOYANO-NAKAGAWA, N., BAIK, J., GARRY, D. J., KYBA, M., LETARTE, M. & PERLINGEIRO, R. C. R. 2012. A critical role for endoglin in the emergence of blood during embryonic development. *Blood,* 119**,** 5417-5428.

BOT, P. T., HOEFER, I. E., SLUIJTER, J. P., VAN VLIET, P., SMITS, A. M., LEBRIN, F., MOLL, F., DE VRIES, J.-P., DOEVENDANS, P. & PIEK, J. J. 2009. Increased expression of the transforming growth factor-β signaling pathway, endoglin, and early growth response-1 in stable plaques. *Stroke,* 40**,** 439-447.

BOUW, G., STOLTE, L., BAAK, J. & OORT, J. 1976. Quantitative morphology of the placenta 1. Standardization of sampling. *European Journal of Obstetrics & Gynecology and Reproductive Biology,* 6**,** 325-331.

BOYD, J. D. & HAMILTON, W. J. 1970. *The human placenta*, Heffer.

BREIER, G., BREVIARIO, F., CAVEDA, L., BERTHIER, R., SCHNÜRCH, H., GOTSCH, U., VESTWEBER, D., RISAU, W. & DEJANA, E. 1996. Molecular cloning and expression of murine vascular endothelial-cadherin in early stage development of cardiovascular system. *Blood,* 87**,** 630-41.

BROUGHTON, B. R., LIM, R., ARUMUGAM, T. V., DRUMMOND, G. R., WALLACE, E. M. & SOBEY, C. G. 2013. Post-stroke inflammation and the potential efficacy of novel stem cell therapies: focus on amnion epithelial cells. *Frontiers in cellular neuroscience,* 6**,** 66.

BUTALIA, S., GUTIERREZ, L., LODHA, A., AITKEN, E., ZAKARIASEN, A. & DONOVAN, L. 2017. Short-and long-term outcomes of metformin compared with insulin alone in pregnancy: a systematic review and meta-analysis. *Diabetic Medicine,* 34**,** 27-36.

BUTLER, J., EPSTEIN, S. E., GREENE, S. J., QUYYUMI, A. A., SIKORA, S., KIM, R. J., ANDERSON, A. S., WILCOX, J. E., TANKOVICH, N.

I. & LIPINSKI, M. J. 2017. Intravenous allogeneic mesenchymal stem cells for nonischemic cardiomyopathy: safety and efficacy results of a phase II-A randomized trial. *Circulation Research,* 120**,** 332-340.

CAGLAYAN, S., AHRENS, T. D., CIEŚLAR-POBUDA, A. & STAERK, J. 2019. Chapter 3 - Modern Ways of Obtaining Stem Cells. *In:* ŁOS, M. J., HUDECKI, A. & WIECHEĆ, E. (eds.) *Stem Cells and Biomaterials for Regenerative Medicine.* Academic Press.

CAMELO CASTILLO, W., BOGGESS, K., STÜRMER, T., BROOKHART, M. A., BENJAMIN, D. K., JR. & JONSSON FUNK, M. 2014. Trends in glyburide compared with insulin use for gestational diabetes treatment in the United States, 2000-2011. *Obstetrics and gynecology,* 123**,** 1177-1184.

CANFIELD, S. G., STEBBINS, M. J., MORALES, B. S., ASAI, S. W., VATINE, G. D., SVENDSEN, C. N., PALECEK, S. P. & SHUSTA, E. V. 2017. An isogenic blood–brain barrier model comprising brain endothelial cells, astrocytes, and neurons derived from human induced pluripotent stem cells. *Journal of neurochemistry,* 140**,** 874-888.

CAO, R., JI, H., FENG, N., ZHANG, Y., YANG, X., ANDERSSON, P., SUN, Y., TRITSARIS, K., HANSEN, A. J. & DISSING, S. 2012. Collaborative interplay between FGF-2 and VEGF-C promotes lymphangiogenesis and metastasis. *Proceedings of the National Academy of Sciences,* 109**,** 15894-15899.

CAPLAN, A. I. & CORREA, D. 2011. The MSC: an injury drugstore. *Cell stem cell,* 9**,** 11-15.

CARMAN, C. V. & SPRINGER, T. A. 2004. A transmigratory cup in leukocyte diapedesis both through individual vascular endothelial cells and between them. *The Journal of cell biology,* 167**,** 377-388.

CARMELIET, P. 2003. Angiogenesis in health and disease. *Nature medicine,* 9**,** 653-660.

CARMELIET, P. & JAIN, R. K. 2011. Molecular mechanisms and clinical applications of angiogenesis. *Nature,* 473**,** 298-307.

CARTER, A. 1997. When is the maternal placental circulation established in man? *Placenta,* 18**,** 83-87.

CASTRO-MANRREZA, M. E. & MONTESINOS, J. J. 2015. Immunoregulation by Mesenchymal Stem Cells: Biological Aspects and Clinical Applications. *Journal of Immunology Research,* 2015**,** 394917.

CATALANO, P. 2014. Trying to understand gestational diabetes. *Diabetic Medicine,* 31**,** 273-281.

CATALANO, P. M. & HAUGUEL-DE MOUZON, S. 2011. Is it time to revisit the Pedersen hypothesis in the face of the obesity epidemic? *Am J Obstet Gynecol,* 204**,** 479-87.

CATALANO, P. M., TYZBIR, E. D., ROMAN, N. M., AMINI, S. B. & SIMS, E. A. 1991. Longitudinal changes in insulin release and insulin

resistance in nonobese pregnant women. *American journal of obstetrics and gynecology,* 165**,** 1667-1672.

CATALANO, P. M., TYZBIR, E. D., WOLFE, R. R., ROMAN, N. M., AMINI, S. B. & SIMS, E. A. 1992. Longitudinal changes in basal hepatic glucose production and suppression during insulin infusion in normal pregnant women. *American journal of obstetrics and gynecology,* 167**,** 913-919.

CETIN, I., DE SANTIS, M. S. N., TARICCO, E., RADAELLI, T., TENG, C., RONZONI, S., SPADA, E., MILANI, S. & PARDI, G. 2005. Maternal and fetal amino acid concentrations in normal pregnancies and in pregnancies with gestational diabetes mellitus. *American journal of obstetrics and gynecology,* 192**,** 610-617.

CHADCHAN, S. B., KUMAR, V., MAURYA, V. K., SONI, U. K. & JHA, R. K. 2016. Endoglin (CD105) coordinates the process of endometrial receptivity for embryo implantation. *Molecular and Cellular Endocrinology,* 425**,** 69-83.

CHANG, P. & SAUER, M. 2002. The oocyte donation model: lessons on endometrial receptivity. *The Endometrium***,** 495-509.

CHARLES, B., NORRIS, R., XIAO, X. & HAGUE, W. 2006. Population pharmacokinetics of metformin in late pregnancy. *Therapeutic drug monitoring,* 28**,** 67-72.

CHEIFETZ, S., BELLÓN, T., CALÉS, C., VERA, S., BERNABEU, C., MASSAGUÉ, J. & LETARTE, M. 1992. Endoglin is a component of the transforming growth factor-beta receptor system in human endothelial cells. *Journal of Biological Chemistry,* 267**,** 19027-19030.

CHEN, L., MERKHAN, M. M., FORSYTH, N. R. & WU, P. 2019. Chorionic and amniotic membrane-derived stem cells have distinct, and gestational diabetes mellitus independent, proliferative, differentiation, and immunomodulatory capacities. *Stem Cell Research,* 40**,** 101537.

CHEN, L., WANG, C.-T., FORSYTH, N. R. & WU, P. 2020. Transcriptional profiling reveals altered biological characteristics of chorionic stem cells from women with gestational diabetes. *Stem cell research & therapy,* 11**,** 1-15.

CHEN, W., HUANG, Y., HAN, J., YU, L., LI, Y., LU, Z., LI, H., LIU, Z., SHI, C. & DUAN, F. 2016. Immunomodulatory effects of mesenchymal stromal cells-derived exosome. *Immunologic research,* 64**,** 831-840.

CHIRAYATH, H. H., WAREING, M., TAGGART, M. J. & BAKER, P. N. 2010. Endothelial dysfunction in myometrial arteries of women with gestational diabetes. *diabetes research and clinical practice,* 89**,** 134-140.

CHO, N. H., SHAW, J., KARURANGA, S., HUANG, Y., DA ROCHA FERNANDES, J., OHLROGGE, A. & MALANDA, B. 2018. IDF Diabetes Atlas: Global estimates of diabetes prevalence for 2017 and

projections for 2045. *Diabetes research and clinical practice,* 138**,** 271-281.

COTON, S. J., NAZARETH, I. & PETERSEN, I. 2016. A cohort study of trends in the prevalence of pregestational diabetes in pregnancy recorded in UK general practice between 1995 and 2012. *BMJ Open,* 6**,** e009494.

CRISAN, M., YAP, S., CASTEILLA, L., CHEN, C.-W., CORSELLI, M., PARK, T. S., ANDRIOLO, G., SUN, B., ZHENG, B. & ZHANG, L. 2008. A perivascular origin for mesenchymal stem cells in multiple human organs. *Cell stem cell,* 3**,** 301-313.

CVITIC, S., NOVAKOVIC, B., GORDON, L., ULZ, C. M., MÜHLBERGER, M., DIAZ-PEREZ, F. I., JOO, J. E., SVENDOVA, V., SCHIMEK, M. G., TRAJANOSKI, S., SAFFERY, R., DESOYE, G. & HIDEN, U. 2018. Human fetoplacental arterial and venous endothelial cells are differentially programmed by gestational diabetes mellitus, resulting in cell-specific barrier function changes. *Diabetologia,* 61**,** 2398-2411.

DA SILVA FLORIM, G. M., CALDAS, H. C., PAVARINO, E. C., BERTOLLO, E. M. G., FERNANDES, I. M. M. & ABBUD-FILHO, M. 2016. Variables associated to fetal microchimerism in systemic lupus erythematosus patients. *Clinical rheumatology,* 35**,** 107-111.

DALY, B., TOULIS, K. A., THOMAS, N., GOKHALE, K., MARTIN, J., WEBBER, J., KEERTHY, D., JOLLY, K., SARAVANAN, P. & NIRANTHARAKUMAR, K. 2018. Increased risk of ischemic heart disease, hypertension, and type 2 diabetes in women with previous gestational diabetes mellitus, a target group in general practice for preventive interventions: a population-based cohort study. *PLoS medicine,* 15**,** e1002488.

DASKALAKIS, G., MARINOPOULOS, S., KRIELESI, V., PAPAPANAGIOTOU, A., PAPANTONIOU, N., MESOGITIS, S. & ANTSAKLIS, A. 2008. Placental pathology in women with gestational diabetes. *Acta Obstetricia et Gynecologica Scandinavica,* 87**,** 403-407.

DAVIES, J. E., WALKER, J. T. & KEATING, A. 2017. Concise Review: Wharton's Jelly: The Rich, but Enigmatic, Source of Mesenchymal Stromal Cells. *STEM CELLS Translational Medicine,* 6**,** 1620-1630.

DAWE, G. S., TAN, X. W. & XIAO, Z.-C. 2007. Cell migration from baby to mother. *Cell Adhesion & Migration,* 1**,** 19-27.

DE BRUYN, C., NAJAR, M., RAICEVIC, G., MEULEMAN, N., PIETERS, K., STAMATOPOULOS, B., DELFORGE, A., BRON, D. & LAGNEAUX, L. 2011. A rapid, simple, and reproducible method for the isolation of mesenchymal stromal cells from Wharton's jelly without enzymatic treatment. *Stem cells and development,* 20**,** 547-557.

DE SOUZA, L. E. B., MALTA, T. M., KASHIMA HADDAD, S. & COVAS, D. T. 2016. Mesenchymal stem cells and pericytes: to what extent are they related? *Stem cells and development,* 25**,** 1843-1852.

DEAGLIO, S., DWYER, K. M., GAO, W., FRIEDMAN, D., USHEVA, A., ERAT, A., CHEN, J.-F., ENJYOJI, K., LINDEN, J. & OUKKA, M. 2007. Adenosine generation catalyzed by CD39 and CD73 expressed on regulatory T cells mediates immune suppression. *The Journal of experimental medicine,* 204**,** 1257-1265.

DEBEBE, S. K., CAHILL, L. S., KINGDOM, J. C., WHITEHEAD, C. L., CHANDRAN, A. R., PARKS, W. T., SERGHIDES, L., BASCHAT, A., MACGOWAN, C. K. & SLED, J. G. 2020. Wharton's jelly area and its association with placental morphometry and pathology. *Placenta,* 94**,** 34-38.

DEJANA, E. & GIAMPIETRO, C. 2012. Vascular endothelial-cadherin and vascular stability. *Current opinion in hematology,* 19**,** 218-223.

DEJANA, E. & ORSENIGO, F. 2013. Endothelial adherens junctions at a glance. *Journal of cell science,* 126**,** 2545-2549.

DEJANA, E., ORSENIGO, F. & LAMPUGNANI, M. G. 2008. The role of adherens junctions and VE-cadherin in the control of vascular permeability. *Journal of Cell Science,* 121**,** 2115.

DEJANA, E., TOURNIER-LASSERVE, E. & WEINSTEIN, B. M. 2009. The control of vascular integrity by endothelial cell junctions: molecular basis and pathological implications. *Developmental cell,* 16**,** 209-221.

DEL MASCHIO, A., ZANETTI, A., CORADA, M., RIVAL, Y., RUCO, L., LAMPUGNANI, M. G. & DEJANA, E. 1996. Polymorphonuclear leukocyte adhesion triggers the disorganization of endothelial cell-to-cell adherens junctions. *The Journal of cell biology,* 135**,** 497-510.

DEMIR, R., KAUFMANN, P., CASTELLUCCI, M., ERBENGI, T. & KOTOWSKI, A. 1989. Fetal vasculogenesis and angiogenesis in human placental villi. *Cells Tissues Organs,* 136**,** 190-203.

DENKER, H.-W. 1990. Trophoblast-endometrial interactions at embryo implantation: a cell biological paradox. *Trophoblast Invasion and Endometrial Receptivity.* Springer.

DENNEDY, M. C. & DUNNE, F. 2010. The maternal and fetal impacts of obesity and gestational diabetes on pregnancy outcome. *Best Practice & Research Clinical Endocrinology & Metabolism,* 24**,** 573-589.

DESFORGES, M. & SIBLEY, C. P. 2009. Placental nutrient supply and fetal growth. *International Journal of Developmental Biology,* 54**,** 377-390.

DESHMUKH, H. & WAY, S. S. 2019. Immunological basis for recurrent fetal loss and pregnancy complications. *Annual review of pathology,* 14**,** 185.

DI CIANNI, G., MICCOLI, R., VOLPE, L., LENCIONI, C. & DEL PRATO, S. 2003. Intermediate metabolism in normal pregnancy and in gestational diabetes. *Diabetes/metabolism research and reviews,* 19**,** 259-270.

DÍAZ-PRADO, S., MUIÑOS-LÓPEZ, E., HERMIDA-GÓMEZ, T., CICIONE, C., RENDAL-VÁZQUEZ, M. E., FUENTES-BOQUETE,

I., DE TORO, F. J. & BLANCO, F. J. 2011. Human amniotic membrane as an alternative source of stem cells for regenerative medicine. *Differentiation,* 81**,** 162-171.

DODD, J. M., LOUISE, J., DEUSSEN, A. R., GRIVELL, R. M., DEKKER, G., MCPHEE, A. J. & HAGUE, W. 2019. Effect of metformin in addition to dietary and lifestyle advice for pregnant women who are overweight or obese: the GRoW randomised, double-blind, placebo-controlled trial. *The lancet Diabetes & endocrinology,* 7**,** 15-24.

DOMINICI, M., LE BLANC, K., MUELLER, I., SLAPER-CORTENBACH, I., MARINI, F. C., KRAUSE, D. S., DEANS, R. J., KEATING, A., PROCKOP, D. J. & HORWITZ, E. M. 2006. Minimal criteria for defining multipotent mesenchymal stromal cells. The International Society for Cellular Therapy position statement. *Cytotherapy,* 8**,** 315-317.

EBERTH, C. 1871. Handbuch der Lehre von der Gewegen des Menschen und der Tiere. *Leipzig: W. Engelman*.

EBRAHIM, N. A. & LEACH, L. 2015. Temporal studies into attachment, VE-cadherin perturbation, and paracellular migration of human umbilical mesenchymal stem cells across umbilical vein endothelial monolayers. *Stem cells and development,* 24**,** 426-436.

EBRAHIM, N. A. & LEACH, L. 2016. Transendothelial migration of human umbilical mesenchymal stem cells across uterine endothelial monolayers: Junctional dynamics and putative mechanisms. *Placenta,* 48**,** 87-98.

EDWARDS, S. S., ZAVALA, G., PRIETO, C. P., ELLIOTT, M., MARTÍNEZ, S., EGAÑA, J. T., BONO, M. R. & PALMA, V. 2014. Functional analysis reveals angiogenic potential of human mesenchymal stem cells from Wharton's jelly in dermal regeneration. *Angiogenesis,* 17**,** 851-866.

ELICEIRI, B. P., PAUL, R., SCHWARTZBERG, P. L., HOOD, J. D., LENG, J. & CHERESH, D. A. 1999. Selective requirement for Src kinases during VEGF-induced angiogenesis and vascular permeability. *Molecular cell,* 4**,** 915-924.

ESFAHANIAN, N., SHAKIBA, Y., NIKBIN, B., SORAYA, H., MALEKI-DIZAJI, N., GHAZI-KHANSARI, M. & GARJANI, A. 2012. Effect of metformin on the proliferation, migration, and MMP-2 and-9 expression of human umbilical vein endothelial cells. *Molecular medicine reports,* 5**,** 1068-1074.

ESSER, S., LAMPUGNANI, M. G., CORADA, M., DEJANA, E. & RISAU, W. 1998. Vascular endothelial growth factor induces VE-cadherin tyrosine phosphorylation in endothelial cells. *J Cell Sci,* 111 (Pt 13)**,** 1853-65.

EVANS, M. J. & KAUFMAN, M. H. 1981. Establishment in culture of pluripotential cells from mouse embryos. *nature,* 292**,** 154-156.

EVERS, I., NIKKELS, P., SIKKEMA, J. & VISSER, G. 2003. Placental pathology in women with type 1 diabetes and in a control group with normal and large-for-gestational-age infants. *Placenta,* 24**,** 819-825.

EYAL, S., EASTERLING, T. R., CARR, D., UMANS, J. G., MIODOVNIK, M., HANKINS, G. D., CLARK, S. M., RISLER, L., WANG, J. & KELLY, E. J. 2010. Pharmacokinetics of metformin during pregnancy. *Drug Metabolism and Disposition,* 38**,** 833-840.

FADL, H. E., GÄRDEFORS, S., HJERTBERG, R., NORD, E., PERSSON, B., SCHWARCZ, E., ÅMAN, J., ÖSTLUND, I. K. & HANSON, U. S. B. 2015. Randomized controlled study in pregnancy on treatment of marked hyperglycemia that is short of overt diabetes. *Acta Obstetricia et Gynecologica Scandinavica,* 94**,** 1181-1187.

FEIG, D. S., DONOVAN, L. E., ZINMAN, B., SANCHEZ, J. J., ASZTALOS, E., RYAN, E. A., FANTUS, I. G., HUTTON, E., ARMSON, A. B. & LIPSCOMBE, L. L. 2020. Metformin in women with type 2 diabetes in pregnancy (MiTy): a multicentre, international, randomised, placebo-controlled trial. *The Lancet Diabetes & Endocrinology,* 8**,** 834-844.

FEIG, D. S., HWEE, J., SHAH, B. R., BOOTH, G. L., BIERMAN, A. S. & LIPSCOMBE, L. L. 2014. Trends in incidence of diabetes in pregnancy and serious perinatal outcomes: a large, population-based study in Ontario, Canada, 1996–2010. *Diabetes care,* 37**,** 1590-1596.

FENG, D., NAGY, J. A., DVORAK, H. F. & DVORAK, A. M. 2002. Ultrastructural studies define soluble macromolecular, particulate, and cellular transendothelial cell pathways in venules, lymphatic vessels, and tumor-associated microvessels in man and animals. *Microscopy research and technique,* 57**,** 289-326.

FERRARA, N. 2009. VEGF-A: a critical regulator of blood vessel growth. *European cytokine network,* 20**,** 158-163.

FERRARA, N. & ADAMIS, A. P. 2016. Ten years of anti-vascular endothelial growth factor therapy. *Nature reviews Drug discovery,* 15**,** 385-403.

FONSATTI, E. & MAIO, M. 2004. Highlights on endoglin (CD105): from basic findings towards clinical applications in human cancer. *Journal of Translational Medicine,* 2**,** 18.

FORRAZ, N. & MCGUCKIN, C. 2011. The umbilical cord: a rich and ethical stem cell source to advance regenerative medicine. *Cell Proliferation,* 44**,** 60-69.

FRIEDENSTEIN, A. J., GORSKAJA, J. & KULAGINA, N. 1976. Fibroblast precursors in normal and irradiated mouse hematopoietic organs. *Experimental hematology,* 4**,** 267-274.

GAITHER, K., QURAISHI, A. N. & ILLSLEY, N. P. 1999. Diabetes alters the expression and activity of the human placental GLUT1 glucose transporter. *The Journal of Clinical Endocrinology & Metabolism,* 84**,** 695-701.

GALARIS, G., MONTAGNE, K., THALGOTT, J. H., GOUJON, G. J. P. E., VAN DEN DRIESCHE, S., MARTIN, S., MAGER, H.-J. J.,

MUMMERY, C. L., RABELINK, T. J. & LEBRIN, F. 2021. Thresholds of Endoglin Expression in Endothelial Cells Explains Vascular Etiology in Hereditary Hemorrhagic Telangiectasia Type 1. *International Journal of Molecular Sciences,* 22**,** 8948.

GAVARD, J. 2009. Breaking the VE-cadherin bonds. *FEBS letters,* 583**,** 1-6.

GAVARD, J. 2013. Endothelial permeability and VE-cadherin: a wacky comradeship. *Cell adhesion & migration,* 7**,** 455-461.

GE, Q., ZHANG, H., HOU, J., WAN, L., CHENG, W., WANG, X., DONG, D., CHEN, C., XIA, J. & GUO, J. 2018. VEGF secreted by mesenchymal stem cells mediates the differentiation of endothelial progenitor cells into endothelial cells via paracrine mechanisms. *Molecular Medicine Reports,* 17**,** 1667-1675.

GEORGIADES, P., OGILVY, S., DUVAL, H., LICENCE, D. R., CHARNOCK-JONES, D. S., SMITH, S. K. & PRINT, C. G. 2002. VavCre transgenic mice: a tool for mutagenesis in hematopoietic and endothelial lineages. *genesis,* 34**,** 251-256.

GERHARDT, H., GOLDING, M., FRUTTIGER, M., RUHRBERG, C., LUNDKVIST, A., ABRAMSSON, A., JELTSCH, M., MITCHELL, C., ALITALO, K. & SHIMA, D. 2003. VEGF guides angiogenic sprouting utilizing endothelial tip cell filopodia. *The Journal of cell biology,* 161**,** 1163-1177.

GOMES, C.P., TORLONI, M.R., GUEUVOGHLANIAN-SILVA, B.Y., ALEXANDRE, S.M., MATTAR, R. AND DAHER, S., 2013. Cytokine levels in gestational diabetes mellitus: a systematic review of the literature. *American Journal of Reproductive Immunology*, *69*, 545-557.

GORE, B., IZIKKI, M., MERCIER, O., DEWACHTER, L., FADEL, E., HUMBERT, M., DARTEVELLE, P., SIMONNEAU, G., NAEIJE, R., LEBRIN, F. & EDDAHIBI, S. 2014. Key role of the endothelial TGF-β/ALK1/endoglin signaling pathway in humans and rodents pulmonary hypertension. *PLoS One,* 9**,** e100310.

GOUGOS, A. & LETARTE, M. 1988. Identification of a human endothelial cell antigen with monoclonal antibody 44G4 produced against a pre-B leukemic cell line. *The Journal of Immunology,* 141**,** 1925-1933.

GREGG, B., ELGHAZI, L., ALEJANDRO, E. U., SMITH, M. R., BLANDINO-ROSANO, M., EL-GABRI, D., CRAS-MÉNEUR, C. & BERNAL-MIZRACHI, E. 2014. Exposure of mouse embryonic pancreas to metformin enhances the number of pancreatic progenitors. *Diabetologia,* 57**,** 2566-2575.

GREGOIRE, F. M., SMAS, C. M. & SUL, H. S. 1998. Understanding adipocyte differentiation. *Physiological reviews,* 78**,** 783-809.

GREGORY, A. L., XU, G., SOTOV, V. & LETARTE, M. 2014. Review: The enigmatic role of endoglin in the placenta. *Placenta,* 35**,** S93-S99.

GUAN, L. X., GUAN, H., LI, H. B., REN, C. A., LIU, L., CHU, J. J. & DAI, L. J. 2015. Therapeutic efficacy of umbilical cord-derived

mesenchymal stem cells in patients with type 2 diabetes. *Experimental and therapeutic medicine,* 9**,** 1623-1630.

GUDE, N. M., ROBERTS, C. T., KALIONIS, B. & KING, R. G. 2004. Growth and function of the normal human placenta. *Thrombosis Research,* 114**,** 397-407.

GUIMARÃES-CAMBOA, N., CATTANEO, P., SUN, Y., MOORE-MORRIS, T., GU, Y., DALTON, N. D., ROCKENSTEIN, E., MASLIAH, E., PETERSON, K. L., STALLCUP, W. B., CHEN, J. & EVANS, S. M. 2017. Pericytes of Multiple Organs Do Not Behave as Mesenchymal Stem Cells In Vivo. *Cell Stem Cell,* 20**,** 345-359.e5.

GUMBINER, B. M. 1996. Cell adhesion: the molecular basis of tissue architecture and morphogenesis. *Cell,* 84**,** 345-357.

GUNDERSEN, H. J. & JENSEN, E. 1987. The efficiency of systematic sampling in stereology and its prediction. *Journal of microscopy,* 147**,** 229-263.

GUO, R., SAKAMOTO, H., SUGIURA, S. & OGAWA, M. 2007. Endothelial cell motility is compatible with junctional integrity. *Journal of cellular physiology,* 211**,** 327-335.

HADDEN, D. R. & MCLAUGHLIN, C. Normal and abnormal maternal metabolism during pregnancy. Seminars in Fetal and Neonatal Medicine, 2009. Elsevier, 66-71.

HAMILTON, R. D. & LEACH, L. 2011. Isolation and properties of an in vitro human outer blood-retinal barrier model. *The Blood-Brain and Other Neural Barriers.* Springer.

HAO, L., ZOU, Z., TIAN, H., ZHANG, Y., ZHOU, H. & LIU, L. 2014. Stem cell-based therapies for ischemic stroke. *BioMed research international,* 2014.

HARE, J. M., DIFEDE, D. L., RIEGER, A. C., FLOREA, V., LANDIN, A. M., EL-KHORAZATY, J., KHAN, A., MUSHTAQ, M., LOWERY, M. H. & BYRNES, J. J. 2017. Randomized comparison of allogeneic versus autologous mesenchymal stem cells for nonischemic dilated cardiomyopathy: POSEIDON-DCM trial. *Journal of the American College of Cardiology,* 69**,** 526-537.

HARE, J. M., FISHMAN, J. E., GERSTENBLITH, G., VELAZQUEZ, D. L. D., ZAMBRANO, J. P., SUNCION, V. Y., TRACY, M., GHERSIN, E., JOHNSTON, P. V. & BRINKER, J. A. 2012. Comparison of allogeneic vs autologous bone marrow–derived mesenchymal stem cells delivered by transendocardial injection in patients with ischemic cardiomyopathy: the POSEIDON randomized trial. *Jama,* 308**,** 2369-2379.

HATANAKA, K., LANAHAN, A. A., MURAKAMI, M. & SIMONS, M. 2012. Fibroblast growth factor signaling potentiates VE-cadherin stability at adherens junctions by regulating SHP2. *PLoS One,* 7**,** e37600.

HAWINKELS, L. J., KUIPER, P., WIERCINSKA, E., VERSPAGET, H. W., LIU, Z., PARDALI, E., SIER, C. F. & TEN DIJKE, P. 2010. Matrix Metalloproteinase-14 (MT1-MMP)–Mediated Endoglin Shedding Inhibits Tumor AngiogenesisMMP-14–Mediated Endoglin Shedding. *Cancer research,* 70**,** 4141-4150.

HAY JR, W. W. 2006. Placental-fetal glucose exchange and fetal glucose metabolism. *Transactions of the American Clinical and Climatological Association,* 117**,** 321.

HE, L. & HANNON, G. J. 2004. MicroRNAs: small RNAs with a big role in gene regulation. *Nature reviews genetics,* 5**,** 522-531.

HE, X., GU, Y., CAO, Y., HU, B., FANG, H., FEI, Y., LV, K., LIU, X., WANG, J. & LIN, C. 2021. Impact of intratumoural CD73 expression on prognosis and therapeutic response in patients with gastric cancer. *European Journal of Cancer,* 157**,** 114-123.

HEILMAIER, C., THIELSCHER, C., ZILLER, M., ALTMANN, V. AND KOSTEV, K., 2014. Use of antidiabetic agents in the treatment of gestational diabetes mellitus in G ermany, 2008–2012. ,. *Journal of Obstetrics and Gynaecology Research,* 40**,** 5.

HEINDEL, J. J. & VANDENBERG, L. N. 2015. Developmental origins of health and disease: a paradigm for understanding disease etiology and prevention. *Current opinion in pediatrics,* 27**,** 248.

HERRERA, M. B., BRUNO, S., BUTTIGLIERI, S., TETTA, C., GATTI, S., DEREGIBUS, M. C., BUSSOLATI, B. & CAMUSSI, G. 2006. Isolation and Characterization of a Stem Cell Population from Adult Human Liver. *STEM CELLS,* 24**,** 2840-2850.

HICKLIN, D. J. & ELLIS, L. M. 2005. Role of the vascular endothelial growth factor pathway in tumor growth and angiogenesis. *Journal of clinical oncology,* 23**,** 1011-1027.

HIRASE, T., STADDON, J. M., SAITOU, M., ANDO-AKATSUKA, Y., ITOH, M., FURUSE, M., FUJIMOTO, K., TSUKITA, S. & RUBIN, L. L. 1997. Occludin as a possible determinant of tight junction permeability in endothelial cells. *J Cell Sci,* 110 (Pt 14)**,** 1603-13.

HOTAMISLIGIL, G.S., 2003. Inflammatory pathways and insulin action. *International Journal of Obesity*, *27*, S53-S55.

HU, J., WANG, Y., GONG, H., YU, C., GUO, C., WANG, F., YAN, S. & XU, H. 2016. Long term effect and safety of Wharton's jelly-derived mesenchymal stem cells on type 2 diabetes. *Experimental and therapeutic medicine,* 12**,** 1857-1866.

HU, S., PARK, J., LIU, A., LEE, J., ZHANG, X., HAO, Q. & LEE, J.-W. 2018. Mesenchymal Stem Cell Microvesicles Restore Protein Permeability Across Primary Cultures of Injured Human Lung Microvascular Endothelial Cells. *Stem Cells Translational Medicine,* 7**,** 615-624.

HUANG, N. F. & LI, S. 2008. Mesenchymal stem cells for vascular regeneration.

HUNT, K. J. & SCHULLER, K. L. 2007. The increasing prevalence of diabetes in pregnancy. *Obstetrics and gynecology clinics of North America,* 34**,** 173-vii.

HUPPERTZ, B. 2008. The anatomy of the normal placenta. *Journal of Clinical Pathology,* 61**,** 1296.

IJÄS, H., VÄÄRÄSMÄKI, M., SAARELA, T., KERAVUO, R. & RAUDASKOSKI, T. 2015. A follow-up of a randomised study of metformin and insulin in gestational diabetes mellitus: growth and development of the children at the age of 18 months. *BJOG: An International Journal of Obstetrics & Gynaecology,* 122**,** 994-1000.

IQBAL, T., SAAIQ, M. & ALI, Z. 2013. Epidemiology and outcome of burns: early experience at the country's first national burns centre. *Burns,* 39**,** 358-362.

ITOH, M., MORITA, K. & TSUKITA, S. 1999. Characterization of ZO-2 as a MAGUK family member associated with tight as well as adherens junctions with a binding affinity to occludin and alpha catenin. *J Biol Chem,* 274**,** 5981-6.

JACKSON, L. 2003. Fetal cells and DNA in maternal blood. *Prenatal Diagnosis: Published in Affiliation With the International Society for Prenatal Diagnosis,* 23**,** 837-846.

JANSSON, T., AYE, I. L. & GOBERDHAN, D. C. 2012. The emerging role of mTORC1 signaling in placental nutrient-sensing. *Placenta,* 33**,** e23-e29.

JANSSON, T., EKSTRAND, Y., BJORN, C., WENNERGREN, M. & POWELL, T. L. 2002. Alterations in the activity of placental amino acid transporters in pregnancies complicated by diabetes. *Diabetes,* 51**,** 2214-2219.

JANSSON, T., EKSTRAND, Y., WENNERGREN, M. & POWELL, T. L. 2001. Placental glucose transport in gestational diabetes mellitus. *American journal of obstetrics and gynecology,* 184**,** 111-116.

JANSSON, T. & POWELL, T. L. 2006. Human placental transport in altered fetal growth: does the placenta function as a nutrient sensor?–a review. *Placenta,* 27**,** 91-97.

JEON, K. W. & KENNEDY, J. R. 1973. The primordial germ cells in early mouse embryos: light and electron microscopic studies. *Developmental biology,* 31**,** 275-284.

JIANG, Y., HUANG, W., WANG, J., XU, Z., HE, J., LIN, X., ZHOU, Z. & ZHANG, J. 2014. Metformin plays a dual role in MIN6 pancreatic β cell function through AMPK-dependent autophagy. *International journal of biological sciences,* 10**,** 268.

JIN, Y., MUHL, L., BURMAKIN, M., WANG, Y., DUCHEZ, A.-C., BETSHOLTZ, C., ARTHUR, H. M. & JAKOBSSON, L. 2017. Endoglin prevents vascular malformation by regulating flow-induced cell migration and specification through VEGFR2 signalling. *Nature cell biology,* 19**,** 639-652.

JOFFRE, J., HELLMAN, J., INCE, C. & AIT-OUFELLA, H. 2020. Endothelial responses in sepsis. *American journal of respiratory and critical care medicine,* 202**,** 361-370.

JOHNSON, K. L., NELSON, J. L., FURST, D. E., MCSWEENEY, P. A., ROBERTS, D. J., ZHEN, D. K. & BIANCHI, D. W. 2001. Fetal cell microchimerism in tissue from multiple sites in women with systemic sclerosis. *Arthritis & Rheumatism,* 44**,** 1848-1854.

JOHNSTONE, B., HERING, T. M., CAPLAN, A. I., GOLDBERG, V. M. & YOO, J. U. 1998. In vitrochondrogenesis of bone marrow-derived mesenchymal progenitor cells. *Experimental cell research,* 238**,** 265-272.

JYOTHI PRASANNA, S. & SOWMYA JAHNAVI, V. 2011. Wharton's jelly mesenchymal stem cells as off-the-shelf cellular therapeutics: a closer look into their regenerative and immunomodulatory properties. *The Open Tissue Engineering and Regenerative Medicine Journal,* 4.

KACZMAREK, I., DEUTSCH, M.-A., ROHRER, M.-E., BEIRAS-FERNANDEZ, A., GROETZNER, J., DAEBRITZ, S., SCHMOECKEL, M., SPANNAGL, M., MEISER, B. & REICHART, B. 2006. HLA-DR matching improves survival after heart transplantation: is it time to change allocation policies? *The Journal of heart and lung transplantation,* 25**,** 1057-1062.

KAMANA, K., SHAKYA, S. & ZHANG, H. 2015. Gestational diabetes mellitus and macrosomia: a literature review. *Annals of Nutrition and Metabolism,* 66**,** 14-20.

KAMOLZ, L.-P., KECK, M. & KASPER, C. 2014. Wharton's jelly mesenchymal stem cells promote wound healing and tissue regeneration. *Stem cell research & therapy,* 5**,** 62-62.

KAUER, J., SCHWARTZ, K., TANDLER, C., HINTERLEITNER, C., ROERDEN, M., JUNG, G., SALIH, H. R., HEITMANN, J. S. & MÄRKLIN, M. 2019. CD105 (Endoglin) as negative prognostic factor in AML. *Scientific Reports,* 9**,** 18337.

KAUFMANN, P. 1992. Placental development. *Maternal-fetal physiology***,** 47-55.

KAUFMANN, P., BLACK, S. & HUPPERTZ, B. 2003. Endovascular trophoblast invasion: implications for the pathogenesis of intrauterine growth retardation and preeclampsia. *Biology of reproduction,* 69**,** 1-7.

KIM, D.-W., STAPLES, M., SHINOZUKA, K., PANTCHEVA, P., KANG, S.-D. & BORLONGAN, C. V. 2013. Wharton's jelly-derived mesenchymal stem cells: phenotypic characterization and optimizing their therapeutic potential for clinical applications. *International journal of molecular sciences,* 14**,** 11692-11712.

KIM, J., PIAO, Y., PAK, Y. K., CHUNG, D., HAN, Y. M., HONG, J. S., JUN, E. J., SHIM, J.-Y., CHOI, J. & KIM, C. J. 2015. Umbilical cord mesenchymal stromal cells affected by gestational diabetes mellitus

display premature aging and mitochondrial dysfunction. *Stem cells and development,* 24**,** 575-586.

KIM, S. U. & DE VELLIS, J. 2009. Stem cell-based cell therapy in neurological diseases: a review. *Journal of neuroscience research,* 87**,** 2183-2200.

KINGDOM, J., HUPPERTZ, B., SEAWARD, G. & KAUFMANN, P. 2000. Development of the placental villous tree and its consequences for fetal growth. *European Journal of Obstetrics & Gynecology and Reproductive Biology,* 92**,** 35-43.

KOBAYASHI, H., TAMATANI, T., TAMURA, T., KUSAFUKA, J., YAMATAKA, A., LANE, G. J., KAWASAKI, S., ISHIZAKI, Y., MIZUTA, K. & KAWARASAKI, H. 2007. Maternal microchimerism in biliary atresia. *Journal of pediatric surgery,* 42**,** 987-991.

KOCH, A. W., BOZIC, D., PERTZ, O. & ENGEL, J. 1999. Homophilic adhesion by cadherins. *Current Opinion in Structural Biology,* 9**,** 275-281.

KOMAROVA, Y. & MALIK, A. B. 2010. Regulation of endothelial permeability via paracellular and transcellular transport pathways. *Annual review of physiology,* 72**,** 463-493.

KOMAROVA, Y. A., KRUSE, K., MEHTA, D. & MALIK, A. B. 2017. Protein Interactions at Endothelial Junctions and Signaling Mechanisms Regulating Endothelial Permeability. *Circulation Research,* 120**,** 179-206.

KONG, C.-M., SUBRAMANIAN, A., BISWAS, A., STUNKEL, W., CHONG, Y.-S., BONGSO, A. & FONG, C.-Y. 2019. Changes in Stemness Properties, Differentiation Potential, Oxidative Stress, Senescence and Mitochondrial Function in Wharton's Jelly Stem Cells of Umbilical Cords of Mothers with Gestational Diabetes Mellitus. *Stem Cell Reviews and Reports,* 15**,** 415-426.

KOVO, M., HAROUTIUNIAN, S., FELDMAN, N., HOFFMAN, A. & GLEZERMAN, M. 2008. Determination of metformin transfer across the human placenta using a dually perfused ex vivo placental cotyledon model. *European Journal of Obstetrics & Gynecology and Reproductive Biology,* 136**,** 29-33.

KROHN-GRIMBERGHE, M., MITCHELL, M. J., SCHLOSS, M. J., KHAN, O. F., COURTIES, G., GUIMARAES, P. P. G., ROHDE, D., CREMER, S., KOWALSKI, P. S., SUN, Y., TAN, M., WEBSTER, J., WANG, K., IWAMOTO, Y., SCHMIDT, S. P., WOJTKIEWICZ, G. R., NAYAR, R., FRODERMANN, V., HULSMANS, M., CHUNG, A., HOYER, F. F., SWIRSKI, F. K., LANGER, R., ANDERSON, D. G. & NAHRENDORF, M. 2020. Nanoparticle-encapsulated siRNAs for gene silencing in the haematopoietic stem-cell niche. *Nat Biomed Eng,* 4**,** 1076-1089.

KRUPA, P., VACKOVA, I., RUZICKA, J., ZAVISKOVA, K., DUBISOVA, J., KOCI, Z., TURNOVCOVA, K., URDZIKOVA, L. M., KUBINOVA, S., REHAK, S. & JENDELOVA, P. 2018. The Effect of

Human Mesenchymal Stem Cells Derived from Wharton's Jelly in Spinal Cord Injury Treatment Is Dose-Dependent and Can Be Facilitated by Repeated Application. *International Journal of Molecular Sciences,* 19.

KWAK, S. H. & PARK, K. S. 2016. Recent progress in genetic and epigenetic research on type 2 diabetes. *Experimental & Molecular Medicine,* 48**,** e220-e220.

KWON, Y.-W., AHN, H.-S., LEE, J.-W., YANG, H.-M., CHO, H.-J., KIM, S. J., LEE, S.-H., YANG, H.-M., JANG, H.-D., KIM, S. J. & KIM, H.-S. 2021. HLA DR Genome Editing with TALENs in Human iPSCs Produced Immune-Tolerant Dendritic Cells. *Stem Cells International,* 2021**,** 8873383.

LABARRERE, C., SEBASTIANI, M., SIMINOVICH, M., TORASSA, E. & ALTHABE, O. 1985. Absence of Wharton's jelly around the umbilical arteries: An unusual cause of perinatal mortality. *Placenta,* 6**,** 555-559.

LAGER, S. & POWELL, T. L. 2012. Regulation of nutrient transport across the placenta. *Journal of pregnancy,* 2012.

LAIN, K. Y. & CATALANO, P. M. 2007. Metabolic changes in pregnancy. *Clinical obstetrics and gynecology,* 50**,** 938-948.

LAMOIA, T. E. & SHULMAN, G. I. 2021. Cellular and molecular mechanisms of metformin action. *Endocrine Reviews,* 42**,** 77-96.

LAMPUGNANI 2017. Vascular Endothelial (VE)-Cadherin, Endothelial Adherens Junctions, and Vascular Disease. *Cold Spring Harb Perspect Biol.* .

LAMPUGNANI, M.-G., RESNATI, M., RAITERI, M., PIGOTT, R., PISACANE, A., HOUEN, G., RUCO, L. & DEJANA, E. 1992. A novel endothelial-specific membrane protein is a marker of cell-cell contacts. *The Journal of cell biology,* 118**,** 1511-1522.

LAMPUGNANI, M. G., CORADA, M., CAVEDA, L., BREVIARIO, F., AYALON, O., GEIGER, B. & DEJANA, E. 1995. The molecular organization of endothelial cell to cell junctions: differential association of plakoglobin, beta-catenin, and alpha-catenin with vascular endothelial cadherin (VE-cadherin). *J Cell Biol,* 129**,** 203-17.

LAMPUGNANI, M. G., ORSENIGO, F., GAGLIANI, M. C., TACCHETTI, C. & DEJANA, E. 2006. Vascular endothelial cadherin controls VEGFR-2 internalization and signaling from intracellular compartments. *The Journal of cell biology,* 174**,** 593-604.

LANDON, M. B. & GABBE, S. G. 2011. Gestational Diabetes Mellitus. *Obstetrics & Gynecology,* 118**,** 1379-1393.

LANGER, O., CONWAY, D. L., BERKUS, M. D., XENAKIS, E. M. J. & GONZALES, O. 2000. A Comparison of Glyburide and Insulin in Women with Gestational Diabetes Mellitus. *New England Journal of Medicine,* 343**,** 1134-1138.

LAPPAS, M. 2014. Markers of endothelial cell dysfunction are increased in human omental adipose tissue from women with pre-existing maternal obesity and gestational diabetes. *Metabolism,* 63**,** 860-873.

LAPPAS, M., HIDEN, U., DESOYE, G., FROEHLICH, J., MOUZON, S. H.-D. & JAWERBAUM, A. 2011. The role of oxidative stress in the pathophysiology of gestational diabetes mellitus. *Antioxidants & redox signaling,* 15**,** 3061-3100.

LASSANCE, L., MIEDL, H., ABSENGER, M., DIAZ-PEREZ, F., LANG, U., DESOYE, G. & HIDEN, U. 2013. Hyperinsulinemia Stimulates Angiogenesis of Human Fetoplacental Endothelial Cells: A Possible Role of Insulin in Placental Hypervascularization in Diabetes Mellitus. *The Journal of Clinical Endocrinology & Metabolism,* 98**,** E1438-E1447.

LASTRES, P., BELLON, T., CABAÑAS, C., SANCHEZ-MADRID, F., ACEVEDO, A., GOUGOS, A., LETARTE, M. & BERNABEU, C. 1992. Regulated expression on human macrophages of endoglin, an Arg-Gly-Asp-containing surface antigen. *European journal of immunology,* 22**,** 393-397.

LEACH, L. 2011. Placental Vascular Dysfunction in Diabetic Pregnancies: Intimations of Fetal Cardiovascular Disease? *Microcirculation,* 18**,** 263-269.

LEACH, L., BABAWALE, M. O., ANDERSON, M. & LAMMIMAN, M. 2002. Vasculogenesis, Angiogenesis and the Molecular Organisation of Endothelial Junctions in the Early Human Placenta. *Journal of Vascular Research,* 39**,** 246-259.

LEACH, L., EATON, B. M., WESTCOTT, E. D. & FIRTH, J. A. 1995. Effect of histamine on endothelial permeability and structure and adhesion molecules of the paracellular junctions of perfused human placental microvessels. *Microvascular research,* 50**,** 323-337.

LEACH, L. & FIRTH, J. A. 1992. Fine structure of the paracellular junctions of terminal villous capillaries in the perfused human placeta. *Cell and tissue research,* 268**,** 447-452.

LEACH, L., GRAY, C., STATON, S., BABAWALE, M., GRUCHY, A., FOSTER, C., MAYHEW, T. & JAMES, D. 2004. Vascular endothelial cadherin and β-catenin in human fetoplacental vessels of pregnancies complicated by Type 1 diabetes: associations with angiogenesis and perturbed barrier function. *Diabetologia,* 47**,** 695-709.

LEACH, L., TAYLOR, A. & SCIOTA, F. 2009. Vascular dysfunction in the diabetic placenta: causes and consequences. *Journal of Anatomy,* 215**,** 69-76.

LEAÑOS-MIRANDA, A., NAVARRO-ROMERO, C. S., SILLAS-PARDO, L. J., RAMÍREZ-VALENZUELA, K. L., ISORDIA-SALAS, I. & JIMÉNEZ-TREJO, L. M. 2019. Soluble endoglin as a marker for preeclampsia, its severity, and the occurrence of adverse outcomes. *Hypertension,* 74**,** 991-997.

LEBRIN, F., GOUMANS, M.-J., JONKER, L., CARVALHO, R. L. C., VALDIMARSDOTTIR, G., THORIKAY, M., MUMMERY, C., ARTHUR, H. M. & TEN DIJKE, P. 2004. Endoglin promotes endothelial cell proliferation and TGF-beta/ALK1 signal transduction. *The EMBO journal,* 23**,** 4018-4028.

LECKBAND, D. & SIVASANKAR, S. 2000. Mechanism of homophilic cadherin adhesion. *Current opinion in cell biology,* 12**,** 587-592.

LEE JANG, H., OKADA, K., KHUSH, K., KOBAYASHI, Y., SINHA, S., LUIKART, H., VALANTINE, H., YEUNG ALAN, C., HONDA, Y. & FEARON WILLIAM, F. 2017. Coronary Endothelial Dysfunction and the Index of Microcirculatory Resistance as a Marker of Subsequent Development of Cardiac Allograft Vasculopathy. *Circulation,* 135**,** 1093-1095.

LEE, N., HEBERT, M. F., WAGNER, D. J., EASTERLING, T. R., LIANG, C. J., RICE, K. & WANG, J. 2018. Organic cation transporter 3 facilitates fetal exposure to metformin during pregnancy. *Molecular pharmacology,* 94**,** 1125-1131.

LEE, S. D., YU, D., LEE, D. Y., SHIN, H.-S., JO, J.-H. & LEE, Y. C. 2019. Upregulated microRNA-193a-3p is responsible for cisplatin resistance in CD44(+) gastric cancer cells. *Cancer Science,* 110**,** 662-673.

LEI, L., CHEN, J., ZHAO, Y., YANG, S. & HE, L. 2016. Resveratrol attenuates senescence of adipose-derived mesenchymal stem cells and restores their paracrine effects on promoting insulin secretion of INS-1 cells through Pim-1. *Eur Rev Med Pharmacol Sci,* 20**,** 1203-1213.

LENTI, M., CIERI, E., DE RANGO, P., POZZILLI, P., COSCARELLA, C., BERTOGLIO, C., TROIANI, R. & CAO, P. 2007. Endovascular treatment of long lesions of the superficial femoral artery: results from a multicenter registry of a spiral, covered polytetrafluoroethylene stent. *Journal of vascular surgery,* 45**,** 32-39.

LEVI, B., WAN, D. C., GLOTZBACH, J. P., HYUN, J., JANUSZYK, M., MONTORO, D., SORKIN, M., JAMES, A. W., NELSON, E. R., LI, S., QUARTO, N., LEE, M., GURTNER, G. C. & LONGAKER, M. T. 2011. CD105 protein depletion enhances human adipose-derived stromal cell osteogenesis through reduction of transforming growth factor β1 (TGF-β1) signaling. *J Biol Chem,* 286**,** 39497-509.

LEVICK, J. & SMAJE, L. 1987. An analysis of the permeability of a fenestra. *Microvascular research,* 33**,** 233-256.

LEVINE, R. J., LAM, C., QIAN, C., YU, K. F., MAYNARD, S. E., SACHS, B. P., SIBAI, B. M., EPSTEIN, F. H., ROMERO, R. & THADHANI, R. 2006. Soluble endoglin and other circulating antiangiogenic factors in preeclampsia. *New England Journal of Medicine,* 355**,** 992-1005.

LI, C., GUO, B., DING, S., RUIS, C., LANGA, C., KUMAR, P., BERNABEU, C. & KUMAR, S. 2003. TNFα down-regulates CD105 expression in vascular endothelial cells: A comparative study with TGFß1.

LI, D., LIU, Q., QI, L., DAI, X., LIU, H. & WANG, Y. 2016. Low levels of TGF-β1 enhance human umbilical cord-derived mesenchymal stem cell fibronectin production and extend survival time in a rat model of lipopolysaccharide-induced acute lung injury. *Molecular medicine reports,* 14**,** 1681-1692.

LIAU, L. L., RUSZYMAH, B. H. I., NG, M. H. & LAW, J. X. 2020. Characteristics and clinical applications of Wharton's jelly-derived mesenchymal stromal cells. *Current Research in Translational Medicine,* 68**,** 5-16.

LINDEN, J. 2001. Molecular Approach to Adenosine Receptors: Receptor-Mediated Mechanisms of Tissue Protection. *Annual Review of Pharmacology and Toxicology,* 41**,** 775-787.

LIU, L., YU, Q., HU, K., WANG, B., ZHANG, Y., XU, Y., FU, S., YU, X. & HUANG, H. 2016. Electro-acupuncture promotes endogenous multipotential mesenchymal stem cell mobilization into the peripheral blood. *Cellular Physiology and Biochemistry,* 38**,** 1605-1617.

LIU, X., ZHENG, P., WANG, X., DAI, G., CHENG, H., ZHANG, Z., HUA, R., NIU, X., SHI, J. & AN, Y. 2014a. A preliminary evaluation of efficacy and safety of Wharton's jelly mesenchymal stem cell transplantation in patients with type 2 diabetes mellitus. *Stem cell research & therapy,* 5**,** 1-9.

LIU, Y., PAAUWE, M., NIXON, A. B. & HAWINKELS, L. J. A. C. 2021. Endoglin Targeting: Lessons Learned and Questions That Remain. *International Journal of Molecular Sciences,* 22**,** 147.

LIU, Z., LEBRIN, F., MARING, J. A., VAN DEN DRIESCHE, S., VAN DER BRINK, S., VAN DINTHER, M., THORIKAY, M., MARTIN, S., KOBAYASHI, K. & HAWINKELS, L. J. 2014b. ENDOGLIN is dispensable for vasculogenesis, but required for vascular endothelial growth factor-induced angiogenesis. *PloS one,* 9**,** e86273.

MACEYKA, M., HARIKUMAR, K. B., MILSTIEN, S. & SPIEGEL, S. 2012. Sphingosine-1-phosphate signaling and its role in disease. *Trends in cell biology,* 22**,** 50-60.

MADAZLı, R., TUTEN, A., CALAY, Z., UZUN, H., ULUDAG, S. & OCAK, V. 2008. The incidence of placental abnormalities, maternal and cord plasma malondialdehyde and vascular endothelial growth factor levels in women with gestational diabetes mellitus and nondiabetic controls. *Gynecologic and obstetric investigation,* 65**,** 227-232.

MADIGAN, M. & ATOUI, R. 2018. Therapeutic use of stem cells for myocardial infarction. *Bioengineering,* 5**,** 28.

MAGARIÑOS, M. P., SÁNCHEZ-MARGALET, V., KOTLER, M., CALVO, J. C. & VARONE, C. L. 2007. Leptin promotes cell proliferation and survival of trophoblastic cells. *Biology of reproduction,* 76**,** 203-210.

MAGEE, T. R., ROSS, M. G., WEDEKIND, L., DESAI, M., KJOS, S. & BELKACEMI, L. 2014. Gestational diabetes mellitus alters apoptotic

and inflammatory gene expression of trophobasts from human term placenta. *Journal of Diabetes and its Complications,* 28**,** 448-459.

MAGNESS, R. R. 1998. Maternal cardiovascular and other physiologic responses to the endocrinology of pregnancy. *Endocrinology of pregnancy***,** 507-539.

MAHMOOD, U. & O'DONOGHUE, K. 2014. Microchimeric fetal cells play a role in maternal wound healing after pregnancy. *Chimerism,* 5**,** 40-52.

MALEKI, M., GHANBARVAND, F., BEHVARZ, M. R., EJTEMAEI, M. & GHADIRKHOMI, E. 2014. Comparison of mesenchymal stem cell markers in multiple human adult stem cells. *International journal of stem cells,* 7**,** 118-126.

MALONEY, S., SMITH, A., FURST, D. E., MYERSON, D., RUPERT, K., EVANS, P. C. & NELSON, J. L. 1999. Microchimerism of maternal origin persists into adult life. *The Journal of clinical investigation,* 104**,** 41-47.

MARINO, L., CASTALDI, M. A., ROSAMILIO, R., RAGNI, E., VITOLO, R., FULGIONE, C., CASTALDI, S. G., SERIO, B., BIANCO, R. & GUIDA, M. 2019. Mesenchymal stem cells from the Wharton's jelly of the human umbilical cord: biological properties and therapeutic potential. *Int J stem cells,* 12**,** 218-226.

MARTIN, K. E., GRIVELL, R. M., YELLAND, L. N. & DODD, J. M. 2015. The influence of maternal BMI and gestational diabetes on pregnancy outcome. *Diabetes research and clinical practice,* 108**,** 508-513.

MARTINEZ, J., PATKANIOWSKA, A., URLAUB, H., LÜHRMANN, R. & TUSCHL, T. 2002. Single-Stranded Antisense siRNAs Guide Target RNA Cleavage in RNAi. *Cell,* 110**,** 563-574.

MARTINO, J., SEBERT, S., SEGURA, M., GARCÍA-VALDÉS, L., FLORIDO, J., PADILLA, M., MARCOS, A., RUEDA, R., MCARDLE, H. & BUDGE, H. 2016. Maternal body weight and gestational diabetes differentially influence placental and pregnancy outcomes. *The Journal of Clinical Endocrinology & Metabolism,* 101**,** 59-68.

MATHEW, S. A., NAIK, C., CAHILL, P. A. & BHONDE, R. R. 2020. Placental mesenchymal stromal cells as an alternative tool for therapeutic angiogenesis. *Cellular and Molecular Life Sciences,* 77**,** 253-265.

MCALLISTER, K., GROGG, K., JOHNSON, D. W., GALLIONE, C., BALDWIN, M., JACKSON, C., HELMBOLD, E., MARKEL, D., MCKINNON, W. & MURREL, J. 1994. Endoglin, a TGF-β binding protein of endothelial cells, is the gene for hereditary haemorrhagic telangiectasia type 1. *Nature genetics,* 8**,** 345-351.

MCBEATH, R., PIRONE, D. M., NELSON, C. M., BHADRIRAJU, K. & CHEN, C. S. 2004. Cell shape, cytoskeletal tension, and RhoA regulate stem cell lineage commitment. *Developmental cell,* 6**,** 483-495.

MCINTYRE, H. D., CATALANO, P., ZHANG, C., DESOYE, G., MATHIESEN, E. R. & DAMM, P. 2019a. Gestational diabetes mellitus. *Nature Reviews Disease Primers,* 5**,** 47.

MCINTYRE, H. D., CATALANO, P., ZHANG, C., DESOYE, G., MATHIESEN, E. R. & DAMM, P. 2019b. Gestational Diabetes Mellitus. *Diabetes Care,* 5**,** 1-19.

MEHTA, D. & MALIK, A. B. 2006. Signaling Mechanisms Regulating Endothelial Permeability. *Physiological Reviews,* 86**,** 279-367.

MEISEL, R., ZIBERT, A., LARYEA, M., GÖBEL, U., DÄUBENER, W. & DILLOO, D. 2004. Human bone marrow stromal cells inhibit allogeneic T-cell responses by indoleamine 2, 3-dioxygenase–mediated tryptophan degradation. *Blood,* 103**,** 4619-4621.

MENDICINO, M., BAILEY, A. M., WONNACOTT, K., PURI, R. K. & BAUER, S. R. 2014. MSC-based product characterization for clinical trials: an FDA perspective. *Cell stem cell,* 14**,** 141-145.

MEURER, S., WIMMER, A. E., VAN DE LEUR, E. & WEISKIRCHEN, R. 2019. Endoglin trafficking/exosomal targeting in liver cells depends on N-glycosylation. *Cells,* 8**,** 997.

MINHAJAT, R., MORI, D., YAMASAKI, F., SUGITA, Y., SATOH, T. & TOKUNAGA, O. 2006. Organ-specific endoglin (CD105) expression in the angiogenesis of human cancers. *Pathology international,* 56**,** 717-723.

MINSHALL, R. D., TIRUPPATHI, C., VOGEL, S. M. & MALIK, A. B. 2002. Vesicle formation and trafficking in endothelial cells and regulation of endothelial barrier function. *Histochemistry and cell biology,* 117**,** 105-112.

MOORE, K. A. & LEMISCHKA, I. R. 2006. Stem cells and their niches. *Science,* 311**,** 1880-1885.

MORTIER, I., BLANC, J., TOSELLO, B., GIRE, C., BRETELLE, F. & CARCOPINO, X. 2017. Is gestational diabetes an independent risk factor of neonatal severe respiratory distress syndrome after 34 weeks of gestation? A prospective study. *Archives of Gynecology and Obstetrics,* 296**,** 1071-1077.

MRIZAK, I., ARFA, A., FEKIH, M., DEBBABI, H., BOUSLEMA, A., BOUMAIZA, I., ZAOUALI, M., KHAN, N. A. & TABKA, Z. 2013. Inflammation and impaired endothelium-dependant vasodilatation in non obese women with gestational diabetes mellitus: preliminary results. *Lipids in health and disease,* 12**,** 1-7.

MUECKLER, M. & THORENS, B. 2013. The SLC2 (GLUT) family of membrane transporters. *Molecular aspects of medicine,* 34**,** 121-138.

MURPHY, M. B., MONCIVAIS, K. & CAPLAN, A. I. 2013. Mesenchymal stem cells: environmentally responsive therapeutics for regenerative medicine. *Experimental & molecular medicine,* 45**,** e54-e54.

MURRAY, S. R. & REYNOLDS, R. M. 2020. Short-and long-term outcomes of gestational diabetes and its treatment on fetal development. *Prenatal Diagnosis*.

MYREN, M., MOSE, T., MATHIESEN, L. & KNUDSEN, L. E. 2007. The human placenta – An alternative for studying foetal exposure. *Toxicology in Vitro,* 21**,** 1332-1340.

NAGY, J. A., BENJAMIN, L., ZENG, H., DVORAK, A. M. & DVORAK, H. F. 2008. Vascular permeability, vascular hyperpermeability and angiogenesis. *Angiogenesis,* 11**,** 109-119.

NAGY, J. A., FENG, D., VASILE, E., WONG, W. H., SHIH, S.-C., DVORAK, A. M. & DVORAK, H. F. 2006. Permeability properties of tumor surrogate blood vessels induced by VEGF-A. *Laboratory investigation,* 86**,** 767-780.

NANOVSKAYA, T. N., NEKHAYEVA, I. A., PATRIKEEVA, S. L., HANKINS, G. D. V. & AHMED, M. S. 2006. Transfer of metformin across the dually perfused human placental lobule. *American Journal of Obstetrics and Gynecology,* 195**,** 1081-1085.

NASDALA, I., WOLBURG-BUCHHOLZ, K., WOLBURG, H., KUHN, A., EBNET, K., BRACHTENDORF, G., SAMULOWITZ, U., KUSTER, B., ENGELHARDT, B. & VESTWEBER, D. 2002. A transmembrane tight junction protein selectively expressed on endothelial cells and platelets. *Journal of Biological Chemistry,* 277**,** 16294-16303.

NEHRING, I., CHMITORZ, A., REULEN, H., VON KRIES, R. & ENSENAUER, R. 2013. Gestational diabetes predicts the risk of childhood overweight and abdominal circumference independent of maternal obesity. *Diabetic medicine,* 30**,** 1449-1456.

NELSON, S. M., COAN, P. M., BURTON, G. J. & LINDSAY, R. S. 2009. Placental structure in type 1 diabetes: relation to fetal insulin, leptin, and IGF-I. *Diabetes,* 58**,** 2634-2641.

NGUYEN-NGO, C., JAYABALAN, N., SALOMON, C. & LAPPAS, M. 2019. Molecular pathways disrupted by gestational diabetes mellitus. *Journal of molecular endocrinology,* 63**,** R51-R72.

NGUYEN, L., CHAN, S.-Y. & TEO, A. K. K. 2018. Metformin from mother to unborn child–Are there unwarranted effects? *EBioMedicine,* 35**,** 394-404.

NICE 2015. Diabetes in pregnancy: management from preconception to the postnatal period, NICE guideline [NG3].

NICE 2021. NICE guideline [NG201]Antenatal care.

O'DONOGHUE, K. & CHAN, J. 2006. Human fetal mesenchymal stem cells. *Current stem cell research & therapy,* 1**,** 371-386.

ODE, A., SCHOON, J., KURTZ, A., GAETJEN, M., ODE, J. E., GEISSLER, S. & DUDA, G. N. 2013. CD73/5′-ecto-nucleotidase acts as a regulatory factor in osteo-/chondrogenic differentiation of mechanically stimulated mesenchymal stromal cells. *Eur Cell Mater,* 25.

OLLAURI-IBÁÑEZ, C., NÚÑEZ-GÓMEZ, E., EGIDO-TURRIÓN, C., SILVA-SOUSA, L., DÍAZ-RODRÍGUEZ, E., RODRÍGUEZ-BARBERO, A., LÓPEZ-NOVOA, J. M. & PERICACHO, M. 2020. Continuous endoglin (CD105) overexpression disrupts angiogenesis and facilitates tumor cell metastasis. *Angiogenesis,* 23**,** 231-247.

WORLD HEALTH ORGANIZATION. 2013. Diagnostic criteria and classification of hyperglycaemia first detected in pregnancy: a World Health Organization guideline.

PAAUWE, M., HEIJKANTS, R., OUDT, C., VAN PELT, G., CUI, C., THEUER, C., HARDWICK, J., SIER, C. & HAWINKELS, L. 2016. Endoglin targeting inhibits tumor angiogenesis and metastatic spread in breast cancer. *Oncogene,* 35**,** 4069-4079.

PAAUWE, M., SCHOONDERWOERD, M. J., HELDERMAN, R. F., HARRYVAN, T. J., GROENEWOUD, A., VAN PELT, G. W., BOR, R., HEMMER, D. M., VERSTEEG, H. H. & SNAAR-JAGALSKA, B. E. 2018. Endoglin expression on cancer-associated fibroblasts regulates invasion and stimulates colorectal cancer metastasis. *Clinical Cancer Research,* 24**,** 6331-6344.

PANG, V., BATES, DAVID O. & LEACH, L. 2017. Regulation of human feto-placental endothelial barrier integrity by vascular endothelial growth factors: competitive interplay between VEGF-A₁₆₅a, VEGF-A₁₆₅b, PIGF and VE-cadherin. *Clinical Science,* 131**,** 2763.

PANKAJAKSHAN, D. & AGRAWAL, D. K. 2014. Mesenchymal stem cell paracrine factors in vascular repair and regeneration. *Journal of biomedical technology and research,* 1.

PANSKY, B. 1982. *Review of MEDICAL EMBRYOLOGY*.

PANTHAM, P., AYE, I. L. M. H. & POWELL, T. L. 2015. Inflammation in maternal obesity and gestational diabetes mellitus. *Placenta,* 36**,** 709-715.

PARANT, O., DUBERNARD, G., CHALLIER, J.-C., OSTER, M., UZAN, S., ARACTINGI, S. & KHOSROTEHRANI, K. 2009. CD34+ cells in maternal placental blood are mainly fetal in origin and express endothelial markers. *Laboratory investigation,* 89**,** 915-923.

PARK, D.-H., LEE, J.-H., BORLONGAN, C. V., SANBERG, P. R., CHUNG, Y.-G. & CHO, T.-H. 2011. Transplantation of umbilical cord blood stem cells for treating spinal cord injury. *Stem Cell Reviews and Reports,* 7**,** 181-194.

PATHAK, S., HOOK, E., HACKETT, G., MURDOCH, E., SEBIRE, N., JESSOP, F. & LEES, C. 2010. Cord coiling, umbilical cord insertion and placental shape in an unselected cohort delivering at term: relationship with common obstetric outcomes. *Placenta,* 31**,** 963-968.

PATI, S., KHAKOO, A. Y., ZHAO, J., JIMENEZ, F., GERBER, M. H., HARTING, M., REDELL, J. B., GRILL, R., MATSUO, Y. & GUHA, S. 2011. Human mesenchymal stem cells inhibit vascular permeability

by modulating vascular endothelial cadherin/β-catenin signaling. *Stem cells and development,* 20**,** 89-101.

PEDERSEN, J. 1977. *The pregnant diabetic and her newborn: problems and management*, Williams & Wilkins Company.

PEREZ-PEREZ, A., MAYMO, J. L., GAMBINO, Y. P., GUADIX, P., DUENAS, J., VARONE, C. L. & SÁNCHEZ-MARGALET, V. 2013. Activated translation signaling in placenta from pregnant women with gestational diabetes mellitus: possible role of leptin. *Hormone and Metabolic Research,* 45**,** 436-442.

PERGIALIOTIS, V., KOTROGIANNI, P., KOUTAKI, D., CHRISTOPOULOS-TIMOGIANNAKIS, E., PAPANTONIOU, N. & DASKALAKIS, G. 2020. Umbilical cord coiling index for the prediction of adverse pregnancy outcomes: a meta-analysis and sequential analysis. *The Journal of Maternal-Fetal & Neonatal Medicine,* 33**,** 4022-4029.

PHERMTHAI, T., ODGLUN, Y., JULAVIJITPHONG, S., TITAPANT, V., CHUENWATTANA, P., VANTANASIRI, C. & PATTANAPANYASAT, K. 2010. A novel method to derive amniotic fluid stem cells for therapeutic purposes. *BMC cell biology,* 11**,** 1-9.

PIERDOMENICO, L., LANUTI, P., LACHMANN, R., GRIFONE, G., CIANCI, E., GIALÒ, L., PACELLA, S., ROMANO, M., VITACOLONNA, E. & MISCIA, S. 2011. Diabetes mellitus during pregnancy interferes with the biological characteristics of Wharton's jelly mesenchymal stem cells. *The Open Tissue Engineering and Regenerative Medicine Journal,* 4.

PITTENGER, M. F., DISCHER, D. E., PÉAULT, B. M., PHINNEY, D. G., HARE, J. M. & CAPLAN, A. I. 2019. Mesenchymal stem cell perspective: cell biology to clinical progress. *npj Regenerative Medicine,* 4**,** 22.

PLOWS, J. F., STANLEY, J. L., BAKER, P. N., REYNOLDS, C. M. & VICKERS, M. H. 2018. The pathophysiology of gestational diabetes mellitus. *International journal of molecular sciences,* 19**,** 3342.

PÖTGENS, A., SCHMITZ, U., BOSE, P., VERSMOLD, A., KAUFMANN, P. & FRANK, H.-G. 2002. Mechanisms of syncytial fusion: a review. *Placenta,* 23**,** S107-S113.

POTTER, M. D., BARBERO, S. & CHERESH, D. A. 2005. Tyrosine phosphorylation of VE-cadherin prevents binding of p120-and β-catenin and maintains the cellular mesenchymal state. *Journal of Biological Chemistry,* 280**,** 31906-31912.

PRANDINI, M.-H., DREHER, I., BOUILLOT, S., BENKERRI, S., MOLL, T. & HUBER, P. 2005. The human VE-cadherin promoter is subjected to organ-specific regulation and is activated in tumour angiogenesis. *Oncogene,* 24**,** 2992.

PRASANNA, S. J., GOPALAKRISHNAN, D., SHANKAR, S. R. & VASANDAN, A. B. 2010. Pro-inflammatory cytokines, IFNγ and

TNFα, influence immune properties of human bone marrow and Wharton jelly mesenchymal stem cells differentially. *PloS one,* 5**,** e9016.

PREDESCU, D., VOGEL, S. M. & MALIK, A. B. 2004. Functional and morphological studies of protein transcytosis in continuous endothelia. *American Journal of Physiology-Lung Cellular and Molecular Physiology,* 287**,** L895-L901.

PRIYA, G. & KALRA, S. 2018. Metformin in the management of diabetes during pregnancy and lactation. *Drugs in context,* 7.

PU, C.-M., LIU, C.-W., LIANG, C.-J., YEN, Y.-H., CHEN, S.-H., JIANG-SHIEH, Y.-F., CHIEN, C.-L., CHEN, Y.-C. & CHEN, Y.-L. 2017. Adipose-derived stem cells protect skin flaps against ischemia/reperfusion injury via IL-6 expression. *Journal of Investigative Dermatology,* 137**,** 1353-1362.

PUJOL-GIMÉNEZ, J., BARRENETXE, J., GONZÁLEZ-MUNIESA, P. & LOSTAO, M. P. 2013. The facilitative glucose transporter GLUT12: what do we know and what would we like to know? *Journal of physiology and biochemistry,* 69**,** 325-333.

PULOUS, F. E., GRIMSLEY-MYERS, C. M., KANSAL, S., KOWALCZYK, A. P. & PETRICH, B. G. 2019. Talin-Dependent Integrin Activation Regulates VE-Cadherin Localization and Endothelial Cell Barrier Function. *Circulation research,* 124**,** 891-903.

QIN, L., ZHAO, D., XU, J., REN, X., TERWILLIGER, E. F., PARANGI, S., LAWLER, J., DVORAK, H. F. & ZENG, H. 2013. The vascular permeabilizing factors histamine and serotonin induce angiogenesis through TR3/Nur77 and subsequently truncate it through thrombospondin-1. *Blood, The Journal of the American Society of Hematology,* 121**,** 2154-2164.

QURESHI, F. & JACQUES, S. M. 1994. Marked segmental thinning of the umbilical cord vessels. *Archives of pathology & laboratory medicine,* 118**,** 826-830.

RAHAVI, H., HASHEMI, S. M., SOLEIMANI, M., MOHAMMADI, J. & TAJIK, N. 2015. Adipose tissue-derived mesenchymal stem cells exert in vitro immunomodulatory and beta cell protective functions in streptozotocin-induced diabetic mice model. *Journal of diabetes research,* 2015.

RAHIMI, N. 2017. Defenders and Challengers of Endothelial Barrier Function. *Frontiers in Immunology,* 8.

REED, A. M., PICORNELL, Y. J., HARWOOD, A. & KREDICH, D. W. 2000. Chimerism in children with juvenile dermatomyositis. *The Lancet,* 356**,** 2156-2157.

RICHARDSON, S. M., KALAMEGAM, G., PUSHPARAJ, P. N., MATTA, C., MEMIC, A., KHADEMHOSSEINI, A., MOBASHERI, R., POLETTI, F. L., HOYLAND, J. A. & MOBASHERI, A. 2016.

Mesenchymal stem cells in regenerative medicine: focus on articular cartilage and intervertebral disc regeneration. *Methods,* 99**,** 69-80.

RIVAS, C., ZUNIGA, F., SALAS-BURGOS, A., MARDONES, L., ORMAZABAL, V. & VERA, J. 2008. Vitamin C transporters. *Journal of physiology and biochemistry,* 64**,** 357-375.

ROBERTS, R. M., GREEN, J. A. & SCHULZ, L. C. 2016. The evolution of the placenta. *Reproduction,* 152**,** R179-89.

RODRÍGUEZ-FUENTES, D. E., FERNÁNDEZ-GARZA, L. E., SAMIA-MEZA, J. A., BARRERA-BARRERA, S. A., CAPLAN, A. I. & BARRERA-SALDAÑA, H. A. 2021. Mesenchymal Stem Cells Current Clinical Applications: A Systematic Review. *Archives of Medical Research,* 52**,** 93-101.

ROMERO, D., O'NEILL, C., TERZIC, A., CONTOIS, L., YOUNG, K., CONLEY, B. A., BERGAN, R. C., BROOKS, P. C. & VARY, C. P. 2011. Endoglin regulates cancer–stromal cell interactions in prostate tumors. *Cancer research,* 71**,** 3482-3493.

ROSATI, D., SUHENDRO, G., DENESKA, R. S., FAUZIAH, D. & ABDULLAH, M. R. 2022. The Effect of CD 90 Expression after Intrasclera Limbal Mesenchymal Stem Cell Injection in Form Deprivation Myopia Animal Model. *The Effect of CD 90 Expression after Intrasclera Limbal Mesenchymal Stem Cell Injection in Form Deprivation Myopia Animal Model,* 94**,** 9-9.

ROSSI, E., GOYARD, C., CRAS, A., DIZIER, B., BACHA, N., LOKAJCZYK, A., GUERIN, C.L., GENDRON, N., PLANQUETTE, B., MIGNON, V. AND BERNABEU, C., 2017. Co-injection of mesenchymal stem cells with endothelial progenitor cells accelerates muscle recovery in hind limb ischemia through an endoglin-dependent mechanism. *Thrombosis and Haemostasis*, *117*,1908-1918.

ROSSI, E., SANZ-RODRIGUEZ, F., ELENO, N., DUEWELL, A., BLANCO, F.J., LANGA, C., BOTELLA, L.M., CABANAS, C., LOPEZ-NOVOA, J.M. AND BERNABEU, C., 2013. Endothelial endoglin is involved in inflammation: role in leukocyte adhesion and transmigration. *Blood, The Journal of the American Society of Hematology*, *121*, 403-415.

ROSU-MYLES, M., FAIR, J., PEARCE, N. & MEHIC, J. 2010. Non-multipotent stroma inhibit the proliferation and differentiation of mesenchymal stromal cells in vitro. *Cytotherapy,* 12**,** 818-830.

ROWAN, J. A., RUSH, E. C., OBOLONKIN, V., BATTIN, M., WOULDES, T. & HAGUE, W. M. 2011. Metformin in gestational diabetes: the offspring follow-up (MiG TOFU) body composition at 2 years of age. *Diabetes care,* 34**,** 2279-2284.

RUIZ-LLORENTE, L., GALLARDO-VARA, E., ROSSI, E., SMADJA, D. M., BOTELLA, L. M. & BERNABEU, C. 2017. Endoglin and alk1 as therapeutic targets for hereditary hemorrhagic telangiectasia. *Expert Opin Ther Targets,* 21**,** 933-947.

RYAN, J., BARRY, F., MURPHY, J. & MAHON, B. P. 2007. Interferon-γ does not break, but promotes the immunosuppressive capacity of adult human mesenchymal stem cells. *Clinical & Experimental Immunology,* 149**,** 353-363.

SADLER, T. 1985. Normal development of the external genitalia. *Sadler TW. Langman's Medical Embryology, 5th Ed., Baltimore, Williams & Wilkins***,** 383.

SADLER, T. 2004. Second week of development: Bilaminar germ disc. *Langman's Medical Embryology. 9th ed. Philadelphia: Lippincott Williams & Wilkins,* 57.

SAEEDI, M., CAO, Y., FADL, H., GUSTAFSON, H. & SIMMONS, D. 2021. Increasing prevalence of gestational diabetes mellitus when implementing the IADPSG criteria: a systematic review and meta-analysis. *diabetes research and clinical practice,* 172**,** 108642.

SAGAR, R., WALTHER-JALLOW, L., DAVID, A. L., GÖTHERSTRÖM, C. & WESTGREN, M. 2018. Fetal Mesenchymal Stromal Cells: an Opportunity for Prenatal Cellular Therapy. *Current stem cell reports,* 4**,** 61-68.

SAITO, S., NAKASHIMA, A., SHIMA, T. AND ITO, M., 2010. Th1/Th2/Th17 and regulatory T-cell paradigm in pregnancy. *American journal of reproductive immunology*, *63*, 601-610.

SAITO, T., BOKHOVE, M., CROCI, R., ZAMORA-CABALLERO, S., HAN, L., LETARTE, M., DE SANCTIS, D. & JOVINE, L. 2017. Structural Basis of the Human Endoglin-BMP9 Interaction: Insights into BMP Signaling and HHT1. *Cell Rep,* 19**,** 1917-1928.

SAMAR SALEM, D. O. B., LOPA LEACH 2022. Effect of gestational diabetes mellitus on human umbilical mesenchymal stem cells: a flow cy tometry study. *Microcirculation,* 29**,** e12739.

SÁNCHEZ-ELSNER, T., BOTELLA, L. M., VELASCO, B., LANGA, C. & BERNABÉU, C. 2002. Endoglin expression is regulated by transcriptional cooperation between the hypoxia and transforming growth factor-β pathways. *Journal of Biological Chemistry,* 277**,** 43799-43808.

SANTIBANEZ, J. F., LETAMENDIA, A., PEREZ-BARRIOCANAL, F., SILVESTRI, C., SAURA, M., VARY, C. P., LOPEZ-NOVOA, J. M., ATTISANO, L. & BERNABEU, C. 2007. Endoglin increases eNOS expression by modulating Smad2 protein levels and Smad2-dependent TGF-β signaling. *Journal of cellular physiology,* 210**,** 456-468.

SASSOLI, C., PINI, A., CHELLINI, F., MAZZANTI, B., NISTRI, S., NOSI, D., SACCARDI, R., QUERCIOLI, F., ZECCHI-ORLANDINI, S. & FORMIGLI, L. 2012. Bone marrow mesenchymal stromal cells stimulate skeletal myoblast proliferation through the paracrine release of VEGF. *PloS one,* 7**,** e37512.

SCARPELLO, J. H. & HOWLETT, H. C. 2008. Metformin therapy and clinical uses. *Diabetes and Vascular Disease Research,* 5**,** 157-167.

SCHAEFER-GRAF, U. M., GRAF, K., KULBACKA, I., KJOS, S. L., DUDENHAUSEN, J., VETTER, K. & HERRERA, E. 2008. Maternal lipids as strong determinants of fetal environment and growth in pregnancies with gestational diabetes mellitus. *Diabetes care,* 31**,** 1858-1863.

SCHMAIER, A. & MCCRAE, K. 2007. The plasma kallikrein–kinin system: its evolution from contact activation. *Journal of thrombosis and haemostasis,* 5**,** 2323-2329.

SCHOONDERWOERD, M. J. A., GOUMANS, M. T. H. & HAWINKELS, L. 2020. Endoglin: Beyond the Endothelium. *Biomolecules,* 10.

SEGURA, M. T., DEMMELMAIR, H., KRAUSS-ETSCHMANN, S., NATHAN, P., DEHMEL, S., PADILLA, M. C., RUEDA, R., KOLETZKO, B. & CAMPOY, C. 2017. Maternal BMI and gestational diabetes alter placental lipid transporters and fatty acid composition. *Placenta,* 57**,** 144-151.

SHPICHKA, A., BUTNARU, D., BEZRUKOV, E. A., SUKHANOV, R. B., ATALA, A., BURDUKOVSKII, V., ZHANG, Y. & TIMASHEV, P. 2019. Skin tissue regeneration for burn injury. *Stem cell research & therapy,* 10**,** 1-16.

SIBIAK, R., OZEGOWSKA, K., WENDER-OZEGOWSKA, E., GUTAJ, P., MOZDZIAK, P. & KEMPISTY, B. 2022. Fetomaternal Expression of Glucose Transporters (GLUTs)-Biochemical, Cellular and Clinical Aspects. *Nutrients,* 14.

SIBLEY, C. 2009. Understanding placental nutrient transfer–why bother? New biomarkers of fetal growth. *The Journal of physiology,* 587**,** 3431-3440.

SIKAVITSAS, V. I., TEMENOFF, J. S. & MIKOS, A. G. 2001. Biomaterials and bone mechanotransduction. *Biomaterials,* 22**,** 2581-2593.

SILVER, R. K., DOOLEY, S. L., TAMURA, R. K. & DEPP, R. 1987. Umbilical cord size and amniotic fluid volume in prolonged pregnancy. *American journal of obstetrics and gynecology,* 157**,** 716-720.

SNODGRASS, R., ARTHUR, H. & CHICO, T. J. 2021. Synergistic TOR and ERK inhibition mitigates the hereditary haemorrhagic telangiectasia-like phenotype and excess kugel formation in endoglin mutant zebrafish. *bioRxiv*.

SOBREVIA, L., ABARZÚA, F., NIEN, J., SALOMÓN, C., WESTERMEIER, F., PUEBLA, C., CIFUENTES, F., GUZMÁN-GUTIÉRREZ, E., LEIVA, A. & CASANELLO, P. 2011. Differential placental macrovascular and microvascular endothelial dysfunction in gestational diabetes. *Placenta,* 32**,** S159-S164.

SORRELL, J. M., BABER, M. A. & CAPLAN, A. I. 2009. Influence of adult mesenchymal stem cells on in vitro vascular formation. *Tissue Engineering Part A,* 15**,** 1751-1761.

SPENCER, R., CARR, D. & DAVID, A. 2014. Treatment of poor placentation and the prevention of associated adverse outcomes–what does the future hold? *Prenatal diagnosis,* 34**,** 677-684.

SPRAGUE, A. H. & KHALIL, R. A. 2009. Inflammatory cytokines in vascular dysfunction and vascular disease. *Biochemical pharmacology,* 78**,** 539-552.

ST-JACQUES, S., FORTE, M., LYE, S. J. & LETARTE, M. 1994. Localization of endoglin, a transforming growth factor-β binding protein, and of CD44 and integrins in placenta during the first trimester of pregnancy. *Biology of reproduction,* 51**,** 405-413.

STANIROWSKI, P. J., SZUKIEWICZ, D., MAJEWSKA, A., WĄTROBA, M., PYZLAK, M., BOMBA-OPOŃ, D. & WIELGOŚ, M. 2022. Placental expression of glucose transporters GLUT-1, GLUT-3, GLUT-8 and GLUT-12 in pregnancies complicated by gestational and type 1 diabetes mellitus. *Journal of Diabetes Investigation,* 13**,** 560-570.

STERN, C., SCHWARZ, S., MOSER, G., CVITIC, S., JANTSCHER-KRENN, E., GAUSTER, M. & HIDEN, U. 2021. Placental Endocrine Activity: Adaptation and Disruption of Maternal Glucose Metabolism in Pregnancy and the Influence of Fetal Sex. *Int J Mol Sci,* 22.

SUBRAMANIAN, A., FONG, C.-Y., BISWAS, A. & BONGSO, A. 2015. Comparative Characterization of Cells from the Various Compartments of the Human Umbilical Cord Shows that the Wharton's Jelly Compartment Provides the Best Source of Clinically Utilizable Mesenchymal Stem Cells. *PloS one,* 10**,** e0127992-e0127992.

SUN, Y., ARBUCKLE, S., HOCKING, G. & BILLSON, V. 1995. Umbilical cord stricture and intrauterine fetal death. *Pediatric Pathology & Laboratory Medicine,* 15**,** 723-732.

SUZUKI, S., SANO, K. & TANIHARA, H. 1991. Diversity of the cadherin family: evidence for eight new cadherins in nervous tissue. *Cell regulation,* 2**,** 261-270.

TADDEI, A., GIAMPIETRO, C., CONTI, A., ORSENIGO, F., BREVIARIO, F., PIRAZZOLI, V., POTENTE, M., DALY, C., DIMMELER, S. & DEJANA, E. 2008. Endothelial adherens junctions control tight junctions by VE-cadherin-mediated upregulation of claudin-5. *Nature Cell Biology,* 10**,** 923-934.

TAKASHIMA, Y., ERA, T., NAKAO, K., KONDO, S., KASUGA, M., SMITH, A. G. & NISHIKAWA, S.-I. 2007. Neuroepithelial cells supply an initial transient wave of MSC differentiation. *Cell,* 129**,** 1377-1388.

TAKECHI, K., KUWABARA, Y. & MIZUNO, M. 1993. Ultrastructural and immunohistochemical studies of Wharton's jelly umbilical cord cells. *Placenta,* 14**,** 235-245.

TAM, C., WONG, J. H., CHEUNG, R. C. F., ZUO, T. & NG, T. B. 2017. Therapeutic potentials of short interfering RNAs. *Appl Microbiol Biotechnol,* 101**,** 7091-7111.

TARICCO, E., RADAELLI, T., DE SANTIS, M. N. & CETIN, I. 2003. Foetal and placental weights in relation to maternal characteristics in gestational diabetes. *Placenta,* 24**,** 343-347.

TARICCO, E., RADAELLI, T., ROSSI, G., NOBILE DE SANTIS, M. S., BULFAMANTE, G. P., AVAGLIANO, L. & CETIN, I. 2009. Effects of gestational diabetes on fetal oxygen and glucose levels in vivo. *Bjog,* 116**,** 1729-35.

TARRY-ADKINS, J. L., AIKEN, C. E. & OZANNE, S. E. 2019. Neonatal, infant, and childhood growth following metformin versus insulin treatment for gestational diabetes: A systematic review and meta-analysis. *PLoS medicine,* 16**,** e1002848.

TARTARIN, P., MOISON, D., GUIBERT, E., DUPONT, J., HABERT, R., ROUILLER-FABRE, V., FRYDMAN, N., POZZI, S., FRYDMAN, R. & LÉCUREUIL, C. 2012. Metformin exposure affects human and mouse fetal testicular cells. *Human Reproduction,* 27**,** 3304-3314.

TEO, G. S., ANKRUM, J. A., MARTINELLI, R., BOETTO, S. E., SIMMS, K., SCIUTO, T. E., DVORAK, A. M., KARP, J. M. & CARMAN, C. V. 2012. Mesenchymal stem cells transmigrate between and directly through tumor necrosis factor-α-activated endothelial cells via both leukocyte-like and novel mechanisms. *Stem cells,* 30**,** 2472-2486.

TERTTI, K., EKBLAD, U., HEIKKINEN, T., RAHI, M., RÖNNEMAA, T. & LAINE, K. 2010. The role of organic cation transporters (OCTs) in the transfer of metformin in the dually perfused human placenta. *European Journal of Pharmaceutical Sciences,* 39**,** 76-81.

THOMSON, L. L. & HOO, J. J. 1996. Linear disruption of umbilical cord: a rare anomaly of the cord associated with acute fetal distress and perinatal death/profound psychomotor retardation. *American journal of medical genetics,* 62**,** 348-349.

TIAN, H., HUANG, J. J., GOLZIO, C., GAO, X., HECTOR-GREENE, M., KATSANIS, N. & BLOBE, G. C. 2018. Endoglin interacts with VEGFR2 to promote angiogenesis. *The FASEB Journal,* 32**,** 2934-2949.

TIEU, J., COAT, S., HAGUE, W., MIDDLETON, P. & SHEPHERD, E. 2017. Oral anti-diabetic agents for women with established diabetes/impaired glucose tolerance or previous gestational diabetes planning pregnancy, or pregnant women with pre-existing diabetes. *The Cochrane database of systematic reviews,* 10**,** CD007724-CD007724.

TIMPSON, P., JONES, G. E., FRAME, M. C. & BRUNTON, V. G. 2001. Coordination of cell polarization and migration by the Rho family GTPases requires Src tyrosine kinase activity. *Current biology,* 11**,** 1836-1846.

TIRUPPATHI, C., MINSHALL, R. D., PARIA, B. C., VOGEL, S. M. & MALIK, A. B. 2002. Role of Ca2+ signaling in the regulation of endothelial permeability. *Vascular Pharmacology,* 39**,** 173-185.

TODESCHI, M. R., EL BACKLY, R., CAPELLI, C., DAGA, A., PATRONE, E., INTRONA, M., CANCEDDA, R. & MASTROGIACOMO, M. 2015. Transplanted umbilical cord mesenchymal stem cells modify the in vivo microenvironment enhancing angiogenesis and leading to bone regeneration. *Stem cells and development,* 24**,** 1570-1581.

TOPORSIAN, M., GROS, R., KABIR, M. G., VERA, S., GOVINDARAJU, K., EIDELMAN, D. H., HUSAIN, M. & LETARTE, M. 2005. A Role for Endoglin in Coupling eNOS Activity and Regulating Vascular Tone Revealed in Hereditary Hemorrhagic Telangiectasia. *Circulation Research,* 96**,** 684-692.

TRAKTUEV, D. O., PRATER, D. N., MERFELD-CLAUSS, S., SANJEEVAIAH, A. R., SAADATZADEH, M. R., MURPHY, M., JOHNSTONE, B. H., INGRAM, D. A. & MARCH, K. L. 2009. Robust functional vascular network formation in vivo by cooperation of adipose progenitor and endothelial cells. *Circulation research,* 104**,** 1410-1420.

TRENTIN BRUM, S., DEMASI, A. P., FANTELLI STELINI, R., CINTRA, M. L., CAVALCANTI DE ARAUJO, V. & BORGES SOARES, A. 2019. Endoglin is Highly Expressed in Human Mast Cells. *Appl Immunohistochem Mol Morphol,* 27**,** 613-617.

TRONCOSO, F., ACURIO, J., HERLITZ, K., AGUAYO, C., BERTOGLIA, P., GUZMAN-GUTIERREZ, E., LOYOLA, M., GONZALEZ, M., REZGAOUI, M. & DESOYE, G. 2017. Gestational diabetes mellitus is associated with increased pro-migratory activation of vascular endothelial growth factor receptor 2 and reduced expression of vascular endothelial growth factor receptor 1. *PLoS One,* 12**,** e0182509.

TROUNSON, A. & MCDONALD, C. 2015. Stem Cell Therapies in Clinical Trials: Progress and Challenges. *Cell Stem Cell,* 17**,** 11-22.

TROYER, D. L. & WEISS, M. L. 2008. Concise review: Wharton's jelly-derived cells are a primitive stromal cell population. *Stem cells,* 26**,** 591-599.

TSAI, P.-J., WANG, H.-S., SHYR, Y.-M., WENG, Z.-C., TAI, L.-C., SHYU, J.-F. & CHEN, T.-H. 2012. Transplantation of insulin-producing cells from umbilical cord mesenchymal stem cells for the treatment of streptozotocin-induced diabetic rats. *Journal of biomedical science,* 19**,** 1-9.

TSAI, T.-L., MANNER, P. & LI, W.-J. 2013. Regulation of mesenchymal stem cell chondrogenesis by glucose through protein kinase C/transforming growth factor signaling. *Osteoarthritis and Cartilage,* 21**,** 368-376.

TSOPANOGLOU, N. E. & MARAGOUDAKIS, M. E. Role of thrombin in angiogenesis and tumor progression. Seminars in thrombosis and hemostasis, 2004. Copyright© 2004 by Thieme Medical Publishers, Inc., 333 Seventh Avenue, New …, 63-69.

TUAL-CHALOT, S., GARCIA-COLLADO, M., REDGRAVE, R. E., SINGH, E., DAVISON, B., PARK, C., LIN, H., LULI, S., JIN, Y. & WANG,

Y. 2020. Loss of endothelial endoglin promotes high-output heart failure through peripheral arteriovenous shunting driven by VEGF signaling. *Circulation research,* 126**,** 243-257.

TUMA, P. L. & HUBBARD, A. L. 2003. Transcytosis: crossing cellular barriers. *Physiological reviews,* 83**,** 871-932.

TUROWSKI, P., MARTINELLI, R., CRAWFORD, R., WATERIDGE, D., PAPAGEORGIOU, A.-P., LAMPUGNANI, M. G., GAMP, A. C., VESTWEBER, D., ADAMSON, P. & DEJANA, E. 2008. Phosphorylation of vascular endothelial cadherin controls lymphocyte emigration. *Journal of cell science,* 121**,** 29-37.

TURTURICI, G., TINNIRELLO, R., SCONZO, G. & GERACI, F. 2014. Extracellular membrane vesicles as a mechanism of cell-to-cell communication: advantages and disadvantages. *American Journal of Physiology-Cell Physiology,* 306**,** C621-C633.

ULLAH, I., SUBBARAO, RAGHAVENDRA B. & RHO, GYU J. 2015. Human mesenchymal stem cells - current trends and future prospective. *Bioscience Reports,* 35**,** e00191.

V., R. 2006. Doubling Time Computing.

VAN DER AA, E. M., COPIUS PEEREBOOM-STEGEMAN, J. H., NOORDHOEK, J., GRIBNAU, F. W. & RUSSEL, F. G. 1998. Mechanisms of drug transfer across the human placenta. *Pharmacy World and Science,* 20**,** 139-148.

VAN WEELDEN, W., WEKKER, V., DE WIT, L., LIMPENS, J., IJÄS, H., VAN WASSENAER-LEEMHUIS, A. G., ROSEBOOM, T. J., VAN RIJN, B. B., DEVRIES, J. H. & PAINTER, R. C. 2018. Long-term effects of oral antidiabetic drugs during pregnancy on offspring: a systematic review and meta-analysis of follow-up studies of RCTs. *Diabetes Therapy,* 9**,** 1811-1829.

VANKY, E., ZAHLSEN, K., SPIGSET, O. & CARLSEN, S. M. 2005. Placental passage of metformin in women with polycystic ovary syndrome. *Fertil Steril,* 83**,** 1575-8.

VASANDAN, A. B., JAHNAVI, S., SHASHANK, C., PRASAD, P., KUMAR, A. & PRASANNA, S. J. 2016. Human Mesenchymal stem cells program macrophage plasticity by altering their metabolic status via a PGE2-dependent mechanism. *Scientific reports,* 6**,** 1-17.

VÁZQUEZ BLANCO, M., RUDA VEGA, H., GUERRI-GUTTENBERG, R., GIULIANO, R., R. GRANA, D., AZZATO, F. & MILEI, J. 2011. *Histopathology and histomorphometry of umbilical cord blood vessels. Findings in normal and high risk pregnancies*.

VELLASAMY, S., SANDRASAIGARAN, P., VIDYADARAN, S., GEORGE, E. & RAMASAMY, R. 2012. Isolation and characterisation of mesenchymal stem cells derived from human placenta tissue. *World journal of stem cells,* 4**,** 53.

VESTWEBER, D., WESSEL, F. & NOTTEBAUM, A.F. 2014. Similarities and differences in the regulation of leukocyte extravasation and vascular permeability. *Seminars in Immunopathology,* 36**,** 177–192.

VESTWEBER, D., WINDERLICH, M., CAGNA, G. & NOTTEBAUM, A. F. 2009. Cell adhesion dynamics at endothelial junctions: VE-cadherin as a major player. *Trends in Cell Biology,* 19**,** 8-15.

VICEN, M., VITVEROVA, B., HAVELEK, R., BLAZICKOVA, K., MACHACEK, M., RATHOUSKA, J., NAJMANOVÁ, I., DOLEZELOVA, E., PRASNICKA, A. & STERNAK, M. 2019. Regulation and role of endoglin in cholesterol-induced endothelial and vascular dysfunction in vivo and in vitro. *The FASEB Journal,* 33**,** 6099-6114.

VILLAR, J., ISMAIL, L. C., VICTORA, C. G., OHUMA, E. O., BERTINO, E., ALTMAN, D. G., LAMBERT, A., PAPAGEORGHIOU, A. T., CARVALHO, M., JAFFER, Y. A., GRAVETT, M. G., PURWAR, M., FREDERICK, I. O., NOBLE, A. J., PANG, R., BARROS, F. C., CHUMLEA, C., BHUTTA, Z. A. & KENNEDY, S. H. 2014. International standards for newborn weight, length, and head circumference by gestational age and sex: the Newborn Cross-Sectional Study of the INTERGROWTH-21st Project. *The Lancet,* 384**,** 857-868.

VILLOTA, S. D., TOLEDO-RODRIGUEZ, M. & LEACH, L. 2021. Compromised barrier integrity of human feto-placental vessels from gestational diabetic pregnancies is related to downregulation of occludin expression. *Diabetologia,* 64**,** 195-210.

VINCENT, P. A., XIAO, K., BUCKLEY, K. M. & KOWALCZYK, A. P. 2004. VE-cadherin: adhesion at arm's length. *American Journal of Physiology-Cell Physiology,* 286**,** C987-C997.

WAJID, N., NASEEM, R., ANWAR, S. S., AWAN, S. J., ALI, M., JAVED, S. & ALI, F. 2015. The effect of gestational diabetes on proliferation capacity and viability of human umbilical cord-derived stromal cells. *Cell and Tissue Banking,* 16**,** 389-397.

WALKER, N., FILIS, P., O'SHAUGHNESSY, P. J., BELLINGHAM, M. & FOWLER, P. A. 2019. Nutrient transporter expression in both the placenta and fetal liver are affected by maternal smoking. *Placenta,* 78**,** 10-17.

WALKNOWSKA, J., CONTE, F. & GRUMBACH, M. 1969. Practical and theoretical implications of fetal/maternal lymphocyte transfer. *The Lancet,* 293**,** 1119-1122.

WANG, W., LIU, T., YANG, L., MA, Y., DOU, F., SHI, L., WEN, A. & DING, Y. 2019. Study on the multi-targets mechanism of triphala on cardio-cerebral vascular diseases based on network pharmacology. *Biomedicine & Pharmacotherapy,* 116**,** 108994.

WANG, X.-Y., LAN, Y., HE, W.-Y., ZHANG, L., YAO, H.-Y., HOU, C.-M., TONG, Y., LIU, Y.-L., YANG, G. & LIU, X.-D. 2008. Identification of mesenchymal stem cells in aorta-gonad-mesonephros and yolk sac of human embryos. *Blood,* 111**,** 2436-2443.

WATSON, N., DIVERS, R., KEDAR, R., MEHINDRU, A., MEHINDRU, A., BORLONGAN, M. C. & BORLONGAN, C. V. 2015. Discarded Wharton jelly of the human umbilical cord: a viable source for mesenchymal stromal cells. *Cytotherapy,* 17**,** 18-24.

WEIS, S., CUI, J., BARNES, L. & CHERESH, D. 2004. Endothelial barrier disruption by VEGF-mediated Src activity potentiates tumor cell extravasation and metastasis. *The Journal of cell biology,* 167**,** 223-229.

WEIS, S. M. 2008. Vascular permeability in cardiovascular disease and cancer. *Current opinion in hematology,* 15**,** 243-249.

WEISS, P. A., KAINER, F. & HAAS, J. 1998. Cord blood insulin to assess the quality of treatment in diabetic pregnancies. *Early Hum Dev,* 51**,** 187-95.

WEISSMAN, A. & JAKOBI, P. 1997. Sonographic measurements of the umbilical cord in pregnancies complicated by gestational diabetes. *Journal of ultrasound in medicine,* 16**,** 691-694.

WENDLAND, E. M., TORLONI, M. R., FALAVIGNA, M., TRUJILLO, J., DODE, M. A., CAMPOS, M. A., DUNCAN, B. B. & SCHMIDT, M. I. 2012. Gestational diabetes and pregnancy outcomes-a systematic review of the World Health Organization (WHO) and the International Association of Diabetes in Pregnancy Study Groups (IADPSG) diagnostic criteria. *BMC pregnancy and childbirth,* 12**,** 23.

WENSINK, M. J., LU, Y., TIAN, L., SHAW, G. M., RIZZI, S., JENSEN, T. K., MATHIESEN, E. R., SKAKKEBÆK, N. E., LINDAHL-JACOBSEN, R. & EISENBERG, M. L. 2022. Preconception antidiabetic drugs in men and birth defects in offspring: a nationwide cohort study. *Annals of Internal Medicine,* 175**,** 665-673.

WHARTON, T. 1730. *Adenographia, sive glandularum totius corporis descriptio*, Typis JG impensis authoris.

WILLIAMS, D. J., VALLANCE, P., NEILD, G., SPENCER, J. & IMMS, F. J. 1997. Nitric oxide-mediated vasodilation in human pregnancy. *American Journal of Physiology-Heart and Circulatory Physiology,* 272**,** H748-H752.

WISSE, E. 1970. An electron microscopic study of the fenestrated endothelial lining of rat liver sinusoids. *Journal of ultrastructure research,* 31**,** 125-150.

WONG, S.-P., ROWLEY, J. E., REDPATH, A. N., TILMAN, J. D., FELLOUS, T. G. & JOHNSON, J. R. 2015. Pericytes, mesenchymal stem cells and their contributions to tissue repair. *Pharmacology & therapeutics,* 151**,** 107-120.

WOODCOCK, T. & WOODCOCK, T. M. 2012. Revised Starling equation and the glycocalyx model of transvascular fluid exchange: an improved paradigm for prescribing intravenous fluid therapy. *British journal of anaesthesia,* 108**,** 384-394.

WOODFIN, A., VOISIN, M.-B. & NOURSHARGH, S. 2007. PECAM-1: a multi-functional molecule in inflammation and vascular biology. *Arteriosclerosis, thrombosis, and vascular biology,* 27**,** 2514-2523.

WOOLARD, J., WANG, W.-Y., BEVAN, H. S., QIU, Y., MORBIDELLI, L., PRITCHARD-JONES, R. O., CUI, T.-G., SUGIONO, M., WAINE, E., PERRIN, R., FOSTER, R., DIGBY-BELL, J., SHIELDS, J. D., WHITTLES, C. E., MUSHENS, R. E., GILLATT, D. A., ZICHE, M., HARPER, S. J. & BATES, D. O. 2004. VEGF₁₆₅b, an Inhibitory Vascular Endothelial Growth Factor Splice Variant. *Cancer Research,* 64**,** 7822.

WRIGHT, S. D., RAMOS, R. A., TOBIAS, P. S., ULEVITCH, R. J. & MATHISON, J. C. 1990. CD14, a receptor for complexes of lipopolysaccharide (LPS) and LPS binding protein. *Science,* 249**,** 1431.

WU, Y., LIU, B., SUN, Y., DU, Y., SANTILLAN, M.K., SANTILLAN, D.A., SNETSELAAR, L.G. AND BAO, W., 2020. Association of maternal prepregnancy diabetes and gestational diabetes mellitus with congenital anomalies of the newborn. *Diabetes Care*, *43*, 2983-2990.

WU, X., WANG, S., CHEN, B. & AN, X. 2010. Muscle-derived stem cells: isolation, characterization, differentiation, and application in cell and gene therapy. *Cell and tissue research,* 340**,** 549-567.

XIANG, A. H., PETERS, R. K., TRIGO, E., KJOS, S. L., LEE, W. P. & BUCHANAN, T. A. 1999. Multiple metabolic defects during late pregnancy in women at high risk for type 2 diabetes. *Diabetes,* 48**,** 848-854.

XU, Z., GU, C., YAO, X., GUO, W., WANG, H., LIN, T., LI, F., CHEN, D., WU, J. & YE, G. 2020. CD73 promotes tumor metastasis by modulating RICS/RhoA signaling and EMT in gastric cancer. *Cell death & disease,* 11**,** 1-15.

YAMAMOTO, J. M., KELLETT, J. E., BALSELLS, M., GARCÍA-PATTERSON, A., HADAR, E., SOLÀ, I., GICH, I., VAN DER BEEK, E. M., CASTAÑEDA-GUTIÉRREZ, E. & HEINONEN, S. 2018. Gestational diabetes mellitus and diet: a systematic review and meta-analysis of randomized controlled trials examining the impact of modified dietary interventions on maternal glucose control and neonatal birth weight. *Diabetes Care,* 41**,** 1346-1361.

YAN, H.-T. & SU, G.-F. 2014. Expression and significance of HIF-1 α and VEGF in rats with diabetic retinopathy. *Asian Pacific Journal of Tropical Medicine,* 7**,** 237-240.

YANG, G.-R., DYE, T. D. & LI, D. 2019. Effects of pre-gestational diabetes mellitus and gestational diabetes mellitus on macrosomia and birth defects in Upstate New York. *Diabetes Research and Clinical Practice,* 155**,** 107811.

YOUNG, B. C., LEVINE, R. J. & KARUMANCHI, S. A. 2010. Pathogenesis of preeclampsia. *Annual review of pathology,* 5**,** 173.

ZACHARY, I. 2003. VEGF signalling: integration and multi-tasking in endothelial cell biology. *Biochemical Society Transactions,* 31**,** 1171-1177.

ZAPPULLI, V., FRIIS, K. P., FITZPATRICK, Z., MAGUIRE, C. A. & BREAKEFIELD, X. O. 2016. Extracellular vesicles and intercellular communication within the nervous system. *The Journal of clinical investigation,* 126**,** 1198-1207.

ZYGMUNT, M., HERR, F., MÜNSTEDT, K., LANG, U. & LIANG, O. D. 2003. Angiogenesis and vasculogenesis in pregnancy. *European Journal of Obstetrics & Gynecology and Reproductive Biology,* 110**,** S10-S18.